Development of electrospun wound-dressings incorporating medicinal plant-extracts

Cláudia Filipa Duarte Mouro

Tese para obtenção do Grau de Doutor em
Materiais e Processamento Avançados
(3º ciclo de estudos)

Orientadora: Prof.ª Doutora Isabel Cristina Aguiar de Sousa e Silva Gouveia
Co-Orientador: Prof. Doutor Raul Manuel Esteves de Sousa Fangueiro

Júri:
Prof. Doutor Joaquim Mateus Paulo Serra
Prof. Doutor Rogério Manuel Santos Simões
Prof. Doutor João Paulo Miranda Ribeiro Borges
Prof.ª Doutora Maria Ascensão Ferreira Silva Lopes
Prof.ª Doutora Isabel Cristina Aguiar de Sousa e Silva Gouveia
Prof. Doutor Nuno José Ramos Belino
Prof.ª Doutora Mariana Contente Rangel Henriques

03 de fevereiro de 2023

Declaração de Integridade

Eu, Cláudia Filipa Duarte Mouro, que abaixo assino, estudante com o número de inscrição D1684 do 3º Ciclo em Materiais e Processamento Avançados da Faculdade de Engenharias, declaro ter desenvolvido o presente trabalho e elaborado o presente texto em total consonância com o **Código de Integridades da Universidade da Beira Interior**.

Mais concretamente afirmo não ter incorrido em qualquer das variedades de Fraude Académica, e que aqui declaro conhecer, que em particular atendi à exigida referenciação de frases, extratos, imagens e outras formas de trabalho intelectual, e assumindo assim na íntegra as responsabilidades da autoria.

Universidade da Beira Interior, Covilhã 13/02/2023

Assinado por: **Cláudia Filipa Duarte Mouro**
Num. de Identificação: 13752254
Data: 2023.02.13 10:52:35+00'00'

Dedicatory

To all the people who have inspired, encouraged, and supported me, and to all those who believe in the richness of learning and continue to research to get results.

I would like to acknowledge the Fundação para a Ciência e Tecnologia (FCT) for the PhD fellowship (PD/BD/113550/2015).

Acknowledgements

This thesis is the result of my endeavor and dedication, but also of all those who deposit their contributions in it. In this way, I would like to express my sincere gratitude towards all those persons who made this thesis possible and a remarkable experience for me.

To start, I would like to express my deepest gratitude to my supervisor Prof. Dr. Isabel Cristina Gouveia, for all availability, knowledge, scientific support, expertise, insightful suggestions, and valuable advices. Her guidance was crucial for the success of this work.

I am also sincerely grateful to Prof. Dr. Raul Fangueiro, for his deepest solicitude.

I have to kindly acknowledge the financial support from the Fundação para a Ciência e Tecnologia (FCT) through the individual PhD fellowship (Ref PD/BD/113550/2015) provided under the Doctoral Program AdvaMTech. I would also like to mention the University of Beira Interior, particularly the FibEnTech - Fiber Materials and Environmental Technologies Research Unit, for give me the opportunity to develop this study in its facilities and the funding from the project UIDB/00195/2020.

Moreover, I would like to express my gratitude to Engª Ana Paula Gomes from Centro de Óptica for contributing with her technical expertise in my work. Her tireless help in SEM and DSC analysis was essential in this thesis. A special thanks to Raquel Nunes, my friend since childhood, for her technical support with cytotoxic analysis.

A special appreciation to my lab colleagues, particularly to Frederico Nogueira and Lúcia Amorim, for all the assistance and friendship. I will never forget your scientific contributions and all the good times we spent together during this journey. Also, my sincere gratitude goes to my friends for the love, care, support, encouragement, and enjoyable moments.

Finally, I couldn't finish the acknowledgments without express my extremely thankful to my parents, sister, and my boyfriend, Mauro, for their patience, unconditional care and love, unfailing support, and incentive during this thesis. This accomplishment would not have been possible without them.

THANK YOU ALL!

Preface

The skin is the largest organ of the human body. It consists of a complex three-layer structure, the epidermis, the dermis, and the hypodermis, which under normal physiological conditions, possess inherent properties of self-renewal and regeneration. However, the skin's integrity can be compromised by both endogenous and exogenous factors and lead to the occurrence of acute and chronic, non-healing wounds.

Chronic wounds associated with several pathological conditions, such as diabetes, obesity, and ageing have demonstrated an increased incidence of bacterial colonization, leading to infections, and consequently delaying the healing. Besides, the persistent microbial colonization observed in chronic wounds makes them an ideal environment for biofilm formation which results in serious complications, like amputations, systemic infections, drug-resistances, and increase the healthcare costs.

In order to prevent this situation and ensure an appropriate wound management, several strategies have been developed not only to protect the wound site from bacterial infection but also to enhance the healing process. Among them, the topical application of various antimicrobial agents, particularly antibiotics, at the wound site has been explored. Nevertheless, when these agents are topically applied to prevent microbial growth, an allergic or irritant response can be induced and these agents can be easily removed from the wound site, resulting in therapeutic failure. Likewise, if these agents are delivered within an adverse wound healing environment, their therapeutic capability can be compromised.

Thus, as a possible solution, researchers have successfully incorporated a wide range of bioactive compounds with antimicrobial activity, like antibiotics, nanoparticles, and natural products, into wound dressing materials from diverse strategies to simultaneously prevent or treat infection and encourage the healing process. In this sense, extensive research efforts have emerged to develop antimicrobial wound dressings from more simple, environmentally friendly, and cost-effective approaches.

So, the motivation behind this doctoral thesis arises from this necessity and is focused on a new type of wound dressing materials, based on nanofibers produced via electrospinning, due to their excellent properties in promoting the healing process, such as high-surface area, micro-porosity, and structural similarity to the natural extracellular matrix (ECM), as well as incomparable ability to load a variety of bioactive compounds. Amongst the various compounds incorporated until now, the plant extracts, a group of interesting natural

products, have received considerable attention due to their high availability, easy extraction, environmentally friendly nature, and absence of adverse side effects.

Hence, different electrospun wound dressings containing medicinal plant extracts were successfully produced in this doctoral thesis, and with hopes that this research work may open up new perspectives to fill the gap that remains between the lab-scale research, clinical trials, and even commercialization of these materials.

List of papers

Papers published in peer-reviewed international journals included in this Doctoral thesis:

I. **Electrospun wound dressings with antibacterial function: A critical review of plant extract and essential oil incorporation.**
Cláudia Mouro and Isabel C. Gouveia
(Under review in Critical Reviews in Biotechnology)

II. **Emulsion Electrospun Fiber Mats of PCL/PVA/Chitosan and Eugenol for Wound Dressing Applications.**
Cláudia Mouro, Manuel Simões, and Isabel C. Gouveia
Advances in Polymer Technology (2019) 2019:9859506
DOI: 10.1155/2019/9859506

III. **Emulsion electrospinning of PLLA/PVA/Chitosan with *Hypericum perforatum* L. as an antibacterial nanofibrous wound dressing.**
Cláudia Mouro, Raul Fangueiro, and Isabel C. Gouveia
(Submitted for publication)

IV. ***Chelidonium majus* L. Incorporated Emulsion Electrospun PCL/PVA_PEC Nanofibrous Meshes for Antibacterial Wound Dressing Applications.**
Cláudia Mouro, Ana P. Gomes, Merja Ahonen, Raul Fangueiro, and Isabel C. Gouveia
Nanomaterials (2021) 11(7):1785
DOI: 10.3390/nano11071785

V. **Double-layer PLLA/PEO_Chitosan nanofibrous mats containing *Hypericum perforatum* L. as an effective approach for wound treatment.**
Cláudia Mouro, Ana P. Gomes, and Isabel C. Gouveia
Polymers for Advanced Technologies (2021) 32(4):1493-1506
DOI: 10.1002/pat.5185

VI. Preparation and Characterization of Electrospun Double-layered Nanocomposites Membranes as a Carrier for *Centella asiatica* (L.).

Cláudia Mouro, Raul Fangueiro, and Isabel C. Gouveia

Polymers (Basel) (2020) 12(11):2653

DOI: 10.3390/polym12112653

VII. Designing New Antibacterial Wound Dressings: Development of a Dual Layer Cotton Material Coated with Poly(Vinyl Alcohol)_Chitosan Nanofibers Incorporating *Agrimonia eupatoria* L. Extract.

Cláudia Mouro, Colum P. Dunne, and Isabel C. Gouveia

Molecules (2021) 26(1):83

DOI: 10.3390/molecules26010083

List of Scientific Communications

Oral scientific communications related with this Doctoral thesis:

I. ***Agrimonia eupatoria* L.-incorporated electrospun nanofibers and cotton composite for antibacterial wound dressing applications.**
Cláudia Mouro, Raul Fangueiro, Isabel C. Gouveia
1st International FibEnTech Congress - New opportunities for fibrous materials in the ecological transition (2021) Covilhã, Portugal (Virtual)

II. **Electrospun nanofibrous membranes containing medicinal plant extracts as natural source of bioactive compounds for wound dressing applications.**
Cláudia Mouro, Isabel C. Gouveia
International Conference on Direct Digital Manufacturing and Polymers (2021) Marinha Grande, Portugal (Virtual)

III. **Development of electrospun wound-dressings incorporating medicinal plant-extracts.**
Cláudia Mouro, Raul Fangueiro, Isabel C. Gouveia
4th General Meeting PhD Program in Advanced Materials and Processing – AdvaMTech (2018) Lisboa, Portugal

IV. **Development of electrospun wound-dressings incorporating medicinal plant-extracts.**
Cláudia Mouro, Raul Fangueiro, Isabel C. Gouveia
3rd General Meeting PhD Program in Advanced Materials and Processing – AdvaMTech (2017) Lisboa, Portugal

V. **Development of electrospun wound-dressings incorporating medicinal plant-extracts.**
Cláudia Mouro, Raul Fangueiro, Isabel C. Gouveia
2nd General Meeting PhD Program in Advanced Materials and Processing – AdvaMTech (2016) Lisboa, Portugal

VI. Development of electrospun wound-dressings incorporating medicinal plant-extracts.

Cláudia Mouro, Raul Fangueiro, Isabel C. Gouveia

1st General Meeting PhD Program in Advanced Materials and Processing – AdvaMTech (2015) Lisboa, Portugal

Poster presentations related with this Doctoral thesis:

I. **Eugenol loaded into electrospun PCL/PVA/Chitosan nanofibrous mats by emulsion electrospinning to development of innovative wound dressings.**
Cláudia Mouro, Manuel Simões, Isabel C. Gouveia
3rd Symposium of the FibEnTech Research Unit: Fiber Materials and Environmental Technologies (2018) Covilhã, Portugal

II. **Emulsion Electrospun Fiber Mats of PCL/PVA/Chitosan and Eugenol aimed for antimicrobial wound healing applications.**
Cláudia Mouro, Manuel Simões, Isabel C. Gouveia
The AMiCI WG2 workshop Antimicrobial Coatings Applied in Healthcare Settings – Efficacy Testing, Federal Institute for Materials Research and Testing (BAM) (2018) Berlin, Germany

Resumo alargado

A pele constitui uma barreira notavelmente eficaz contra a invasão de agentes patogénicos externos. No entanto, quando a integridade da pele é comprometida pela ocorrência de feridas, a possibilidade de microrganismos patogénicos colonizarem o local e desencadearem uma infeção, aumenta. Normalmente, logo após a lesão ocorrer, inicia-se uma série sequencial e ordenada de eventos regulada pelo sistema imunitário, de forma a restaurar a estrutura e as funções da pele nativa. Contudo, múltiplos fatores podem impedir que o processo de cicatrização ocorra de maneira eficaz. Entre estes, a presença e permanência de elevados níveis de bactérias patogénicas na ferida, mais comum em pacientes imunocomprometidos, prevalecem como um dos principais responsáveis pelo atraso ou falha no processo de cicatrização.

As infeções da pele e tecidos moles (IPTM), especialmente as causadas por bactérias, estão entre as infeções mais comuns que podem progredir rapidamente para complicações potencialmente fatais. Além disso, o envelhecimento da população, a obesidade e o consequente aumento da incidência de doenças crónicas têm contribuído para uma maior prevalência de feridas suscetíveis à colonização bacteriana e infeção. Neste contexto, para prevenir a penetração de bactérias no local da ferida e evitar o seu crescimento e proliferação, têm sido produzidos pensos para feridas, a partir de diferentes materiais, com formas distintas, contendo agentes antimicrobianos na sua estrutura para aprimorar as propriedades antimicrobianas destes materiais. Entre estes agentes, destacam-se os antibióticos, as nanopartículas (NPs) e os produtos de origem natural. Contudo, apesar de estarem disponíveis vários antibióticos para o tratamento de infeções de feridas, o seu uso recorrente e indiscriminado tem desencadeado uma taxa alarmante de bactérias multirresistentes capazes de resistir mesmo aos antibióticos mais recentes e eficazes. Nesse sentido, as NPs surgiram como uma alternativa terapêutica aos antibióticos mais comuns. No entanto, a possível toxicidade associada à sua utilização tem limitado a sua aplicação em pensos. Deste modo, temos vindo a assistir a uma crescente procura por compostos obtidos a partir de fontes naturais, em particular a partir de plantas medicinais, como uma alternativa mais eficaz e segura.

As plantas medicinais têm sido consideradas desde os tempos ancestrais poderosos suplementos naturais por desempenharem um papel importante na cura e tratamento de diferentes tipos de feridas. Estas são de fácil acesso e reconhecidas devido às inúmeras propriedades terapêuticas que exibem, como propriedades antimicrobianas, anti-

inflamatórias, antioxidantes, anestésicas e analgésicas, as quais estão relacionadas com a presença de uma vasta gama de substâncias bioativas. Além disso, as plantas medicinais são também capazes de melhorar o processo de cicatrização por exibirem a capacidade de acelerar a proliferação de fibroblastos, revascularização, síntese e deposição de colagénio. Desta forma, pensos para feridas contendo compostos naturais provenientes de plantas, mais ecológicos, sustentáveis, eficazes e seguros, bem como economicamente viáveis, com atividade antimicrobiana intrínseca e, ao mesmo tempo, com a capacidade de acelerar o processo de cicatrização, têm-se revelado de extrema importância e despertado o interesse dos investigadores nos últimos anos a fim de prevenir ou mesmo eliminar infeções indesejáveis.

Entre as diferentes técnicas utilizadas para produzir pensos para feridas, o *electrospinning* tem merecido um maior destaque no desenvolvimento de membranas nanofibrosas devido à sua simplicidade, relação custo-eficácia e versatilidade. Além disso, as membranas produzidas por *electrospinning* têm demonstrado propriedades com notável potencial terapêutico, tais como uma estrutura tridimensional que mimetiza as características morfológicas da matriz extracelular da pele (ECM), uma elevada área de superfície e porosidade que lhes permite controlar o exsudado e gerir o ambiente húmido no local da ferida, bem como garantir a oxigenação e o fornecimento necessário de nutrientes. Estes materiais têm ainda a capacidade de promover a adesão e proliferação celular e potencial para libertar compostos bioativos no local da ferida.

Assim sendo, e de forma a proteger as feridas de agressões externas e evitar possíveis complicações, a nossa proposta prevê a utilização de diferentes estratégias/ metodologias para produzir, através de *electrospinning*, materiais com as características adequadas para aplicação na área do tratamento de feridas. Com esse objetivo, os trabalhos realizados ao longo deste projeto exploram diferentes misturas de biopolímeros com polímeros sintéticos biodegradáveis e biocompatíveis, bem como vários extratos brutos de plantas medicinais e seus derivados, como óleos essenciais, com reconhecidas propriedades antimicrobianas, a fim de reduzir o risco de infeção bacteriana e permitir que a cicatrização ocorra num curto espaço de tempo.

Numa primeira abordagem, o Eugenol (EUG), um óleo essencial extraído do cravo-da-índia, conhecido por apresentar propriedades terapêuticas muito interessantes, foi incorporado com sucesso em uma mistura polimérica composta de Policaprolactona (PCL), Álcool Polivinílico (PVA) e Quitosano (CS) por *electrospinning* de emulsão. O EUG foi incorporado pela primeira vez em duas emulsões distintas, água-em-óleo (A/O) e óleo-em-água (O/A), para investigar qual seria a combinação que apresentava melhores propriedades para

aplicação como penso para feridas. Neste estudo, o EUG incorporado na emulsão do tipo O/A revelou resultados mais promissores e demonstrou capacidade para inibir o crescimento de *Staphylococcus aureus* (*S. aureus*) e *Pseudomonas aeruginosa* (*P. aeruginosa*) sem induzir qualquer efeito citotóxico em fibroblastos dérmicos humanos normais (NHDF).

No entanto, apesar do *electrospinning* de emulsão se ter revelado uma técnica auspiciosa para preservar a estabilidade e bioatividade do EUG, a obtenção de óleos essenciais exige quantidades elevadas de planta, requer métodos de preparação que envolvem várias etapas, bem como equipamentos específicos de laboratório. Além disso, estes derivados de plantas podem ser facilmente degradados e são suscetíveis a perdas por volatilização e/ou decomposição térmica.

Para superar as limitações apresentadas pelos óleos essenciais, dois diferentes extratos brutos de plantas medicinais foram preparados e incorporados em duas misturas poliméricas distintas, por *electrospinning* de emulsão, a fim de corroborar a eficácia e potencialidade desta técnica. Os extratos brutos destacam-se dos óleos essenciais por serem facilmente obtidos a partir de plantas secas e moídas, através de métodos de extração simples, de fácil execução e baixo custo.

Além disso, os extratos brutos são misturas ecologicamente sustentáveis que possuem diversas substâncias com múltiplas propriedades terapêuticas e têm demonstrado ser mais efetivos, comparativamente aos seus derivados, devido à sua disponibilidade e acessibilidade. Também as interações sinérgicas estabelecidas entre os diferentes compostos têm-se revelado favoráveis e resultado em uma melhor proteção contra possíveis degradações. Neste sentido, um extrato bruto de *Hypericum perforatum* L. (HP) foi incorporado numa mistura polimérica de Poli (L-ácido láctico) (PLLA), PVA e CS enquanto um extrato bruto de *Chelidonium majus* L. (CM) foi incorporado numa mistura composta por PCL, PVA e Pectina (PEC). Os resultados revelaram que as membranas de nanofibras fabricadas a partir de emulsões A/O contendo os extratos brutos de plantas medicinais exibiram propriedades adequadas para utilização como pensos para feridas. Além disso, estas membranas demonstraram ser capazes de inibir o crescimento de bactérias patogénicas e comprovaram ser sistemas versáteis para libertação controlada de agentes bioativos e/ou terapêuticos. Porém, a membrana de nanofibras em que o extrato de CM foi incorporado na mistura polimérica PCL/PVA_PEC demonstrou uma maior atividade antibacteriana, obtendo-se um ~4 Log de redução.

Portanto, o *electrospinning* de emulsão comprovou exibir a inigualável capacidade de produzir, numa única etapa, pensos para feridas compostos de uma única camada

incorporados com produtos naturais e a substituição do EUG por extratos brutos de plantas medicinais revelou-se uma alternativa atrativa e promissora.

Por outro lado, materiais produzidos por deposição de duas diferentes camadas foram desenhados na tentativa de mimetizar a estrutura nativa da pele, bem como as suas funções e tornar o processo de cicatrização mais rápido e eficaz. Assim, uma membrana de dupla camada constituída por uma camada superior de PLLA, desenhada para atuar como uma barreira protetora contra a entrada de agentes patogénicos, e uma camada inferior de Óxido de Polietileno (PEO), CS e HP, destinada a ser utilizada em contacto com a ferida, a fim de dotar a membrana com propriedades antimicrobianas e promover a regeneração da pele, foi fabricada com sucesso por *electrospinning*. Os resultados obtidos revelaram que a camada superior pode atuar como uma barreira impermeável, mas respirável, capaz de impedir a entrada de bactérias no local da ferida, enquanto a camada inferior exibiu a porosidade, molhabilidade e *swelling* (inchamento por efeito de absorção de líquidos) adequados à manutenção de um ambiente húmido favorável ao processo de cicatrização. Além disso, as propriedades antimicrobianas do CS e HP foram demonstradas pela capacidade desta camada inibir o crescimento de *S. aureus* e *P. aeruginosa*, sem causar efeitos citotóxicos. Similarmente, uma membrana de dupla camada foi produzida por *electrospinning* com uma camada superior de PCL. Esta camada exibiu a porosidade e a molhabilidade desejáveis para atuar como uma barreira física contra ameaças externas, nomeadamente contra a invasão de bactérias. Por sua vez, o CS foi reticulado com tripolifosfato de sódio (TPP) e combinado com PVA a fim de testar a sua adequabilidade para atuar como um transportador de *Centella asiatica* L. (CA), a ser libertada no local da ferida e melhorar o potencial terapêutico da camada inferior. Devido às suas propriedades, esta camada demonstrou ser capaz de promover o processo de cicatrização e de oferecer uma libertação controlada de CA, desejável para evitar o crescimento bacteriano no local da ferida, observando-se uma redução de *S. aureus* e *P. aeruginosa* de 3 Log.

Finalmente, o Algodão, normalmente utilizado em pensos para feridas, foi combinado com nanofibras de PVA e CS incorporadas com *Agrimonia eupatoria* L. (AG) a fim de produzir um *nano-coating* capaz de acelerar o processo de cicatrização. Para isso, o algodão foi primeiramente oxidado com o radical 2,2,6,6-tetrametil-1-piperidinoxil (TEMPO) para dota-lo com cargas negativas e de seguida foi utilizado como substrato na produção das nanofibras de PVA, CS e AG. Através dos resultados obtidos foi possível verificar que a camada de nanofibras incorporada com o extrato de AG exibiu propriedades adequadas para prevenir a desidratação, bem como a adesão das fibras de algodão ao leito da ferida. Além

disso, as nanofibras revelaram-se não tóxicas para fibroblastos humanos, bem como apropriadas para inibir o crescimento bacteriano quando em contacto com a pele lesada.
No geral, o trabalho realizado no âmbito desta tese pretende incentivar a comunidade científica a dar particular relevância aos produtos de origem natural com baixa propensão ao desenvolvimento de resistências bacterianas e ao uso de estratégias relativamente simples, versáteis e de baixo custo para obtenção de materiais avançados para a fabricação de pensos para feridas com propriedades antimicrobianas, adequados para combater possíveis infeções e melhorar o processo de cicatrização.

Palavras-chave

Pensos antimicrobianos para a cicatrização de feridas, produtos naturais, plantas medicinais, polímeros biodegradáveis e biocompatíveis, electrofiação de emulsão, membranas de dupla camada, cicatrização de feridas

Abstract

Human skin is a remarkably effective barrier against the invasion of external pathogens. However, when the occurrence of wounds compromises the skin's integrity, the possibility of pathogenic microorganisms to colonize the wound site increase as well as the risk of acquiring an infection. In particular, the presence and permanence of high levels of pathogenic bacteria in the wound have been identified as the main responsible for the delay or failure in the healing process, especially in patients with a compromised immune system. The skin and soft tissue infections (SSTIs), particularly those caused by bacteria, are among the most common infections that can progress quickly to life-threatening complications. Besides, the aging population, combined with the increased rates of obesity and chronic diseases, like diabetes, have contributed to a higher prevalence of wounds susceptible to bacterial colonization and infection. In this context, to prevent the penetration of bacteria at the wound site and its growth and proliferation, wound dressings have been produced from different materials, with diverse shapes, containing antimicrobial agents into their structure. Among these agents, antibiotics, nanoparticles (NPs), and natural products have been the most used. However, the excessive and indiscriminate use of antibiotics has triggered an alarming rate of multidrug-resistant bacteria. Also, the possible toxicity associated with the use of NPs has limited its application in dressing materials. In this way, we have been witnessing an increasing demand for compounds obtained from natural sources, in particular from medicinal plants, as a more effective and efficient alternative.

Medicinal plants are natural sources of bioactive substances that may exert significant effects on the management and treatment of wounds. Besides, the numerous therapeutic properties of the medicinal plants, such as antimicrobial, anti-inflammatory, antioxidant, anesthetic, and analgesic, are helpful in the treatment of injured skin by enhancing fibroblast proliferation, angiogenesis, and collagen biosynthesis. Thus, wound dressing materials containing plant extracts and some compounds obtained from plants, with intrinsic antimicrobial activity and ability to accelerate the healing process, have captured the interest of researchers in recent years in order to avoid or even eliminate undesirable pathogenic infections.

Among the different techniques used to produce wound dressing materials, the electrospinning has been highlighted in the development of wound dressings based on bioactive nanofibers due to its simplicity, cost-effectiveness, and versatility.

The nanofiber membranes produced by electrospinning have demonstrated properties with remarkable therapeutic potential, such as a 3D architecture that mimics the morphological features of the skin's extracellular matrix (ECM), a high surface area to volume ratio, and porosity that allow them to control the exudate effectively. These characteristics are also able to maintain a moist environment at the wound site and ensure a continuous supply of nutrients and oxygen that promotes wound healing. Furthermore, the electrospun nanofibrous membranes have been incorporated with different types of bioactive or therapeutic agents, improving the desirable wound healing properties.

Therefore, in this doctoral work, new electrospun wound dressing materials containing crude medicinal plant extracts and plant essential oils with remarkable antimicrobial and healing effects were developed from several strategies to protect the wound from both external agents and pathogenic invasion, as well as improve the skin tissue regeneration.

In a first approach, Eugenol (EUG), an essential oil extracted from cloves, was incorporated into a polymeric blend composed of Polycaprolactone (PCL), Polyvinyl Alcohol (PVA), and Chitosan (CS) by electrospinning from water-in-oil (W/O) and oil-in-water (O/W) emulsions. From this work, it was achieved better wound healing properties when O/W emulsion was used. However, although emulsion electrospinning shows promising potential for preserving the EUG's stability and bioactivity, the essential oils require large amounts of raw material, as well as multiple step preparation methods and special laboratory facilities.

To overcome the limitations presented by essential oils, two different crude medicinal plant extracts, which are easily obtained from dried and milled plants, were prepared through a simple, easy to perform, and low-cost extraction method, and then incorporated in two different polymeric blends by emulsion electrospinning to corroborate the effectiveness and potential of this technique. Regarding that, a crude extract of *Hypericum perforatum* L. (HP) was incorporated into a polymeric blend of Poly(L-lactic acid) (PLLA), PVA, and CS, while a crude extract of *Chelidonium majus* L. (CM) was loaded into a blend of PCL, PVA, and Pectin (PEC). The results revealed that the manufactured nanofiber membranes exhibited suitable properties for use as wound dressing materials. Besides, these membranes have been shown to inhibit the growth of pathogenic bacteria, namely *Staphylococcus aureus* (*S. aureus*) and *Pseudomonas aeruginosa* (*P. aeruginosa*), and proved to be versatile systems for controlled release of bioactive and/or therapeutic agents. From these studies, the CM extract loaded into electrospun PCL/PVA_PEC nanofibrous membrane achieved a better antibacterial activity, reaching a ~4 Log reduction.

Therefore, emulsion electrospinning has demonstrated to exhibit the incomparable ability to produce, in a single step, single-layer wound dressings incorporated with natural

products, and the replacement of EUG by crude medicinal plant extracts proved to be an attractive and promising alternative.

In a different approach, double-layered electrospun nanofibrous membranes containing crude medicinal plant extracts were produced, aiming to restore the structure and functions of the native skin.

Concerning that, two different double-layer materials were developed from electrospinning. PLLA and PCL's top layers were designed to act as breathable and waterproof protective barriers, capable of preventing bacteria penetration into the wound. In turn, lower layers of Polyethylene oxide (PEO), CS, and HP, as well as Chitosan-Sodium Tripolyphosphate (CS-TPP), combined with PVA and *Centella asiatica* L. (CA) were produced to improve the biologic performance of these materials. Due to their properties, the lower layers demonstrated to be able to promote the healing process and inhibit the growth of *S. aureus* and *P. aeruginosa* without inducing any cytotoxic effect. However, the PVA_CS-TPP_CA revealed a higher bacterial inhibitory effect, reaching a 3 Log reduction.

Finally, a cotton gauze bandage, traditionally used to provide support and confer robust protection against external threats, was successfully combined with PVA and CS nanofibers containing *Agrimonia eupatoria* L. (AG) to produce a nano-coating capable of inhibiting the growth of bacteria at the wound site and support skin regeneration.

Overall, the scientific work performed in this thesis has been conducted to encourage the scientific community to give more attention to the potential benefits of bioactive natural products as medicinal plants, which exhibit a low tendency to develop bacterial resistance. Moreover, it has been shown that the use of relatively simple, versatile, and low-cost strategies to produce wound dressing materials displaying antimicrobial properties have an essential impact on the control of bacterial colonization but also prevent bacterial wound infection and consequently accelerate the healing process.

Keywords

Antimicrobial wound dressings, natural products, medicinal plants, biodegradable and biocompatible polymers, emulsion electrospinning, double-layered membranes, wound healing

Thesis Overview

The present thesis was divided into 4 main chapters.

Chapter 1 is based on a review paper (**Paper 1 - Electrospun wound dressings with antibacterial function: A critical review of plant extract and essential oil incorporation**) and makes a literature review of the main topics involved in the research work performed during this thesis, in order to contextualize the reader.
This introductory chapter focus on the prevention, treatment, and management of bacterial infected wounds. Concerning that, a description of the different wound dressings used over time is exhibited and the importance of producing nanofibers through electrospinning displaying antimicrobial activity is highlighted. Also, the different functionalization strategies used for this purpose are described, as well as the most common antimicrobial agents incorporated into the electrospun nanofibers, focusing on the effectiveness of the natural extracts from plants.

Chapter 2 identifies the main purpose and specific goals to be achieved with this doctoral thesis.

Chapter 3 presents the results obtained during this thesis and has the purpose of showing the practical achievements of the goals considered in **Chapter 2**, Figure 1. This chapter comprises three different parts in the form of original research papers, respectively:

Part I - Emulsion Electrospinning for Wound Dressing Applications:
Paper 2 - Emulsion Electrospun Fiber Mats of PCL/PVA/Chitosan and Eugenol for Wound Dressing Applications

This research work describes for the first time the loading of Eugenol (EUG), an essential oil (EO), known for its therapeutic properties, into the electrospun Polycaprolactone (PCL)/ Polyvinyl Alcohol (PVA)/ Chitosan (CS) fiber mats. The fiber mats were produced from water-in-oil (W/O) and oil-in-water (O/W) emulsions to reach the best strategy. Several techniques were performed to assess their suitability as a wound dressing material.

Paper 3 - Emulsion electrospinning of PLLA/PVA/Chitosan with *Hypericum perforatum* L. as an antibacterial nanofibrous wound dressing

The incorporation of the hydro-ethanolic extract of *Hypericum perforatum* L. (HP) in a Poly(L-lactic acid) (PLLA)/PVA/CS emulsion blend was explored in this work to endow the produced fibers with antimicrobial activity, improving the healing process and avoiding of wound infection. For that purpose, a crude HP extract was easily prepared from dried and powdered aerial plant parts and two different weight percentages applied to accomplish a functional antimicrobial dressing. This approach highlights the benefits of using cost-effective and eco-friendly natural bioactive agents for wound management, and the capacity to produce, by emulsion electrospinning, wound dressing materials incorporated with these agents, in a single step.

Paper 4 - *Chelidonium majus* L. Incorporated Emulsion Electrospun PCL/PVA_PEC Nanofibrous Meshes for Antibacterial Wound Dressing Applications

In this paper, electrospun nanofibrous meshes composed of PCL, PVA, and Pectin (PEC) were incorporated with *Chelidonium majus* L. (CM), known for displaying a broad spectrum of pharmacological activities, and their properties (morphological, chemical, physical, mechanical, and biological) analyzed. The obtained meshes revealed suitable features to be applied as wound dressings. Also, the produced electrospun PCL/PVA_PEC nanofibrous meshes played an enhanced bactericidal activity against *Staphylococcus aureus* (*S. aureus*) and *Pseudomonas aeruginosa* (*P. aeruginosa*) and presented non-toxic effects to normal human dermal fibroblast (NHDF) cells.
Overall, these findings emphasize the potential that emulsion electrospinning has received, among the different functionalization strategies, to develop less expensive, functional, and versatile electrospun polymeric nanofibers for the sustained release of natural products, like medicinal plants.

Part II - Electrospun Double-Layered for Wound Dressing Applications:
Paper 5 - Double-layer PLLA/PEO_Chitosan nanofibrous mats containing *Hypericum perforatum* L. as an effective approach for wound treatment

In this study, a new double-layer nanofibrous dressing was produced through electrospinning. The upper layer, composed by PLLA, was fabricated to act as a protective

barrier, avoiding the bacteria penetration, while the Polyethylene oxide (PEO)_CS lower layer containing crude HP extract was designed to improve the healing process.
Consequently, the HP extract incorporation granted antimicrobial properties to the lower layer, which is essential to provide an aseptic environment at the wound site. Besides, the double-layer PLLA/PEO_HP_CS nanofibrous mats' properties revealed important insights into the behavior of this material as a wound dressing.

Paper 6 - Preparation and Characterization of Electrospun Double-layered Nanocomposites Membranes as a Carrier for *Centella asiatica* (L.)

This research work reports the development of a novel electrospun double-layered wound dressing membrane. To accomplish that, PVA, and CS-Sodium Tripolyphosphate (CS-TPP) incorporated with *Centella asiatica* L. (CA), commonly known as a medicinal plant able to improve its antimicrobial and biological properties, was successfully electrospun directly over a recently produced PCL layer. The CS was cross-linked with the TPP to comprehensively analyze its *in vitro* performance as a carrier for CA release.
The produced double-layered PCL/PVA_CS_TPP membrane containing CA did not exhibit any cytotoxic effect for fibroblasts while also ensuring a controlled release of CA, as well as an excellent antibacterial effect against *S. aureus* and *P. aeruginosa*, which is advantageous to prevent skin infections.

Part III – Cotton based composites for Wound Dressing Applications:
Paper 7 - Designing New Antibacterial Wound Dressings: Development of a Dual Layer Cotton Material Coated with Poly(Vinyl Alcohol)_Chitosan Nanofibers Incorporating *Agrimonia eupatoria* L. Extract

In the present study, cotton, a natural textile material, often used for gauze bandage dressings, was combined with PVA_CS nanofibers containing *Agrimonia eupatoria* L. (AG) to confer antimicrobial activity and towards an improved skin wound healing, avoiding the limitations of the textile dressings. In this strategy, the cellulose cotton was firstly oxidized with the 2,2,6,6 tetramethylpiperidine-1-oxyl radical (TEMPO), and then the PVA_CS blend added with AG extract was electrospun using Nanospider™ electrospinning on top of pre-activated cotton gauze bandage. The surface morphology, chemical, physical, mechanical, and biological properties of the produced dual-layer material were characterized to reinforce its application as a wound dressing displaying antimicrobial activity.

Accordingly, the dual-layer composite material's performance was influenced by the combination of the benefits of two distinct materials.

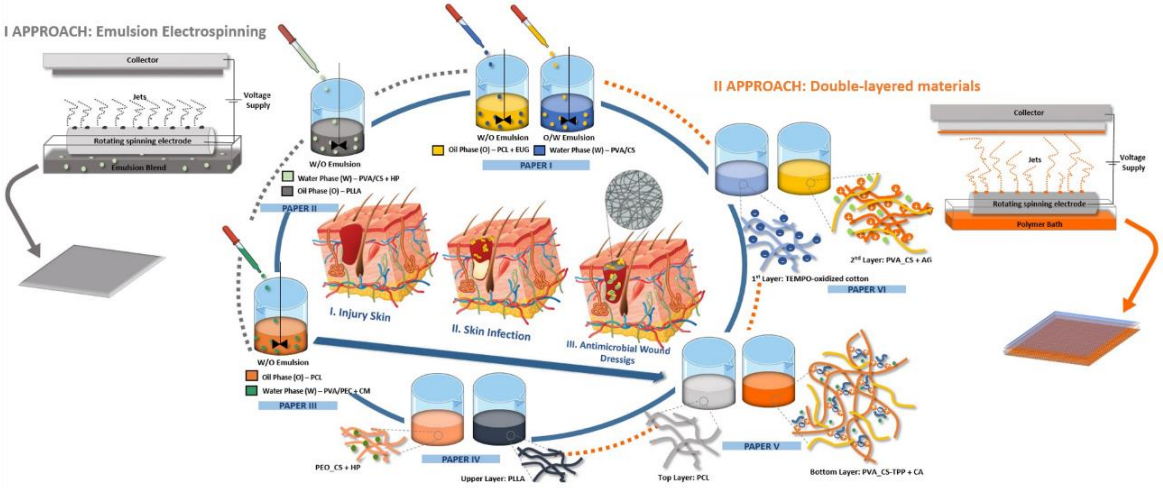

Figure 1 – Schematic representation of the approaches used during this thesis. (**I**) Emulsion electrospinning; (**II**) Double-layered materials.

Finally, the **Chapter 4** summarizes the concluding remarks and contains a general discussion of the results obtained, as well as the contributions of this thesis. Also, some suggestions and future trends are mentioned as eventual works to be carried out to complement the findings reported in this doctoral thesis.

Index

CHAPTER 1

General Introduction

This chapter is based on a review manuscript submitted for publication:

Cláudia Mouro and Isabel C. Gouveia. Electrospun wound dressings with antibacterial function: A critical review of plant extract and essential oil incorporation. *(Under review in Critical Reviews in Biotechnology)* (**Paper 1**)

Paper 1 - Electrospun wound dressings with antibacterial function: A critical review of plant extract and essential oil incorporation

Abstract

The wounds provide an ideal environment for bacterial growth, which may lead to infections, the most common cause of delayed healing. This situation becomes more alarming in patients with weakened immune systems, like those with diabetes, since there is an increased susceptibility to biofilm formation.

Nowadays, the bacterial biofilms are a serious global health concern, being responsible for persistent infections highly resistant to antibiotics, resulting in serious treatment failure and life-threatening complications. For this reason, and to overcome these limitations, researchers have incorporated several bioactive compounds with antimicrobial properties into different wound dressing materials to promote healing as well as prevent and treat bacterial infections.

Among the many different types of wound dressings, nanofiber-based materials produced through electrospinning are claimed to be ideal because of their auspicious intrinsic properties and the feasibility of employing several strategies to load bioactive compounds into their structure. Besides, bioactive compounds from natural sources, such as medicinal plant extracts and essential oils (EOs), have proven to be particularly attractive due to their non-toxic nature, minor side effects, desirable bioactive properties, and favorable effects on the healing process.

Concerning that, this review provides an exhaustive and up-to-date revision of the most prominent plant extracts and EOs with antimicrobial properties that have been incorporated into nanofiber-based wound dressings. The most common methods used for incorporating bioactive compounds into electrospun nanofibers include pre-electrospinning (blend, encapsulation, coaxial, and emulsion electrospinning) and post-electrospinning (physical adsorption, chemical immobilization, and layer-by-layer assembly). Furthermore, a general overview of the benefits of EOs and medicinal plant extracts is presented, describing their intrinsic properties and techniques for their incorporation into wound dressings. Finally, the current challenges and safety issues that need to be adequately clarified and addressed are discussed.

Graphical Abstract

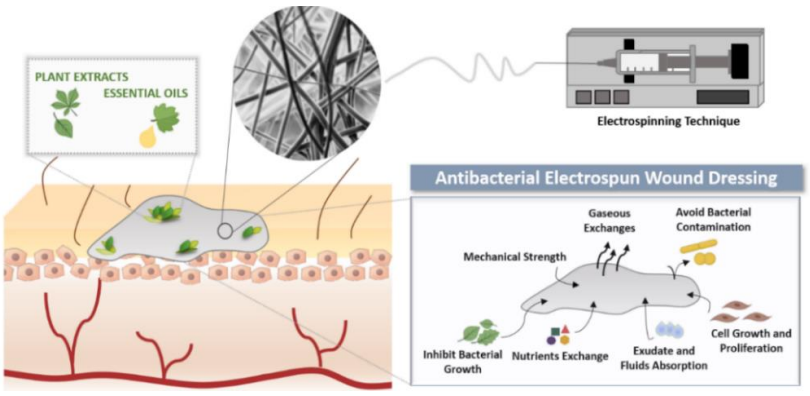

Keywords: Electrospun nanofibers; antimicrobial wound dressings; natural products; plant extracts; essential oils; electrospinning.

1. Introduction

The skin is the outer covering and largest organ of the human body that protects the underlying muscles, bones, ligaments, and internal organs from external threats. Besides, the skin is a sensory organ with the ability to regulate body temperature and water balance, play an essential role in both innate and adaptive immune responses and is responsible for producing vitamin D [1–7]. However, the structure and function of skin can be affected by several injuries, which lead to wounding. Wounds can have an accidental or intentional etiology, such as cuts, burns, and surgical incisions or arise from diseases, such as diabetes [3,5,6,8–10]. Hence, under certain conditions, when skin integrity is lost, the structural and functional features of the native skin must be rapidly re-established to ensure hemostasis and minimize the risk of microbial contamination, Figure 1.

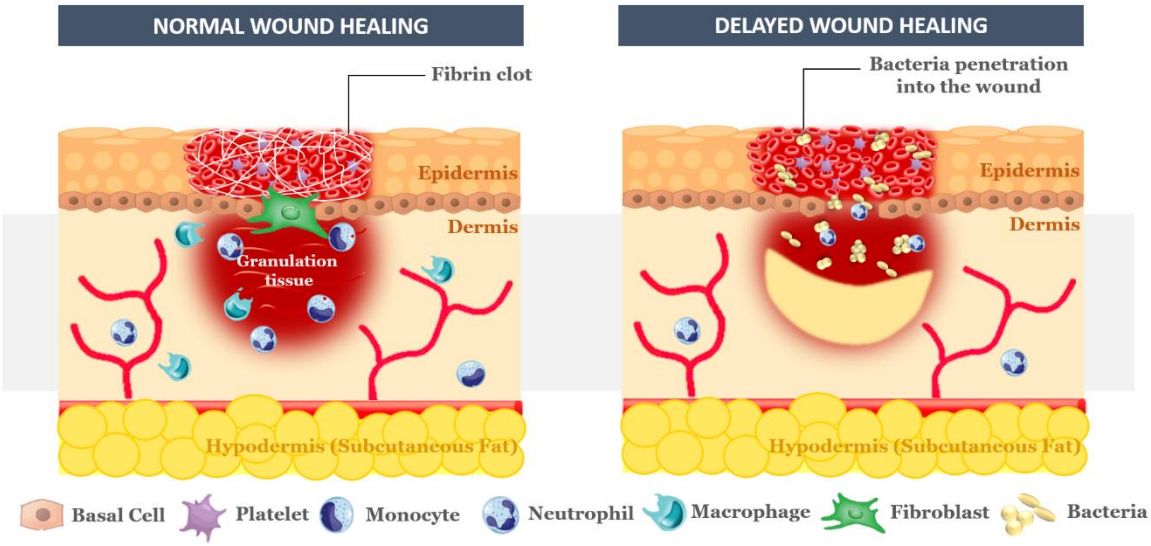

Figure 1 – Schematic representation of the normal healing process of a wound and the wounds' susceptibility to bacteria invasion and subsequent infection.

Upon the occurrence of a wound, the normal wound healing process begins as soon as possible after the skin injury with the hemostasis and is followed by three successive and overlapping phases, i.e., inflammation, proliferation, and remodeling [2,3,5,6,8,9,11,12].

However, the wounds are a favorable microenvironment for bacterial colonization and proliferation, resulting in subsequent infections, especially in patients with an impaired immune system. Concerning that, when the skin barrier is compromised, bacterial infections impair the healing process, resulting in chronic wounds and high rates of morbidity and mortality [2,4,5,7–10].

Skin and soft tissue infections (SSTIs) produced by bacteria are among the most common infections and range from superficial to life-threatening skin infections. *Staphylococcus aureus* (*S. aureus*) and *Streptococcus pyogenes* (*S. pyogenes*) are the most common Gram-positive bacteria found during the initial phases of chronic wound construction, while Gram-negative bacteria, like *Pseudomonas aeruginosa* (*P. aeruginosa*) and *Escherichia coli* (*E. coli*) are the

predominant pathogens in the later stages of the wound infectious process and tend to penetrate the skin's deeper layers, contributing to significant tissue damage [5,9,10]. In addition, polymicrobial infections are prevalent in chronic wounds due to the synergistic bacterial development patterns [9]. For example, aerobic bacteria require more oxygen to grow and survive leading to a hypoxic wound environment favourable to the development of anaerobic bacteria which produce short chain fatty acids that are able of inhibit the phagocytic activity of host defense cells, allowing more pathogens to colonize the wound [9].

Furthermore, the persistent bacterial colonization in infected wounds induces an extended inflammatory response once the inflammatory cells into the wound area release higher levels of destructive proteases, such as metalloproteinases (MMPs) and reactive oxygen species (ROS) that degrade extracellular matrix (ECM) components and compromise wound healing [5,10]. Besides, the infected wounds provide also an ideal environment for the formation of antibiotic-resistant biofilms [5,9,10,13].

Therefore, developing wound dressings that can prevent bacterial penetration into the wound and subsequent infection is imperative. To achieve this, wound dressings exhibiting antimicrobial activities have been fabricated from different materials and of various shapes using several techniques [1,2,4,5,7,9,10,12–14]. Among the many available wound dressings (*e.g.*, films, foams, hydrogels, and hydrocolloids), nanofiber membranes have attracted much attention in recent years. In addition, among the different techniques of nanofiber production, such as drawing, self-assembly, phase separation, and template synthesis, electrospinning has emerged as the ideal approach to overcome the problems of high cost, time consumption, and low efficiency of these methods. Based on these advantages, nanofibrous materials produced through electrospinning from naturally derived or synthetic biopolymer blends have been designed as promising materials for promoting the wound healing process while conferring protection against bacterial invasion. These effects result from the remarkable properties of these materials, such as their three-dimensional structure resembling the ECM of the natural skin, their ability to promote cell adhesion and proliferation, and their capability to deliver therapeutic and/or bioactive compounds to the wound site [1–3,5,7,11–17]. Among these, bioactive compounds obtained from natural sources, such as medicinal plants have emerged as attractive alternatives owing to their health benefits, easy availability, inexpensiveness, and safety [1,14–18]. Medicinal plants possess an enormous potential to overcome certain limitations of the currently available therapeutic products, such as the growing concerns regarding antimicrobial resistance and biofilm-associated infections, which constitute serious global public health threats, estimated to cause 10 million death per year by 2050 and incur a cumulative healthcare cost of US$100 trillion [14–19].

Herein, an overview of the most prominent antimicrobial agents that have thus far been incorporated into electrospun nanofiber materials to both prevent wound infection and promote wound healing is provided. In addition, particular attention has been devoted to natural products, such as medicinal plants and essential oils (EOs), given ability to prevent bacteria penetration and growth into the wound, low propensity to develop bacterial resistance, and capability to accelerate wound healing.

2. Electrospun nanofibers used as wound dressings

When the skin tissue is disrupted or wounding compromises skin's cellular integrity, dressing materials are required to act as a temporary barrier for protecting against external threats and simultaneously promote healing of the damaged skin [2,4,5,7,10,12,15]. An ideal wound dressing must fulfil several inherent requirements to successfully support the healing process and reduce the risk of infection. As such, it must be able to absorb and retain fluids, maintain a moist wound environment, ensure gas exchange and nutrient supply, support cell adhesion, migration, growth, and differentiation, and prevent bacterial growth [1,2,4,9,10,12,13,15,16,20]. In addition, wound dressings should be comfortable and conformable, biocompatible, non-toxic, and non-allergenic [1,2]. To meet these requirements, diverse types of wound dressings, such as films, foams, hydrogels, hydrocolloids, and micro/nanofibers membranes, have been developed depending on the severity of the wound and stage of the wound healing process [2,5,9,12,16,20].

For instance, semipermeable films, such as Opsite®, Tegaderm™, Bioclusive®, and Dermafilm™, are thin pellicles that are impermeable to bacteria and are compatible with gas exchange. They allow air permeation and supply the oxygen required for cellular respiration [4,5,16,21–23]. However, these dressings can cause exudate accumulation, leading to tissue maceration and/or infection [4,5,10,16]. On the other hand, several solid foams with different capacity for fluids absorption have emerged as a viable option [16,22,23]. These dressing materials are soft and porous and can easily adapt to wounds. In addition, they can maintain excellent thermal insulation performance, create an appropriate moist environment, and avoid fluid and exudate accumulation at the wound site [5,10,16,22–24]. However, these materials are generally non-adhesive dressings and consequently require a secondary dressing [16]. Some foam-based wound dressings available on the market include Lyofoam®, Tielle® Plus, Biatain® Adhesive, PermaFoam®, and Mepilex® [25,26]. Furthermore, hydrogels, a quite comprehensive class of dressings, have been widely used because of their capacity to store large amounts of water inside a three-dimensional polymeric network and/or their ability to absorb excessive amounts of exudate [5,16,22–24]. Typically, a hydrogel contains approximately 96% water, which allows for maintaining a moist environment at the wound surface [4,10,16,22–24]. However, hydrogels naturally display a weak capacity for exudate absorption, resulting in fluid accumulation and skin maceration [16,23,24]. Therefore, dehydrated hydrogels with a higher capacity to absorb excessive exudates from the wound site have been considered an alternative for wounds with high exudate levels [10,22]. Hydrogel-based dressings are available in the form of patches (*e.g.*, Aquaflo™ Hydrogel) or as thick and viscous gels (amorphous) (*e.g.*, Nu-Gel™, Intrasite®, and Solosite®) [26]. Amorphous hydrogels exhibit unique features that ensure optimal hydration of dry wounds because of their ability to act as water donors [10,22]. Nonetheless, hydrogels exhibit weak mechanical properties, requiring the application of a secondary dressing [4,5,16]. More recently, hydrocolloids produced from particles uniformly dispersed in an elastic adhesive matrix have been applied. The adhesive matrix maintains the dressing on the wound, and the hydrocolloid particles absorb and retain fluids, creating a hydrogel suitable for reducing the risk

of skin maceration [4,16,22,27]. In addition, the produced hydrogels can ensure a favorable moist environment at the wound site. Thus, these dressings do not adhere to the wounds and are painless for patients [16,22,24]. However, hydrocolloids gels can develop an unpleasant odor and are easily mistaken for infection [4,5,16,22,24]. Commercially available hydrocolloid dressings include Alione®, Granuflex®, CombiDERM® ACD®, DuoDERM®, Ultec™, Comfeel®, Hydrocoll®, Nu-Derm™, Granugel®, and Versiva® [4,22,26]. In turn, alginate (*e.g*. Kaltostat®, Sorbsan®, and Algisite M), chitosan (CS) (*e.g*. HemCon® Bandage, Syvek-Patch®, Chitopack C®, Chitopack S®, Beschitin®, Chitodine®, and Trauma DEX®), and collagen (*e.g*. Alloderm®, Integra®, PuraPly®, FIBRACOL™ Plus, Apligraft®, and Orcel®) dressings have become popular because of their intrinsic properties [4,16,22–24,27,28].

Nevertheless, despite the great diversity of dressings currently available on the market, nanofiber wound dressings have shown promising properties for promoting the healing process.

Among the different methods used to fabricate micro-to-nano-scale fibrous wound dressing materials (*e.g*. phase separation, self-assembly, drawing, and template synthesis), electrospinning has become one of the most desirable and attractive techniques owing to its simplicity, cost-effectiveness, and functional versatility to produce nanofibrous meshes that can re-establish native skin features, Figure 2 [1–3,12–16,24,29]. Electrospun nanofibrous membranes can mimic the three-dimensional architecture of the natural skin ECM, which is essential to ensure additional support for cell adhesion and proliferation as well as promote skin regeneration with minimal scarring [1–3,7,12–16,24,29–32]. Moreover, the inherently high surface-to-volume ratio and porosity of electrospun nanofibers are conducive to hemostasis and allow for adequate gas permeability, efficient water and nutrient supply, and effective fluid absorption while maintaining the moisture balance at the wound site [1–3,7,12–16,24,29–32]. In addition, nonwoven structures are flexible, which ensures their conformability to the wound site and provides an effective physical barrier to protect the wound surface from further injury and bacterial invasion [1,14,33]. Furthermore, several bioactive and/or therapeutic compounds, such as growth factors, vitamins, analgesics, mineral supplements, antimicrobial, and anti-inflammatory agents, can be efficiently incorporated using different approaches into synthetic and natural polymers and blends of them, and thus electrospinning has been reported as a promising method for controlling drug release and enhancing desirable wound healing properties [2,7,12–14,16,29].

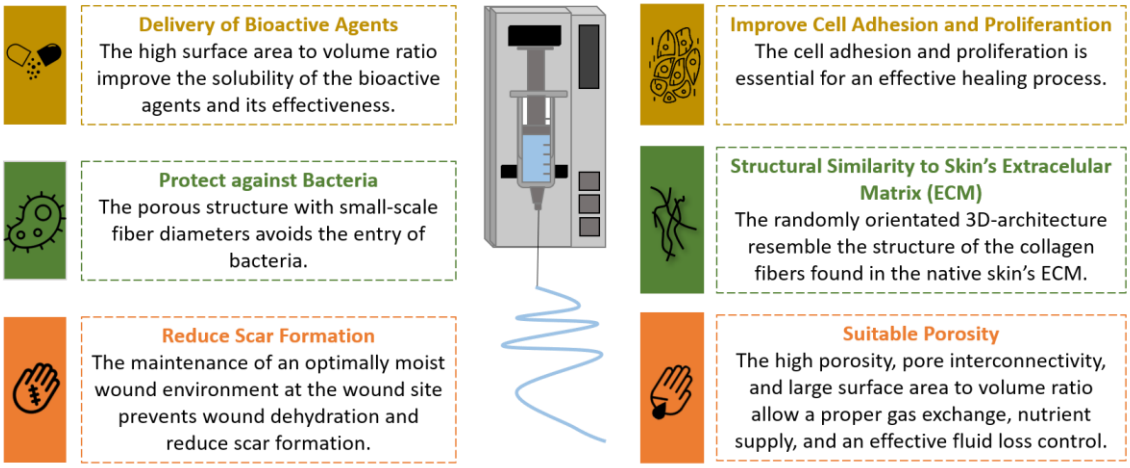

Figure 2 – Representation of the most promising properties of electrospun fibers display for application as antimicrobial wound dressings.

3. Electrospinning techniques for antimicrobial agent delivery

A wide range of bioactive compounds with antimicrobial activities have been incorporated into the structure of wound dressing materials for preventing bacterial penetration into the wound and simultaneously promote the healing process [2,5,15,16,29,34].

Among the different strategies explored for the incorporation of these compounds into electrospun nanofibrous membranes, pre-spinning methods, such as the blending of polymer solution before spinning and core-shell fibers (from emulsion and coaxial electrospinning), as well as post-spinning methods, such as chemical immobilization, physical adsorption, and layer-by-layer (LbL) assembly, have been widely employed to manipulate the release of incorporated compounds from the nanofibers. However, the selection and/or a combination of these methods are affected by the roles of bioactive compounds in the healing process as well as by the desirable release rates and profiles [2,13–16,20,29,30]. The most common methodologies for the incorporation of these compounds into nanofibers are presented in Figure 3 and described below.

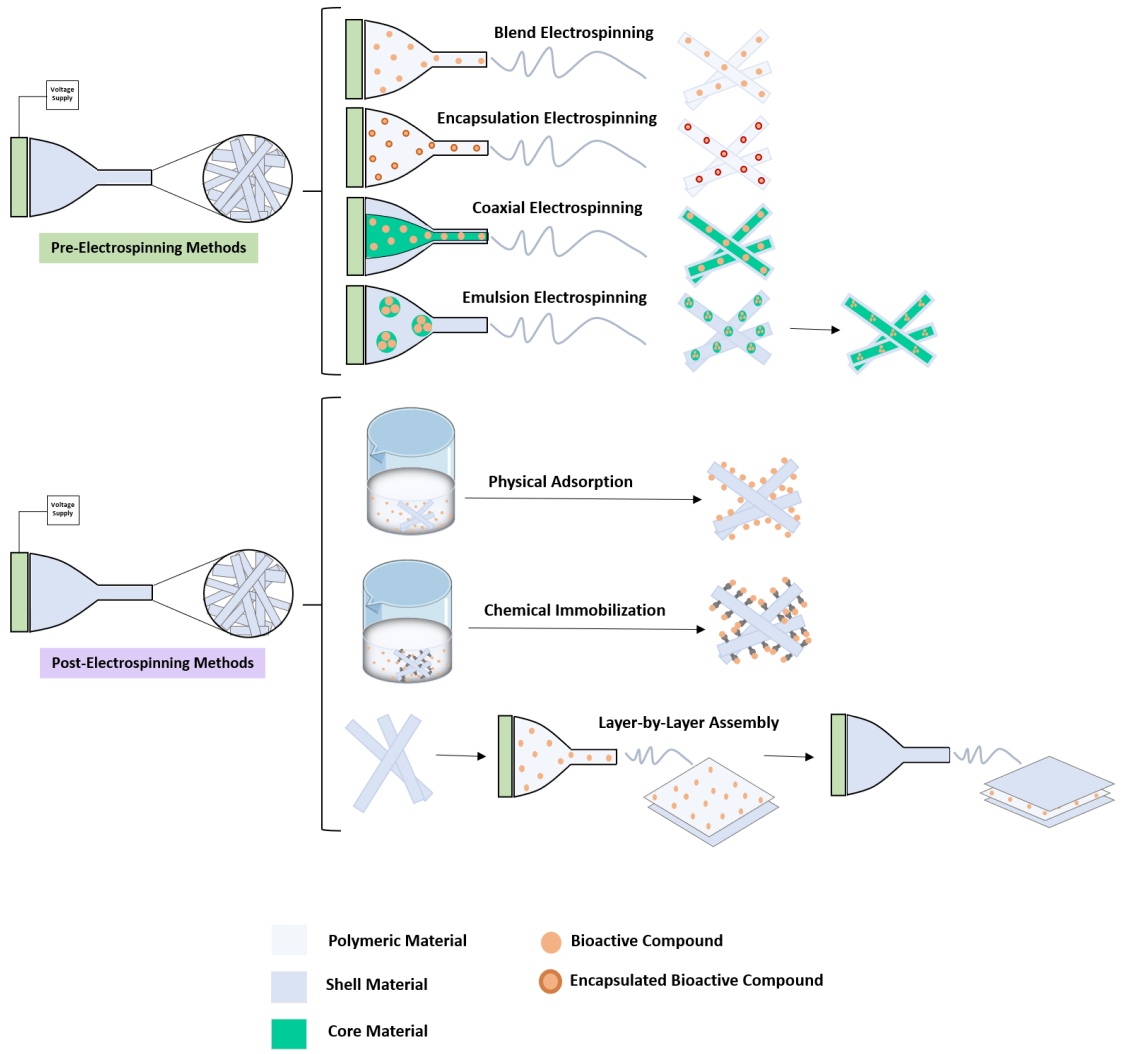

Figure 3 – Schematic representation of the most common electrospinning techniques used for the incorporation of bioactive compounds into nanofibers: pre-electrospinning (blend, encapsulation, coaxial, and emulsion electrospinning) and post-electrospinning (physical adsorption, chemical immobilization, and layer-by-layer (LbL) assembly).

▪ **Polymer blend electrospinning -** The simplest method to incorporate bioactive compounds into nanofibers is by blending/dispersing them into the polymer solution before electrospinning [12,16,20,29,35]. However, when this method is applied, the bioactive compounds are immediately released from the nanofiber surface. Moreover, the structural integrity and bioactivity of these compounds can be compromised and potentially harmful to the healing process, particularly when a lasting therapeutic effect on the wound site is desired. Thus, to ensure sustained release and, in particular, to avoid an initial burst effect, it is desirable to absorb and/or encapsulate the bioactive compounds into nanostructures before dispersion in the polymer solution [12,35,36].

▪ **Core-shell structures -** Another strategy to incorporate bioactive compounds is based on the production of core-shell nanofibers through coaxial electrospinning [12,16,37]. Coaxial electrospinning uses two concentrically arranged capillaries instead of a single capillary, as in

conventional electrospinning. These concentric capillaries are connected to two separate reservoirs. The outer capillary is attached to the reservoir containing the shell solution and allows the production of nanofibers that provided protection to the core. Meanwhile, the inner capillary is connected to the reservoir containing the core solution, and this is where the bioactive compounds are generally incorporated [16,29,35,37,38]. Hence, core-shell nanofibers provide an added advantage as carriers for the delivery of bioactive compounds, protecting the native structure of these compounds and their bioactivity from harsh environments during nanofibers fabrication. In addition, the incorporation of bioactive compounds into the core of nanofibers can significantly decrease the initial burst effect and maintain a sustained release, and the nanofiber shell can act as a barrier to the diffusion of incorporated compounds [16,20,35,37,38]. However, although two different and incompatible polymer solutions can be simultaneously applied through coaxial electrospinning, the technique requires a special apparatus and careful selection of operating conditions to ensure desirable results [39,40]. To overcome the limitations associated with coaxial electrospinning, emulsion electrospinning has attracted growing interest for the production of core-shell nanofibers in recent years. This method is similar to conventional electrospinning except that the solution is replaced with a water-in-oil (W/O) or oil-in-water (O/W) emulsion [12,16,29,40–42]. During the emulsion electrospinning process, the continuous-phase solvent evaporates more swiftly than the disperse droplets, resulting in a viscosity gradient between the two phases. Subsequently, this gradient guides the emulsion droplets from the surface to the center, and the droplets are stretched into elliptical shapes along the axial region of the fibers under a high voltage [43,44]. Most emulsions used in electrospinning are of the W/O type. These emulsions comprise an aqueous phase composed mainly of water-soluble polymers or bioactive compounds dissolved in an aqueous solution, whereas the oil phase is composed of polymers dissolved in an organic solvent [16,39]. Hence, W/O emulsions are particularly useful for controlled or sustained release of water-soluble bioactive compounds. This is because the compounds encapsulated in the core of the nanofibers structure must pass through the core-shell matrix before being released [40,42]. Furthermore, the core-shell structure of the nanofibers produced through emulsion electrospinning may improve their poor solubility, enhance the affinity of hydrophilic compounds to hydrophobic polymers, and protect the bioactive compounds from the harmful effects of the external environment [40,42].

- **Post-electrospinning treatments -** Bioactive compounds can also be physically adsorbed on the surface of nanofibers following electrospinning, given that most of these compounds exhibit functional groups that facilitate their attachment to nanofibers [16,29,35,45]. Generally, when these compounds are adsorbed on the nanofibers surface via physical forces, weak nonspecific intermolecular interactions, such as electrostatic interactions, hydrogen bonding, hydrophobic interactions, and Van der Waals forces, are established between the compounds and electrospun nanofibers [29,45]. Alternatively, these compounds can be covalently immobilized onto the surface of nanofibers using the wet chemical method, plasma treatment, and graft polymerisation to obtain more consistent and potent bioactivity. In this approach, the surface of the nanofibers can be modified using various treatments, and functional groups can be added to

their surfaces. Moreover, recently LbL assembly has been used as a simple, useful, and versatile surface modification method, which allows the formation of surface coatings via successive deposition of polymer layers of opposite charges [29,45]. This alternating depositing of polymers using the LbL technique allows effortless incorporation of bioactive compounds along with the multilayer assembly and accurate control of desired thickness, which can affect the release profile of these compounds. Electrostatic interactions are the major driving force of assembly [29,45].

In recent years, different electrospinning methods have been developed to provide specific release profiles of bioactive compounds. Among them, two needles side-by-side have been applied to produce nanofibers with Janus structures and materials with two distinct layers [12,46]. Meanwhile, multiple-jet electrospinning has been used to simultaneously produce multiple nanofibers, and a modified coaxial electrospinning technique using multiple concentric needles has been explored to ensure sustained release of the incorporated bioactive compounds, Figure 4 [12,46,47].

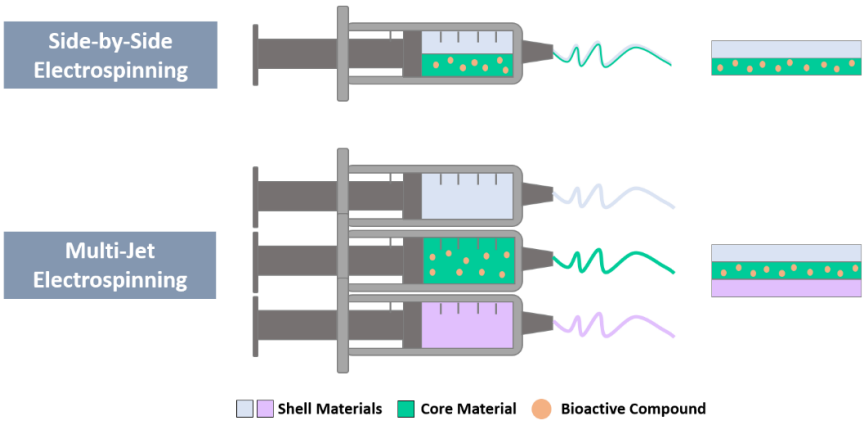

Figure 4 – Illustration of the side-by-side and multi-jet electrospinning for the incorporation of bioactive compounds into electrospun nanofibers.

4. Incorporation of natural plant extracts with antimicrobial properties into electrospun materials

As previously described, several bioactive compounds have been incorporated into electrospun wound dressings to improve their biological performance [2,6,16,29]. Among them, antimicrobial agents, such as antibiotics (*e.g.* gentamicin, tetracycline hydrochloride, ciprofloxacin, and silver sulfadiazine), nanoparticles (NPs) (*e.g.* metallic NPs (silver (Ag), zinc oxide (ZnO), titanium dioxide (TiO_2), iron oxide (Fe_3O_4), and copper (Cu))) and natural products (*e.g.*, medicinal plants and EOs) have been used to prevent infections at the wound site and further promote the healing process [2,5,6,14,17,29].

Although many studies have reported the beneficial effects of these bioactive agents, natural product-based compounds, particularly plant-derived compounds, have emerged as promising approaches to develop new therapeutic alternatives that can provide an effective antimicrobial activity and prevent deleterious effects of infections on the healing process [1,5,14–17,33,34,48].

4.1. Plant extracts

The growing trends of using alternative and complementary medicines to explore innovative and effective wound healing therapies as well as the recognition and awareness of the advantages and feasibility of using medicinal plants as powerful natural supplements for wound management and treatment have garnered much attention from the researcher community working in the fabrication of wound dressings with antimicrobial properties [14,16,17,48].

Since long, medicinal plants have been explored and recognized as a major source of therapeutic agents for improving wound healing. Medicinal plants contain a wide variety of biologically active and effective components, such as flavonoids, alkaloids, terpenoids, phenolics, fatty acids, and EOs, which confer antimicrobial, anti-inflammatory, antioxidant, analgesic, anesthetic, antiviral, and anticancer effects [16,17,48]. In addition, medicinal plants promote the wound healing process by enhancing fibroblast proliferation, neovascularization, and collagen deposition [16,17,48]. Moreover, these natural healing agents have been proven an interesting approach to overcome certain limitations of various current bioactive compounds incorporated into wound dressing materials owing to their low cost, environmental sustainability, limited adverse effects, easy availability, extraction, and efficacy [1,14–16,48]. In recent years, crude medicinal plant extracts and their derivatives, such as EOs, have gained great interest, achieving higher therapeutic potential for preventing infections and treating infected wounds [14,16,17,48]. Several plant-derived natural compounds with bactericidal activity have been incorporated into wound dressing materials, and a few of these, including the Gentell® Hydrogel *Aloe vera* wound dressing and *Curcuma longa* L. (turmeric)-based bandage (patents) used by Johnson &Johnson in Band-Aid®, have been approved by the United States Food and Drug Administration (US FDA) and other drug regulatory agencies [33,49,50]. Likewise, a number of studies have been performed integrating the unique features of the electrospun nanofibers with single- and multi-layered structures and the benefits of the natural bioactive compounds for effective wound healing, Figure 5 [1,14,16,17,48].

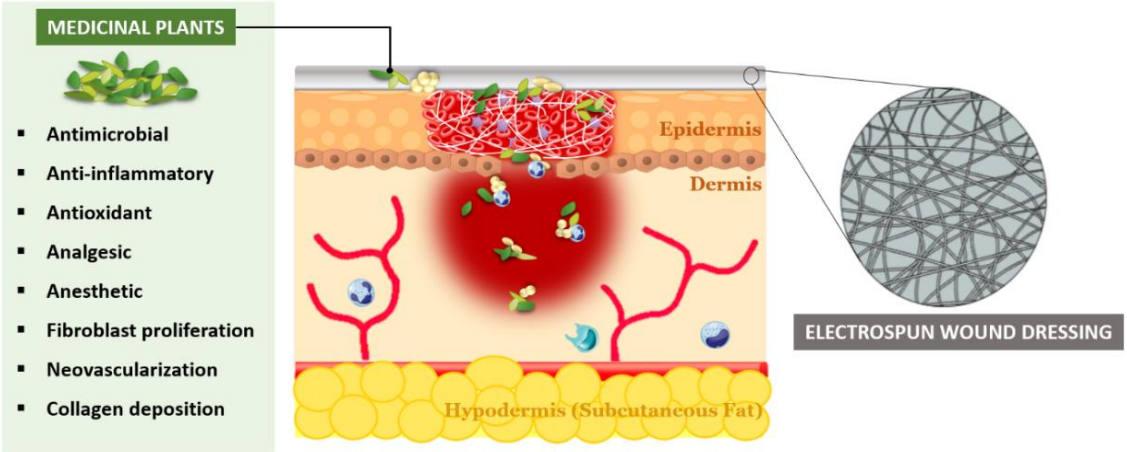

Figure 5 – Representation of the electrospun wound dressings containing medicinal plant extracts and their key roles in the healing process.

4.1.1. Crude medicinal plant extracts

Crude medicinal plant extracts are ecologically sustainable mixtures of compounds with multiple therapeutic properties, which support their potential role in wound healing [14,16,17,48]. These extracts can be obtained from fresh or milled, dried plants and can be easily extracted using various methods [14,17]. In addition, crude plant extracts produce stronger effects than specific compounds isolated from the same plants owing to the promising synergistic interactions between their bioactive components [51]. These favorable interactions provide better protection against enzymatic degradation and promote transport through cell barriers. Typically, crude plant extracts are considered a promising approach to overcome multi-drug resistance in pathogenic bacteria [16,17,48,51].

The antimicrobial properties of crude medicinal plant extracts are mainly attributed to their active metabolites, which can alter the permeability of bacterial membranes, leading to cell wall disruption and lysis. Moreover, plant extracts can interfere with fundamental cellular processes and metabolic pathways [52,53].

Crude extracts with high antibacterial activity of several medicinal plants have been applied as electrospun dressing materials from different strategies. Among them, *Aloe vera*, *Azadirachta indica, Calendula officinalis, Centella asiatica, Chamomilla recutita, Curcuma longa, Garcinia mangostana*, *Lawsonia* inermis, and *Tridax procumbens* are commonly used for the production of the bioactive plant-based wound dressings [1,5,16,17,33,48,54].

In 2015, Yao et al. produced Gelatin/Polyvinyl Alcohol (PVA) nanofibers containing *Centella asiatica* extract for application as a wound dressing material to treat skin wounds [55]. The electrospun Gelatin/PVA nanofibers incorporated with *Centella asiatica* extract significantly increased cell growth and proliferation as well as enhanced antibacterial activity compared with neat Gelatin/PVA membranes. Moreover, *in vivo* data revealed that, after 7 days of treatment, animals treated with Gelatin/PVA membranes containing *Centella asiatica* extract displayed a slightly higher wound recovery rate and collagen synthesis rate than those treated with neat Gelatin/PVA membranes, gauze (control), and a commercial wound dressing (Comfeel®, Peterborough, United Kindom). Further histopathological assessments supported the results of the animal experimentation [55].

In addition, Pourhojat et al. assessed the performance of the electrospun Polylactic-co-glycolic acid (PLGA) nanofibers containing *Hypericum perforatum* as antimicrobial coverage for wounds [56]. The developed membranes better controlled the water vapor transmission rate (WVTR) and presented a greater exudate absorption capacity and a burst drug release kinetics, which followed the Higuchi kinetic model. Moreover, *in vitro* evaluation of the biologic properties of the membranes revealed their capacity to inhibit the growth of bacteria at the wound site as well as their biocompatibility [56]. Shokrollahi et al. developed patches based on *Chamomilla recutita* L. (chamomile)-loaded carboxyethyl chitosan (CECS)/PVA and Polycaprolactone (PCL) [57]. Compared with the commercial Ag coating, the developed multilayered nanofibrous patches exhibited increased antibacterial efficiency, antioxidant activity, and biocompatibility, as well as enhanced cell viability with increasing culture time [57].

Recently, Mouro et al. incorporated *Chelidonium majus* L., a medicinal plant known to display a broad spectrum of pharmacological activities, into electrospun nanofibers composed of PCL, PVA, and Pectin (PEC) using emulsion electrospinning. The developed membranes exhibited suitable features for application as wound dressings. As such, they presented enhanced bactericidal activity against *S. aureus* and *P. aeruginosa* and did not cause cytotoxicity in normal human dermal fibroblasts (NHDF) [58].

Various medicinal plant extracts with antibacterial activity that have been incorporated in electrospun wound dressings to prevent bacterial infections and enhance healing are listed in Table 1.

Table 1 – Examples of plant extracts that have been incorporated into electrospun wound dressing materials.

Plant extracts	Materials / Polymers	Main findings	Ref.
Acacia tortilis	Chitosan (CS)/ Polyethylene Oxide (PEO)/Cellulose nanocrystals (CNC)	The incorporation of *Acacia tortilis* extract improved the antibacterial and antifungal properties of nanofiber membranes. Moreover, evaluation of the biologic performance of membranes revealed their biocompatibility.	[59]
Acalypha indica	Guar gum/Polyvinyl Alcohol (PVA)	The incorporation of *Acalypha indica* into electrospun nanofibers improved bactericidal activity and promoted cell adhesion and proliferation.	[60]
Achyranthes aspera and *Datura metel*	Polycaprolactone (PCL)	PCL/*Achyranthes aspera* and PCL/*Datura metel* nanofibrous mats showed potent antibacterial activity and biocompatibility, as well as promoted healing.	[61]
Agrimonia eupatoria L.	PVA/CS	The PVA_CS blend loaded with *Agrimonia eupatoria* L. was electrospun using Nanospider electrospinning on top of a pre-activated cotton gauze bandage. The produced dual-layer composite material displayed suitable properties for use as a wound dressing and prevented bacterial infection of the wound.	[62]
Aloe vera	Polyvinylpyrrolidone (PVP)	The composite nanofibers of PVP with *Aloe vera* and *Aloe vera* acetate demonstrated no bacterial and viral growth and suitability for wound healing.	[63]
	PCL and CS/Polyethylene Oxide (PEO)	The asymmetric electrospun membrane with a top layer made of PCL and a bottom layer of PEO, CS, and *Aloe vera* prevented the invasion and growth of *S. aureus* and *E. coli* and promoted the healing process.	[64]
Annona muricata L.	PVA	The electrospun PVA nanofibers loaded with *Annona muricata* L. (Soursop) leaves extract inhibited the growth of S. *aureus,* indicating the potential application of the developed nanofibers as a viable antibacterial wound dressing material.	[65]
Artemisia annua L.	PCL and Gelatin	A double-layer wound dressing composed by an electrospun Gelatin/*Artemisia annua* L. active layer and a PCL nanofibrous base layer displayed no cytotoxicity against fibroblasts and promoted cell adhesion and proliferation. Moreover, the produced nanofibrous wound dressing exhibited potent antibacterial activity against *S. aureus*.	[66]
Azadirachta indica	PVA and CS	The bi-layered PVA-CS blend nanofibrous mat incorporated with *Azadirachta indica* (neem) extract revealed suitable properties for application as a biodegradable and an antibacterial wound dressing material.	[67]

Calendula officinalis	PCL/Gum Arabic	The PCL/*Calendula officinalis*/Gum arabic nanofibrous membranes exhibited excellent mechanical properties and porosity favorable for cell proliferation. Moreover, the produced membranes showed antibacterial activity as well as good cytocompatibility and biocompatibility.	[68]
	CS/PEO	The CS/PEO nanofibers containing *Calendula officinalis* extract showed strong antibacterial properties against both *E. coli* and *S. aureus* and enhanced the proliferation, growth, and attachment of fibroblast cells, indicating wound healing ability.	[69]
Camellia sinensis	CS/PEO	The CS/PEO/*Camellia sinensis* (green tea) extract nanofibers exhibited favorable antibacterial and inflammation activity and promoted healing.	[70]
Capparis spinosa L.	Poly(lactic acid) (PLA)	The incorporation of *Capparis spinosa* L. extract into PLA nanofiber membranes improved the wettability, mechanical properties, oxidation resistance, and inhibitory effect on *E. coli* and *S. aureus* of the developed material.	[71]
Centella asiatica	PCL and PVA_CS	The produced double-layered PCL/PVA_CS-Sodium tripolyphosphate (TPP) membrane containing *Centella asiatica* extract did not exhibit cytotoxicity against fibroblasts while also ensuring a controlled release of *Centella asiatica*, as well as producing excellent antibacterial effect against *S. aureus* and *P. aeruginosa*, which is advantageous to prevent skin infections.	[72]
Chamomilla recutita L.	PCL/Polystyrene (PS)	Both *in vitro* and *in vivo* assays showed that the loading of *Chamomilla recutita* L. (chamomile) into PCL/PS nanofibrous mats improved the healing process while protecting the wound from infection.	[73]
Chromolaena odorata L.	PVA	The optimized electrospun PVA/ *Chromolaena odorata* L. nanofibers were suitable for antimicrobial wound dressing applications.	[74]
Clerodendrum phlomidis	PCL	The loading of *Clerodendrum phlomidis* extract into PCL nanofibers mats enhanced mechanical properties, wettability, and antibacterial and antioxidant activities.	[75]
Curcuma longa L.	PCL/Polyethylene glycol (PEG)	The curcumin-loaded PCL/PEG nanofiber mats exhibited enhanced biological properties. These nanofibrous mats showed excellent antibacterial and anti-inflammatory activities and promoted cell proliferation. Moreover, wound closure occurred in a shorter period.	[76]

Elaeagnus angustifolia	Silk Fibroin (SF)/PVA	Different concentrations of *Elaeagnus angustifolia* extract were incorporated in SF/PVA nanofibers. The incorporation of *Elaeagnus angustifolia* extract into the nanofibrous dressings improved their antioxidant and antibacterial properties. Moreover, cell viability slightly increased with increasing *Elaeagnus angustifolia* concentration.	[77]
Garcinia mangostana	CS-Ethylenediaminetetraacetic acid (EDTA)/PVA	The electrospun CS-EDTA/PVA nanofiber mats containing *Garcinia mangostana* exhibited antioxidant and antibacterial activities. Moreover, these mats accelerated the rate of healing compared with the control (gauze-covered) material.	[78]
	PLLA	The *Garcinia mangostana*-loaded PLLA fiber mats exhibited the highest antibacterial activity against *S. aureus*. Moreover, the electrospun PLLA fibers containing *Garcinia mangostana* showed excellent antioxidant properties and did not manifest cytotoxicity against fibroblasts at lower extraction ratios.	[79]
Grewia mollis	Polyurethane (PU)	The PU nanofibers containing *Grewia mollis* extract inhibited the growth of the bacterial strains, acting as a potential antimicrobial agent.	[80]
Gymnema sylvestre	PCL	Electrospun PCL nanofibrous mats incorporated with *Gymnema sylvestre* extract prevented biofilm formation and promoted normal human dermal fibroblast (NHDF) cell attachment.	[81]
Hypericum capitatum var. capitatum	Polylactic-co-glycolic acid (PLGA)/Gelatin	The electrospun PLGA/Gelatin membranes containing *Hypericum capitatum var. capitatum* (HCC) showed antibacterial activity against *S. aureus* and *E. coli*, when HCC was added at ≥5 wt%. Moreover, these electrospun membranes did not compromise the cell viability.	[82]
Hypericum perforatum L.	PLLA and PEO_CS	*Hypericum perforatum* L. incorporation granted additional antimicrobial properties to the PEO_CS's lower layer, which is essential to provide an aseptic environment at the wound site. Moreover, the properties of double-layer PLLA/PEO_*Hypericum perforatum* L._CS nanofibrous mats offered important insights into the behavior of this material as a wound dressing.	[83]
Ipomoea pes-caprae L.	PVA	The *Ipomoea pes-caprae* L. extract-loaded electrospun hydrogels showed a superior antibacterial activity against *S. aureus* compared with a commercial dressing patch. This material may be used as a wound dressing for infected wounds.	[84]
Juniperus chinensis	PVA	The *Juniperus chinensis*-incorporated PVA nanofibers presented excellent antibacterial activity against *S. aureus* and *K. pneumonia*.	[85]

Lawsonia inermis	PEO/PVA	The electrospun PEO/PVA nanofibers containing *Lawsonia inermis* (Henna), a potent eco-friendly antimicrobial agent, exhibited antibacterial activity against *S. aureus* and *E. coli*.	[86]
	CS/PEO	The electrospun CS/PEO nanofibrous mats incorporated with different concentrations of traditional *Lawsonia inermis* leaf extract displayed antibacterial activity against *S. aureus* and *E. coli* and accelerated the wound healing process.	[87]
	Gelatin/Oxidized starch (OST)	The Gelatin/OST nanofibers containing *Lawsonia inermis* (Henna) enhanced cell adhesion and proliferation, collagen synthesis, and antibacterial activity. Further, *in vivo* assays demonstrated that the nanofibers loaded with Henna extract remarkably accelerated wound closure.	[88]
	PLLA/Gelatin	*Lawsonia inermis* loading into PLLA-Gelatin nanofibrous membranes inhibited the growth of both *E. coli* and *S. aureus*. These biocompatible membranes were suitable to control wound infections.	[89]
Melilotus officinalis	PCL/CS	The incorporation of *Melilotus officinalis* extract into the PCL/CS nanofibrous mats improved the antibacterial activity. Moreover, the PCL/CS/*Melilotus officinalis* mats did not display any cytotoxic effect but promoted cell adhesion and proliferation.	[90]
Momordica charantia	PVA	The electrospun PVA/*Momordica charantia* nanofibers displayed potential antibacterial activity against both *B. subtilis* and *E. coli* and did not produce any cytotoxic effect.	[91]
Nigella sativa	PVA	The incorporation of *Nigella sativa* extract into PVA mats enhanced their antibacterial, moisture management, and wound healing properties.	[92]
Phaeodactylum tricornutum	Gelatin	The *Phaeodactylum tricornutum*-loaded Gelatin nanofiber mats exhibited antimicrobial activity against *E. coli* and Methicillin-resistant *Staphylococcus aureus* (MRSA). Moreover, these nanofibers did not show cytotoxicity.	[93]
Tecomella undulata	PCL/PVP	*Tecomella undulata*-loaded PCL/PVP nanofiber mats inhibited the growth of *P. aeruginosa*, *S. aureus*, and *E. coli*, highlighting their potential as antimicrobial wound dressing materials.	[94]
Tridax procumbens	PVA	The electrospun PVA nanofibrous mats containing *Tridax procumbens* exhibited antibacterial activity against *S. aureus* and *E. coli*.	[95]
	PCL	The *Tridax procumbens*-PCL nanofibers exhibited potent antibacterial activity, acting as a wound healing enhancer.	[96]

Zataria multiflora	Cellulose acetate/Gelatin	A multifunctional nanofibrous Cellulose acetate/Gelatin/*Zataria multiflora*-nano-emulsion wound dressing material exhibited antibacterial activity against *E. coli* and *S. aureus*, and considerably promoted the healing process.	[97]
Achillea millefolium, Calendula officinalis, Chamomilla recutita, Echinacea purpurea, Hypericum perforatum	Carboxymethyl cellulose (CMC)/PEO	Electrospun mats containing plant extracts were produced using a needless electrospinning. The obtained electrospun materials loaded with plant extracts exhibited bactericidal properties against *S. aureus* as well as antioxidant properties.	[98]
Hypericum perforatum, *Agrimonia eupatoria,* and *Satureja hortensis*	Thermoplastic Polyurethane (TPU)	The electrospun TPU nanofibers loaded with *Satureja hortensis* displayed the highest antibacterial activity against *S. aureus* and *P. aeruginosa*.	[99]
Indigofera aspalathoides, *Azadirachta indica*, *Memecylon edule*, and *Myristica andamanica*	PCL	The electrospun PCL nanofibers containing *Memecylon edule* (*M. edule*) exhibited the highest cell proliferation and showed the least cytotoxicity among all the other electrospun nanofibrous membranes. Moreover, the biocompatibility and antimicrobial activity of the PCL/*M. edule* nanofibers promoted healing and skin regeneration.	[100]

4.2. Essential oils (EOs)

EOs are secondary metabolites typically extracted from aromatic plants, and they exhibit a wide range of therapeutic properties, including antimicrobial, antioxidant, anti-inflammatory, anti-allergic, anticancer, and antiviral properties, as well as repellent effects [5,9,17,34,48]. However, these volatile natural mixtures require multiple step preparation methods and special laboratory facilities as well as a large amount of raw material. In addition, their effectiveness is limited by the fact that EOs are easily degraded and more susceptible to losses by volatilization or thermal decomposition [14,101,102].

The antimicrobial activity of EOs is attributed to their phenolic compounds, which are typically hydrophobic. In this context, the mechanisms of action are based on their partitioning into the phospholipid bilayer present in the bacterial cell membrane and the lipids on the cell wall. The establishment of such different interactions increases membrane permeability to ions and other cellular contents, causing cytoplasmic leakage and pH decrease and inhibiting vital cellular processes, such as ATP biosynthesis, DNA transcription, and protein synthesis, with ultimately lead to the disruption of cell structure and cell death. Moreover, the EOs can interfere with the function of the cytoplasmic membrane by blocking the transfer of nutrients through the cell membrane and coagulation of bacteria cell constituents [4,5,9,17,34].

Amongst the known EOs, cinnamon, lavender, olive, peppermint, tea tree, and thymol (THY) oils have been used in electrospun materials for antibacterial purposes, Table 2 [5,16,17,34,103].

For instance, Hajiali et al. produced Alginate–lavender nanofibers for burn management. In both *in vitro* and *in vivo* assays, the nanofibrous dressings of Sodium Alginate (SA) and lavender oil displayed promising antibacterial and anti-inflammatory activities, highlighting their potential for improving the burn healing process [104]. Furthermore, Gámez-Herrera et al. electrosprayed THY-loaded PLGA microparticles onto electrospun PCL-based nanofibers [105]. The dressings successfully inhibited *S. aureus* growth and did not compromise the cell viability. In addition, when infected wounds inoculated with *S. aureus* were treated with the dressings, these materials could minimize the growth of bacteria into the wound site [105]. In a recent study, Zare et al. prepared core-shell nanofibers composed of Gelatin/PVA/*Trachyspermum ammi* (Ajwain) EO (core) and *Aloe vera*/Arabinose/Polyvinylpyrrolidone (PVP) (shell) using coaxial electrospinning [106]. The produced membranes exhibited excellent antioxidant and antimicrobial properties through prolonged release of the Ajwain EO, and accelerated bacteria-infected wound healing [106].

Table 2 – Examples of electrospun wound dressing materials incorporated with essential oils (EOs).

Essential Oils (EOs)	Materials / Polymers	Main findings	Ref.
Eugenol	Polycaprolactone (PCL)/ Polyvinyl Alcohol (PVA)/Chitosan (CS)	Eugenol, an essential oil known for its therapeutic properties, was incorporated into electrospun PCL/PVA/CS fiber mats. The obtained fiber mats were suitable for use as wound dressing material and exhibited inhibitory effects against *S. aureus* and *P. aeruginosa*.	[107]
Hypericum perforatum oil	PCL and Polyethylene glycol (PEG)/PCL	An electrospun bi-layered membrane was produced with an upper layer of PCL to protect the wound from external factors and confer mechanical support and a lower PEG/PCL layer incorporated with *Hypericum perforatum* oil to prevent the growth of *S. aureus* and *E. coli*.	[108]
Lavender oil	Polyurethane (PU)	The electrospun PU nanofiber mats containing lavender oil and Ag NPs displayed synergistic antibacterial activity against *E. coli* and *S. aureus* and promoted cell growth and proliferation.	[109]
Origanum minutiflorum oil	CS	The CS core–shell nanofibers loaded with *Origanum minutiflorum* oil improved antibacterial activity against *S. aureus* and *P. aeruginosa* and exhibited controlled and tunable drug release.	[110]
Olive oil	Polyethylene oxide (PEO)/CS/PCL	The electrospun PEO/CS/PCL nanofibrous scaffolds containing olive oil exhibited potent antibacterial activity, promoted cell adhesion, spread, and proliferation, and showed no cytotoxicity.	[111]
Peppermint oil	PCL	The peppermint oil-loaded PCL electrospun fiber mats displayed antibacterial activity against *S. aureus* and *E. coli* and did not show cytotoxicity against normal human dermal fibroblast (NHDF) cells.	[112]
Tea tree oil	CS/PCL	The electrospun CS/PCL fiber mats containing tea tree oil presented wide-spectrum antibacterial properties and accelerated healing.	[113]
Zataria multiflora oil	CS/PVA/Gelatin	CS/PVA/Gelatin nanofiber mats successfully incorporated with different concentrations of *Zataria multiflora* oil (0, 2, 5, and 10%) exhibited good antibacterial activity against *Candida albicans* (*C. albicans*), *P. aeruginosa*, and *S. aureus*, without any cytotoxicity.	[114]
Cinnamon oil, clove oil, and lavender oil	Sodium Alginate (SA)/PVA	Cotton-gauzed SA/PVA nanofibers incorporated with three different concentrations (0.5, 1, and 1.5%) of cinnamon, clove, and lavender oils exhibited excellent antibacterial properties against *S. aureus*.	[115]

Palmarosa oil and phytoncide oil	PVA	The electrospun PVA nanofibrous membranes containing palmarosa oil and phytoncide were successful produced from emulsion electrospinning. The membranes containing palmarosa oil exhibited a stronger antimicrobial effect as well as better air/moisture vapor transport and water uptake properties.	[116]
Satureja mutica or *Oliveria decumbens* oils	CS/PVA (core) and Polyvinylpyrrolidone (PVP)/Maltodextrin (MD) (shell)	The core-shell nanofibres loaded with essential oils (EOs) showed potent antioxidant and antimicrobial activities, which are essential for promoting the healing process.	[117]
Tea tree oil, Manuka oil	Poly(lactic acid) (PLA)	The incorporation of EOs derived from *Melaleuca alternifolia* (Tea Tree oil) and *Leptospermum scoparium (*Manuka oil) into PLA nanofibers enhanced both mechanical and antibacterial properties. Manuka oil was particularly effective in preventing bacterial colonization and biofilm formation.	[118]

Conclusions

Despite the efforts devoted, the susceptibility of the wounds to bacteria growth and subsequent risk of infection remains a concern, particularly among people with weakened immune systems. Up to now, numerous studies have been conducted to develop different types of dressing materials that can act as a physical barrier to protect the wound from microbial invasion and simultaneously boost the healing process. Among the available wound dressings, nanofibers produced through electrospinning - simple, cost-effective, versatile, easy scale-up technique - are one of the most efficient materials that can reproduce the native three-dimensional structure of the skin ECM, and further enhance healing. Thus, electrospun nanofibers represent a biocompatible and biodegradable option with unique properties that fulfil the requirements of an ideal wound dressing material. In addition, the easy incorporation of several bioactive compounds, particularly eco-friendly, inexpensive, non-toxic, and efficient alternatives against drug-resistant bacteria, such as natural agents (*e.g.* plant extracts and EOs) into electrospun nanofibers using diverse strategies (*e.g.* blend, coaxial, emulsion, LbL, and multi-jet electrospinning) highlights their potential to both prevent wound bacterial colonization at the wound site and promote the re-establishment of the structural and functional integrity of the damaged skin.

Nevertheless, despite the efforts performed until now, several challenges in the application of electrospun nanofibers for wound dressing remain to be addressed. For example, some of the available materials cannot precisely reproduce the structure and functions of the native skin. Therefore, the orientation of the nanofibers should be optimized and their arrangement and porosity controlled to improve their performance. Likewise, different techniques should be integrated and diverse natural antimicrobial agents should be loaded into electrospun nanofibers to control their release profiles for specific applications.

Additionally, in the near future, the incorporation of sensors in electrospun nanofibers materials containing natural bioactive agents must be explored to successfully control their release from nanofibers as well as detect bacteria at the wound site, avoid bacterial growth in wounds, and ensure a non-infectious healing environment.

Finally, efforts are warranted to transfer the electrospun wound dressing materials containing natural products from the laboratory and clinical scale to the industrial and even commercial scale. For this purpose, additional assays and validation processes, are essential to ensure the quality, safety, and functional performance of these dressing materials.

Funding Sources

The authors are grateful for the funding granted by the Portuguese Foundation for Science and Technology (FCT), I.P./MCTES through national funds (PIDDAC), in the scope of the FibEnTech Research Unit project (UIDB/00195/2020). Cláudia Mouro also acknowledges a PhD fellowship from the Foundation for Science and Technology (FCT) (PD/BD/113550/2015).

Notes

The authors declare no conflicts of interest, financial or otherwise.

References

1. Adamu, B.F.; Gao, J.; Jhatial, A.K.; Kumelachew, D.M. A Review of Medicinal Plant-Based Bioactive Electrospun Nano Fibrous Wound Dressings. *Mater. Des.* **2021**, *209*, 109942.
2. Azimi, B.; Maleki, H.; Zavagna, L.; de la Ossa, J.G.; Linari, S.; Lazzeri, A.; Danti, S. Bio-Based Electrospun Fibers for Wound Healing. *J. Func. Biomater.* **2020**, *11* (3), 67.
3. Juncos Bombin, A.D.; Dunne, N.J.; McCarthy, H.O. Electrospinning of Natural Polymers for the Production of Nanofibres for Wound Healing Applications. *Mater. Sci. Eng. C.* **2020**, *114*, 110994.
4. Negut, I.; Grumezescu, V.; Grumezescu, A.M. Treatment Strategies for Infected Wounds. *Molecules* **2018**, *23* (9), 2392.
5. Simões, D.; Miguel, S. P.; Ribeiro, M.P.; Coutinho, P.; Mendonça, A.G.; Correia, I.J. Recent Advances on Antimicrobial Wound Dressing: A Review. *Eur. J. Pharm. Biopharm.* **2018**, *127*, 130–141.
6. Sousa Coelho, D.; Veleirinho, B.; Alberti, T.; Maestri, A.; Yunes, R.; Fernando Dias, P.; Maraschin, M. Electrospinning Technology: Designing Nanofibers toward Wound Healing Application. In *Nanomaterials - Toxicity, Human Health and Environment*; IntechOpen, 2018; pp 1–19.
7. Wang, F.; Hu, S.; Jia, Q.; Zhang, L. Advances in Electrospinning of Natural Biomaterials for Wound Dressing. *J. Nanomater.* **2020**, *2020,* 8719859.
8. Chouhan, D.; Dey, N.; Bhardwaj, N.; Mandal, B.B. Emerging and Innovative Approaches for Wound Healing and Skin Regeneration: Current Status and Advances. *Biomaterials* **2019**, *216*, 119267.
9. Mihai, M.M.; Dima, M.B.; Dima, B.; Holban, A.M. Nanomaterials for Wound Healing and Infection Control. *Materials* **2019**, *12* (13), 2176.
10. Sarheed, O.; Ahmed, A.; Shouqair, D.; Boateng, J. Antimicrobial Dressings for Improving Wound Healing. In *Wound Healing - New insights into Ancient Challenges*; InTech, 2016; pp 373–398.
11. Gizaw, M.; Thompson, J.; Faglie, A.; Lee, S. Y.; Neuenschwander, P.; Chou, S.F. Electrospun Fibers as a Dressing Material for Drug and Biological Agent Delivery in Wound Healing Applications. *Bioengineering* **2018**, *5* (1), 1–28.
12. Liu, X.; Xu, H.; Zhang, M.; Yu, D.G. Electrospun Medicated Nanofibers for Wound Healing: Review. *Membranes* **2021**, *11* (10), 770
13. Jeckson, T.A.; Neo, Y.P.; Sisinthy, S.P.; Gorain, B. Delivery of Therapeutics from Layer-by-Layer Electrospun Nanofiber Matrix for Wound Healing: An Update. *J. Pharm. Sci.* **2021**, *110* (2), 635–653.

14. Fatehi, P.; Abbasi, M. Medicinal Plants Used in Wound Dressings Made of Electrospun Nanofibers. *J. Tissue Eng. Regen. Med.* **2020**, *14* (11), 1527–1548.

15. Croitoru, A. M.; Ficai, D.; Ficai, A.; Mihailescu, N.; Andronescu, E.; Turculet, C.F. Nanostructured Fibers Containing Natural or Synthetic Bioactive Compounds in Wound Dressing Applications. *Materials*. **2020**, *13* (10), 2407.

16. Pilehvar-Soltanahmadi, Y.; Dadashpour, M.; Mohajeri, A.; Fattahi, A.; Sheervalilou, R.; Zarghami, N. An Overview on Application of Natural Substances Incorporated with Electrospun Nanofibrous Scaffolds to Development of Innovative Wound Dressings. *Mini-Rev. Med. Chem.* **2017**, *18* (5), 414–427.

17. Zhang, W.; Ronca, S.; Mele, E. Electrospun Nanofibres Containing Antimicrobial Plant Extracts. *Nanomaterials* **2017**, *7* (2), 1–17.

18. Mulat, M.; Pandita, A.; Khan, F. Medicinal Plant Compounds for Combating the Multi-Drug Resistant Pathogenic Bacteria: A Review. *Current Pharmaceutical Biotechnology* **2019**, *20* (3), 183–196.

19. O'Neill, J. Tackling Drug-Resistant Infections Globally: Final Report and Recommendations, 2016. https://amr-review.org/sites/default/files/160525_Final%20paper_with%20cover.pdf (accessed February 28, 2022).

20. Ambekar, R.S.; Kandasubramanian, B. Advancements in Nanofibers for Wound Dressing: A Review. *Eur. Polym. J.* **2019**, *117*, 304–336.

21. Ding, J.; Zhang, J.; Li, J.; Li, D.; Xiao, C.; Xiao, H.; Yang, H.; Zhuang, X.; Chen, X. Electrospun Polymer Biomaterials. *Prog. Polym. Sci.* **2019**, *90*, 1–34.

22. Qin, Y. Medical Textile Materials. *Elsevier Inc.*, 2015.

23. Rajendran, S. Advanced Textiles for Wound Care. *Woodhead Publishing Limited*, 2009.

24. Abrigo, M.; McArthur, S.L.; Kingshott, P. Electrospun Nanofibers as Dressings for Chronic Wound Care: Advances, Challenges, and Future Prospects. *Macromol. Biosci.* **2014**, *14* (6), 772–792.

25. Echague, C.G.; Hair, P.S.; Cunnion, K.M. A Comparison of Antibacterial Activity against Methicillin-Resistant *Staphylococcus Aureus* and Gram-Negative Organisms for Antimicrobial Compounds in a Unique Composite Wound Dressing. *Adv. Skin Wound Care* **2010**, *23* (9), 406–413.

26. Kadunc, B., Palermo, E., Addor, F., Metsavaht, L., Rabello, L., Mattos, R., Martins, S. Tratado de Cirurgia Dermatológica, Cosmiatria e Laser: Da Sociedade Brasileira de Dermatologia. *Elsevier Health Sciences*, 2013.

27. Vasconcelos, A.; Cavaco-Paulo, A. Wound Dressings for a Proteolytic-Rich Environment. *Appl. Microbiol. Biotechnol.* **2011**, *90* (2), 445–460.

28. Jayakumar, R.; Prabaharan, M.; Sudheesh Kumar, P.T.; Nair, S.V.; Tamura, H. Biomaterials Based on Chitin and Chitosan in Wound Dressing Applications. *Biotechnol. Adv.* **2011**, *29* (3), 322–337.

29. Miguel, S.P.; Figueira, D.R.; Simões, D.; Ribeiro, M.P.; Coutinho, P.; Ferreira, P.; Correia, I.J. Electrospun Polymeric Nanofibres as Wound Dressings: A Review. *Colloid Surf. B-Biointerface*. **2018**, *169*, 60–71.

30. Goh, Y.F.; Shakir, I.; Hussain, R. Electrospun Fibers for Tissue Engineering, Drug Delivery, and Wound Dressing. *J. Mater. Sci.* **2013**, *48* (8), 3027–3054.

31. Sell, S.A.; Wolfe, P.S.; Garg, K.; McCool, J.M.; Rodriguez, I.A.; Bowlin, G.L. The Use of Natural Polymers in Tissue Engineering: A Focus on Electrospun Extracellular Matrix Analogues. *Polymers* **2010**, *2* (4), 522–553.

32. Zamani, M.; Prabhakaran, M.P.; Ramakrishna, S. Advances in Drug Delivery via Electrospun and Electrosprayed Nanomaterials. *Int. J. Nanomed.* **2013**, *8*, 2997–3017.

33. Bhullar, S.K.; Buttar, H.S. Perspectives on Nanofiber Dressings for the Localized Delivery of Botanical Remedies in Wound Healing. *AIMS Mater. Sci.* **2017**, *4* (2), 370–382.

34. Mohammadi, M.A.; Rostami, M.; Beikzadeh, S.; Raeisi, M.; Tabibiazar, M.; Yousefi, M. Electrospun nanofibers as advanced antibacterial platforms: A review of recent studies. *Int. J. Pharm. Sci.* **2018**, *10* (2), 463–473.

35. Gao, Y.; Bach Truong, Y.; Zhu, Y.; Louis Kyratzis, I. Electrospun Antibacterial Nanofibers: Production, Activity, and *in Vivo* Applications. *J. Appl. Polym. Sci.* **2014**, *131* (18), 40797.

36. Wade, R.J.; Burdick, J.A. Advances in Nanofibrous Scaffolds for Biomedical Applications: From Electrospinning to Self-Assembly. *Nano Today*. **2014**, *9* (6), 722–742.

37. Kriegel, C.; Arrechi, A.; Kit, K.; Mcclements, D.J.; Weiss, J. Fabrication, Functionalization, and Application of Electrospun Biopolymer Nanofibers. *Crit. Rev. Food Sci. Nutr.* **2008**, *48* (8), 775–797.

38. Haider, A.; Haider, S.; Kang, I.K. A Comprehensive Review Summarizing the Effect of Electrospinning Parameters and Potential Applications of Nanofibers in Biomedical and Biotechnology. *Arab. J. Chem.* **2018**, *11* (8), 1165–1188.

39. Hu, J.; Wei, J.; Liu, W.; Chen, Y. Preparation and Characterization of Electrospun PLGA/Gelatin Nanofibers as a Drug Delivery System by Emulsion Electrospinning. *J. Biomater. Sci.-Polym. Ed.* **2013**, *24* (8), 972–985.

40. Wang, X.; Yuan, Y.; Huang, X.; Yue, T. Controlled Release of Protein from Core-Shell Nanofibers Prepared by Emulsion Electrospinning Based on Green Chemical. *J. Appl. Polym. Sci.* **2015**, *132* (16), 1–9.

41. Hu, J.; Prabhakaran, M.P.; Ding, X.; Ramakrishna, S. Emulsion Electrospinning of Polycaprolactone: Influence of Surfactant Type towards the Scaffold Properties. *J. Biomater. Sci.-Polym. Ed.* **2015**, *26* (1), 57–75.

42. Viry, L.; Moulton, S.E.; Romeo, T.; Suhr, C.; Mawad, D.; Cook, M.; Wallace, G.G. Emulsion-Coaxial Electrospinning: Designing Novel Architectures for Sustained Release of Highly Soluble Low Molecular Weight Drugs. *J. Mater. Chem.* **2012**, *22* (22), 11347–11353.

43. Shahriar, S.M.S.; Mondal, J.; Hasan, M.N.; Revuri, V.; Lee, D.Y.; Lee, Y.K. Electrospinning Nanofibers for Therapeutics Delivery. *Nanomaterials* **2019**, *9* (4), 532.

44. Zhang, C.; Feng, F.; Zhang, H. Emulsion Electrospinning: Fundamentals, Food Applications and Prospects. *Trends Food Sci. Technol.* **2018**, *80*, 175–186.

45. Yoo, H.S.; Kim, T.G.; Park, T.G. Surface-Functionalized Electrospun Nanofibers for Tissue Engineering and Drug Delivery. *Adv. Drug Deliv. Rev.* **2009**, *61* (12), 1033–1042.

46. Teixeira, M.A.; Amorim, M.T.P.; Felgueiras, H.P. Poly(Vinyl Alcohol)-Based Nanofibrous Electrospun Scaffolds for Tissue Engineering Applications. *Polymers* **2020**, *12* (1), 7.

47. Li, Y.; Zhu, J.; Cheng, H.; Li, G.; Cho, H.; Jiang, M.; Gao, Q.; Zhang, X. Developments of Advanced Electrospinning Techniques: A Critical Review. *Adv. Mater. Technol.* **2021**, *6* (11), 2100410.

48. Hajialyani, M.; Tewari, D.; Sobarzo-Sánchez, E.; Nabavi, S.M.; Farzaei, M.H.; Abdollahi, M. Natural Product-Based Nanomedicines for Wound Healing Purposes: Therapeutic Targets and Drug Delivery Systems. *Int. J. Nanomed.* **2018**, *13*, 5023–5043.

49. Agarwal, R.; Sarwar Alam, M.; Gupta, B. Preparation of Curcumin Loaded Poly(Vinyl Alcohol)-Poly(Ethylene Oxide)-Carboxymethyl Cellulose Membranes for Wound Care Application. *J. Biomater. Tissue Eng.* **2013**, *3* (3), 273–283.

50. Gupta, B.; Agarwal, R.; Sarwar Alam, M. Aloe Vera Loaded Poly(Vinyl Alcohol)-Poly(Ethylene Oxide)-Carboxymethyl Cellulose-Polyester Nonwoven Membranes. *J. Biomater. Tissue Eng.* **2013**, *3* (5), 503–511.

51. El-Hamid, MIA. A New Promising Target for Plant Extracts: Inhibition of Bacterial Quorum Sensing. *J. Mol. Biol. Biotech.* **2016**, *1* (1).

52. Gonelimali, F.D.; Lin, J.; Miao, W.; Xuan, J.; Charles, F.; Chen, M.; Hatab, S.R. Antimicrobial Properties and Mechanism of Action of Some Plant Extracts against Food Pathogens and Spoilage Microorganisms. *Front. Microbiol.* **2018**, *9*, 1639.

53. Omojate, G.C.; Enwa, F.O.; Jewo, A.O.; Eze, C.O. Mechanisms of Antimicrobial Actions of Phytochemicals against Enteric Pathogens – A Review. *J. pharm. chem. biol. sci.* **2014**, *2* (2), 77–85.

54. Firdous, S.M.; Sautya, D. Medicinal Plants with Wound Healing Potential. *Bangladesh J. Pharmacol.* **2018**, *13* (1), 41–52.

55. Yao, C.H.; Yeh, J.Y.; Chen, Y.S.; Li, M.H.; Huang, C.H. Wound-Healing Effect of Electrospun Gelatin Nanofibres Containing *Centella asiatica* Extract in a Rat Model. *J. Tissue Eng. Regen. Med.* **2015**, *11* (3), 905–915.

56. Pourhojat, F.; Shahab, S.; Sohrabi, M.; Mahdavi, H.; Asadpour, L. Preparation of Antibacterial Electrospun Poly Lactic-Co–Glycolic Acid Nanofibers Containing *Hypericum perforatum* with Bedsore Healing Property and Evaluation of Its Drug Release Performance. *Int. J. Nano Dimens.* **2018**, *9* (3), 286–297.

57. Shokrollahi, M.; Bahrami, S.H.; Nazarpak, M.H.; Solouk, A. Multilayer Nanofibrous Patch Comprising Chamomile Loaded Carboxyethyl Chitosan/Poly(Vinyl Alcohol) and Polycaprolactone as a Potential Wound Dressing. *Int. J. Biol. Macromol.* **2020**, *147*, 547–559.

58. Mouro, C.; Gomes, A.P.; Ahonen, M.; Fangueiro, R.; Gouveia, I.C. *Chelidonium majus* L. Incorporated Emulsion Electrospun PCL/PVA_PEC Nanofibrous Meshes for Antibacterial Wound Dressing Applications. *Nanomaterials* **2021**, *11* (7), 1785.

59. Ribeiro, A.S.; Costa, S.M.; Ferreira, D.P.; Calhelha, R.C.; Barros, L.; Stojković, D.; Soković, M.; Ferreira, I.C.F.R.; Fangueiro, R. Chitosan/Nanocellulose Electrospun Fibers with Enhanced Antibacterial and Antifungal Activity for Wound Dressing Applications. *React. Funct. Polym.* **2021**, *159*, 104808.

60. Jenifer, P.; Kalachaveedu, M.; Viswanathan, A.; Gnanamani, A.; Mubeena. Fabricated Approach for an Effective Wound Dressing Material Based on a Natural Gum Impregnated with *Acalypha Indica* Extract. *J. Bioact. Compat. Polym.* **2018**, *33* (6), 612–628.

61. Suryamathi, M.; Viswanathamurthi, P.; Seedevi, P. Herbal Plant Leaf Extracts Immobilized PCL Nanofibrous Mats as Skin-Inspired Anti-Infection Wound Healing Material. *Regen. Eng. Transl. Med.* **2021**.

62. Mouro, C.; Dunne, C.P.; Gouveia, I.C. Designing New Antibacterial Wound Dressings: Development of a Dual Layer Cotton Material Coated with Poly(Vinyl Alcohol)_Chitosan Nanofibers Incorporating *Agrimonia eupatoria* L. Extract. *Molecules* **2020**, *26* (1), 83.

63. Aghamohamadi, N.; Sanjani, N.S.; Majidi, R.F.; Nasrollahi, S.A. Preparation and Characterization of Aloe Vera Acetate and Electrospinning Fibers as Promising Antibacterial Properties Materials. *Mater. Sci. Eng. C* **2019**, *94*, 445–452.

64. Miguel, S.P.; Ribeiro, M.P.; Coutinho, P.; Correia, I.J. Electrospun Polycaprolactone/Aloe Vera_Chitosan Nanofibrous Asymmetric Membranes Aimed for Wound Healing Applications. *Polymers* **2017**, *9* (5).

65. Aruan, N.M.; Sriyanti, I.; Edikresnha, D.; Suciati, T.; Munir, M.M.; Khairurrijal, K. Polyvinyl Alcohol/Soursop Leaves Extract Composite Nanofibers Synthesized Using Electrospinning Technique and Their Potential as Antibacterial Wound Dressing. *Procedia Eng.* **2017**, *170*, 31–35.

66. Mirbehbahani, F.S.; Hejazi, F.; Najmoddin, N.; Asefnejad, A. *Artemisia annua* L. as a Promising Medicinal Plant for Powerful Wound Healing Applications. *Prog. Biomater.* **2020**, *9* (3), 139–151.

67. Ali, A.; Shahid, M.A.; Hossain, M.D.; Islam, M.N. Antibacterial Bi-Layered Polyvinyl Alcohol (PVA)-Chitosan Blend Nanofibrous Mat Loaded with *Azadirachta indica* (Neem) Extract. *Int. J. Biol. Macromol.* **2019**, *138*, 13–20.

68. Pedram Rad, Z.; Mokhtari, J.; Abbasi, M. Preparation and Characterization of *Calendula officinalis*-Loaded PCL/Gum Arabic Nanocomposite Scaffolds for Wound Healing Applications. *Iran. Polym. J.* **2019**, *28* (1), 51–63.

69. Kharat, Z.; Amiri Goushki, M.; Sarvian, N.; Asad, S.; Dehghan, M.M.; Kabiri, M. Chitosan/PEO Nanofibers Containing *Calendula officinalis* Extract: Preparation, Characterization, in Vitro and in Vivo Evaluation for Wound Healing Applications. *Int. J. Pharm.* **2021**, *609*, 121132.

70. Sadri, M.; Arab-Sorkhi, S.; Vatani, H.; Bagheri-Pebdeni, A. New Wound Dressing Polymeric Nanofiber Containing Green Tea Extract Prepared by Electrospinning Method. *Fiber. Polym.* **2015**, *16* (8), 1742–1750.

71. Zhu, P.; Zhang, X.; Wang, Y.; Li, C.; Wang, X.; Tie, J.; Wang, Y. Electrospun Polylactic Acid Nanofiber Membranes Containing *Capparis spinosa* L. Extracts for Potential Wound Dressing Applications. *J. Appl. Polym. Sci.* **2021**, *138* (32), 50800.

72. Mouro, C.; Fangueiro, R.; Gouveia, I.C. Preparation and Characterization of Electrospun Double-Layered Nanocomposites Membranes as a Carrier for *Centella asiatica* (L.). *Polymers* **2020**, *12* (11), 1–18.

73. Motealleh, B.; Zahedi, P.; Rezaeian, I.; Moghimi, M.; Abdolghaffari, A.H.; Zarandi, M.A. Morphology, Drug Release, Antibacterial, Cell Proliferation, and Histology Studies of Chamomile-Loaded Wound Dressing Mats Based on Electrospun Nanofibrous Poly(ε-Caprolactone)/Polystyrene Blends. *J. Biomed. Mater. Res. Part B* **2014**, *102* (5), 977–987.

74. Sriyanti, I.; Marlina, L.; Jauhari, J. Optimization of The Electrospinning Process for Preparation of Nanofibers From Poly (Vinyl Alcohol) (PVA) and *Chromolaena odorata* L. Extrac (COE). *J. Pendidik. Fis. Indones.* **2020**, *16* (1), 47–56.

75. Ravichandran, S.; Radhakrishnan, J.; Jayabal, P.; Venkatasubbu, G.D. Antibacterial Screening Studies of Electrospun Polycaprolactone Nano Fibrous Mat Containing *Clerodendrum phlomidis* Leaves Extract. *Appl. Surf. Sci.* **2019**, *484*, 676–687.

76. Bui, H.T.; Chung, O.H.; dela Cruz, J.; Park, J.S. Fabrication and Characterization of Electrospun Curcumin-Loaded Polycaprolactone-Polyethylene Glycol Nanofibers for Enhanced Wound Healing. *Macromol. Res.* **2014**, *22* (12), 1288–1296.

77. Nourmohammadi, J.; Hadidi, M.; Nazarpak, M.H.; Mansouri, M.; Hasannasab, M. Physicochemical and Antibacterial Characterization of Nanofibrous Wound Dressing from Silk Fibroin-Polyvinyl Alcohol- *Elaeagnus angustifolia* Extract. *Fiber. Polym.* **2020**, *21* (3), 456–464.

78. Charernsriwilaiwat, N.; Rojanarata, T.; Ngawhirunpat, T.; Sukma, M.; Opanasopit, P. Electrospun Chitosan-Based Nanofiber Mats Loaded with *Garcinia mangostana* Extracts. *Int. J. Pharm.* **2013**, *452* (1–2), 333–343.

79. Suwantong, O.; Pankongadisak, P.; Deachathai, S.; Supaphol, P. Electrospun Poly(l-Lactic Acid) Fiber Mats Containing Crude *Garcinia mangostana* Extracts for Use as Wound Dressings. *Polym. Bull.* **2014**, *71* (4), 925–949.

80. Amina, M.; Al-Youssef, H.M.; Amna, T.; Hassan, S.; El-Shafae, A.M.; Kim, H.Y.; Khil, M.-S. Poly(Urethane)/*G. Mollis* Composite Nanofibers for Biomedical Applications. *J. Nanoeng. Nanomanuf.* **2012**, *2* (1), 85–90.

81. Ramalingam, R.; Dhand, C.; Leung, C.M.; Ong, S.T.; Annamalai, S.K.; Kamruddin, M.; Verma, N.K.; Ramakrishna, S.; Lakshminarayanan, R.; Arunachalam, K.D. Antimicrobial Properties and

Biocompatibility of Electrospun Poly-ε-Caprolactone Fibrous Mats Containing *Gymnema sylvestre* Leaf Extract. *Mater. Sci. Eng. C* **2019**, *98*, 503–514.

82. Akşit, N.N.; Gürdap, S.; İşoğlu, S.D.; İşoğlu, İ.A. Preparation of Antibacterial Electrospun Poly(D, L-Lactide-Co-Glycolide)/Gelatin Blend Membranes Containing *Hypericum Capitatum Var. Capitatum*. *Int. J. Polym. Mater. Polym. Biomat.* **2021**, *70* (11), 797–809.
83. Mouro, C.; Gomes, A.P.; Gouveia, I.C. Double-Layer PLLA/PEO_Chitosan Nanofibrous Mats Containing *Hypericum perforatum* L. as an Effective Approach for Wound Treatment. *Polym. Adv. Technol.* **2021**, *32* (4), 1493–1506.
84. Eakwaropas, P.; Ngawhirunpat, T.; Rojanarata, T.; Akkaramongkolporn, P.; Opanasopit, P.; Patrojanasophon, P. Fabrication of Electrospun Hydrogels Loaded with *Ipomoea Pes-Caprae* (L.) R. Br Extract for Infected Wound. *J. Drug Deliv. Sci. Technol.* **2020**, *55*, 101478.
85. Kim, J.H.; Lee, H.; Jatoi, A. W.; Im, S.S.; Lee, J.S.; Kim, I.S. *Juniperus Chinensis* Extracts Loaded PVA Nanofiber: Enhanced Antibacterial Activity. *Mater. Lett.* **2016**, *181*, 367–370.
86. Avci, H.; Monticello, R.; Kotek, R. Preparation of Antibacterial PVA and PEO Nanofibers Containing *Lawsonia inermis* (Henna) Leaf Extracts. *J. Biomater. Sci.-Polym. Ed.* **2013**, *24* (16), 1815–1830.
87. Yousefi, I.; Pakravan, M.; Rahimi, H.; Bahador, A.; Farshadzadeh, Z.; Haririan, I. An Investigation of Electrospun Henna Leaves Extract-Loaded Chitosan Based Nanofibrous Mats for Skin Tissue Engineering. *Mater. Sci. Eng. C* **2017**, *75*, 433–444.
88. Hadisi, Z.; Nourmohammadi, J.; Nassiri, S.M. The Antibacterial and Anti-Inflammatory Investigation of *Lawsonia inermis*-Gelatin-Starch Nano-Fibrous Dressing in Burn Wound. *Int. J. Biol. Macromol.* **2018**, *107* (Pt B), 2008–2019.
89. Vakilian, S.; Norouzi, M.; Soufi-Zomorrod, M.; Shabani, I.; Hosseinzadeh, S.; Soleimani, M. *L. inermis*-Loaded Nanofibrous Scaffolds for Wound Dressing Applications. *Tissue Cell* **2018**, *51*, 32–38.
90. Shahrousvand, M.; Haddadi-Asl, V.; Shahrousvand, M. Step-by-Step Design of Poly (ε-Caprolactone) /Chitosan/*Melilotus officinalis* Extract Electrospun Nanofibers for Wound Dressing Applications. *Int. J. Biol. Macromol.* **2021**, *180*, 36–50.
91. Hashmi, M.; Ullah, S.; Kim, I.S. Electrospun *Momordica charantia* Incorporated Polyvinyl Alcohol (PVA) Nanofibers for Antibacterial Applications. *Mater. Today Commun.* **2020**, *24*, 101161.
92. Ali, A.; Mohebbullah, Md.; Shahid, Md.A.; Alam, S.; Uddin, Md.N.; Miah, Md.S.; Jamal, M.S.I.; Khan, Md.S. PVA-*Nigella sativa* Nanofibrous Mat: Antibacterial Efficacy and Wound Healing Potentiality. *J. Text. Inst.* **2021**, *112* (10), 1611–1621.
93. Kwak, H.W.; Kang, M.J.; Bae, J.H.; Hur, S.B.; Kim, I.S.; Park, Y.H.; Lee, K.H. Fabrication of *Phaeodactylum Tricornutum* Extract-Loaded Gelatin Nanofibrous Mats Exhibiting Antimicrobial Activity. *Int. J. Biol. Macromol.* **2014**, *63*, 198–204.
94. Suganya, S.; Senthil Ram, T.; Lakshmi, B.S.; Giridev, V.R. Herbal Drug Incorporated Antibacterial Nanofibrous Mat Fabricated by Electrospinning: An Excellent Matrix for Wound Dressings. *J. Appl. Polym. Sci.* **2011**, *121* (5), 2893–2899.
95. Ganesan, P.; Pradeepa, P. Development and Characterization of Nanofibrous Mat from PVA/*Tridax Procumbens* (TP) Leaves Extracts. *Wound Med.* **2017**, *19*, 15–22.
96. Suryamathi, M.; Ruba, C.; Viswanathamurthi, P.; Balasubramanian, V.; Perumal, P. *Tridax Procumbens* Extract Loaded Electrospun PCL Nanofibers: A Novel Wound Dressing Material. *Macromol. Res.* **2019**, *27* (1), 55–60.
97. Farahani, H.; Barati, A.; Arjomandzadegan, M.; Vatankhah, E. Nanofibrous Cellulose Acetate/Gelatin Wound Dressing Endowed with Antibacterial and Healing Efficacy Using Nanoemulsion of *Zataria multiflora*. *Int. J. Biol. Macromol.* **2020**, *162*, 762–773.

98. Maver, T.; Kurečič, M.; Pivec, T.; Maver, U.; Gradišnik, L.; Gašparič, P.; Kaker, B.; Bratuša, A.; Hribernik, S.; Stana Kleinschek, K. Needleless Electrospun Carboxymethyl Cellulose/Polyethylene Oxide Mats with Medicinal Plant Extracts for Advanced Wound Care Applications. *Cellulose* **2020**, *27* (8), 4487–4508.

99. Avci, H.; Gergeroglu, H. Synergistic Effects of Plant Extracts and Polymers on Structural and Antibacterial Properties for Wound Healing. *Polym. Bull.* **2019**, *76* (7), 3709–3731.

100. Jin, G.; Prabhakaran, M.P.; Kai, D.; Annamalai, S.K.; Arunachalam, K.D.; Ramakrishna, S. Tissue Engineered Plant Extracts as Nanofibrous Wound Dressing. *Biomaterials* **2013**, *34* (3), 724–734.

101. Bilia, A.R.; Guccione, C.; Isacchi, B.; Righeschi, C.; Firenzuoli, F.; Bergonzi, M.C. Essential Oils Loaded in Nanosystems: A Developing Strategy for a Successful Therapeutic Approach. *Evid.-based Complement Altern. Med.* **2014**, *2014*, 651593.

102. Moure, A.; Cruz, J.M.; Franco, D.; Manuel Domínguez, J.; Sineiro, J.; Domínguez, H.; Núñez, M.J.; Carlos Parajó, J. Natural Antioxidants from Residual Sources. *Food Chem.* **2001**, *72* (2), 145–171.

103. Liakos, I.; Rizzello, L.; Scurr, D.J.; Pompa, P.P.; Bayer, I.S.; Athanassiou, A. All-Natural Composite Wound Dressing Films of Essential Oils Encapsulated in Sodium Alginate with Antimicrobial Properties. *Int. J. Pharm.* **2014**, *463* (2), 137–145.

104. Hajiali, H.; Summa, M.; Russo, D.; Armirotti, A.; Brunetti, V.; Bertorelli, R.; Athanassiou, A.; Mele, E. Alginate-Lavender Nanofibers with Antibacterial and Anti-Inflammatory Activity to Effectively Promote Burn Healing. *J. Mat. Chem. B* **2016**, *4* (9), 1686–1695.

105. Gámez-Herrera, E.; García-Salinas, S.; Salido, S.; Sancho-Albero, M.; Andreu, V.; Pérez, M.; Luján, L.; Irusta, S.; Arruebo, M.; Mendoza, G. Drug-Eluting Wound Dressings Having Sustained Release of Antimicrobial Compounds. *Eur. J. Pharm. Biopharm.* **2020**, *152*, 327–339.

106. Zare, M.R.; Khorram, M.; Barzegar, S.; Asadian, F.; Zareshahrabadi, Z.; Saharkhiz, M.J.; Ahadian, S.; Zomorodian, K. Antimicrobial Core–Shell Electrospun Nanofibers Containing Ajwain Essential Oil for Accelerating Infected Wound Healing. *Int. J. Pharm.* **2021**, *603*, 120698

107. Mouro, C.; Simões, M.; Gouveia, I.C. Emulsion Electrospun Fiber Mats of PCL/PVA/Chitosan and Eugenol for Wound Dressing Applications. *Adv. Polym. Technol.* **2019**, *2019*, 9859506.

108. Eğri, Ö.; Erdemir, N. Production of *Hypericum perforatum* Oil-Loaded Membranes for Wound Dressing Material and in Vitro Tests. *Artif. Cell. Nanomed. Biotechnol.* **2019**, *47* (1), 1404–1415.

109. Sofi, H.S.; Akram, T.; Tamboli, A. H.; Majeed, A.; Shabir, N.; Sheikh, F.A. Novel Lavender Oil and Silver Nanoparticles Simultaneously Loaded onto Polyurethane Nanofibers for Wound-Healing Applications. *Int. J. Pharm.* **2019**, *569*, 118590.

110. Avci, H.; Ghorbanpoor, H.; Nurbas, M. Preparation of Origanum Minutiflorum Oil-Loaded Core–Shell Structured Chitosan Nanofibers with Tunable Properties. *Polym. Bull.* **2018**, *75* (9), 4129–4144.

111. Zarghami, A.; Irani, M.; Mostafazadeh, A.; Golpour, M.; Heidarinasab, A.; Haririan, I. Fabrication of PEO/Chitosan/PCL/Olive Oil Nanofibrous Scaffolds for Wound Dressing Applications. *Fiber. Polym.* **2015**, *16* (6), 1201–1212.

112. Unalan, I.; Slavik, B.; Buettner, A.; Goldmann, W.H.; Frank, G.; Boccaccini, A.R. Physical and Antibacterial Properties of Peppermint Essential Oil Loaded Poly (ε-Caprolactone) (PCL) Electrospun Fiber Mats for Wound Healing. *Front. Bioeng. Biotechnol.* **2019**, *7*, 346.

113. Bai, M.Y.; Chang, Y.T.; Tsai, J.C.; Wei, D.J. Tea Tree Oil-Containing Chitosan/Polycaprolactone Electrospun Nonwoven Mats: A Systematic Study of Its Anti-Bacterial Properties in Vitro. *Int. J. Nanotechnol.* **2013**, *10* (10–11), 959–972.

114. Ardekani, N.T.; Khorram, M.; Zomorodian, K.; Yazdanpanah, S.; Veisi, H.; Veisi, H. Evaluation of Electrospun Poly (Vinyl Alcohol)-Based Nanofiber Mats Incorporated with *Zataria multiflora* Essential Oil as Potential Wound Dressing. *Int. J. Biol. Macromol.* **2019**, *125*, 743–750.

115. Rafiq, M.; Hussain, T.; Abid, S.; Nazir, A.; Masood, R. Development of Sodium Alginate/PVA Antibacterial Nanofibers by the Incorporation of Essential Oils. *Mater. Res. Express* **2018**, *5* (3), 035007.

116. Lee, K.; Lee, S. Electrospun Nanofibrous Membranes with Essential Oils for Wound Dressing Applications. *Fiber. Polym.* **2020**, *21* (5), 999–1012.

117. Barzegar, S.; Zare, M.R.; Shojaei, F.; Zareshahrabadi, Z.; Koohi-Hosseinabadi, O.; Saharkhiz, M.J.; Iraji, A.; Zomorodian, K.; Khorram, M. Core-Shell Chitosan/PVA-Based Nanofibrous Scaffolds Loaded with *Satureja Mutica* or *Oliveria Decumbens* Essential Oils as Enhanced Antimicrobial Wound Dressing. *Int. J. Pharm.* **2021**, *597*, 120288.

118. Zhang, W.; Huang, C.; Kusmartseva, O.; Thomas, N.L.; Mele, E. Electrospinning of Polylactic Acid Fibres Containing Tea Tree and Manuka Oil. *React. Funct. Polym.* **2017**, *117*, 106–111.

CHAPTER 2

Global Aims

This doctoral project is focused on the use of plant extracts to efficiently produce antibacterial dressings, by electrospinning, for wound healing applications. To accomplish this, several medicinal plants with well-known therapeutic properties and intrinsic antibacterial activity are selected, and new and promising approaches applied to develop wound dressing materials that can prevent skin infections as well as maintain an appropriate wound environment for healing.

Accordingly, to achieve the aim purposed, this doctoral research work has been developed under the following specific aims:

1. Careful selection of the polymer blends and the medicinal plant extracts concerning the information found in the literature

To achieve this task, several polymer blends from natural and synthetic biodegradable polymers (*e.g.*, Polycaprolactone (PCL)/ Polyvinyl Alcohol (PVA)/ Chitosan (CS), Poly(L-lactic acid) (PLLA)/PVA/CS, PCL/PVA/Pectin (PEC), PLLA/ Poly(ethylene oxide) (PEO)_CS) are chosen according to their promising wound healing properties, namely their biocompatibility, bioactivity, and ability to control the water vapor transmission rate, the oxygen permeability, and the fluid drainage, as well as the capacity to promote cell adhesion and proliferation, combined with their strength and durability. Also, different crude plant extracts (*e.g.*, *Hypericum perforatum* L. (HP), *Chelidonium majus* L. (CM), *Centella asiatica* L. (CA), and *Agrimonia eupatoria* L. (AG) and their derivatives, like Eugenol (EUG)) are selected due to their inherent antimicrobial, anti-inflammatory, and antioxidant activities, as well as unique healing characteristics.

2. Production and development of new electrospun wound dressings

The plant extracts and their derivatives are blended or dispersed in the selected biodegradable and biocompatible polymer blends, prior to electrospinning using different strategies, namely various emulsions and layer-by-layer depositions. Electrospinning processing conditions were optimized and the nanofibers were produced using the needle-free Nanospider™ technology, an electrospinning equipment which is highly productive and whose process is easily transferable from the laboratory to industrial scale.

3. Characterization of the produced electrospun wound dressings

The morphological, chemical, physical, and mechanical features of the produced electrospun wound dressing materials are evaluated, as well as their *in vitro* release profiles. The biological properties, such as the antibacterial activity and cell viability, are further assessed to confirm the suitability of these materials for being used as wound dressings with antimicrobial properties.

CHAPTER 3

Research Work

Part I

Emulsion Electrospinning for Wound Dressing Applications

This part describes the development of the electrospun nanofibrous membranes from either water-in-oil (W/O) or oil-in-water (O/W) emulsions and the ability of emulsion electrospinning to directly incorporate hydrophilic or hydrophobic antibacterial plant compounds into the electrospun nanofibers for a sustained release. The produced electrospun membranes were evaluated in terms of morphological, physicochemical, mechanical, and biological properties. Overall, the gathered data emphasize the potential of emulsion electrospinning to produce single-layer nanofibrous structures to be used as antibacterial wound dressings.

This part includes the following scientific publications:

Cláudia Mouro, Manuel Simões, and Isabel C. Gouveia. Emulsion Electrospun Fiber Mats of PCL/PVA/Chitosan and Eugenol for Wound Dressing Applications. Advances in Polymer Technology (2019) 2019:9859506. (**Paper 2**)

Cláudia Mouro, Raul Fangueiro, and Isabel C. Gouveia. Emulsion electrospinning of PLLA/PVA/Chitosan with *Hypericum perforatum* L. as an antibacterial nanofibrous wound dressing. *(Submitted for publication)* (**Paper 3**)

Cláudia Mouro, Ana P. Gomes, Merja Ahomen, Raul Fangueiro, and Isabel C. Gouveia. *Chelidonium majus* L. Incorporated Emulsion Electrospun PCL/PVA_PEC Nanofibrous Meshes for Antibacterial Wound Dressing Applications. Nanomaterials (2021) 11(7):1785. (**Paper 4**)

Paper 2 - Emulsion Electrospun Fiber Mats of PCL/PVA/Chitosan and Eugenol for Wound Dressing Applications

Abstract

In recent years, the damaging effects of antimicrobial resistance relating to wound management and infections have driven the ongoing development of composite wound dressing mats containing natural compounds, such as plant extracts and their derivatives. The present research reports the fabrication of novel electrospun Polycaprolactone (PCL)/Polyvinyl Alcohol (PVA)/Chitosan (CS) fiber mats loaded with Eugenol (EUG), an essential oil, known for its therapeutic properties. The electrospun fiber mats were prepared via electrospinning from either water-in-oil (W/O) or oil-in-water (O/W) emulsions and characterized using scanning electron microscopy (SEM), Fourier-transform infrared spectroscopy (FT-IR), total porosity measurements, and water contact angle. The *in vitro* EUG release profile and antibacterial activity against *Staphylococcus aureus* (*S. aureus*) and *Pseudomonas aeruginosa* (*P. aeruginosa*) were also evaluated. The obtained results proved that the EUG was loaded efficiently into electrospun PCL/PVA/CS fiber mats and the two W/O and O/W emulsions prepared from the PCL/PVA/CS (7:3:1) and PCL/PVA/CS (3:7:1) revealed porosity within the ideal range of 60–90%, even when EUG was loaded. The measured contact angle values showed that the O/W emulsion exhibited a more hydrophilic character and the wettability noticeably decreased after adding EUG in both emulsion blends. Furthermore, the electrospun PCL/PVA/CS fiber mats demonstrated a rapid release of EUG during the first 8 hours, which enhanced gradually afterward (up to 120 hours). Moreover, an efficient antibacterial activity against *S. aureus* (inhibition ratios of 92.43% and 83.08%) and *P. aeruginosa* (inhibition ratios of 94.68% and 87.85%) was displayed and the *in vitro* cytotoxic assay demonstrated that the normal human dermal fibroblasts (NHDF) remained viable for at least 7 days, after direct contact with the produced electrospun fiber mats. Therefore, such findings support the biocompatibility and suitability of using these EUG-loaded electrospun PCL/PVA/CS fiber mats as a new innovative wound dressing material with potential for preventing and treating microbial wound infections.

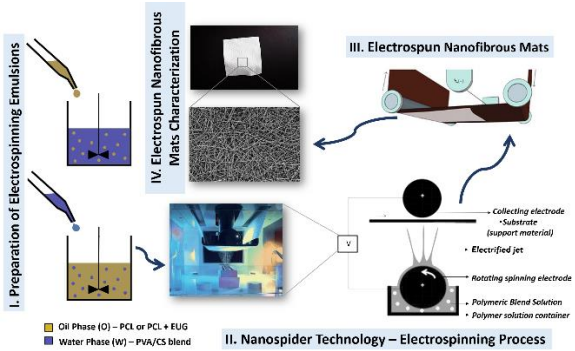

Keywords: Emulsion electrospinning; eugenol; essential oils; wound dressing; wound healing material.

1. Introduction

The integrity of the skin can be affected by several disorders. When the skin is injured, it becomes more susceptible to microbial infections, which can have negative consequences on the healing process [1,2]. Therefore, the development of materials with suitable barrier properties using different antimicrobial agents have shown to prevent and suppress the microbial invasion and colonization by pathogenic bacteria [3]. However, it is still a challenge to achieve the release of these agents directly onto the damaged tissue to ensure the correct therapeutic dosage and prevent the wound from getting infections. Recently, composite wound dressing mats produced by electrospinning have attracted research attention due to their unique properties like extremely high surface area, high porosity, and small pore size [4,5]. In addition, these materials are known in the wound management field for their capability to absorb excess exudate from the wound, while they create and maintain a moist environment. Moreover, electrospun fiber mats provide wound protection from mechanical trauma and bacterial colonization, exhibit high air, and oxygen permeability, as well as mimic the properties of natural extracellular matrix (ECM) ensuring additional support for cell growth and proliferation in order to promote the wound healing with the minimum scar formation [4–6]. Also, electrospinning has the ability to incorporate different types of bioactive or therapeutic agents, thus leading to the enhancing of the desirable wound healing properties [6]. Antibiotics, growth factors (GFs), vitamins, antimicrobial, analgesics, and anti-inflammatory compounds are among the most successful bioactive agents so far loaded into electrospun fiber mats [7]. Nevertheless, medicinal plant extracts, and their derivatives, such as essential oils, have captured the attention of researchers due to their traditional therapeutic properties, cost-effectiveness, and availability [6]. Eugenol (EUG), a naturally occurring phenolic component extracted from cloves, is known for its analgesic, antimicrobial, antioxidant, anti-inflammatory, and anticarcinogenic properties and has demonstrated abilities to improve the healing process and tissue regeneration [8–10]. However, EUG presents poor water solubility, and its stability can be affected by chemical and enzymatic degradation, losses by volatilization or thermal decomposition [11,12]. In order to overcome EUG disadvantages, emulsion electrospinning is of particular interest to successfully incorporate both hydrophilic and hydrophobic bioactive agents, while preventing the loss of their structural integrity and bioactivity [13]. Emulsion electrospinning is a novel and straightforward technique similar to the traditional electrospinning, where water-in-oil (W/O) or oil-in-water (O/W) emulsions are used instead of a conventional polymer solution [14,15]. This modified electrospinning method does not require a special apparatus, neither a careful selection of the operating conditions to ensure desirable results. In addition, emulsion electrospinning has been used to improve the solubility of poorly soluble bioactive agents and, consequently, their therapeutic effectiveness. Furthermore, this approach also increases the affinity of the oil and water phases and plays a significant role in the stability of low molecular weight polymers and diluted polymer solutions [13]. In this context, the present work describes the innovative development of EUG-loaded into electrospun Polycaprolactone (PCL)/Polyvinyl Alcohol

(PVA)/Chitosan (CS) fiber mats through W/O and O/W emulsions by nanospider technology, a needle-free electrospinning equipment, based on a rotating spinning electrode immersed into a liquid polymer bath. The modern nanospider technology differs from conventional electrospinning because it allows the formation of many Taylor cones (the source of nanofibers) simultaneously on the surface of the rotating spinning electrode, and hence this technology is highly productive and more effective to produce high-quality nanofibers [16,17]. In this way, a nontoxic hydrophobic synthetic polymer, PCL, known for its many advantages over the main synthetic polymers was used to act as a protective barrier against external threats. However, the data available in the literature showed that cells are more prone to adhere, proliferate, and grow on a moderate hydrophilic surface than on a hydrophobic or super-hydrophilic surface [18,19]. Therefore, CS, a naturally occurring polysaccharide, was selected for its abilities, namely by supporting cell adhesion and growth of several cell types and also by exhibiting hemostatic and antimicrobial properties [20]. Nevertheless, CS is difficult to electrospun into a fibrous structure and exhibits low mechanical properties, which restricts its use in medical applications [21,22]. To overcome these limitations, CS has been blended with other biocompatible hydrophilic synthetic polymers, like PVA [23]. Herein, in this study, CS and PVA were blended in order to ensure efficient exudate management and provide a moist wound environment. Moreover, the PVA/CS blend exhibits an inhibitory effect on microbial growth and promote cell adhesion and proliferation [24]. The biological abilities of EUG, mainly analgesic, anti-inflammatory, and antimicrobial properties have also been exploited to strengthen the healing process. Therefore, we present new findings claiming the development of new EUG-loaded electrospun PCL/PVA/CS fiber mats prepared from W/O and O/W emulsions, for wound dressing applications. The results obtained revealed that mixing PCL, PVA, and CS enhanced the final properties of the blend. CS formed miscible blends with PVA, which acted as a good emulsifying and dispersing agent and made CS/PVA blend compatible with the PCL. The antimicrobial and non-cytotoxic effect of EUG was also seen as a promising strategy to develop new innovative wound dressings, with the potential to prevent and treat microbial-resistant wound infections.

2. Materials and Methods

2.1. Materials

Polycaprolactone (PCL) (MW 80,000 g/mol) and Chitosan (CS) (MW 50,000–190,000 g/mol, degree of deacetylation 75–85%) and Eugenol (EUG) were purchased from Sigma-Aldrich. Polyvinyl Alcohol (PVA) (MW 115,000g/mol) was purchased from VWR Chemicals. Chloroform (analytical grade), Dimethylformamide (DMF) (analytical grade), Glacial acetic acid, and Ethanol absolute were purchased from Fisher Chemical. Normal human dermal fibroblasts (NHDF) cells were acquired from ATCC—American Type Culture Collection. Brain Heart Infusion (BHI) Broth was provided from Panreac. Nutrient Agar (NA), Nutrient Broth (NB), and Agar for microbiology were purchased from

Fluka. Sodium chloride (NaCl), Mueller-Hinton Broth (MHB), Dimethyl sulfoxide (DMSO) anhydrous ≥99.9%, Tween 80, Trypsin, and 3-(4,5-Dimethyl-2-thiazolyl)-2,5-diphenyl-2H-tetrazolium bromide (MTT) were purchased from Sigma Aldrich. Phosphate-buffered saline (PBS), pH 7.4 was purchased from Alfa Aesar. All solvents were used as received without further purification.

2.2. Determination of Minimum Inhibitory Concentration (MIC) of EUG

Minimal Inhibitory Concentration (MIC) of EUG was applied against two bacterial strains: *Staphylococcus aureus* ATTC 6538 and *Pseudomonas aeruginosa* PA25 by the broth microdilution method according to NCLS M07-A6 guidelines. Briefly, EUG stock solution was prepared in DMSO (10% (v/v)) to yield a concentration of 20 μL/mL. Serial dilutions of EUG were made in MHB with concentrations ranging from 10 to 1 μL/mL. Then, overnight liquid bacterial cultures were adjusted to 0.5 McFarland turbidity standards with sterile water. Afterward, bacterial work suspensions were formed from 500 μL of the 0.5 McFarland suspensions and 4500 μL of MHB. A volume of 50 μL of bacterial work suspensions and 50 μL of the EUG dilutions were added into 96 multi-well polystyrene plates (Sigma-Aldrich). The multi-well plates were incubated for 24 hours at 37 °C. Deposited bacteria (dot-shaped) in the bottom of each well were evaluated. The last well in the dilution series that showed deposit (bacterial killing) corresponded to MIC of EUG. All the determinations were performed in triplicate.

2.3. Preparation of Electrospinning Emulsions

PCL solution (8% w/v) was prepared by dissolving PCL in chloroform/DMF (volume ratio of 30:20) at 50 °C under magnetic stirring until complete dissolution. Afterward, the solution was left to stir overnight to ensure proper dissolution of the PCL before being blended with the PVA/CS blend. CS solution (4% w/v) was prepared by dissolving CS in acetic acid (14%) at room temperature. Also, a PVA solution (10% w/v) in distilled water was prepared at 90 °C. PVA and CS solutions were then mixed in two different ratios, 7:1 and 3:1 (v/v), to form the PVA/ CS blend solution. The W/O emulsion blend 8% PCL/10% PVA/4% CS (7:3:1) was prepared by simultaneous adding of PVA/CS blend solution to PCL solution, followed by mixing with high-speed homogenizer (Techmatic S2), while the O/W emulsion blend 8% PCL/10% PVA/4% CS) (3:7:1) was prepared by simultaneous adding of PCL solution to PVA/ CS blend solution. The final mixtures were stirred at room temperature for 4 hours to ensure complete dissolution and to obtain uniform emulsions. PCL/PVA/CS blends were also loaded with EUG. The final concentration of the EUG was 5% (w/w) (based on the weight of the PCL powder), i.e., 5% over the weight of the fiber (owf) EUG. All emulsions were immediately used for electrospinning.

2.4. Electrospinning

The stable and homogenous emulsions were electrospun using Nanospider Technology (Nanospider laboratory machine NS LAB 500S from Elmarco s.r.o., Czech Republic, http://www.elmarco.com). Electrospinning of the emulsions was carried out with a distance between the spinning electrode and collecting electrode of 13 cm at a driving voltage of 75.0 kV and a rotating spinning electrode of 9.6 rpm (60Hz). The collection time was ~1.0 hour at 25 °C and relative humidity up to 35%. The electrospun fiber mats were collected on polypropylene nonwoven fabric and were dried in the hood at room temperature till constant weight. The same electrospinning conditions were used to pure PCL and PVA/CS blend as a reference for electrospun PCL/PVA/CS fiber mats with and without loaded EUG.

2.5. Electrospun Fiber Mats Characterization

2.5.1. Fourier Transform Infrared Spectroscopy (FT-IR)

The chemical composition of pure PCL, PVA/CS, and electrospun PCL/PVA/CS fiber mats with and without loaded EUG were analysed on FT-IR. Measurements were performed on Thermo-Nicolet is10 FT-IR spectrophotometer over the range 500–4000 cm^{-1} with a spatial frequency resolution of 4 cm^{-1} and each sample was scanned 64 times.

2.5.2. Surface Morphology of Electrospun Fiber Mats

The surface morphology of the electrospun PCL/PVA/CS fiber mats with and without loaded EUG was investigated with the help of scanning electron microscope (SEM) Hitachi S2700 at a high voltage of 20 kV. The fiber diameters were directly measured from SEM images using public domain software (Image J, National Institutes of Health, USA). After that, the average diameter and diameter distribution were determined by applying SPSS Statistics 21.0 software (SPSS Inc. Chicago, USA).

2.5.3. Porosity Measurement

The total porosity of the dry electrospun fiber mats was measured using a liquid displacement method, as described by Chitrattha et al. [25]. Ethanol was used as the displacement liquid because it readily penetrated into the pores of the matrices and did not induce shrinkage or swelling of these materials. Briefly, a pre-weighed porous membrane (W_s) was immersed in a cylinder containing 20 mL of ethanol (W_1) and placed in a water sonicator bath (Ultrasons-H, P-Selecta) for 40 min at 30 °C to assist the penetration of ethanol into the porous structure. Subsequently, the volume in the sonicated cylinder containing porous membrane impregnated with ethanol was readjusted to 20 mL

and weighed (W_2). After that, the membrane saturated with ethanol was removed from the cylinder and the cylinder was reweighed (W_3). The porosity (ε) of these porous materials was determined using the following Equation (1) [25]:

$$\varepsilon(\%) = (W_2 - W_3 - W_s) / (W_1 - W_3) \times 100 \quad (1)$$

2.5.4. Water Contact-Angle Determination

The surface wettability of pure PCL, PVA/CS, and electrospun PCL/PVA/CS fiber mats with and without loaded EUG were determined through water contact angle (WCA) using a data physics contact angle system OCAH-200 apparatus. To accomplish that, deionized water droplets were placed on the surface of each sample at room temperature and the contact angle was calculated after 10 seconds of incubation time to avoid discrepancy in the contact angle values measured. The measurements were conducted on different sample locations and the average was reported as the contact angle of each sample.

2.6. Release *In Vitro* of EUG from EUG-Loaded Electrospun PCL/PVA/CS Fiber Mats

Release of EUG from EUG-loaded electrospun PCL/PVA/CS fiber mats was studied by UV–Vis spectrometry. To perform this assay, standard solutions of EUG with concentrations from 0.00 μL/mL to 10.00 μL/mL were prepared and a calibration curve was drawn at 282 nm (maximum wavelength of EUG). Samples (2×2 cm) of EUG-loaded electrospun PCL/PVA/CS fiber mats were immersed in 10 mL of phosphate-buffered saline (PBS, pH=7.4) at 37 °C with constant rotation at a speed of 100 rpm. Afterward, 3 mL of release medium was recovered at specified time intervals, ranging between 0 and 120 hours, and at the same time, an equal volume of the fresh PBS solution was replenished to maintain a constant volume. The concentration of EUG that remained in the release medium at each time point was quantified at 282 nm using UV–Vis spectrophotometer. All measurements were carried out in triplicate.

2.7. Estimation of Antibacterial Activity of EUG-Loaded Electrospun PCL/PVA/CS Fiber Mats

The antibacterial effect of EUG loaded into electrospun PCL/PVA/CS fiber mats was carried out according to E 2180-07 standard test method for determining the activity of incorporated antimicrobial agent(s) in polymeric or hydrophobic materials. *S. aureus* and *P. aeruginosa* were selected, once they are the most common bacteria present in wound infections [26].

To perform the assay, a bacterial suspension (1–5×10^8 CFU/mL) was added in an agar slurry previously prepared from 0.85 (w/v) NaCl and 0.3 (w/v) agar-agar in deionized water. Afterward, a thin layer of inoculated agar slurry was poured onto 3×3 cm square samples of electrospun PCL/PVA/CS fiber mats with and without EUG loaded. The samples were evaluated immediately after adding the inoculated agar slurry (T_{oh}) and after 18–24 hours in contact with the inoculated agar slurry at 37 °C for 18–24 hours (T_{24h}). For each sample, serial dilutions of the agar slurry were done with 0.85 (w/v) NaCl, plated in agar plates, and incubated for 18–24 hours at 37 °C. The antimicrobial efficiency was quantitatively expressed in percentage of bacterial reduction (%R) using Equation (2) by comparing the CFU on the control samples (electrospun PCL/PVA/CS fiber mats), *C*, with the CFU on the samples loaded with 5% owf EUG (5% EUG-loaded electrospun PCL/PVA/CS fiber mats), *A* [27].

$$\text{Percentage Reduction (\%R)} = ((C-A)/C) \times 100 \quad (2)$$

According to Japanese Industrial Standard JIS L 1902:2002, the bacteriostatic or bactericidal effect of the electrospun PCL/PVA/CS fiber mats containing EUG was then calculated using Equations (3) and (4):

$$\text{Bacteriostatic activity value} = M_B - M_C \quad (3)$$

$$\text{Bactericidal activity value} = M_A - M_C \quad (4)$$

where M_A is the average of the common logarithm of the number of living bacteria in control samples immediately after adding the inoculated agar slurry (T_{oh}), M_B is the average of the common logarithm of the number of living bacteria in control samples after 18–24 hours in contact with the inoculated agar slurry (T_{24h}), and M_C is the average of the common logarithm of the number of living bacteria in samples containing 5% owf EUG after 18–24 hours in contact with the inoculated agar slurry (T_{24h}).

2.8. Characterization of the Cytotoxicity Profile of the EUG-Loaded Electrospun PCL/PVA/CS Fiber Mats

The cytotoxic profiles of the produced electrospun PCL/PVA/CS fiber mats with and without EUG were performed *in vitro* following ISO 10993–5 (Biological evaluation of medical devices-Part 5: Tests for *in vitro* cytotoxicity). Briefly, the samples were placed in 24-well plates (Sigma-Aldrich) at the center of each well occupying <1/10 of its area and then sterilized under UV irradiation (254 nm, ~7 $mWcm^{-2}$) for 1 hour. After that, normal human dermal fibroblast (NHDF) cells were used as a model to seed each well at a density of 1 × 10^4 cells/well and incubated at 37 °C, in an incubator under a humidified atmosphere containing 5% CO_2. After an incubation period of 1, 3, and 7 days, the mitochondrial redox activity of the viable cells was assessed through the reduction of the MTT into an insoluble blue formazan dye. In this way, the medium of each well was removed and it was replaced with a mixture of fresh culture medium and the MTT reagent solution. After 4 hours of incubation at

37 °C and 5% CO_2 humidified atmosphere, the MTT solution was removed and DMSO was added to each well in order to dissolve the formazan crystals. Finally, the absorbance of each sample was measured at 570 nm using a microplate reader (Biorad xMark microplate spectrophotometer). Wells containing cells cultured without the materials and wells containing cells cultured with EtOH (96%) were also included as a negative control (K^-) and positive control (K^+), respectively.

2.9. Statistical Analysis

Data were analyzed statistically by the one-way analysis of variance (ANOVA) and Tukey Post-Hoc test using SPSS 21.0 (SPSS Inc. Chicago, USA). Statistical calculations were based on a confidence level ≥95% (values of $p < 0.05$ were considered statistically significant).

3. Results and Discussion

3.1. Determination of Minimum Inhibitory Concentration (MIC) of EUG

Minimal Inhibitory Concentration (MIC) of EUG against *S. aureus* and *P. aeruginosa* was found to be 4.25 µL/mL and 3.00 µL/mL, respectively. Several other studies have confirmed the significant antibacterial activity of EUG against *S. aureus* and *P. aeruginosa*. For example, Sanla-Ead et al. [28] described MIC of 25.00 µL/mL against *S. aureus* and 50.00 µL/mL against *P. aeruginosa*, which were higher than those found in this study. However, the MIC values for specific alkaloids obtained from plants, namely the bioactive properties of these natural compounds depend on various factors, including the environmental condition and seasonal variables, as well as the geographical location and method of extraction.

3.2. Electrospun Fiber Mats Characterization

3.2.1. Fourier Transform Infrared Spectroscopy (FT-IR)

The FT-IR spectra of pure PCL, PVA/CS and electrospun PCL/PVA/CS fiber mats with and without EUG were acquired and represented in Figure 1. The FT-IR spectrum of pure PCL exhibits its characteristic peaks, Figures 1(a)(i) and 1(b)(i). Peaks at 2866.05 and 2945.76 cm^{-1} are attributed to symmetric and asymmetric CH_2 stretching vibrations. At 1722.51 cm^{-1} occurs an intense, sharp peak, which corresponds to carbonyl stretching vibration of the ester group, while the peaks at 1293.80, 1239.67, and 1164.76 cm^{-1} are associated for C-O and C-C stretching, asymmetric and symmetric –C-O-C stretching, respectively [29]. On the other hand, the characteristic bands of both PVA and CS are displayed in the FT-IR spectrum of the PVA/CS blend. Figures 1(a)(ii) and 1(b)(ii) shows the

characteristic peaks at 1558.80 cm^{-1} and 1653.25 cm^{-1}, corresponding to N-H bending vibrations in secondary amides and C=O stretching vibrations of the amide bond, respectively. Moreover, the spectrum of PVA/CS blend exhibits a broad peak at 3118.56 cm^{-1}, which is assigned to O-H and N-H stretching.

Additionally, the emulsion blends of PCL/PVA/CS (Figures 1(a)(iii) and 1(b)(iii)) display a sharp peak at around 1720.00 cm^{-1} which corresponds to the PCL and a broad peak in the region between 3000 and 3500 cm^{-1} that belongs to PVA/CS blend. Likewise, the FT-IR spectra of electrospun PCL/PVA/CS fiber mats containing EUG (Figures 1(a)(iv) and 1(b)(iv)) exhibit those peaks and other characteristic peaks at around 1033.00 and 1267.00 cm^{-1}, regarding the stretching vibration of symmetric and asymmetric C-O-C, which demonstrate the presence of the methoxy group of EUG. Moreover, the presence of all characteristic peaks of the components used to produce the electrospun fiber mats proves the successful blending of the EUG with the PCL/PVA/CS emulsions.

However, the FT-IR analysis suggests that there is no evidence of chemical bonding between each component of the blend because new absorption peaks are not seen in FT-IR spectra. Nevertheless, some chemical interactions could have occurred among carboxyl, amino, and hydroxyl groups of the PCL, PVA, CS, and bioactive agent. These interactions can be suggested by slight displacement of absorption peaks, as well as by different peak intensities and peak widths.

Similar results were presented by Ajalloueian et al. [20]. The FT-IR spectrum of PLGA/CS/PVA nanofibers displayed the characteristic peaks of PLGA, CS, and PVA, and when they removed the PVA from the blend fewer hydroxyl groups were detected as shown by a narrower and shorter peak at 3400–3700 cm^{-1}. Furthermore, Zarghami et al. [19] demonstrated by FT-IR that olive oil was successfully embedded within the PCL/Olive oil composite nanofibers. Nevertheless, in the FT-IR spectrum of the PEO/CS/PCL/Olive oil composite nanofibers were not evident chemical bonding between the PEO/CS and PCL/Olive oil.

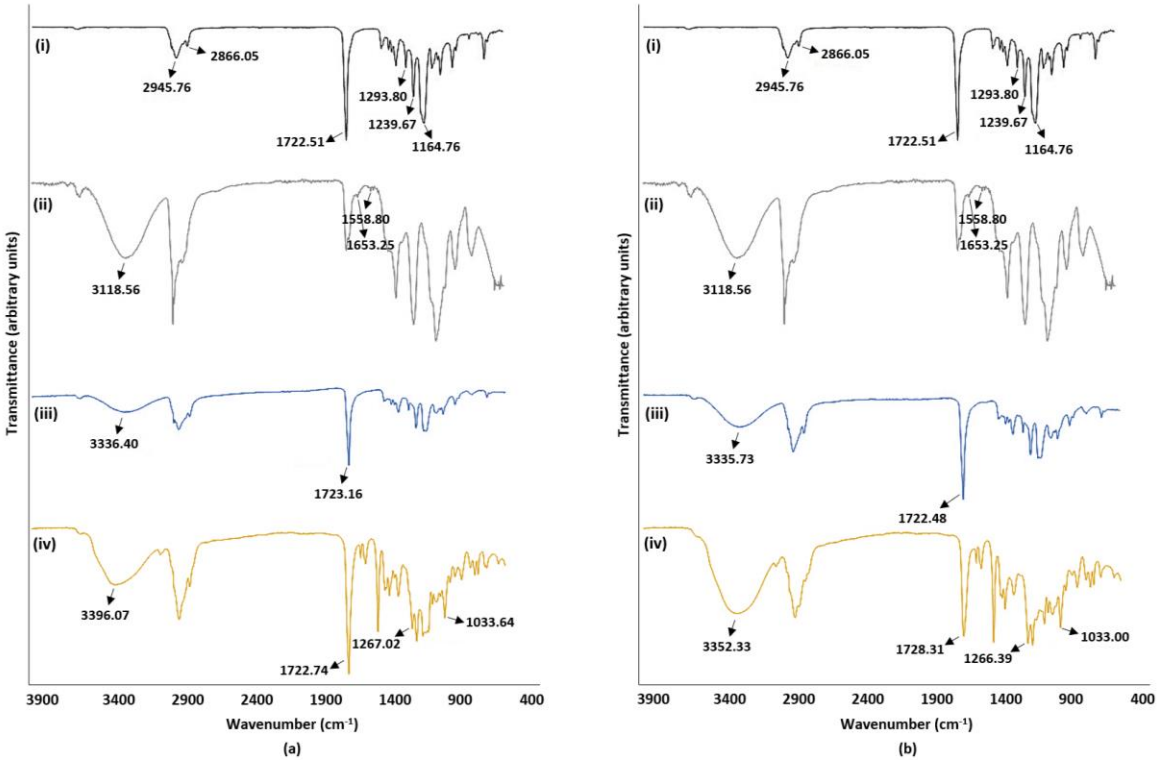

Figure 1 – FT-IR spectrums of pure PCL (**i**), PVA/CS (**ii**) and electrospun PCL/PVA/CS fiber mats from W/O emulsion (**a**) and from O/W emulsion (**b**). Electrospun PCL/PVA/CS fiber mats without loaded EUG (**iii**) and with 5% owf EUG (**iv**).

3.2.2. Surface Morphology of Electrospun Fiber Mats

SEM micrographs and fiber diameter distributions of EUG-loaded electrospun PCL/PVA/CS fiber mats, prepared via electrospinning from either W/O or O/W emulsions, are shown in Figure 2. The electrospun PCL/PVA/CS fiber mats produced from W/O emulsion displayed beads and fibers, known as the spindles or bead-on-a-string morphologies, with an average diameter of 379.05 ± 161.95 nm, Figure 2(a). When 5% owf EUG was incorporated, nanofibers with similar morphology were produced with a mean diameter of 387.07 ± 179.51 nm, Figure 2(b). In turn, the electrospun PCL/PVA/CS fiber mats produced from O/W emulsion, with and without EUG loaded, demonstrated thinner and more uniform fibers with fewer beads, with an average diameter of 174.47 ± 38.93 nm and 199.90 ± 48.86 nm, Figures 2(c) and 2(d), respectively. It showed that the PVA, which acts as an emulsifying agent, is the most critical component of the blend which controls the process of emulsion electrospinning [30]. Thus, PVA decreases the surface tension between immiscible phases and contributes towards the formation of more uniform nanofibers [30,31]. Moreover, the O/W emulsions are especially useful for controlled or sustained release of the oil-soluble bioactive compounds, as the EUG. Hajiali et al. [32] obtained similar results to Sodium Alginate (SA)-Polyethylene Oxide (PEO) nanofibers and SA-PEO containing 5% v/v of Lavender oil nanofibers. In both cases, 85% of fibers exhibited diameters in the range of 50–125 nm, with a most representative

percentage between 75 and 100 nm. This result confirmed that the addition of essential oil to the polymer solution did not have a significant effect on fiber diameters. Moreover, Gholipour-Kanani et al. [33] produced PCL/PVA/CS nanofibrous mats by adding PVA to PCL/CS in 2:1:1.33 (PCL/PVA/CS) blend ratio and obtained uniform fibers with diameters in the range of 136 ± 37.00 nm. This study revealed a mean diameter lower than the average diameter of fibers found for PCL/PVA/CS (7:3:1) (379.05 ± 161.95 nm) and PCL/PVA/CS (3:7:1) (174.47 ± 38.93 nm), confirming that both the composition and ratio of each component in the blend influence the fiber diameters.

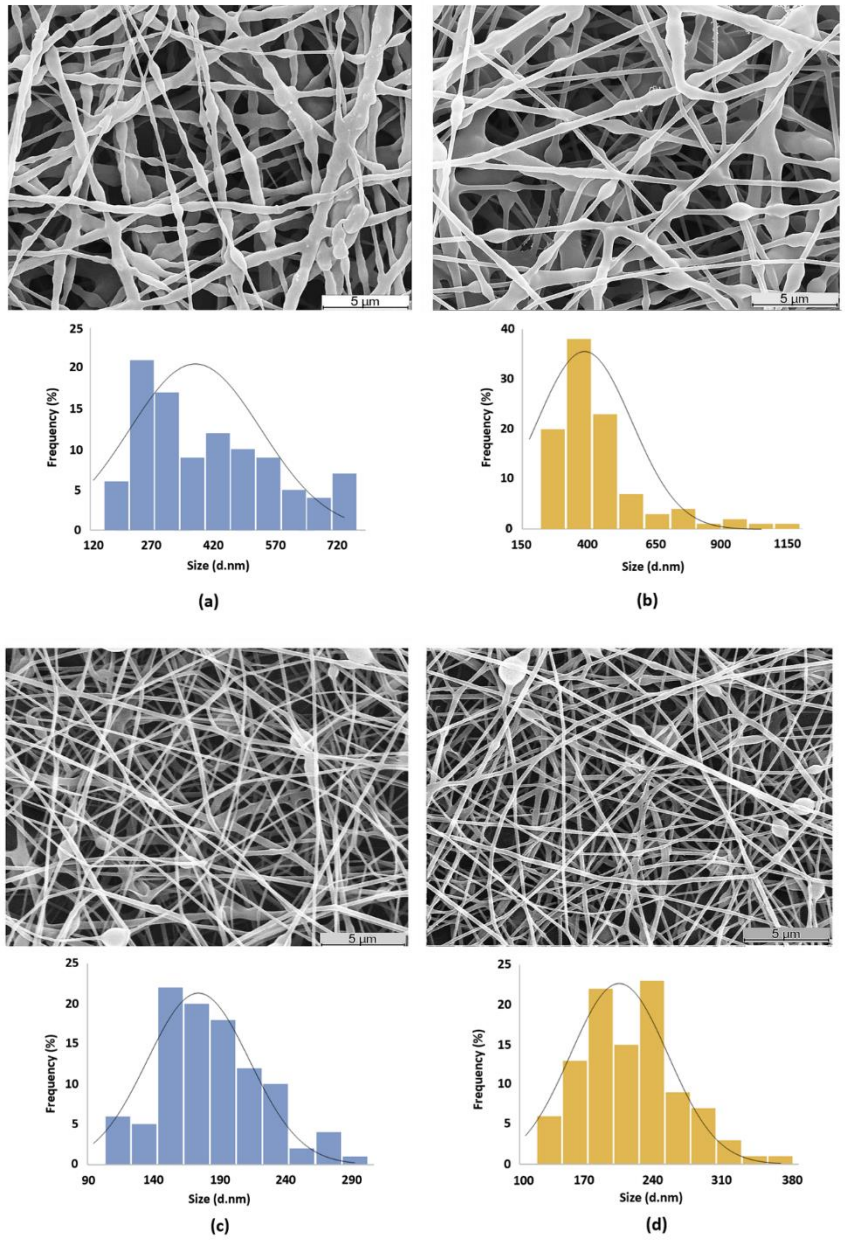

Figure 2 – SEM images with fiber diameters distribution obtained from electrospun (**a**) PCL/PVA/CS fiber mats prepared via W/O emulsion without EUG loaded, (**b**) and with 5% owf EUG, (**c**) PCL/PVA/CS fiber mats prepared via O/W emulsion without EUG loaded, (**d**) and with 5% owf EUG.

3.2.3. Porosity Measurement

The wound dressings' porosity contributes to a correct gas, nutrient, and fluid exchange, as well as drug release. The porosity of a material is also essential to support cell adhesion and proliferation in the wound site [25]. Herein, the electrospun PCL/PVA/CS fiber mats produced from W/O and O/W emulsions presented a total porosity of 88.74 ± 2.27% and 90.46 ± 2.15%, respectively, as demonstrated in Table 1. The porosity values slightly decreased when the ratio of PCL in the emulsion blend increased, namely to W/O emulsion, and when EUG was loaded. Moreover, the electrospun PCL/PVA/CS fiber mats prepared from W/O emulsion loaded with EUG exhibited a total porosity of 84.44 ± 3.10%, while a value of 88.52 ± 4.09% was observed from the O/W emulsion loaded with EUG. The total porosity values of the electrospun PCL/PVA/CS fiber mats, with and without EUG, are within the preferred range of 60–90% for an effective wound healing process [34]. Indeed, the high porosity exhibited by the produced electrospun fiber mats is more proper to provide a suitable pore structure for cell migration, nutrient exchange, and development of a new ECM, although it depends on the wound characteristics and the aim of wound management [25].

Table 1 – Porosity measurement of electrospun PCL/PVA/CS fiber mats with and without loaded EUG.

Samples	Porosity (%)
W/O emulsion blend PCL/PVA/CS	88.74 ± 2.27
W/O emulsion blend PCL/PVA/CS + 5% owf EUG	84.44 ± 3.10
O/W emulsion blend PCL/PVA/CS	90.46 ± 2.15
O/W emulsion blend PCL/PVA/CS + 5% owf EUG	88.52 ± 4.09

3.2.4. Water Contact-Angle Determination

Surface wettability of electrospun fiber mats is one of the most desirable material properties to the wound dressing applications, which may influence the initial adhesion and migration of cells, as well as their proliferation to the wound site [29,35]. Therefore, the contact angle between water droplets and the electrospun fiber mats (WCA) was determined to assess the wettability of the pure PCL, PVA/CS, and electrospun PCL/PVA/CS fiber mats with and without EUG (Figure 3). In this study, a hydrophobic polymer, PCL, 90.2 ± 7.30°, was blended with a hydrophilic polymer PVA/CS blend, 28.8 ± 5.50°, to improve the hydrophilic features of electrospinning emulsions [36]. WCA values of 61.2 ± 4.24° and 42.85 ± 3.95° were obtained for electrospun PCL/PVA/CS fiber mats prepared from W/O and O/W emulsions, respectively. The O/W emulsion presented a more hydrophilic character than W/O emulsion, due to inherent hydrophilic nature of both PVA and CS. However, the

incorporation of EUG through the electrospun fiber mats was more hydrophobic. WCA values of 70.70 ± 4.62° and 59.37 ± 5.11° were displayed for electrospun PCL/PVA/CS fiber mats loaded with 5% owf EUG from W/O and O/W emulsions, respectively. Hence, the addition of EUG improves the most hydrophilic character of the O/W emulsion.

Similar results found by Cui et al. [35] showed that increasing the PVA-SbQ amount in comparison with the Zein amount resulted in a lower WCA. The reason for this was because Zein, a predominantly corn-based protein, exhibits a more hydrophobic character due to a higher amount of hydrophobic (nonpolar) amino acids than hydrophilic (polar) ones.

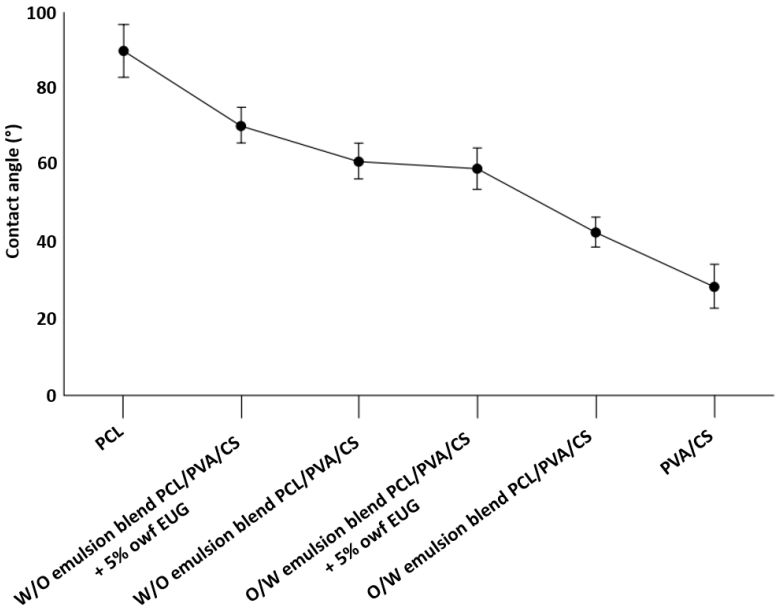

Figure 3 – Variation of contact angle on pure PCL, PVA/CS and electrospun PCL/PVA/CS fiber mats prepared from W/O and O/W emulsions, with and without EUG.

3.3. Release *In Vitro* of EUG from EUG-Loaded Electrospun PCL/PVA/CS Fiber Mats

Figure 4 shows the cumulative release of 5% owf EUG loaded into electrospun PCL/PVA/CS fiber mats produced from W/O and O/W emulsions. The release profiles revealed a burst effect of 65.05 ± 3.58% and 54.61 ± 3.19% during the initial 8 hours, followed by a continuous slow and sustained release over the next days. The observed initial burst could be due to the EUG adsorbed on or near the surface of the electrospun nanofibers, while the sustained release might be due to the diffusion of EUG from electrospun nanofibers. During the period of incubation, 80.37 ± 2.19% and 70.15 ± 1.63% of total EUG were released from W/O and O/W emulsions, respectively. This result can be explained by the higher affinity of EUG for PCL phase, which results in a faster EUG release from W/O emulsions. In addition, the EUG loaded into electrospun PCL/PVA/CS fiber mats prepared from O/W

emulsion need to pass through the shell PVA/CS barrier before being released. In turn, the PVA/CS blend exhibits better wettability than the PCL and, consequently, the PVA/CS matrix is easily penetrated by the release medium, releasing the EUG quickly. Therefore, the initial EUG burst release observed is a predictable result, due to the chosen polymer blend to produce the electrospun fiber mats and selected method. The burst release can improve the therapeutic effect and accelerate the healing process, once EUG is suitable to reach some relief at the beginning of wound treatment and to stimulate an adequate initial inflammatory response, essential to proper tissue repair. These results are in agreement with Motealleh et al. [37] in that electrospun PS fibers exhibited a lower chamomile release than electrospun PCL fibers. In this study, PCL revealed greater compatibility with the chamomile extract and its flavonoid apigenin. A similar trend was displayed by EUG loaded into W/O emulsion blend. Controlling the rapid initial release of the biologically active compounds can be needed to treat specific types of wounds at different stages of healing. A variety of approaches have been employed to reduce and avoid the occurrence of an early burst release. Among them, the capacity of diffusion of a bioactive agent from electrospun nanofibers and the wetting properties of the electrospun nanofibers have been explored to achieve a desirable release profile. In addition, environmental factors, such as temperature, pH, or light response, have been considered as a stimulus for bioactive agent release.

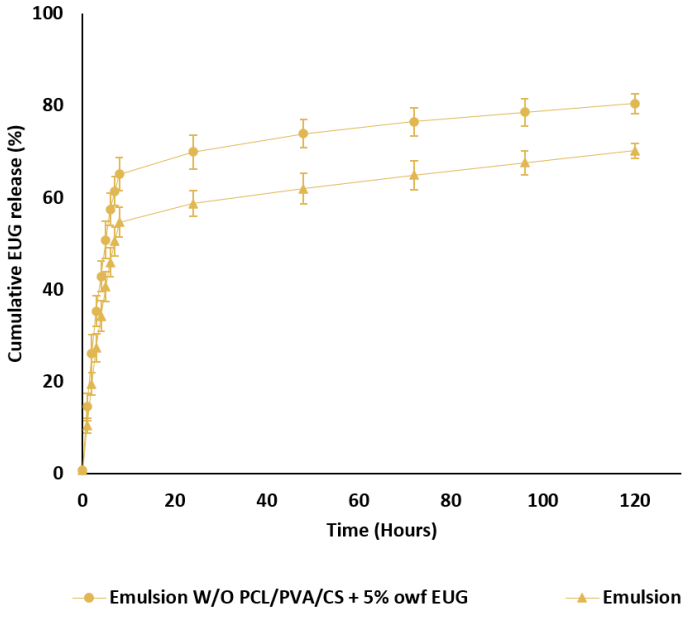

Time (h)	W/O emulsion	O/W emulsion
0	0.68 ± 0.02	0.60 ± 0.03
1	14.44 ± 3.02	10.38 ± 1.59
2	26.05 ± 4.20	19.47 ± 2.50
3	35.29 ± 3.29	27.34 ± 3.08
4	42.84 ± 3.40	34.18 ± 3.32
5	50.73 ± 4.07	40.63 ± 3.20
6	57.37 ± 3.51	45.56 ± 3.16
7	61.31 ± 3.16	50.43 ± 3.09
8	65.05 ± 3.58	54.61 ± 3.19
24	69.84 ± 3.69	58.63 ± 2.79
48	73.85 ± 3.10	61.92 ± 3.28
72	76.42 ± 3.03	64.84 ± 3.16
96	78.47 ± 2.96	67.51 ± 2.56
120	80.37 ± 2.19	70.15 ± 1.63

Figure 4 – *In vitro* release study of EUG loaded into electrospun PCL/PVA/CS fiber mats at a physiological pH of 7.4 in a PBS buffer solution for 120 hours.

3.4. Estimation of Antibacterial Activity of EUG-Loaded Electrospun PCL/PVA/CS Fiber Mats

The antibacterial efficiency of EUG loaded into electrospun PCL/PVA/CS fiber mats was quantitatively expressed as a percentage of bacterial reduction (%R) and evaluated after 24 hours against *S. aureus* and *P. aeruginosa*, two bacteria commonly present in wound infections [26].
The results showed an inhibitory effect against selected bacteria (Table 2). Interestingly, electrospun PCL/PVA/CS fiber mats obtained from W/O emulsion revealed a higher bacterial reduction against *S. aureus* (92.43%), comparatively to O/W emulsion (83.08%). The same pattern was observed for *P. aeruginosa*. The W/O emulsion showed an increased inhibitory effect in bacterial growth (94.68%) when compared to O/W emulsion (87.85%).

Table 2 – Antibacterial efficiency of EUG loaded into electrospun PCL/PVA/CS fiber mats against *S. aureus* and *P. aeruginosa*, expressed in percentage of bacterial reduction (%R).

Samples		*S. aureus* CFU/mL	*S. aureus* Growth Reduction (%)		*P. aeruginosa* CFU/mL	*P. aeruginosa* Growth Reduction (%)
W/O emulsion blend PCL/PVA/CS	oh	8.86E+04	-	oh	1.77E+06	-
	24h	3.04E+06	-	24h	6.02E+07	-
W/O emulsion blend PCL/PVA/CS + 5% owf EUG		2.30E+05	92.43%		3.20E+06	94.68%
O/W emulsion blend PCL/PVA/CS	oh	9.78E+04	-	oh	2.21E+06	-
	24h	2.51E+06	-	24h	1.90E+08	-
O/W emulsion blend PCL/PVA/CS + 5% owf EUG		4.25E+05	83.08%		2.31E+07	87.85%

These results can be explained by the difference in EUG's affinity for the polymeric blend. Such values are in agreement with those obtained for EUG release at 24 hours (58.63 ± 2.79% from O/W emulsion and 69.84 ± 3.69% from W/O emulsion (Figure 4)), where a higher EUG release from W/O resulted in a stronger inhibition of bacterial growth.
Moreover, the electrospun PCL/PVA/CS fiber mats loaded with 5% owf EUG proved to have a bacteriostatic effect (Table 3). The bacteriostatic activity values were 1.12 and 0.77 for *S. aureus*, while for *P. aeruginosa* were 1.27 and 0.92 to W/O and O/W emulsions, respectively.

Table 3 – Antibacterial activity values (bacteriostatic and bactericidal activity values).

Sample	*S. aureus* $M_B - M_C$	*S. aureus* $M_A - M_C$	*P. aeruginosa* $M_B - M_C$	*P. aeruginosa* $M_A - M_C$
W/O emulsion blend PCL/PVA/CS + 5% owf EUG	1.12	-0.23	1.27	-0.26
O/W emulsion blend PCL/PVA/CS + 5% owf EUG	0.77	-0.64	0.92	-1.02

Therefore, the antibacterial efficiency of the electrospun PCL/PVA/CS fiber mats, conferred by natural properties of CS, can be strengthened with the use of EUG, as a natural antibacterial agent. The hydrophobic nature of EUG was responsible by its mechanism of action against common pathogens present in wounds. Thus, when the EUG is partitioned into the lipid bilayer of the bacterial membrane, it changes its permeability and, consequently, rupture and release of cellular contents occur [5]. Bai et al. [38] reported the production of PCL/Chitosan nanofibers that were incorporated with tea tree oil (TTO) to improve their antibacterial ability.

3.5. Characterization of the Cytotoxicity Profile of the EUG-Loaded Electrospun PCL/PVA/CS Fiber Mats

The cytotoxic profile of the electrospun PCL/PVA/CS fiber mats with and without loaded EUG was evaluated from O/W emulsions, once these samples displayed a better capability to be applied as wound dressing materials. The results showed that the produced fiber mats did not induce any cytotoxic effect on the NHDF cells for at least 7 days, as shown in Figure 5. Moreover, the incorporation of 5% owf EUG into the emulsion blend did not compromise the cell viability. Therefore, these data reinforce the suitability of the EUG-loaded electrospun PCL/PVA/CS fiber mats for wound healing applications.

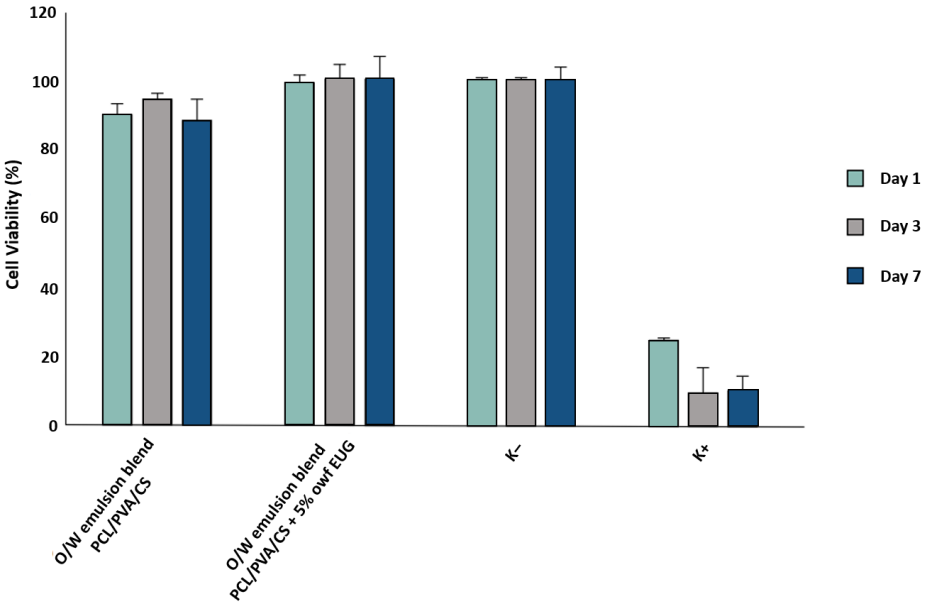

Figure 5 – NHDF cell viability percentage after 1, 3, and 7 days in direct contact with the electrospun PCL/PVA/CS fiber mats prepared from O/W emulsion, with and without loaded EUG.

4. Conclusion

In this study, EUG, an essential oil extracted from cloves, was successfully loaded into electrospun PCL/PVA/CS fiber mats in an amount of 5% (w/w), based on the weight of PCL powder, via electrospinning from either W/O or O/W emulsion. The results attained showed that the produced electrospun PCL/PVA/CS fiber mats with and without loaded EUG presented a high porous structure similar to the fibrous structure of native ECM. Moreover, these electrospun nanofibers exhibited surfaces with moderate wettability, which are able to provide suitable moisture at the wound site and better fibroblast attachment and proliferation. In addition, the antibacterial ability of EUG loaded into electrospun PCL/PVA/CS fiber mats was examined against *S. aureus* and *P. aeruginosa* and displayed the potential to inhibit bacterial growth. The *in vitro* EUG release study showed a burst release of EUG in the first 8 hours, followed by a continuous slow and sustained release over the next days. The O/W emulsion revealed a better release behaviour compared to W/O emulsion, once the cumulative EUG release from W/O emulsion resulted in a faster release rate.

Therefore, the incorporation of plant essential oils, such as EUG, which exhibit unique therapeutic properties, into electrospun fiber mats from O/W emulsion revealed better results and proved to be a noncytotoxic and highly promising approach for improving the wound healing process.

Data Availability

The data used to support the findings of this study are included in the article.

Conflicts of Interest

The authors declare that they have no conflicts of interest.

Acknowledgments

The authors acknowledge the Portuguese Foundation for Science and Technology (FCT) for funding the PhD grant PD/ BD/113550/2015. The manuscript was presented as a poster in the AMiCI WG2 workshop “Antimicrobial Coatings Applied in Healthcare Settings–Efficacy Testing”, Berlin, Germany.

References

1. Qin, Y. Medical Textile Materials. Woodhead Publishing Series in Textiles, An Imprint of Elsevier. 2016.
2. Liakos, I.; Rizzello, L.; Hajiali, H.; Brunetti, V.; Carzino, R.; Pompa, P.P.; Athanassiou, A.; Mele, E. Fibrous wound dressings encapsulating essential oils as natural antimicrobial agents. *J. Mat. Chem. B* **2015**, *3(8)*, 1583–1589.
3. Augustine, R.; Kalarikkal, N.; Tomas, S. Electrospun PCL membranes incorporated with biosynthesized silver nanoparticles as antibacterial wound dressings. *Appl. Nanosci.* **2016**, *6(3)*, 337–344.
4. Panichpakdee, P.; Pavasant, P.; Supahol, P. Electrospun cellulose acetate fiber mats containing emodin with potential for use as wound dressing. *Chiang Mai J. Sci.* **2016**, *43(1)*, 195–205.
5. Zhang, W.; Ronca, S.; Mele, E. Electrospun nanofibres containing antimicrobial plant extracts. *Nanomaterials* **2017**, *7(2)*, 42.
6. Pilehvar-Soltanahmadi, Y.; Dadashpour, M.; Mohajeri, A.; Fattahi, A.; Sheervalilou, R.; Zarghami, N. An overview on application of natural substances incorporated with electrospun nanofibrous scaffolds to development of innovative wound dressings. *Mini-Reviews in Medicinal Chemistry*. **2018**, *18*(5), 414–427.
7. Hu, X.; Liu, S.; Zhou, G.; Huang, Y.; Xie, Z.; Jig, X. Electrospinning of polymeric nanofibers for drug delivery applications. *J. Control. Release* **2014**, *185*, 12–21.
8. Raja, M.R.C.; Srinivasan, V.; Selvaraj, S.; Mahapatra, S.K. Versatile and synergistic potential of eugenol: a review. *Pharm. Anal. Acta* **2015**, *6(5)*, 367–372.
9. Kong, X.; Liu, X.; Li, J.; Yang, Y. Advances in pharmacological research of eugenol. *Curr. Opin. Complement. Altern. Med.* **2014**, *1*, 8–11.
10. Gomes, I.B.; Malheiro, J.; Mergulhão, F.; Maillard, J.-Y.; Simões, M. Comparison of the efficacy of natural-based and synthetic biocides to disinfect silicone and stainless steel surfaces. *Pathog. Dis.* **2016**, *74(4)*, fw014.
11. Moure, A.; Cruz, J.M.; Franco D.; Domínguez, J.M.; Sineiro, J.; Domínguez, H.; Núnez, M.J. Natural antioxidants from residual sources. *Food Chem.* **2001**, *72(2)*, 145–171.
12. Semnani, K.; Shams-Ghahfarokhi, M.; Afrashi, M.; Fakhrali, A.; Semnani, D. Antifungal activity of eugenol loaded electrospun PAN nanofiber mats against *Candida albicans*. *Curr. Drug Deliv.* **2018**, *15(6)*, 860–866.
13. Wang, X.; Yuan, Y.; Huang, X.; Yue, T. Controlled release of protein from core–shell nanofibers prepared by emulsion electrospinning based on green chemical. *J. Appl. Polym. Sci.* **2015**, *132(16)*, 41811.
14. Yan, S.; Xiaoqiang, L.; Shuiping, L.; Xiumei, M.; Ramakrishna, S. Controlled release of dual drugs from emulsion electrospun nanofibrous mats. *Colloids Surf. B: Biointerface* **2009**, *73(2)*, 376–381.
15. Qi, H.; Hu, P.; Xu, J.; Wang, A. Encapsulation of drug reservoirs in fibers by emulsion electrospinning: morphology characterization and preliminary release assessment. *Biomacromolecules* **2006**, *7(8)*, 2327–2330.
16. El-Newehy, M.H.; Al-Deyab, S.S.; Kenawy, E.-R.; AbdelMegeed, A. Fabrication of electrospun antimicrobial nanofibers containing metronidazole using nanospider technology. *Fiber. Polym.* **2012**, *13(6)*, 709–717.
17. Adomaviciute, E.; Milasius, R.; Levinskas, R. The influence of main technological parameters on the diameter of poly(vinyl alcohol) (PVA) nanofibre and morphology of manufactured mat. *Mater. Sci.* **2007**, *13(2)*, 152–155.

18. Liao, N.; Unnithan, A.R.; Joshi, M.K. Electrospun bioactive poly(ε-caprolactone)-cellulose acetate-dextran antibacterial composite mats for wound dressing applications. *Colloid Surf. A-Physicochem. Eng. Asp.* **2015**, *469*, 194–201.

19. Zarghami, A.; Irani, M.; Mostafazadeh, A.; Golpour, M.; Heidarinasab, A.; Haririan, I. Fabrication of PEO/chitosan/ PCL/olive oil nanofibrous scaffolds for wound dressing applications. *Fiber. Polym.*, **2015**, *16(6)*, 1201–1212.

20. Ajalloueian, F.; Tavanai, H.; Hilborn, J. Emulsion electrospinning as an approach to fabricate PLGA/chitosan. *BioMed Res. Int.* **2014**, *2014*, 475280.

21. Chen, J.-P.; Chang, G.-Y.; Chen, J.-K. Electrospun collagen/ chitosan nanofibrous membrane as wound dressing. Colloid. Surf. A-Physicochem. Eng. Asp. **2008**, *313*, 183–188.

22. Zhou, Y.; Yang, H.; Mao, J.; Gu, S.; Xu, W.; Liu, X. Electrospinning of carboxyethyl chitosan/poly(vinyl alcohol)/ silk fibroin nanoparticles for wound dressings. *Int. J. Biol. Macromol.* **2013**, *53*, 88–92.

23. Zhang, R.; Xu, W.; Jiang, F. Fabrication and characterization of dense chitosan/polyvinyl-alcohol/ poly-lactic-acid blend membranes. *Fiber. Polym.* **2012**, *13(5)*, 571–575.

24. Liang, D.; Lu, Z.; Yang, H.; Gao, J.; Chen, R. Novel asymmetric wettable AgNPs/chitosan wound dressing. *In vitro* and *in vivo* evaluation. *ACS Appl. Mater. Interfaces* **2016**, *8(6)*, 3958–3968.

25. Chitrattha, S.; Phaechamud, T. Porous poly(DL-lactic acid) matrix film with antimicrobial activities for wound dressing application. *Mater. Sci. Eng. C* **2016**, *58*, 1122–1130.

26. Bessa, L.J.; Fazii, P.; Di Giulio, M.; Cellini, L. Bacterial isolates from infected wounds and their antibiotic susceptibility pattern: some remarks about wound infection. *Int. Wound J.* **2015**, *12*, 47–52.

27. Tang, B.; Wang, J.; Xu, S. Application of anisotropic silver nanoparticles: multifunctionalization of wool fabric. *J. Colloid Interface Sci.* **2011**, *356*, 513–518.

28. Sanla-Ead, N.; Jangchud, A.; Chonhenchob, V.; Suppakul, P. Antimicrobial activity of cinnamaldehyde and eugenol and their activity after incorporation into cellulose-based packaging films. *Packag. Technol. Sci.* **2012**, *25*, 7–17.

29. Mary, S.A.; Giri Dev, V.R. Electrospun herbal nanofibrous wound dressings for skin tissue engineering. *J. Text. Inst.* **2015**, *106(8)*, 886–895.

30. Hu, J.; Prabhakaran, M.P.; Ding, X.; Ramakrishn, S. Emulsion electrospinning of polycaprolactone: influence of surfactant type towards the scaffold properties. *J. Biomater. Sci.-Polym. Ed.* **2015**, *26(1)*, 57–75.

31. Briggs T.; Arinzeh, T.L. Examining the formulation of emulsion electrospinning for improving the release of bioactive proteins from electrospun fibers. *J. Biomed. Mater. Res. Part A* **2014**, *102(3)*, 674–684.

32. Hajiali, H.; Summa, M.; Russo D.; Armirotti, A.; Brunetti, V.; Bertorelli, R.; Athanassiou, A.; Mele, E. Alginate–lavender nanof ibers with antibacterial and anti-inflammatory activity to effectively promote burn healing. *J. Mat. Chem. B* **2016**, *4(9)*, 1686–1695.

33. Gholipour-Kanani, A.; Bahrami, S.H.; Rabbani, S. Effect of novel blend nanofibrous scaffolds on diabetic wounds healing. *IET Nanobiotechnol.* **2016**, *10*, 1–7.

34. Lim, M.M.; Sun, T.; Sultana, N. *In vitro* biological evaluation of electrospun polycaprolactone/gelatine nanofibrous scaffold for tissue engineering. *J. Nanomater.* **2015**, *2015*, 303426.

35. Cui, J.; Qiu, L.; Qiu, Y.; Wang, Q.; Wei, Q. Co-electrospun nanofibers of PVA-SbQ and zein for wound healing. *J. Appl. Polym. Sci.* **2015**, *132(39)*, 42565.

36. Maretschek, S.; Greiner, A.; Kissel, T. Electrospun biodegradable nanofiber nonwovens for controlled release of proteins. *J. Control. Release* **2008**, *127(2)*, 180–187.

37. Motealleh, B.; Zahedi, P.; Rezaeian, I.; Moghimi, M.; Abdolghafari, A.H.; Zarandi, M.A. Morphology, drug release, antibacterial, cell proliferation, and histology studies of chamomile-loaded wound dressing mats based on electrospun nanofibrous poly(E-caprolactone)/polystyrene blends. *J. Biomed. Mater. Res. Part B* **2014**, *102*, 977–987.

38. Bai, M.-Y.; Chou, T.-C.; Tsai, J.-C.; Yu, W.-C. The effect of active ingredient-containing chitosan/polycaprolactone nonwoven mat on wound healing: *In vitro* and *in vivo* studies. *J. Biomed. Mater. Res. Part A* **2014**, *102(7)*, 2324–2333.

Paper 3 - Emulsion electrospinning of PLLA/PVA/Chitosan with *Hypericum perforatum* L. as an antibacterial nanofibrous wound dressing

Abstract

Chronic wounds are one of the most severe health problems that affect millions of people worldwide. These types of injuries impair healing and lead to life-threatening complications. Therefore, suitable wound dressing materials are essential to prevent the risk of infection and to provide an excellent healing environment.

The present research reports the development of an electrospun Poly(L-lactic acid) (PLLA)/ Poly(vinyl alcohol) (PVA)/ Chitosan (CS) wound dressing materials, produced via emulsion electrospinning in a single step. The electrospun PLLA/PVA/CS fiber mats were loaded with two different amounts of *Hypericum perforatum* L. (HP) (2.5% and 5.0% owf). The results revealed that the produced electrospun PLLA/PVA/CS fiber mats displayed ideal properties as a wound dressing due to a total porosity, wettability, water vapor transmission rate (WVTR), and swelling properties similar to those reported for the extracellular matrix (ECM) of the skin, mainly when 2.5% owf HP was incorporated. Moreover, the electrospun PLLA/PVA/CS fiber mats containing HP were able to prevent the growth of *Staphylococcus aureus* (*S. aureus*) without causing cytotoxicity to normal human dermal fibroblasts (NHDF). These findings suggest that these electrospun dressing mats are helpful to prevent wound infections as well as an appropriate support and microenvironment for wound healing.

Graphical Abstract

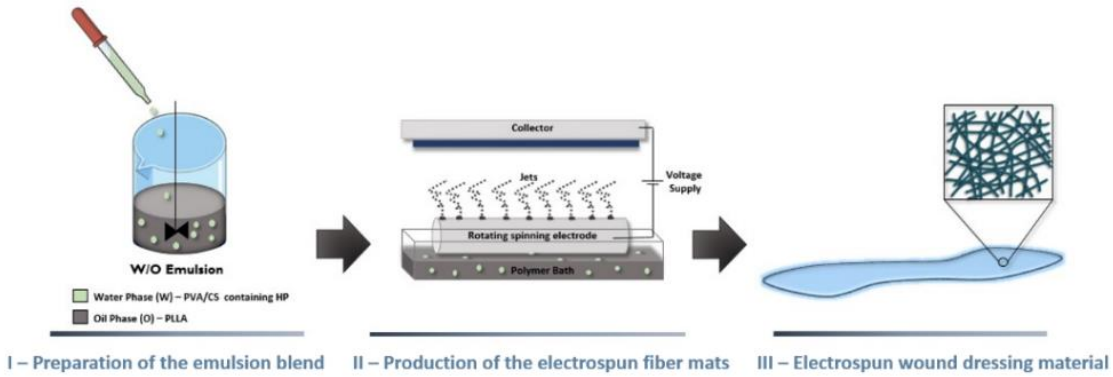

Keywords: Emulsion electrospinning; crude plant extracts; *Hypericum perforatum* L.; antimicrobial wound dressing, chronic wounds.

1. Introduction

Skin damages usually result in a dynamic and complex process mediated through a coordinated cascade of biological events, which are traditionally divided into four distinct but overlapping phases: hemostasis, inflammation, proliferation, and maturation [1-5]. Nevertheless, the healing process can be severely impaired by several factors, and consequently, the wound repair cannot proceed in a timely and orderly manner, resulting in chronic, hard-healing wounds [3,4,6].

Chronic wounds have become a severe public healthcare concern and are strongly associated with significant morbidity and mortality [1-4,6,7]. Nowadays, more than 10 million people around the world are affected by this problem, and it is expected to increase due to an aging population and the sharp rise of diabetes and obesity [4,7,8]. Their higher incidence is generally associated with venous or arterial insufficiency, prolonged pressure, or diabetes [7,9,10].

So far, diverse approaches have been employed for the management of these wounds. Among them, the application of an antimicrobial dressing, which helps in reducing inflammation and prevent wound contamination, has been regarded as a useful practice to treat and avoid chronic wounds occurring [5,8,11]. However, successful healing of chronic wounds often requires long periods of treatment, and as expected, their management is costly. To overcome these limitations, suitable wound dressing materials that actively promote wound regeneration have attracted researchers' attention due to their therapeutic potential. More specifically, wound dressings which protect the wound from external threats and subsequent infection, while absorbing wound exudate, creating and maintaining a moist wound environment, as well as nutrients and gas exchange have been developed to encourage the healing process [5,12-14].

Nowadays, many different techniques are being employed to produce micro to nanoscale materials, including electrospinning, phase separation, and self-assembly. Nevertheless, electrospinning has become one of the most desirable and attractive methods to develop nanofiber-based dressings, due to its remarkable properties, as the extremely high surface area to volume ratio and high porosity, as well as the potential of mimicking the skin extracellular matrix (ECM) composition. These features are essential to keep an appropriate microenvironment for cell adhesion and proliferation [4,5,8,12-16]. Moreover, electrospinning allows the incorporation of bioactive agents into the electrospun nanofibers to enhance the functional and biologic performance of these wound dressing materials [4,5,8,12]. Among the numerous bioactive compounds, antibiotics, antimicrobial, anti-inflammatories, analgesics, vitamins, growth factors, and natural agents as medicinal plants, have been considered as a promising supplement for the management and treatment of wounds [3,5].

Accordingly, this research work describes the innovative use of the nanospider technology, a modified electrospinning technique based on a rotating spinning electrode to produce electrospun Poly(L-lactic acid) (PLLA)/ Poly(vinyl alcohol) (PVA)/ Chitosan (CS) fiber mats containing *Hypericum perforatum* L. (HP), St. John's Wort, via emulsion electrospinning [3,17].

HP has been applied for the treatment of different skin disorders like eczema, burns, and diabetic wounds [3,17]. Besides, different bioactive metabolites such as naphthodianthrones, phloroglucinols, flavonoids, bioflavonoids, and phenylpropanoids have been found in HP extracts and associated with antifungal, antimicrobial, antiviral, and anti-inflammatory activities [3]. In turn, the PLLA, a synthetic tissue-compatible polymer approved by the US Food and Drug Administration (FDA) for direct contact with biological fluids, was used to provide mechanical protection against external threats and prevent fluid loss from the wound surface [18,19]. Additionally, CS was blended with a carrier polymer like the highly hydrophilic, non-toxic, biocompatible, and biodegradable PVA to suppress the difficulty of producing pure CS nanofibers by electrospinning due to its high viscosity in an acidic aqueous solution. CS has revealed promising wound healing abilities and scar-prevention properties, once it can stimulate collagen synthesis and displays antimicrobial and hemostatic properties [20-25].

Herein, the electrospun PLLA/PVA/CS materials were loaded with crude HP extracts to prevent bacterial growth and facilitate the healing process. The effective loading of crude HP extracts into PLLA/PVA/CS emulsions was evaluated, and the results revealed that this cost-effective and eco-friendly natural bioactive agent was successfully applied to these wound dressing materials. Furthermore, emulsion electrospinning revealed to be an alternative approach to produce, in a single step, wound dressings made up from multiple polymers, and displaying antimicrobial activity.

2. Experimental

2.1. Materials

The aerial parts of *Hypericum perforatum* L. (HP) was bought from a Portuguese botanic shop. Poly(L-lactic acid) (PLLA) with an average molecular weight of 217,000-225,000 g/mol, Purasorb® (PL18), was provided from Corbion Purac. Poly(vinyl alcohol) (PVA) (MW 115,000 g/mol) was purchased from VWR Chemicals, and Chitosan (CS) (MW 50,000-190,000 g/mol, degree of deacetylation 75-85%) was obtained from Sigma-Aldrich. Chloroform (analytical grade), dimethylformamide (DMF) (analytical grade), glacial acetic acid, and ethanol absolute were purchased from Fisher Chemical. Nutrient agar (NA), nutrient broth (NB), and agar for microbiology were obtained from Fluka. Sodium chloride (NaCl), mueller-hinton broth (MHB), tween 80, dimethyl sulfoxide (DMSO) anhydrous ≥99.9%, trypsin, and 3-(4,5-Dimethyl-2-thiazolyl)-2,5-diphenyl-2H-tetrazolium bromide (MTT) were provided from Sigma Aldrich. Normal human dermal fibroblasts (NHDF) cells were acquired from ATCC – American Type Culture Collection. Phosphate-buffered saline (PBS) was purchased from Alfa Aesar. All solvents were used as received without further purification.

2.2. Crude ethanol HP extract

2.2.1. Preparation of crude HP extract

Ethanol extracts from the aerial parts of the HP species were obtained by direct maceration of dried and powdered plant material (2.50 g) in 80% ethanol for 24 hours at room temperature. Extracts were filtered, and the solvent was evaporated by Rotavapor (Buchi Rotavapor RE 111) to give dried extracts. The extract yield percentage based on the starting material was 20.44%. Finally, the dried HP extract was used for all experiments, as described below.

2.2.2. Quantification of total Hypericin (Hyp) content in crude ethanol HP extract

The total content of Hyp, one of the main bioactive agents present in the crude HP extract, was analyzed by the spectrophotometric method. For this purpose, standard solutions of dried crude HP extract with concentrations from 6000 to 50 ppm were prepared. Then, the Hyp content (% Hyp (w/w)) was determined by the optical absorbance of each HP solution at 587 nm, using phosphate buffer saline (PBS) pH=5.5 as control. These measurements were performed according to describe by Pourhojat et al. and calculated using the following Equation (1) [26]:

$$\text{Hyp } (\%) = \frac{A}{780}\frac{100}{m} \quad (1)$$

Where A is the measured absorbance, m the weight of HP extract after drying of 25 mL of crude extract, and 780 the specific absorbance of Hyp at 587 nm.

2.3. Determination of Minimum Inhibitory Concentration (MIC) of crude ethanol HP extract

Minimal Inhibitory Concentration (MIC) of crude ethanol HP extract against *Staphylococcus aureus* (ATTC 6538) (gram-positive) (*S. aureus*), was measured by broth microdilution assay according to NCLS M07-A6 guidelines. Briefly, crude ethanol HP extract stock solution was prepared to a final concentration of 20 mg/mL and then serially diluted with sterile Mueller-Hinton Broth (MHB) on range from 0.1 to 10 mg/mL.

Afterward, an overnight liquid culture of *S. aureus* was adjusted to 0.5 McFarland turbidity standards using sterile water and the bacterial work suspension prepared from 500 µL of the 0.5 McFarland suspension and 4500 µL of MHB. Then, 50 µL of bacterial work suspension and 50 µL of the crude ethanol HP extract dilutions were added into 96 multi-well plates.

The multi-well plates were incubated for 24 hours at 37 °C. After the incubation period, the MIC corresponded to the well containing the lowest HP concentration, which did not show visible bacterial growth or turbidity in the culture medium. All the determinations were performed in triplicate.

2.4. Preparation of Electrospinning Emulsions

CS (4% w/v) and PVA (8% w/v) solutions were initially prepared separately by dissolving CS in acetic acid (14%) at room temperature and PVA in deionized water at 90 °C. Then, the PVA/CS binary blend solution was obtained by the blending of PVA and CS with a ratio of 2:1 and stirring at room temperature during a few minutes. Also, PLLA (10% w/v) was dissolved in chloroform and DMF (9:1 volume ratio) at room temperature using a magnetic stirrer until complete polymer dissolution.
The emulsions were prepared by simultaneous adding of PVA/CS binary blend solution to PLLA solution, followed by mixing with a high-speed homogenizer (Techmatic S2) for 4 hours at room temperature to ensure complete dissolution and obtain homogenous emulsions.

2.5. Electrospinning

2.5.1. Preparation of electrospun PLLA/PVA/CS fiber mats containing crude HP extracts

The stable and homogenous PLLA/PVA/CS emulsions were electrospun using Nanospider Technology (Nanospider laboratory machine NS LAB 500S from Elmarco s.r.o., Czech Republic, *http://www.elmarco.com*). Electrospun fiber mats containing different amounts of crude HP extract were also produced. The crude HP extracts were added to the PVA/CS blend to obtain solutions containing 2.5 and 5.0% (based on the weight of PVA/CS blend (owf)). All resulting solutions were electrospun at an applied voltage of 80.0 kV, using a working distance (distance from the electrode to collector) of 10 cm and an electrode rotation rate of 70 Hz. Each solution was electrospun for 1 hour on polypropylene non-woven fabric (collector) at 25 °C and relative humidity up to 35%. After spinning, the produced electrospun PLLA/PVA/CS fiber mats with and without crude HP extracts were dried and stored in a vacuum desiccator until constant weight and then used for characterization and bioactive experiments.

2.6. Nanofibers Characterization

2.6.1. Surface Morphology of Electrospun Fiber Mats

The morphology of the electrospun PLLA/PVA/CS fiber mats with and without crude HP extracts was observed by a scanning electron microscope (SEM; Hitachi S2700) at a high voltage of 20 kV. The

fiber diameters were analysed with the help of the Image J software (National Institutes of Health, Bethesda, MD, USA) while both average diameter and diameter distribution were evaluated using GraphPad Prism 6 software (Prism Software, USA).

2.6.2. Fourier Transform Infrared Spectroscopy (FT-IR)

The differences in chemical structure between the electrospun PLLA/PVA/CS fiber mat and the electrospun PLLA/PVA/CS fiber mats loaded with crude HP extracts were analysed using Thermo-Nicolet is10 FT-IR spectrophotometer over the range 400-4000 cm^{-1}. FT-IR spectra were collected from 64 scans at 4 cm^{-1} resolution.

2.6.3. Porosity Measurement

The porosity values of dry raw electrospun PLLA/PVA/CS fiber mat and the electrospun PLLA/PVA/CS fiber mats loaded with crude HP extracts were determined by using a liquid displacement technique as described previously by Chitrattha et al. [27]. Ethanol was chosen as the displacement liquid due to high penetrating power into the pores and because it did not cause shrinking or swelling of the samples.

Briefly, the dried samples were weighed (W_s) and placed in a graduated cylinder with a known volume (20 mL) of displacement liquid (W_1). Then, the cylinders containing the electrospun fiber mats immersed into the displacement liquid were placed in a water sonicator bath (Ultrasons-H, P-Selecta) for 40 minutes at 30 °C to force the penetration of ethanol into the pores. After that, the volume of displacement liquid in the sonicated cylinders containing the ethanol-impregnated samples was readjusted to 20 mL and reweighed (W_2). Subsequently, the cylinders were weighed again after removing the saturated samples with ethanol (W_3). The total porosity (ε) of the electrospun fiber mats was determinate using the following Equation (2) [27]:

$$\varepsilon\ (\%) = \frac{(W_2 - W_3 - W_S)}{(W_1 - W_3)} \times 100 \quad (2)$$

2.6.4. Water Contact-Angle Determination

The static contact angles for water (WCA) on the electrospun PLLA/PVA/CS fiber mats with and without crude HP extracts were measured using Data Physics Contact Angle System OCAH-200 apparatus to characterize the surface wettability. For each sample, the contact angle was determined from sessile drop method, i.e., deionised water droplets were deposited on the surface of the dried electrospun fiber mats at room temperature. The contact angles were reported as the average of three independent measurements.

2.6.5. Water Vapor Transmission Rate (WVTR)

Water vapor diffusion rates were measured following the ASTM E96/E96M-15 standard method, for all the samples, i.e., raw electrospun PLLA/PVA/CS fiber mat, and electrospun PLLA/PVA/CS fiber mats loaded with crude HP extracts. Briefly, each sample was attached to the opening of a glass test tube (1.20 cm in diameter) with 10 mL of deionized water using parafilm tape to prevent any moisture loss. Subsequently, the samples-glass tubes assembly was incubated at 37 °C. The water evaporation from each sample was determined by weight loss at predetermined intervals through Equation (3):

$$\text{Water Vapor Transmission Rate (WVTR)} = \frac{W_{loss}}{A} \quad (3)$$

Where W_{loss} is the daily weight loss of water, and A is the area of the glass tube opening. All the measurements were performed in triplicate.

2.6.6. Swelling Determination

The swelling behavior of the electrospun PLLA/PVA/CS fiber mat with and without crude HP extracts was evaluated by the water retention test. Briefly, pre-weighted dried samples (W_{dry}) were immersed in phosphate-buffered saline (PBS, pH=5.5) during 120 hours at 37 °C, which plays a crucial role in the maintenance of healthy skin microbiome and has beneficial wound healing effects. At specific periods, the weights of the swollen samples (W_{wet}) were determined after removing the PBS solution excess present at the surface of each sample by carefully with a filter paper. All measurements were conducted in triplicate, and the swelling ratio calculated using Equation (4):

$$\text{Swelling Ratio (\%)} = \frac{(W_{wet} - W_{dry})}{W_{dry}} \times 100 \quad (4)$$

2.7. *In vitro* release study of HP-loaded electrospun PLLA/PVA/CS fiber mats

In vitro releasing of crude HP extracts from electrospun PLLA/PVA/CS fiber mats containing different amounts of HP was carried out, and analysed by UV-Vis spectrometry. To accomplish this, standard HP solutions were prepared with different concentrations to draw a calibration curve at 587 nm [26]. Afterward, 2 cm × 2 cm samples were immersed in 10 mL of PBS at pH=5.5 and then incubated in an incubator shaker at 37 °C under constant rotation at a speed of 100 rpm to measure the HP amount released into the PBS release medium. After specific time intervals, 3 mL of release medium was recovered and, at the same time, replenished with an equal volume of the fresh PBS. The HP concentration that remained in the release medium at each time point was quantified at 587 nm using a UV-Vis spectrophotometer. All measurements were carried out in triplicate.

2.8. Antibacterial Activity Assessment

The antibacterial effect of crude HP extracts loaded into electrospun PLLA/PVA/CS fiber mats was tested through ASTM E2180-07. Briefly, a bacterial suspension (*S. aureus* (ATTC 6538), 1-5×10^8 CFU/mL) was prepared from overnight liquid culture, added in an agar slurry (0.85 (w/v) NaCl and 0.30 (w/v) agar-agar in deionized water) and then spread over the 3 cm x 3 cm square samples. The samples were assessed immediately after inoculum application (T_{oh}) and after 18-24 hours in contact with the inoculum agar slurry at 37 °C for 18-24 hours (T_{24h}). To accomplish this, 0.85 (w/v) NaCl was used to do serial dilutions and then plated in the NA medium and incubated for 18-24 hours at 37 °C.

The antimicrobial activity was calculated to determine bacterial growth inhibition (%Inhibition) by the following Equation (5):

$$\text{Bacterial growth inhibition (\%)} = \frac{C-S}{C} \times 100 \quad (5)$$

Where C is the average value of Colony Forming Units (CFU) on the control sample (electrospun PCL/PVA/CS fiber mat), and S is the average value of CFU on the samples containing different amounts of crude HP extract (electrospun HP-loaded PLLA/PVA/CS fiber mats) [28].

2.9. *In vitro* cytotoxicity Evaluation

Changes in cell viability produced by the electrospun fiber mats were evaluated by direct cytotoxicity assay using 3-(4,5-dimethylthiazol- 2-yl)-2,5-diphenyltetrazolium bromide (MTT) colorimetric method following ISO 10993–5 (Biological evaluation of medical devices-Part 5: Tests for *in vitro* cytotoxicity). Briefly, the samples were placed in 24-well plates occupying < 10% of its area and then sterilized by UV irradiation (254 nm, ~7 mW cm^{-2}) for 1 hour. After that, normal human dermal fibroblasts (NHDF) cells were seeded onto the samples at a cell density of 1×10^4 cells/well and then incubated during 1, 3, and 7 days at 37 °C, in an incubator under a 5% CO_2 humidified atmosphere. After the incubation period, the cellular metabolic activities were evaluated through the cleavage of the MTT tetrazolium ring and formation of the formazan blue crystals. For this purpose, the medium of each well was removed and then a mixture of fresh culture medium containing the MTT solution added to each well. After 4 hours of incubation, the content of each well was replaced by DMSO to dissolve the formazan crystals. After shaking, the optical densities (OD) of each sample (n=5) were measured at 570 nm using a microplate reader (Biorad xMark microplate spectrophotometer). Cells only in the culture medium and cells cultured in EtOH (96%) were included as a negative (K^-) and positive (K^+) controls, respectively.

2.10. Statistical Analysis

The statistical analysis of the results obtained was carried out by analysis of variance (ANOVA) followed by multiple comparison tests using Turkey's test at the 95% confidence level. Statistical analyses were performed in GraphPad Prism 6 software (Prism Software, USA).

3. Results and Discussion

3.1. Quantification of total Hypericin (Hyp) content in crude ethanol extract of HP

The content of the Hyp present in the ethanol extract of HP was measured by the spectrophotometric method. The Hyp is one of the main bioactive agents present in HP extracts, and it is responsible for several therapeutic properties. As seen in Table 1, the total Hyp content was 0.30 ± 0.07 (%), according to the calibration equation (y = 0.0002x - 0.0234) with an $r^2 = 0.99$. These results showed a linear relationship between the concentration of Hyp and absorbance at 587 nm. Similar results have been already reported by Pourhojat et al., who obtained a total Hyp content from HP extract of 0.23 ± 0.06 (%) [26]. Therefore, the extraction method was efficiently accomplished.

Table 1 – Determination of Hypericin (Hyp) content in crude ethanol extract of HP.

Samples	Dried extract (ppm)	Dried extract (g)	Absorbance in λ_{587}	***Hyp*** (%)
1	6000	0.30	0.86	0.37
2	4000	0.20	0.64	0.41
3	3000	0.15	0.39	0.33
4	1000	0.05	0.07	0.19
5	500	0.025	0.04	0.21
6	200	0.01	0.02	0.27
7	100	0.005	0.01	0.26
8	50	0.0025	0.01	0.33
				Average = 0.30 ± 0.07

3.2. Determination of Minimum Inhibitory Concentration (MIC) of crude HP extract

MIC value of crude ethanol extract of HP against *S. aureus* was found to be 2.50 mg/mL. According to Okmen et al., methanol HP flower extracts gave a MIC value against *S. aureus – 17* of 3.25 mg/mL and a MIC value of 1.63 mg/mL against *S. aureus – 18*, respectively [29]. On the other hand, Reichling et al. obtained MIC values of 2.50 mg/mL and in the range of 1.3-2.50 mg/mL, for several filtered teas and loose teas from HP against *S. aureus*, which were similar to the MIC value obtained in this study (2.50 mg/mL), and therefore in the expected range [30].

3.3. Electrospun Fiber Mats Characterization

3.3.1. Surface Morphology of Electrospun Fiber Mats

The morphological properties of electrospun PLLA/PVA/CS fiber mats with and without crude HP extracts were analysed by SEM. SEM micrographs and the fiber-diameter frequency distribution of the samples are shown in Figure 1. The electrospun PLLA/PVA/CS fiber mats displayed fibers uniformly distributed and randomly oriented with a mean diameter of 173.57 ± 41.00 nm. Nevertheless, when 2.5% owf crude HP extract was loaded, the surface morphology exhibited thinner fibers with a mean diameter of 119.96 ± 29.90 nm. Therefore, the addition of HP extract reduced the viscosity of the electrospun solution, and consequently, the average fiber diameters decreased. However, spindles or bead-on-a-string fiber morphologies with a mean of 194.61 ± 40.30 nm were formed when the ratio of crude HP extract increased further to 5.0% owf, due to the difficulty in obtaining stable electrospun jets.

Similar results were found by Zarghami et al., who produced PCL/olive oil nanofibers with three different concentrations of olive oil (1.0%, 2.0%, and 3.0%) [20]. They found homogeneous and uniformly dispersed nanofibers when 1.0% and 2.0% olive oil were incorporated, while PCL loaded with 3.0% olive oil was difficult to produce uniform fibers. Consequently, beads and droplets alongside were observed.

Furthermore, Zarghami et al. also revealed that thinner and homogeneous nanofibers with minimum diameter are preferred to obtain a maximum surface area and porosity structure [20]. In this context, the production of electrospun PLLA/PVA/CS fiber mats by incorporating two different weight percentages of crude HP extract demonstrated that 2.5% owf of HP is required to improve the healing process.

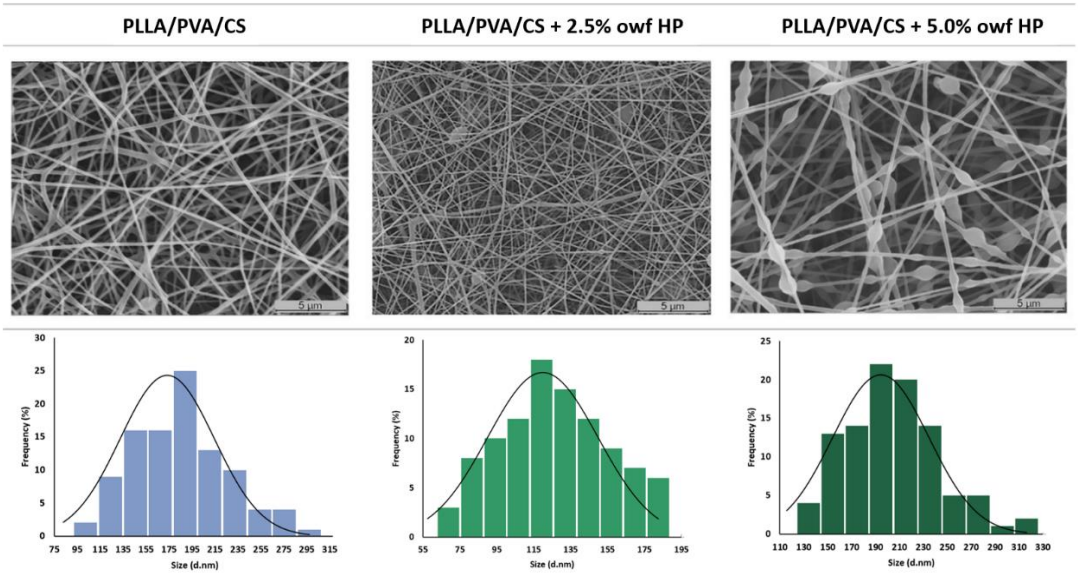

Figure 1 – Characterization of the morphologic features of the electrospun PLLA/PVA/CS fiber mats with and without crude HP extracts. SEM images, fiber diameter, and the size distribution of the fibers.

3.3.2. Attenuated Total reflectance-Fourier transform infrared spectroscopy (ATR-FTIR) Analysis

ATR-FTIR spectra of the raw electrospun PLLA/PVA/CS fiber mats and electrospun PLLA/PVA/CS fiber mats containing crude HP extracts are presented in Figure 2. All the acquired spectra exhibit the characteristic bands of both CS and PVA, as well as PLLA. A broad band is observed in ATR-FTIR spectra around 3000-3500 cm^{-1} due to O-H and N-H stretching vibrations of both CS and PVA backbone [31]. On the other hand, the C=O stretching of PLLA is observed as a strong band around 1755.00 cm^{-1}, while the C-O-C stretching vibration appears as a band near 1183.00 cm^{-1} [32]. Moreover, the spectra of electrospun PLLA/PVA/CS fiber mats loaded with crude HP extracts present bands at 880 cm^{-1}, between 1500 cm^{-1} and 1600 cm^{-1}, as well as near 1200 cm^{-1}, representing the aromatic rings of HP extract, the C=C stretching vibrations, and C-O phenolic groups, respectively [26].

Furthermore, the FT-IR spectra of the electrospun PLLA/PVA/CS fiber mats suggest that the intensity of bands increases as the concentration of crude plant extract. Therefore, the higher intensity of the broad peak at 3400 cm^{-1} is consistent with the concentration of HP incorporated, and consequently proves the successful blending of the crude HP extracts with electrospun PLLA/PVA/CS fiber mats.

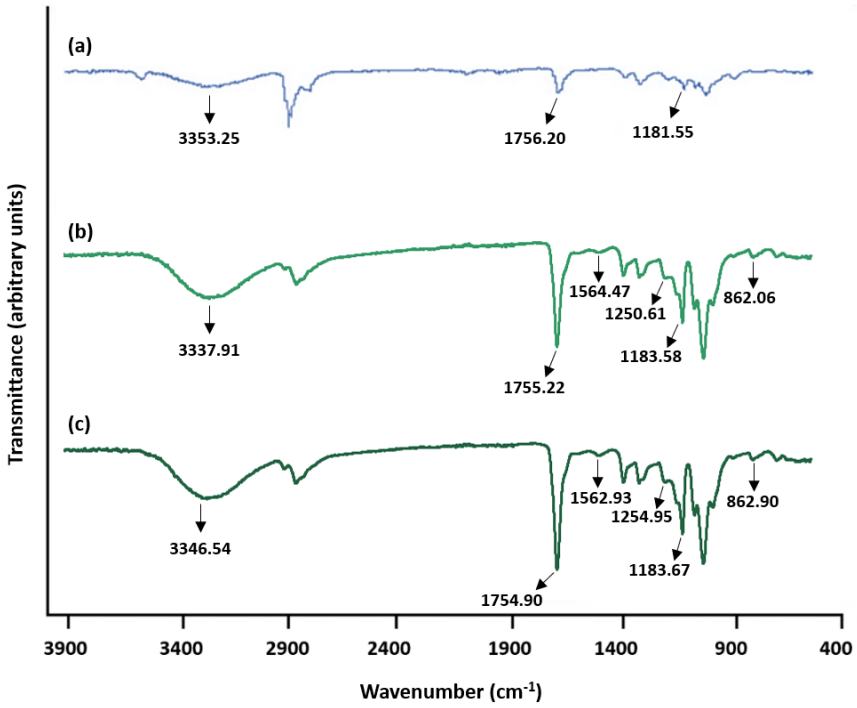

Figure 2 – FT-IR spectra of the raw electrospun PLLA/PVA/CS fiber mats (**a**) and electrospun PLLA/PVA/CS nanofiber mats containing 2.5% and 5.0% owf crude HP extract, (**b**) and (**c**), respectively.

3.3.3. Porosity Measurement

All the electrospun PLLA/PVA/CS fiber mats with and without crude HP extracts showed a highly porous structure. The total porosity of the raw electrospun PLLA/PVA/CS fiber mats was 84.52 ± 6.88%. In comparison, electrospun PLLA/PVA/CS fiber mats containing 2.5% and 5.0% owf HP presented a total porosity of 93.30 ± 1.24% and 80.03 ± 2.08%, respectively.

The slightly higher porosity value measured for the electrospun PLLA/PVA/CS fiber mats containing 2.5% HP owf can be related to the lower fiber diameters, which promote the available pore spacing between fibers. On the other hand, the difficulty in producing uniform and thinner fibers when 5.0% owf HP was loaded resulted in a lower porosity value.

Recently, Yousefi et al. produced electrospun fiber mats loaded with multiple Henna extracts (0-2 wt%) [33]. Their results revealed that the incorporation of 2 wt% Henna led to the production of uniform fibers with thinner diameters. Furthermore, several researchers have recently highlighted that highly porous structures with porosities above 90% are most suitable to provide the required space for cell adhesion, spreading, and migration, which promotes the production of the new ECM [34].

In this context, 2.5% owf crude HP extract proved to be the most effective amount of crude plant extract used to display a proper oxygen permeability, as well as providing nutrients and fluids exchange through the skin surface, promoting the wound healing process.

3.3.4. Water Contact-Angle Determination

WCA on the electrospun PLLA/PVA/CS fiber mats with and without crude HP extracts were measured to assess the surface wettability and hydrophilicity of these materials. Based on the previously described in the literature to polymer surfaces, WCA values ranging 40-70° correspond to a moderate wettability surface, which is optimal for cell adhesion, while WCA values > 90° and WCA values < 20° report that the surface is hydrophobic and highly hydrophilic, respectively [35,36].

In the present study, the raw electrospun PLLA/PVA/CS fiber mats revealed a hydrophobic character (WCA of 94.94 ± 3.45°), while the electrospun PLLA/PVA/CS fiber mats loaded with 2.5 and 5.0% owf crude HP extracts presented WCA values of 52.22 ± 8.17° and 48.10 ± 7.01°, respectively. Such values demonstrated a more hydrophilic character when crude HP extracts were incorporated, due to their hydrophilic functional groups. Moreover, these WCA values showed a moderate wettability that is essential to improve the initial adhesion and migration of cells, as well as their proliferation to the wound site. Furthermore, moderate hydrophilic materials are suitable to assure the maintenance of an optimally moist wound environment to prevent wound dehydration [37,38].

Similarly, Jin et al. showed that the highly hydrophobic electrospun PCL fibers became more hydrophilic when plant extracts (*Indigofera aspalathoides*, *Azadirachta indica*, *Memecylon edule*,

and *Myristica andamanica*) were incorporated [38]. The study also revealed that moderate hydrophilic surfaces displayed a better affinity toward cells.

3.3.5. Water Vapor Transmission Rate (WVTR)

WVTR was measured to evaluate the ability of the produced electrospun fiber mats to provide an optimal moist wound environment, which plays a vital role in the wound healing process by preventing dehydration and fluids accumulation while enhancing the re-epithelization process [39,40].

Depending on the type of wound and stage of healing, the WVTR from skin can change in a broad range. Typically, an WVTR for healthy skin is reported as 204 g m^{-2} day^{-1} while that for injured skin can range from 279 g m^{-2} day^{-1} to 5138 g m^{-2} day^{-1} [39-41].

The electrospun PLLA/PVA/CS fiber mat resulted in a WVTR of 1890.71 ± 104.50 g m^{-2} day^{-1}, while electrospun PLLA/PVA/CS fiber mats loaded with 2.5% and 5.0% owf crude HP extracts reported WVTRs of 2230.58 ± 39.49 and 1729.50 ± 38.47 g m^{-2} day^{-1}, respectively. Hence, the electrospun PLLA/PVA/CS fiber mats loaded with 2.5% owf HP revealed a higher WVTR than the ones achieved by using a higher crude HP extract ratio, mainly due to the high porosity and hydrophilic character.

Chitrattha *et al.* revealed that the hydrophilic character of PLA was improved when PEG was incorporated, and consequently enhanced their WVTR values [27]. On the other hand, Alippilakkotte *et al.* produced PLA/silver nanofibers by electrospinning [42]. The silver-extract nanoparticles were synthesized from *Momordica charantia* fruit extract and loaded with three different concentrations (1.0 wt% (PLA-1Ag), 2.0 wt% (PLA-2Ag) and 3.0 wt% (PLA-3Ag)). Their results demonstrated that the WVTR rate of PLA-2Ag sample was significantly lower than the PLA-1Ag and PLA-3Ag samples, respectively. The acquired data were explained by the lower porosity for this sample, and are in accordance with the WVTR of the electrospun PLLA/PVA/CS fiber mats containing 5.0% owf crude HP extract. Therefore, the WVTR values obtained in the present study suggest that the electrospun PLLA/PVA/CS fiber mat loaded with 2.5% owf crude HP extract can provide the most suitable moist environment.

3.3.6. Swelling Determination

The swelling ability of the electrospun PLLA/PVA/CS fiber mats loaded with crude HP extracts was studied in a PBS solution and overtime periods of 0, 24, 48, 72, 96, and 120 hours, Figure 3. The curves showed a rapid swelling rate during the first 24 hours and then leveled off as time passed. The electrospun PLLA/PVA/CS fiber mat was able to swell up to 401.19 ± 25.14%, while electrospun PLLA/PVA/CS fiber mats containing 2.5% and 5.0% owf crude HP extracts exhibited swelling rates of 510.53 ± 15.71% and 603.19 ± 21.34%, respectively. The results demonstrated that the highest swelling rate was obtained when the crude HP extract concentration increase to 5.0% owf. Such behavior can be explained by the hydrophilic character of crude HP extract, due to the presence of

hydrophilic functional groups on its structure, which can be easily hydrated, like hydroxyl, amino, and carboxyl groups. Therefore, in these conditions, the fluids quickly enter into the pores of the electrospun fiber mats and gradually diffuse into the fibers while creating and maintaining a moist wound environment to facilitate the wound healing process [43]. Moreover, the high swelling can prevent the dressing from sticking to the wound surface and improve the transport of oxygen to the wound surface, resulting in a rapid and better healing and recovery of the wound [33,44].
Sadri et al. proved that the swelling properties also enhanced with the amount of green tea leaf extract loaded [44]. Thus, polymeric nanofiber composite holds more moisture in its structure when a higher concentration of green tea is used.

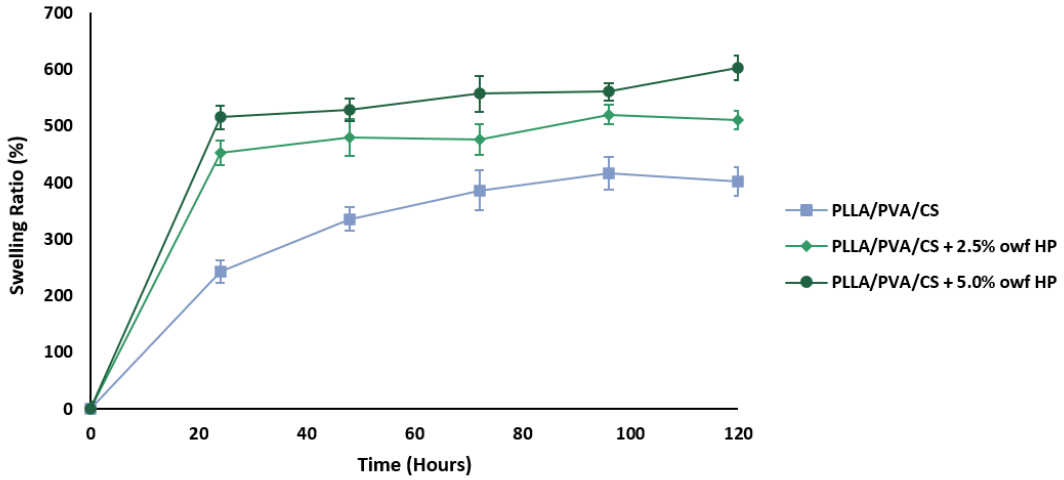

Figure 3 – Characterization of the effect of crude HP extracts on the degree of swelling (%) in PBS (pH=5.5) for 120 hours at 37 °C.

3.4. *In vitro* release study of HP-loaded electrospun PLLA/PVA/CS fiber mats

The release profiles of crude HP extract from electrospun PLLA/PVA/CS fiber mats containing HP at different concentrations (2.5% and 5.0% owf) were reported by the total immersion method using PBS at pH=5.5 as release medium, Figure 4. *In vitro* release profiles exhibited a sustained release of the crude HP extracts during 72 hours, which is appropriate for improving the healing process.
Evidently, electrospun PLLA/PVA/CS fiber mats containing 5.0% owf HP exhibited a faster release rate (78.99 ± 3.14%) than for 2.5% owf of HP (61.89 ± 2.36%). These results suggest that the highest amount of crude plant extract loading displays a faster diffusion, and consequently, the release rate increases with enhancing the degree of swelling of the electrospun PLLA/PVA/CS fiber mats.
The data obtained is in agreement with the previously reported by Panichpakdee et al., who reported the production of the ultra-fine cellulose acetate (CA) fiber mats loaded with emodin, an active herbal substance for use in wound healing extracted from the plant *Polygonum cuspidatum p.e*, at various

amounts (0.01 %wt., 0.05 %wt., and 0.10 %wt.) [15]. In both cases, the electrospun fibers containing the highest concentration of loaded extract exhibited the maximum release rate, as well as a faster release process.

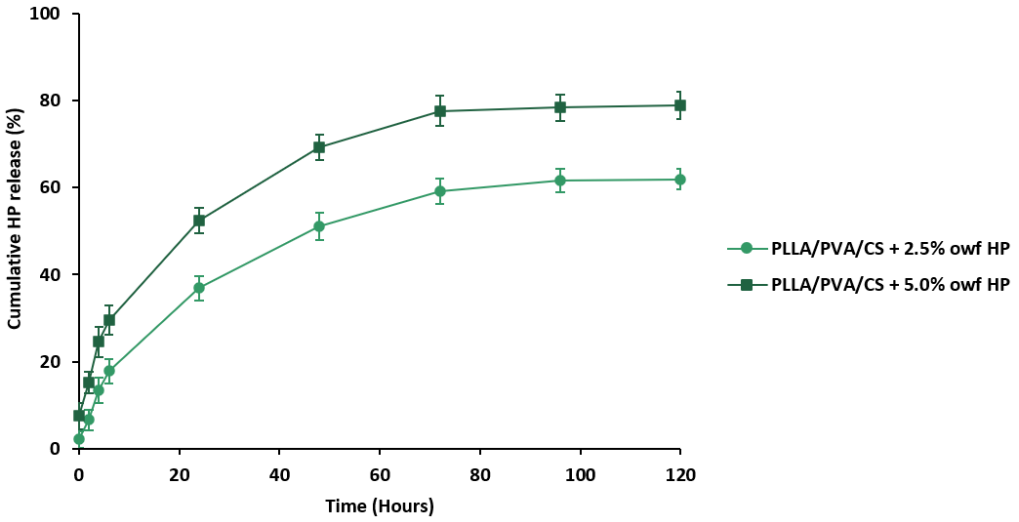

Figure 4 – *In vitro* release study of crude HP extract loaded into electrospun PLLA/PVA/CS fiber mats in a PBS buffer solution (pH=5.5) for 120 hours at 37 °C.

3.5. Antibacterial Activity Assessment

The antibacterial efficiency of the electrospun PLLA/PVA/CS fiber mats loaded with crude HP extracts was successfully evaluated against *S. aureus*, one of the most common bacteria isolates from chronic wounds [11].

The quantitative assay showed that after 24 hours of contact with crude HP extracts-loaded electrospun PLLA/PVA/CS fiber mats there was a percentage of microbial inhibition against *S. aureus* of 93.11 ± 3.53% and 83.97 ± 6.95% when 2.5% and 5.0% owf HP were incorporated, respectively, Figure 5. This evaluation demonstrated that 2.5% owf HP exhibit a higher ability to inhibit the bacterial growth and revealed its effectiveness. Moreover, as expected, the antibacterial properties of the electrospun PLLA/PVA/CS fiber mats, conferred by CS's inherent antimicrobial action, were strengthened with the adding of the crude HP extracts.

These results are in accordance with the data previously reported by Bai et al., who found that the extra loading of tea tree oil (TTO) in the PCL/Chitosan dressings increase the antimicrobial activity [45].

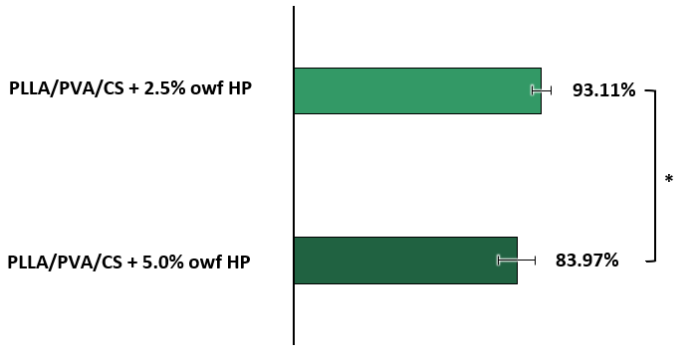

Figure 5 – Antibacterial efficiency of crude HP extract-loaded electrospun PLLA/PVA/CS fiber mats against *S. aureus*, expressed in percentage of microbial inhibition (%R). These values were obtained by comparison with the results of the raw electrospun PLLA/PVA/CS fiber mats. (Data are presented as the mean ± SD, * $p < 0.05$).

3.6 *In vitro* Cytotoxicity Evaluation

The suitability of the produced electrospun fiber mats for being applied as wound dressing materials was assessed from direct cytotoxicity assay using NHDF cells. The raw electrospun PLLA/PVA/CS fiber mats and electrospun PLLA/PVA/CS fiber mats containing 2.5% owf HP, which resulted in better wound dressing properties, were investigated. The results revealed that the presence of the crude HP extract into the fiber mats did not produce any cytotoxic effect on the viability of the NHDF cells, over 7 days, Figure 6. In both cases, the cell viability was higher than 70% (non-cytotoxic effect), confirming that the incorporation of the crude HP extract in the electrospun PLLA/PVA/CS did not affect their biocompatibility.

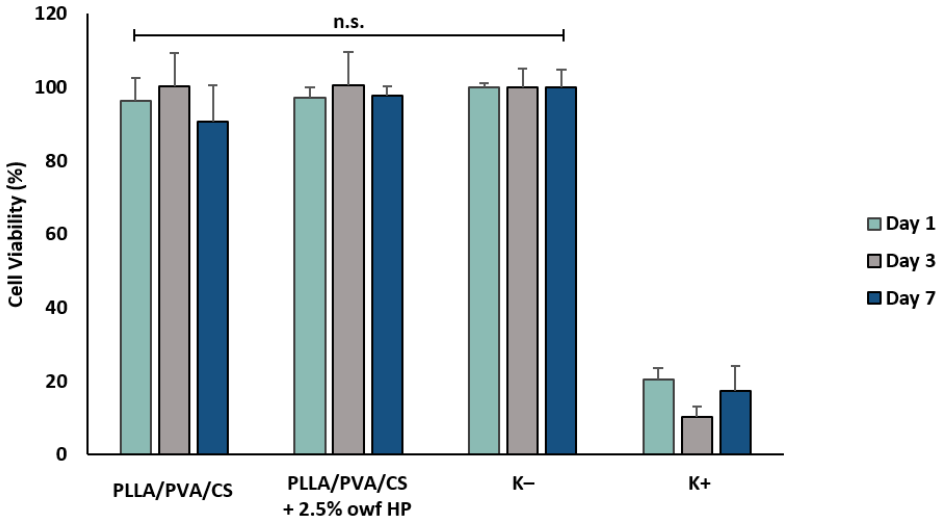

Figure 6 – Evaluation of the *in vitro* cytotoxic profile of the produced electrospun PLLA/PVA/CS fiber mats with and without HP extract. Analysis of the NHDF cell viability via MTT assay after 1, 3, and 7 days.

4. Conclusion

This research work describes the development of new non-woven electrospun wound dressing materials for the treatment and avoidance of skin wound infections. These materials composed of PLLA, PVA, and CS were produced from W/O emulsions by emulsion electrospinning using a Nanospider technology and effectively loaded with two different concentrations of crude HP extract (2.5 and 5.0% owf). The electrospun PLLA/PVA/CS fiber mats proved to be suitable to mimic the properties of native skin structure, mainly when 2.5% owf crude HP extract was incorporated. It was proposed by the fact that thinner fibers were produced with diameters within the preferred size range to the development of a new ECM. Besides, electrospun PLLA/PVA/CS fiber mats loaded with 2.5% owf crude HP extract displayed a most proper porosity, wettability, and degree of swelling, which enables the establishment of a moist wound environment, improving the capability of absorbing and retaining the remaining wound exudate. Furthermore, this dressing material exhibited an enhanced antibacterial activity against *Staphylococcus aureus* (*S. aureus*) (93.11% ± 3.53%), without significantly affecting the viability of NHDF cells.

Therefore, the obtained results showed that electrospun PLLA/PVA/CS fiber mats containing 2.5% crude HP are a promising approach for the development of antibacterial wound dressings.

Declaration of competing interest

The authors declare no conflict of interest, financial or otherwise.

Acknowledgments

The authors thank Ana Raquel Nunes for her help in the cytotoxic assay. The authors are also grateful for the support given by FibEnTech Research Unit (Project UIDB/00195/2020). Cláudia Mouro also acknowledges a PhD fellowship from Foundation for Science and Technology (FCT) (PD/BD/113550/2015).

References

1. Wang, J.; Windbergs, M. Functional electrospun fibers for the treatment of human skin wounds. *Eur. J. Pharm. Biopharm.* **2017**, *119*, 283–299.
2. Prisăcaru, A.I.; Andriţoiu, C. V.; Andriescu, C.; Hăvârneanu, E.C.; Popa, M.; Motoc, A.G.M.; Sava, A. Evaluation of the wound-healing effect of a novel *Hypericum perforatum* ointment in skin injury. *Rom. J. Morphol. Embryol.* **2013**, *54*, 1053–1059.
3. Yadollah-Damavandi, S.; Chavoshi-Nejad, M.; Jangholi, E.; Nekouyian, N.; Hosseini, S.; Seifaee, A.; Rafiee, S.; Karimi, H.; Ashkani-Esfahani, S.; Parsa, Y.; Mohsenikia, M. Topical *Hypericum*

perforatum improves tissue regeneration in full-thickness excisional wounds in diabetic rat model. *Evidence-based Complement. Altern. Med.* **2015**, 245328.

4. Juncos Bombin, A.D.; Dunne, N.J.; McCarthy, H.O. Electrospinning of natural polymers for the production of nanofibres for wound healing applications. *Mater. Sci. Eng. C* **2020**, *114*, 110994.
5. Azimi, B.; Maleki, H.; Zavagna, L.; de la Ossa, J.G.; Linari, S.; Lazzeri, A.; Danti, S. Bio-based electrospun fibers for wound healing. *J. Funct. Biomater.* **2020**, *11*, 67.
6. Chen, H.; Peng, Y.; Wu, S.; Tan, L.P. Electrospun 3D fibrous scaffolds for chronic wound repair. *Materials (Basel).* **2016**, *9*, 1–12.
7. Lagoumintzis, G.; Zagoriti, Z.; Jensen, M.S.; Argyrakos, T.; Koutsojannis, C.; Poulas, K. Wireless direct microampere current in wound healing: Clinical and immunohistological data from two single case reports. *Biosensors* **2019**, *9*, 1–13.
8. Fatehi, P.; Abbasi, M. Medicinal plants used in wound dressings made of electrospun nanofibers. *J. Tissue Eng. Regen. Med.* **2020**, term.3119.
9. Simões, D.; Miguel, S.P.; Ribeiro, M.P.; Coutinho, P.; Mendonça, A.G.; Correia, I.J. Recent advances on antimicrobial wound dressing: A review. *Eur. J. Pharm. Biopharm.* **2018**, *127*, 130–141.
10. Rieger, K.A.; Birch, N.P.; Schiffman, J.D. Designing electrospun nanofiber mats to promote wound healing-a review. *J. Mater. Chem. B* **2013**, *1*, 4531–4541.
11. Gizaw, M.; Thompson, J.; Faglie, A.; Lee, S.Y.; Neuenschwander, P.; Chou, S.F. Electrospun fibers as a dressing material for drug and biological agent delivery in wound healing applications. *Bioengineering* **2018**, *5*, 1–28.
12. Liu, Y.; Zhou, S.; Gao, Y.; Zhai, Y. Electrospun nanofibers as a wound dressing for treating diabetic foot ulcer. *Asian J. Pharm. Sci.* **2019**, *14*, 130–143.
13. Liu, J.; Zheng, H.; Dai, X.; Sun, S.; Machens, H.G.; Schilling, A.F. Biomaterials for Promoting Wound Healing in Diabetes. *J. Tissue Sci. Eng.* **2017**, *8*, 1–4.
14. Moura, L.I.F.; Dias, A.M.A.; Carvalho, E.; De Sousa, H.C. Recent advances on the development of wound dressings for diabetic foot ulcer treatment - A review. *Acta Biomater.* **2013**, *9*, 7093–7114.
15. Panichpakdee, J.; Pavasant, P.; Supaphol, P. Electrospun cellulose acetate fiber mats containing emodin with potential for use as wound dressing. *Chiang Mai J. Sci.* **2016**, *43*, 195–205.
16. Zhang, W.; Ronca, S.; Mele, E. Electrospun nanofibres containing antimicrobial plant extracts. *Nanomaterials* **2017**, *7*, 1–17.
17. Öztürk, N.; Korkmaz, S.; Öztürk, Y. Wound-healing activity of St. John's Wort (*Hypericum perforatum* L.) on chicken embryonic fibroblasts. *J. Ethnopharmacol.* **2007**, *111*, 33–39.
18. Santos, D.; Silva, D.M.; Gomes, P.S.; Fernandes, M.H.; Santos, J.D.; Sencadas, V. Multifunctional PLLA-ceramic fiber membranes for bone regeneration applications. *J. Colloid Interface Sci.* **2017**, *504*, 101–110.
19. Ferri, J.M.; Garcia-Garcia, D.; Carbonell-Verdu, A.; Fenollar, O.; Balart, R. Poly(lactic acid) formulations with improved toughness by physical blending with thermoplastic starch. *J. Appl. Polym. Sci.* **2018**, *135*, 45751.
20. Zarghami, A.; Irani, M.; Mostafazadeh, A.; Golpour, M.; Heidarinasab, A.; Haririan, I. Fabrication of PEO/chitosan/PCL/olive oil nanofibrous scaffolds for wound dressing applications. *Fibers Polym.* **2015**, *16*, 1201–1212.
21. Jayakumar, R.; Prabaharan, M.; Sudheesh Kumar, P.T.; Nair, S. V.; Tamura, H. Biomaterials based on chitin and chitosan in wound dressing applications. *Biotechnol. Adv.* **2011**, *29*, 322–337.
22. Chen, J.P.; Chang, G.Y.; Chen, J.K. Electrospun collagen/chitosan nanofibrous membrane as wound dressing. *Colloids Surfaces A Physicochem. Eng. Asp.* **2008**, *313–314*, 183–188.

23. Zhou, Y.; Yang, H.; Liu, X.; Mao, J.; Gu, S.; Xu, W. Electrospinning of carboxyethyl chitosan/poly(vinyl alcohol)/silk fibroin nanoparticles for wound dressings. *Int. J. Biol. Macromol.* **2013**, *53*, 88–92.

24. Zhang, R.; Xu, W.; Jiang, F. Fabrication and characterization of dense Chitosan/polyvinyl-alcohol/poly-lactic-acid blend membranes. *Fibers Polym.* **2012**, *13*, 571–575.

25. He, Z.; Xiong, L. Evaluation of physical and biological properties of polyvinyl alcohol/chitosan blend films. *J. Macromol. Sci. Part B Phys.* **2012**, *51*, 1705–1714.

26. Pourhojat, F.; Sohrabi, M.; Shariati, S.; Mahdavi, H.; Asadpour, L. Evaluation of poly ε-caprolactone electrospun nanofibers loaded with *Hypericum perforatum* extract as a wound dressing. *Res. Chem. Intermed.* **2017**, *43*, 297–320.

27. Chitrattha, S.; Phaechamud, T. Porous poly(dl-lactic acid) matrix film with antimicrobial activities for wound dressing application. *Mater. Sci. Eng. C* **2016**, *58*, 1122–1130.

28. Shi, R.; Geng, H.; Gong, M.; Ye, J.; Wu, C.; Hu, X.; Zhang, L. Long-acting and broad-spectrum antimicrobial electrospun poly (ε-caprolactone)/gelatin micro/nanofibers for wound dressing. *J. Colloid Interface Sci.* **2018**, *509*, 275–284.

29. Okmen, G.; Balpınar, N. The Biological Activities Of *Hypericum perforatum* L.. *African J. Tradit. Complement. Altern. Med. AJTCAM* **2017**, *14*, 213–218.

30. Reichling, J.; Weseler, A.; Saller, R. A Current Review of the Antimicrobial Activity of *Hypericum perforatum* L. *Pharmacopsychiatry* **2001**, *34*, 116–118.

31. Sharma, P.; Mathur, G.; Dhakate, S.R.; Chand, S.; Goswami, N.; Sharma, S.K.; Mathur, A. Evaluation of physicochemical and biological properties of chitosan/poly (vinyl alcohol) polymer blend membranes and their correlation for Vero cell growth. *Carbohydr. Polym.* **2016**, *137*, 576–583.

32. Yan, Y.; Sencadas, V.; Jin, T.; Huang, X.; Chen, J.; Wei, D.; Jiang, Z. Tailoring the wettability and mechanical properties of electrospun poly(L-lactic acid)-poly(glycerol sebacate) core-shell membranes for biomedical applications. *J. Colloid Interface Sci.* **2017**, *508*, 87–94.

33. Yousefi, I.; Pakravan, M.; Rahimi, H.; Bahador, A.; Farshadzadeh, Z.; Haririan, I. An investigation of electrospun Henna leaves extract-loaded chitosan based nanofibrous mats for skin tissue engineering. *Mater. Sci. Eng. C* **2017**, *75*, 433–444.

34. Lawrence, B.J.; Madihally, S. V. Cell colonization in degradable 3D porous matrices. *Cell Adh. Migr.* **2008**, *2*, 9–16.

35. Kumbar, S.G.; Nukavarapu, S.P.; James, R.; Nair, L.S.; Laurencin, C.T. Electrospun poly(lactic acid-co-glycolic acid) scaffolds for skin tissue engineering. *Biomaterials* **2008**, *29*, 4100–4107.

36. Oliveira, S.M.; Alves, N.M.; Mano, J.F. Cell interactions with superhydrophilic and superhydrophobic surfaces. *J. Adhes. Sci. Technol.* **2014**, *28*, 843–863.

37. Perumal, G.; Pappuru, S.; Chakraborty, D.; Maya Nandkumar, A.; Chand, D.K.; Doble, M. Synthesis and characterization of curcumin loaded PLA—Hyperbranched polyglycerol electrospun blend for wound dressing applications. *Mater. Sci. Eng. C* **2017**, *76*, 1196–1204.

38. Jin, G.; Prabhakaran, M.P.; Kai, D.; Annamalai, S.K.; Arunachalam, K.D.; Ramakrishna, S. Tissue engineered plant extracts as nanofibrous wound dressing. *Biomaterials* **2013**, *34*, 724–734.

39. Trinca, R.B.; Westin, C.B.; da Silva, J.A.F.; Moraes, Â.M. Electrospun multilayer chitosan scaffolds as potential wound dressings for skin lesions. *Eur. Polym. J.* **2017**, *88*, 161–170.

40. Chin, C.Y.; Jalil, J.; Ng, P.Y.; Ng, S.F. Development and formulation of *Moringa oleifera* standardised leaf extract film dressing for wound healing application. *J. Ethnopharmacol.* **2018**, *212*, 188–199.

41. Lin, W.C.; Lien, C.C.; Yeh, H.J.; Yu, C.M.; Hsu, S.H. Bacterial cellulose and bacterial cellulose-chitosan membranes for wound dressing applications. *Carbohydr. Polym.* **2013**, *94*, 603–611.

42. Alippilakkotte, S.; Kumar, S.; Sreejith, L. Fabrication of PLA/Ag nanofibers by green synthesis method using *Momordica charantia* fruit extract for wound dressing applications. *Colloids Surfaces A Physicochem. Eng. Asp.* **2017**, *529*, 771–782.

43. Lin, H.Y.; Chen, H.H.; Chang, S.H.; Ni, T.S. Pectin-chitosan-PVA nanofibrous scaffold made by electrospinning and its potential use as a skin tissue scaffold. *J. Biomater. Sci. Polym. Ed.* **2013**, *24*, 470–484.

44. Sadri, M.; Arab-Sorkhi, S.; Vatani, H.; Bagheri-Pebdeni, A. New wound dressing polymeric nanofiber containing green tea extract prepared by electrospinning method. *Fibers Polym.* **2015**, *16*, 1742–1750.

45. Bai, M.Y.; Chou, T.C.; Tsai, J.C.; Yu, W.C. The effect of active ingredient-containing chitosan/polycaprolactone nonwoven mat on wound healing: *In vitro* and *in vivo* studies. *J. Biomed. Mater. Res. - Part A* **2014**, *102*, 2324–2333.

Paper 4 - *Chelidonium majus* L. Incorporated Emulsion Electrospun PCL/PVA_PEC Nanofibrous Meshes for Antibacterial Wound Dressing Applications

Abstract

Presently, there are many different types of wound dressings available on the market. Nonetheless, there is still a great interest to improve the performance and efficiency of these materials. Concerning that, new dressing materials containing natural products, such as medicinal plants that protect the wound from infections but also enhance skin regeneration have been or are being developed. Herein, we used for the first time a needleless emulsion electrospinning technique for incorporating *Chelidonium majus* L. (*C. majus*), a medicinal plant widely known for its traditional therapeutic properties, in Polycaprolactone (PCL)/Polyvinyl Alcohol (PVA)_Pectin (PEC) nanofibrous meshes. Moreover, the potential use of these electrospun nanofibers as a carrier for *C. majus* was also explored. The results obtained revealed that the produced PCL/PVA_PEC nanofibrous meshes containing *C. majus* extract displayed morphological characteristics similar to the natural extracellular matrix of the skin (ECM). Furthermore, the produced meshes showed beneficial properties to support the healing process. Additionally, the *C. majus*-loaded PCL/PVA_PEC nanofibrous meshes inhibited *Staphylococcus aureus* (*S. aureus*) and *Pseudomonas aeruginosa* (*P. aeruginosa*) growth, reaching a 3.82 Log reduction, and showed to be useful for controlled release, without causing any cytotoxic effect on the normal human dermal fibroblasts (NHDF) cells. Hence, these findings suggest the promising suitability of this novel wound dressing material for prevention and treatment of bacterial wound infections.

Graphical Abstract

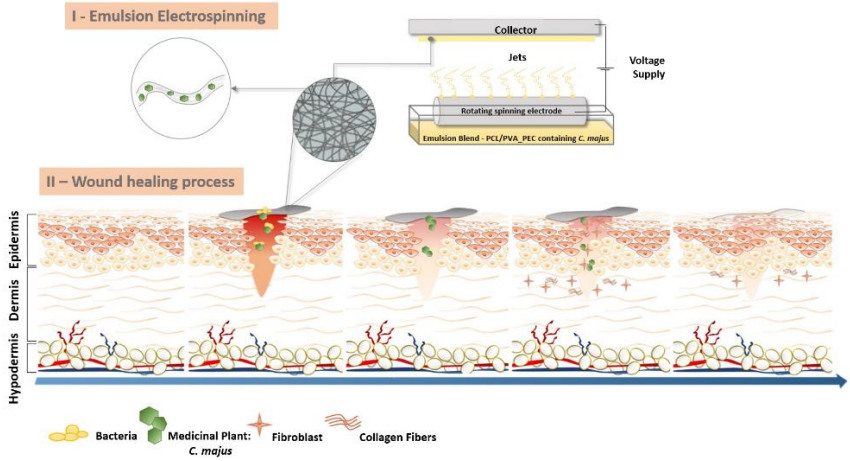

Keywords: Emulsion electrospinning; needleless electrospinning; natural compounds; *C. majus*; antimicrobial wound dressing.

1. Introduction

Over recent decades, traditional wound dressings have been applied to protect the wound from mechanical and bacterial injuries, and simultaneously to absorb low levels of exudates. However, although these dressings are cheaper and provide an essential environment for wound healing, they are not efficient enough to promote hemostasis and maintain a moist wound environment, which has been shown to enhance wound healing [1–6]. To overcome such limitations and improve the healing process, different modern wound dressings such as films, foams, hydrogels, hydrocolloids, and micro to nanofibers meshes have been fabricated from a wide range of natural and synthetic biomaterials and selected based on the type of wounds [4–7]. Among them, nanofiber meshes produced from several methods, including self-assembly, phase separation, drawing, template synthesis, and electrospinning have been regarded as one of the most efficient wound dressing materials, especially those produced by electrospinning, due to its simplicity, cost-effectiveness, and functional versatility [1,2,4,6,8,9].

The electrospun nanofibrous meshes exhibit desirable features for wound healing occurs, once they form randomly orientated 3D-structures which resemble the skin's extracellular matrix (ECM) [4,6,8–11]. Moreover, these meshes display high surface area, high porosity, and interconnected pores, which provide a suitable microenvironment for cell attachment, growth, and differentiation, as well as angiogenesis and collagen synthesis [3,4,6,8,9,12–14]. Furthermore, the electrospun nanofibers can control gas exchanges, supply water and nutrients to the wound site, and assist in fluids absorption, maintaining a moisture balance at the wound dressing interface [4,6,13]. These materials also exhibit potential to scar-free repair and regeneration, and the loading ability for a wide variety of bioactive or therapeutic agents, including antimicrobials, anti-inflammatories, growth factors, vitamins, and even cells [4,6,8,9,12–16]. The incorporation of these agents into electrospun nanofibrous meshes has been performed using different strategies, including blend, co-axial, and emulsion electrospinning. However, post-electrospinning surface modifications, such as chemical immobilization, coating, and physical absorption, as well as layer-by-layer assembly have also been considered [4,6,9,14,17,18]. Among the different methods used until now to add bioactive agents to electrospun nanofibers, emulsion electrospinning has gained considerable attention for successfully loading both hydrophilic and hydrophobic agents, and capability to protect the structural integrity and bioactivity of these agents [4,19]. Additionally, it does not require any specific setup and can enhance the solubility of the components of the blend, as well as act as delivery systems, improving its therapeutic performance [4,18–20]. In this method, an emulsion is electrospun into core-sheath structured fibers due to the difference in volatility between the two liquid phases, i.e., one liquid is dispersed into the other in the form of droplets, and during the electrospinning process, the solvent of the continuous phase evaporates more rapidly while the emulsion droplets move inward and merge in the core of the fibers [18,20]. Moreover, the electrospun nanofibrous meshes prepared by emulsion electrospinning have shown high encapsulation efficiency [4]. Despite the efficient incorporation of a

wide range of bioactive and therapeutic agents into electrospun nanofibers, the interest for natural compounds remains high [4,9,21]. Recent studies report the development of electrospun nanofibrous membranes containing medicinal plant extracts, and their constituents, such as essential oils for wound dressing applications due to their therapeutic properties, cost-effectiveness, and few adverse effects [4,9,21–28]. Plant-derived medicines have a long history of use in traditional medicine, namely in the treatment of different kinds of wounds [22,27,28]. Hence, the electrospun nanofibrous meshes containing plant extracts are a promising therapeutic option, and some practical examples were already successfully applied as an advantageous approach to prevent wound bacterial colonization and infection, while provide an appropriate environment for healing [4,6,9,21–28]. Herein, we aimed to fabricate electrospun Polycaprolactone (PCL)/Polyvinyl Alcohol (PVA)_Pectin (PEC) nanofibrous meshes containing crude *Chelidonium majus* L. (*C. majus*) extract from emulsion electrospinning. *C. majus* is a member of the *Papaveraceae* family, and it is used for the treatment of different types of warts and various inflammatory diseases, including atopic dermatitis [29–32]. The crude *C. majus* extract, as well as purified compounds derived from it, exhibit a broad spectrum of biological properties. The flavonoids and isoquinoline alkaloids, such as chelidonine, berberine, coptisine, sanguinarine, and chelerythrine, are responsible for conferring anti-inflammatory, antimicrobial, anticancer, analgesic, antioxidant, and hepatoprotective properties to *C. majus* [29–32]. On the other hand, the hydrophobic character, strength, and durability of the synthetic polymer, PCL, was combined with the intrinsic biological properties displayed by PEC [29,33–36]. The PEC is a natural polysaccharide, known for its biocompatible, biodegradable, and non-toxicity. Additionally, this natural biopolymer can promote a favorable environment for cell adhesion and proliferation and provide an acid environment which may act as a barrier against bacteria [29,36,37]. Nonetheless, natural biopolymers, as polysaccharides are usually tricky to electrospun into nanofibers, and therefore PVA, one of the most frequently used synthetic water-soluble polymer for the preparation of wound dressings was added to improve PEC electro-spinnability [36]. As a result, PVA is an excellent emulsifying and dispersing agent and can facilitate emulsification and promote emulsion stability [38]. To the best of our knowledge, this is the first time that electrospun PCL/PVA_PEC nanofibrous meshes containing crude *C. majus* extract were successfully fabricated. The obtained results revealed the appropriateness of incorporating a medicinal plant into nanofiber-based wound dressings via emulsion electrospinning, aiming to prevent bacterial infection at the wound site and enhance the healing process.

2. Materials and Methods

2.1. Materials

Chelidonium majus L. (*C. majus*) was bought from a Portuguese botanic shop. Normal human dermal fibroblasts (NHDF) cells were acquired from ATCC (American Type Culture Collection, Manassas,

VA, USA). Polycaprolactone (PCL) (MW 80,000 g/mol) was purchased from Sigma-Aldrich (St. Louis, MO, USA). Polyvinyl Alcohol (PVA) (MW 115,000 g/mol) was obtained from VWR Chemicals (Geldenaaksebaan, Leuven, Belgium). Pectin (PEC) was purchased from Acros Organics (Fisher Scientific, Göteborg, Sweden). Chloroform (analytical grade), Dimethylformamide (DMF) (analytical grade), and ethanol absolute were acquired from Fisher Chemical (Leicestershire, UK). Nutrient agar (NA), Nutrient broth (NB), and agar for microbiology were bought from Fluka (Barcelona, Spain). Brain Heart Infusion (BHI) broth was purchased from Panreac (Barcelona, Spain). Sodium chloride (NaCl), Mueller-Hinton broth (MHB), tween 80, trypsin, fetal bovine serum (FBS), 3-(4,5-Dimethyl-2-thiazolyl)-2,5-diphenyl-2H-tetrazolium bromide (MTT), and Dimethyl Sulfoxide (DMSO) anhydrous ≥99.9% were provided from Sigma-Aldrich. Phosphatebuffered saline (PBS) was purchased from Alfa Aesar (Kandel, Germany). All solvents were used as received without further purification.

2.2. Preparation of Crude C. majus Extract

Ethanol Crude Extraction of *C. majus*

Dried plant material (2.5 g) was extracted using 80% ethanol at room temperature. After that, the plant extract was collected and filtered with filter paper (Whatman No. 1, 11 µm pore size), and the filtrate was then subjected to evaporation by rotavapor (Buchi Rotavapor RE 111, Allschwil, Switzerland) to obtain a soft extract. The yield of the extract was 11.29% (w/w). The crude *C. majus* extract was re-suspended in ethanol and used for all experiments, as described below.

2.3. *In Vitro* Minimum Inhibitory Concentration (MIC) Test of the Crude Extract of *C. majus*

Minimum inhibitory concentration (MIC) of the crude *C. majus* extract against *Staphylococcus aureus* (ATTC 6538) (*S. aureus*) and *Pseudomonas aeruginosa* (PA25) (*P. aeruginosa*) was determined according to NCLS M07-A6 guidelines—Methods for Dilution Antimicrobial Susceptibility Tests for Bacteria That Grow Aerobically. The tests were performed using the broth microdilution method on 96 multi-well polystyrene plates (Sigma-Aldrich, (St. Louis, MO, USA)). First, a stock of *C. majus* solutions was prepared in a range from 0.15 to 10 mg/mL in sterile MHB. Then, 50 µL of each *C. majus* dilution was added to microplate wells containing 50 µL of the bacterial suspension, previously adjusted to approximately ~10^7 CFU/mL in MHB. The assay was performed in triplicate, and the 96-well plates incubated for 24 hours at 37 °C. The MIC of *C. majus* was defined as the lowest concentration at which no visible bacterial growth could be detected on the bottom of each well (medium-turbidity not identified).

2.4. Emulsion Electrospinning Process

A PCL solution was prepared by dissolving (8% w/v) PCL in a chloroform/DMF (volume ratio of 30:20) mixture at 50 °C. This solution was kept under magnetic stirring overnight to ensure the proper dissolution of the polymer. To prepare the PVA_PEC blend, 8% PVA (w/v) and 2% PEC (w/v) solutions were dissolved in distilled water at 90 °C and at room temperature, respectively. These solutions were first prepared separately and then blended with a 7:3 ratio of PVA and PEC. Then, this blend was further incorporated with 2.5% on weight of fiber (owf) of crude *C. majus* extract. After that, the PVA_PEC blend containing *C. majus* extract was added into the PCL solution with a ratio of 1:1 (v/v), and the resultant mixture was stirred using a high-speed stirrer Techmatic S2 to produce the water-in-oil (W/O) emulsion. The final blend was stirred at room temperature for 4 hours to ensure stable and uniform emulsion. As the control, PCL, PVA_PEC, and plain PCL/PVA_PEC were prepared in the same conditions. After preparation, the solutions were immediately electrospun using Nanospider Technology (Nanospider laboratory machine NS LAB 500S from Elmarco s.r.o., Liberec, Czech Republic), a needle-free electrospinning apparatus, based on a rotating spinning electrode, and then the electrospun nanofibrous meshes were fabricated. The PCL was electrospun using an applied voltage of 80.0 kV with a working distance (distance from the electrode to collector) of 13 cm and an electrode rotation rate of 55 Hz, while PVA/PEC blend was electrospun applying 75.0 kV, a working distance of 15 cm and an electrode rotation rate of 45 Hz. In the case of emulsions (PCL/PVA_PEC and PCL/PVA_PEC containing crude *C. majus* extract), processing conditions were respectively set at 80 kV, 15 cm, 55 Hz. All solutions were electrospun for 1 hour at 25 °C and relative humidity up to 35%. The electrospun nanofibrous meshes were collected on polypropylene non-woven fabric and dried in the hood at room temperature till constant weight.

2.5. Characterization of the Produced Electrospun Nanofibrous Meshes

2.5.1. Fourier Transform Infrared Spectroscopy Study

Attenuated total reflectance Fourier transform infrared (ATR-FTIR) spectroscopy (Thermo-Nicolet is10 FT-IR Spectrophotometer, Waltham, MA, USA) was used to analyze the functional groups present in the electrospun nanofibrous meshes produced through emulsion electrospinning. Samples were recorded over the range of 400–4000 cm^{-1} at 32 scans min^{-1} and averaged at the resolution of 4 cm^{-1}.

2.5.2. Scanning Electron Microscopy (SEM) Imaging and Analysis

The morphology and surface topography of raw electrospun PCL nanofibers, PVA_PEC blend, and both the plain and the *C. majus*-loaded PCL/PVA_PEC nanofibrous meshes were examined using an

SEM (Hitachi S2700, Tokyo, Japan). First, the samples were made electrically conductive by coating with a thin gold layer using an Emitech K550 sputter coater (Emitech Ltd., Ashford, Kent, UK) and then imaged at 5000× magnification. The obtained SEM images were analyzed by an image-processing software (ImageJ, National Institutes of Health, Bethesda, MD, USA) for the determination of the diameters of the fibers. The diameter frequency distributions were further assessed with GraphPad Prism 6 software (Prism Software, La Jolla, CA, USA).

2.5.3. Mechanical Properties Characterization

The mechanical properties of both the plain and the *C. majus*-loaded PCL/PVA_PEC nanofibrous meshes were determined in dry conditions with a universal tensile test machine (DY-35 Adamel Lhomargy, Paris, France), according to the American Society for Testing and Materials (ASTM) standard D3039/D3039M (The standard test method for tensile properties of polymer matrix composite materials) by applying a 10-N load cell at a crosshead speed of 2 mm/min, under ambient conditions. All the samples (n = 5) were cut into a rectangular shape with dimensions of 1 cm × 4 cm (width × length), and then were vertically fixed between the two automatic gripping units of the tensile tester, leaving a 1 cm gauge length for mechanical loading. The sample thicknesses were measured using an electronic micrometer (Adamel Lhomargy MI20, Draveil, France). Tensile strength and elongation at break were determined from the tensile stress-strain curves, as well as Young's modulus. The results were expressed as the mean ± standard deviation (SD).

2.5.4. Porosity Measurements

The porosity of the produced electrospun nanofibrous meshes was measured using a liquid displacement method, as described previously by Yeh et al. [39]. The displacement liquid used in this study was absolute ethanol since it penetrates quickly into the pores of materials without inducing any significant shrinkage or swelling of the polymers. Briefly, a dried sample with a known weight (W_s) was immersed in a graduated cylinder containing a known volume of displacement liquid (W_1) and sonicated at 30 °C in an ultrasonic bath (Ultrasons-H, P-Selecta) for 40 minutes. The total amount of ethanol in the cylinder and the ethanol-impregnated sample was market as W_2. The ethanol-impregnated sample was removed from the displacement liquid, and the volume of remaining ethanol was recorded as W_3. The porosity (ε) of porous electrospun nanofibrous meshes was determined as follows (Equations (1)–(3)):

$$V_p = \frac{(W_2 - W_3 - W_S)}{\rho_\varepsilon} \quad (1)$$

$$V_s = \frac{(W_1 - (W_2 - W_S))}{\rho_\varepsilon} \quad (2)$$

$$\varepsilon\,(\%) = \frac{V_p}{(V_p + V_S)} \times 100 \;\Leftrightarrow\; \varepsilon\,(\%) = \frac{(W_2 - W_3 - W_s)}{(W_1 - W_3)} \times 100 \quad (3)$$

where V_p is the volume of the sample pores, V_s is the volume of the sample, and ρ_ε is the density of ethanol (g/mL). For each sample, the porosity measurements were performed in triplicate, and the average values reported below.

2.5.5. Analysis of the *In Vitro* Swelling Behavior

The swelling properties of both the plain and the *C. majus*-loaded PCL/PVA_PEC nanofibrous meshes were investigated using a gravimetric method. The pre-weighed dry samples (W_{dry}) were immersed in a PBS buffer solution with pH = 5.5 at 37 °C for 30 days. The swollen samples were taken out from the PBS buffer solution at specific time points, and their wet weight measured after gently removing the excess water with a filter paper (W_{wet}). All measurements were conducted in triplicate, and the swelling ratio calculated according to Equation (4):

$$\text{Swelling Ability (\%)} = \frac{(W_{wet} - W_{dry})}{W_{dry}} \times 100 \quad (4)$$

2.5.6. Study of the *In Vitro* Degradation Profile

The hydrolytic degradation profile of the plain and the *C. majus*-loaded electrospun PCL/PVA_PEC nanofibrous meshes was evaluated by immersing the samples at 37 °C in PBS solution (pH = 5.5) for different periods up to 30 days. Briefly, at specific time points (1, 4, 8, 16, and 30 days), the samples were taken out from the PBS solution and then were dried and weighed. Finally, the degradation percentage was determined using the following Equation (5):

$$\text{Weight loss (\%)} = \frac{W_i - W_t}{W_t} \times 100 \quad (5)$$

where W_i is the initial weight of the samples, and W_t is the weight of the sample at time t.

2.5.7. Wettability Studies

The wettability of both the plain and the *C. majus*-loaded PCL/PVA_PEC nanofibrous meshes was measured using a contact angle measurement instrument OCAH-200 (DataPhysics Instruments GmbH, Filderstadt, Germany) operating in static mode at 25 °C. First, samples were placed on the measuring stage. Subsequently, water droplets of size 4 μL were placed at different locations on the sample surfaces from a motorized syringe, and the angle was measured immediately (within 10 seconds). The mean value was determined from five different points and reported as the contact angle of each sample.

2.5.8. Water Vapor Transmission Rate (WVTR) Analysis

The water vapor transmission rate (WVTR) of both the plain and the *C. majus*-loaded PCL/PVA_PEC nanofibrous meshes was measured according to the ASTM E96/E96M15 (Standard Test Methods for Water Vapor Transmission of Materials) to evaluate the moisture permeability of the samples. Briefly, each sample was cut into a round shape of 1.2 cm diameter and carefully placed on top of test tubes filled with 10 mL of deionized water at the initial time. Afterward, the samples-glass tubes assembly was placed in an incubator at 37 °C. The weights of the samples were recorded at specific time points, and the weight loss versus time was linearly filled to calculate the WVTR values. WVTR was determined using Equation (6):

$$\text{Water vapor transmission rate (WVTR)} = \frac{W_{loss}}{A} \ (\text{g}/m^2/day) \ (6)$$

where W_{loss} is the daily weight loss of water, and A is the glass tube open area in m^2.

2.6. Determination of *In Vitro* Release Profile

The crude *C. majus* extract release was characterized by an *in vitro* study. The electrospun PCL/PVA_PEC nanofibrous meshes loaded with crude *C. majus* extracts were immersed in PBS pH = 5.5 release medium and stirred at 100 rpm and 37 °C to provide an environment favorable for wound healing. At predetermined time intervals, a fixed volume of release medium was taken out, and an equal amount of fresh PBS refilled. The concentration of crude *C. majus* extract was measured by UV-Vis spectrometry at a wavelength of 360 nm [40]. The absorbance values were converted to release percentages according to the calibrated curve constructed from a series of *C. majus* standard solutions with concentrations from 0.00 mg/mL to 5.00 mg/mL. Finally, the *in vitro* crude *C. majus* extract release curve was drawn over 30 days. All the measurements were performed in triplicate.

2.7. Antibacterial Properties Assessment

The antibacterial properties of the electrospun PCL/PVA_PEC containing crude *C. majus* extracts were evaluated according to ASTM E2180-07 standard (Test Method for Determining the Activity of Incorporated Antimicrobial Agent(s) In Polymeric or Hydrophobic Materials). Briefly, bacterial suspensions of *S. aureus* (ATTC 6538) and *P. aeruginosa* (A25) of ~10^8 CFU/mL (corresponding to the exponential growth phase) were inoculated into a semi-solid agar slurry prepared by adding 0.30% agar to a 0.85% NaCl solution. Then, a thin layer of the inoculated slurry was spread over on top of each sample. After that, the samples were allowed to gel at room temperature and were analyzed immediately (T_{oh}) and 18–24 hours after incubation (T_{24h}) at 37 °C. The samples were subjected to

vigorous vortex mixing for 1 minute in a neutralizing solution to release the agar slurry from the sample. The resultant suspension was serially diluted with saline solution (0.85% NaCl) and plated on growth plates. The agar plates were incubated at 37 °C for 18–24 hours, and the number of viable bacterial colonies determined as colony forming units (CFU). For this purpose, viable bacterial colonies were counted after incubation, and CFU mL^{-1} calculated to determine the antibacterial effectiveness. All samples and control were tested in triplicate, and the results presented as mean values of log (CFU) with SD.

2.8. *In Vitro* Cell Viability Assay

The cytotoxicity of both the plain and the *C. majus*-loaded PCL/PVA_PEC nanofibrous meshes and their effect on cellular viability was evaluated with the colorimetric MTT assay according to ISO 10993–5 (Biological evaluation of medical devices—Part 5: Tests for *in vitro* cytotoxicity). First, the NHDF cells were cultured in medium supplemented with 10% FBS in a humidified incubator at 37 °C under a 5% CO_2 atmosphere. The culture medium was replenished with fresh media every two days. On the other hand, the samples cut into round disks were placed at the center of each well in 24-well plates covering 1/10 of their area, and then sterilized by UV irradiation (254 nm, ≈7 mW cm^{-2}) for 1 hour. After that, 1×10^4 cells/well were seeded in each well containing the sterilized electrospun nanofibrous meshes and incubated with 5% CO_2 at 37 °C for 1, 3, and 7 days. During these intervals of time, the medium was removed and 1 mL of 0.5 mg/mL MTT reagent solution in fresh culture medium was added to each well and incubated for 4 hours under the same conditions. After 4 hours, the content of each well was replaced by DMSO to dissolve the formazan crystals. The absorbance of each sample was measured at 570 nm using a xMark™ microplate spectrophotometer (Bio-Rad Laboratories, Inc., Hercules, CA, USA). The cells incubated without samples (K^-) and cells incubated with ethanol (96%) (K^+) were chosen as control groups.

2.9. Statistical Analysis

Statistical analysis was performed from the one-way analysis of variance (ANOVA), followed by multiple comparison test Turkey using GraphPad Prism 6 software (GraphPad Software, La Jolla, CA, USA) with a statistical significance of $p < 0.053$.

3. Results and Discussion

3.1. *In Vitro* Minimum Inhibitory Concentration (MIC) Test of the Crude Extract of *C. majus*

The MIC values of crude *C. majus* extract against *S. aureus* and *P. aeruginosa* were found to be 0.625 mg/mL and 1.25 mg/mL, respectively. Zuo et al. [41] reported a MIC value of 1.56 mg/mL for crude *C. majus* extract against *Escherichia coli* ATCC25922 (*E. coli*, Gram-negative bacteria). Such a result agrees with the MIC value of *C. majus* extract obtained in this study against *P. aeruginosa*, a Gram-negative bacterium too. On the other hand, the European Medicines Agency revealed that specific alkaloids extracted from *C. majus*, such as quaternary benzophenanthridine and chelerythrine, exhibited MIC values of 5 μg/mL and 10 μg/mL against *S. aureus* [42]. The results obtained confirmed that MIC values for specific alkaloids obtained from plants are lower than those obtained for the crude extract of the same plant and that the concentration of each phytoconstituent in the plant may differ depending on several factors, such as the plant geographic location, the time of year the plant is harvested, and the chosen extraction method, consequently influencing the obtained MIC values.

3.2. Characterization of the Produced Electrospun Nanofibrous Meshes

3.2.1. Fourier Transform Infrared Spectroscopy Study

The ATR-FTIR spectra of the PCL, PVA_PEC, and both the plain PCL/PVA_PEC and *C. majus*-loaded PCL/PVA_PEC nanofibers are shown in Figure 1. All the acquired spectra exhibit the characteristic peaks of PCL near 2890 and 2980 cm^{-1} (symmetric and asymmetric CH_2 stretching vibration), 1721 cm^{-1} (carbonyl stretching vibration), 1293 cm^{-1} (C-O and C-C stretching vibration), 1240 and 1167 cm^{-1} (symmetric and asymmetric C-O-C stretching vibration) [43]. On the other hand, the spectra of PVA_PEC presents a broad peak around 3320 cm^{-1} (O-H stretching vibration), and bands between 2980 cm^{-1} and 2887 cm^{-1} (C-H stretching vibration), near 1380 cm^{-1} (C-H deformation vibration), 1439 cm^{-1} (CH_2 deformation vibration), and 1251 cm^{-1} (C-O-C stretching vibration) [35]. Therefore, the spectra of PCL/PVA_PEC and PCL/PVA_PEC containing *C. majus* display the characteristic peaks of both PCL and PVA/PEC, but all the other bands of *C. majus* extract are masked by the vibrations of the functional groups in the PCL/PVA_PEC emulsion blend. However, the intensity of the broad peak around 3300 cm^{-1} increased slightly by the addition of crude *C. majus* extract while no distinct peak shifts were identified. This result suggests that the crude plant extract was well incorporated within the electrospun PCL/PVA_PEC nanofibrous meshes.

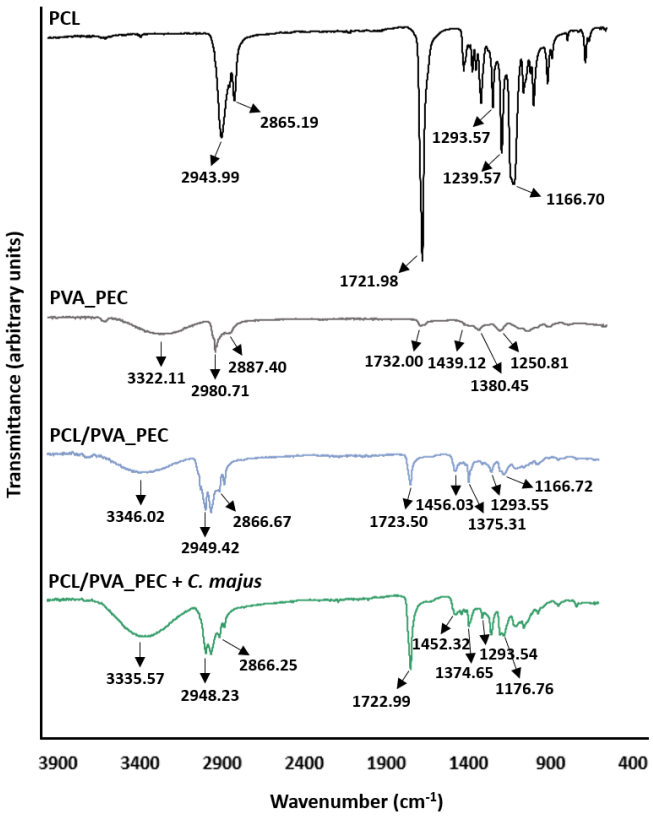

Figure 1 – Attenuated total reflection-Fourier transform infrared (ATR-FTIR) spectra of PCL, PVA_PEC, and both the plain and the *C. majus*-loaded electrospun PCL/PVA_PEC nanofibrous meshes.

3.2.2. Scanning Electron Microscopy (SEM) Imaging and Analysis

The surface morphology and the diameters of the nanofibers produced were assessed through SEM analysis, Figure 2. The PCL (260.56 ± 68.29 nm) and PVA_PEC (208.00 ± 45.46 nm) nanofibers displayed randomly orientated fibers with interconnected pores. On the other hand, the PCL/PVA_PEC and PCL/PVA_PEC containing *C. majus* presented an average fiber diameter of 254.33 ± 64.94 nm and 190.53 ± 56.07 nm, respectively. These results revealed the production of thinner fibers in the presence of *C. majus* extract, due to the reduction of the viscosity of the electrospun solution. Motealleh et al. [44] also showed a similar effect when chamomile, an herbal drug, was incorporated into electrospun PCL/Polystyrene (PS) (65/35) nanofibers. In this previous study, the authors reported a decrease in the average nanofiber diameters from 268 to 175 nm with chamomile extract incorporation. Furthermore, such morphological features mimic the collagen fibers present in native ECM (50–500 nm) and can support cell adhesion and proliferation, prevent fluid accumulation, and enhance moisture vapor transmission, which ensures an effective wound healing process [8,13,44].

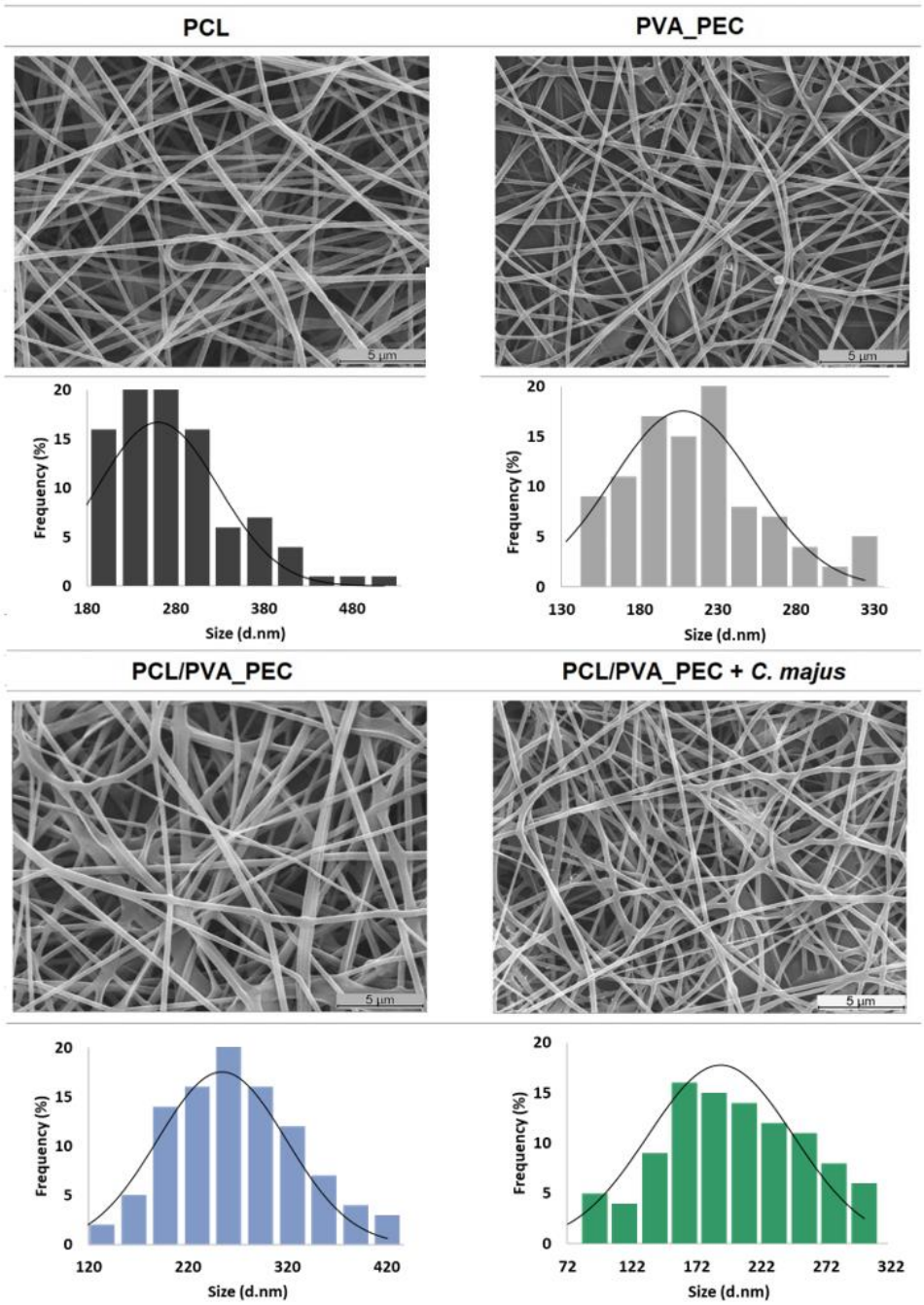

Figure 2 – Nanofiber morphology and fiber size distribution of raw electrospun PCL nanofibers, PVA_PEC blend, and both the plain and the *C. majus*-loaded electrospun PCL/PVA_PEC nanofibrous meshes.

3.2.3. Mechanical Properties Characterization

The mechanical features of a wound dressing material should be in agreement with the parameters established to the skin's native structure to prevent displacement of the dressing after it has been applied, as well as the pain during muscular movement [45,46]. To perform this, a synthetic polymer,

PCL, which exhibits excellent mechanical strength, was blended with a blend of PVA_PEC and PVA_PEC containing *C. majus*, which display high cell affinity but poor mechanical properties [47]. The tensile strength, Young's modulus, and elongation at break for these materials were assessed in dry conditions and presented in Table 1.

Table 1 – Characterization of the mechanical behavior of the produced PCL/PVA_PEC nanofibrous meshes with and without *C. majus* and comparison with the mechanical features of the native human skin.

	Tensile strength (MPa)	**Young's modulus (MPa)**	**Elongation at break (%)**	**Thickness (mm)**
PCL/PVA_PEC	3.17 ± 1.18	17.64 ± 5.30	17.75 ± 1.34	0.22 ± 0.01
PCL/PVA_PEC_*C. majus*	2.96 ± 0.03	15.75 ± 6.46	20.50 ± 8.20	0.22 ± 0.03
Native skin	2.50-30.00 [a]	0.40-20.00 [a]	10.00-115.00 [a]	-

[a] From reference [45].

The electrospun PCL/PVA_PEC nanofibrous meshes showed a value of the Tensile Strength of 3.17 ± 1.18 MPa, whereas the electrospun PCL/PVA_PEC nanofibrous meshes containing *C. majus* exhibited a value of 2.96 ± 0.03 MPa. Moreover, Young's modulus obtained for PCL/PVA_PEC nanofibers was 17.64 ± 5.30 MPa, whereas for PCL/PVA_PEC nanofibers incorporated with *C. majus* decreased to 15.75 ± 6.46 MPa. The elongation at break assays report that the electrospun PCL/PVA_PEC nanofibrous meshes without and with *C. majus* extract can bear a strain of 17.75 ± 1.34% and 20.50 ± 8.20%, respectively. Hence, these results are in accordance with previously reported values for the mechanical properties of the human skin, demonstrating that the produce electrospun nanofibrous meshes can provide appropriate mechanical support during the healing process [45].

3.2.4. Porosity Measurements

The porosity of a biomaterial for the regeneration of skin has a significant impact on its performance [4,18,48]. The porous structure displayed by the electrospun nanofibrous meshes should allow them to perform gas and fluids exchanges, exudate absorption, and promote cell adhesion, migration, and proliferation, improving a new ECM production during wound healing and regeneration [4,18]. The total porosity of the electrospun nanofibrous meshes is presented in Figure 3a and reveals that PCL/PVA_PEC nanofibers have the lowest porosity (85.95 ± 5.75%), whereas PCL/PVA_PEC containing *C. majus* displayed the highest porosity (94.38 ± 4.08%), due to the higher number of void spaces available between nanofibers with thinner diameters. Such a result is in agreement with the findings reported by Yousefi et al. [48], who demonstrated a similar effect when they incorporated *Lawsonia inermis* (Henna) extracts into Chitosan/Poly(ethylene oxide) (PEO) nanofibrous scaffolds.

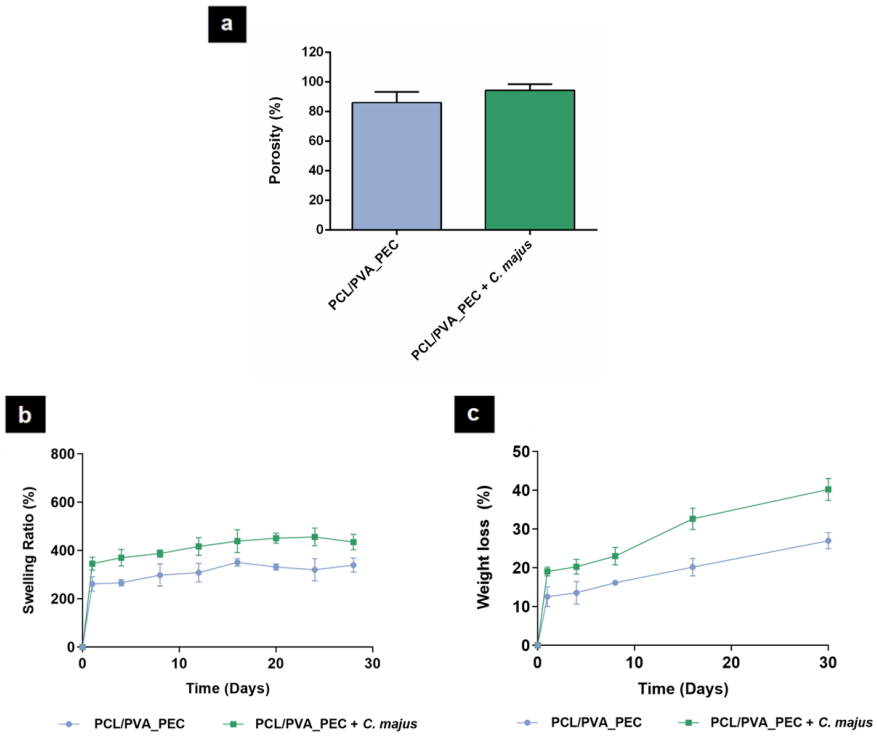

Figure 3 – Characterization of the total porosity (**a**), swelling behavior (**b**), and biodegradation profile (Weight loss) (**c**) of the produced electrospun nanofibrous meshes.

Also recently, researchers have reported that porosities above 90% are the most suitable for facilitating skin tissue repair since they can provide support for cell accommodation and migration and confer a functional environment to promote their growth [4,48].

3.2.5. Analysis of the *In Vitro* Swelling Behavior

The swelling capability of the biomaterials for wound healing applications is fundamental to absorb excessive amounts of exudate, which are produced mainly during the inflammatory phase of healing. The absorption rate of wound exudates can avoid impaired cell adhesion and migration, maceration of the surrounding tissue, as well as bacterial invasion and consequently, wound infections [48]. In this context, the swelling ratio of the produced electrospun nanofibrous meshes was measured in a PBS solution at specific time points, Figure 3b. The obtained results showed that the *C. majus*-loaded electrospun PCL/PVA_PEC nanofibers exhibit a higher swelling ability (~400%) than the plain PCL/PVA_PEC nanofibers (~300%). This result may be attributed to an increase in the number of polar and hydrophilic functional groups, higher surface area, and porosity of the *C. majus*-loaded nanofibers. Therefore, the obtained results showed that the higher swelling capability displayed by electrospun PCL/PVA_PEC nanofibrous meshes containing *C. majus* extract is more proper for effective exudate absorption and able to promote the healing of damaged skin. According to a similar

study by Yousefi et al. [48], the *Lawsonia inermis* extract loaded into Chitosan/PEO nanofibers showed the same effect on swelling behavior of the scaffolds produced. The swelling ratios indicated that the Chitosan/PEO nanofibers, both hydrophilic polymers, provided higher hydrophilic character and surface area for water absorption when *Lawsonia inermis* extract was loaded [48].

3.2.6. Study of the *In Vitro* Degradation Profile

Although there is a wide variety of wound dressings available on the market, most of them still need to be replaced or removed from the wound site, which can lead to scar tissue formation and the risk of bacterial infection can also be increased [4,18,48]. Presently, to minimize this drawback, researchers are developing new biodegradable wound dressing materials as drug carriers to enhance the wound healing rate and skin tissue regeneration. In this study, the degradation profile of the produced electrospun nanofibrous meshes was analyzed for 30 days in a PBS solution, Figure 3c. The obtained results showed that the *C. majus*-loaded PCL/PVA_PEC nanofibers exhibited a weight loss of 40.22 ± 2.86%, while the plain PCL/PVA_PEC nanofibers only lost 26.96 ± 2.09% of the initial weight. The increase in the degradation rate when *C. majus* extract was incorporated into electrospun PCL/PVA_PEC nanofibrous meshes is mainly due to the lower fiber thickness that provides a higher porosity and consequently improves the contact with PBS solution, accelerating their degradation. A similar *in vitro* degradation profile was reported by Yousefi et al. [48], when *Lawsonia inermis* extract was added to the Chitosan/PEO blend solution.

3.2.7. Wettability Studies

Material surface wettability is a critical parameter for the application of the electrospun nanofibrous materials in skin tissue engineering [49,50]. In this context, the water contact angle (WCA) determination has been used to characterize the surface wettability of these materials. According to literature WCA values between 40° and 70° are characteristic of moderate hydrophilic materials and are more proper for supporting cell adhesion, spreading, and proliferation, in comparison with very hydrophilic (WCA < 20°) or hydrophobic (WCA > 90°) surfaces [49,50]. Regarding the obtained results, the plain PCL/PVA_PEC nanofibers exhibited a WCA of 73.85 ± 11.21°, while the *C. majus*-loaded PCL/PVA_PEC nanofibers presented WCA value of 60.30 ± 14.99°. In this case, the produced electrospun PCL/PVA_PEC nanofibrous meshes displayed a moderate hydrophilic character. Moreover, the incorporation of the *C. majus* extract led to a lower WCA value, which might be due to the presence of polar functional groups in the crude plant extract, such as esters and hydroxyl groups that confer a more hydrophilic character to the nanofibers [29]. Therefore, the *C. majus*-loaded PCL/PVA_PEC nanofibrous meshes are more suitable to provide a moist wound environment while supporting cell adhesion and proliferation, and hence can be potentially used to improve the healing process.

3.2.8. Water Vapor Transmission Rate (WVTR) Analysis

A wound dressing material should provide a proper moist environment at the wound site, avoid wound dehydration, and exudates accumulation [4,44,49]. Therefore, the wound surface moisture can be controlled using wound dressing materials with different WVTRs. Herein, the plain PCL/PVA_PEC nanofibers exhibited a WVTR of 1853.04 ± 204.65 g/m²/day, while *C. majus*-loaded PCL/PVA_PEC nanofibers displayed a WVTR of 2019.82 ± 151.01 g/m²/day. The determined WVTR values showed that the incorporation of *C. majus* extract into the electrospun PCL/PVA_PEC nanofibrous meshes improved their performance. Previous literature data repeatedly showed that WVTR values in the range of 2000-2500 g/m²/day are more suitable to keep the wound moist, as well as to create an ideal healing environment able to avoid fluid accumulation and potential infection [4,51]. On the other hand, a higher WVTR can lead to the wound dehydration, and a lower WVTR may cause an accumulation of exudate at the wound site, resulting in the breakdown of extracellular matrix components or maceration of the wound and surrounding skin, and consequently delaying the healing [4,51]. Regarding the obtained results, the highly porous *C. majus*-loaded PCL/PVA_PEC nanofibrous meshes presented a better capability to create and maintain a moist wound environment during the skin's regeneration process. This result is in agreement with the data previously described by Vakilian et al. [52], who also reported a better water vapor exchange between the wound and surrounding environment when a smooth structure with interconnected pores was fabricated from *Lawsonia inermis*-loaded Poly-L-lactic acid (PLLA)/Gelatin nanofibers.

3.3. Determination of *In Vitro* Release Profile

During the healing process, the sustained release of the bioactive compounds from electrospun nanofibers to the wound site has been studied to enhance the desirable wound healing properties and skin regeneration [4,50]. In this way, the *in vitro* release study was carried out to check the capability and performance of electrospun PCL/PVA_PEC nanofibrous meshes to provide a controlled release of the bioactive compounds present in the crude *C. majus* extract. Herein, the release profile was analyzed, and the amount of *C. majus* released from electrospun nanofibers measured with UV/VIS spectroscopy, Figure 4. The obtained results showed that electrospun PCL/PVA_PEC nanofiber meshes were able to sustain the release of the crude *C. majus* extract for 30 days, which is essential to prevent bacterial infection and maintain an appropriate wound healing environment. Approximately 65.70 ± 4.13% of crude *C. majus* extract was released from electrospun PCL/PVA_PEC nanofibrous meshes during the test period. This result proved that the application of emulsion electrospinning using W/O emulsions could provide an improved drug sustained release profile when hydrophilic bioactive compounds, such as medicinal plant extracts, are incorporated [53].

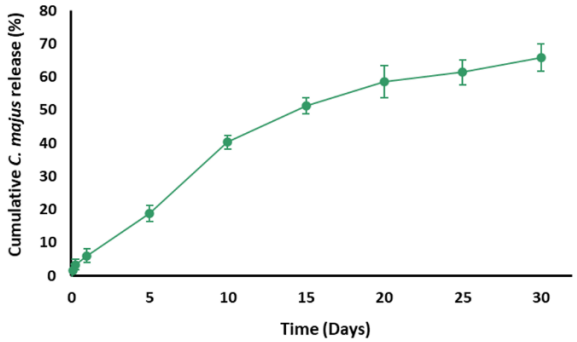

Figure 4 – *In vitro* release profile of *C. majus* from the produced electrospun PCL/PVA_PEC nanofibrous meshes.

3.4. Antibacterial Properties Assessment

Several therapeutic agents have been incorporated into electrospun nanofibers to avoid bacterial colonization to the wound surface and subsequent infections, which may lead to bacterial biofilms, delaying the healing process [4,54]. Herein, the antibacterial properties of the electrospun PCL/PVA_PEC nanofibrous meshes containing *C. majus* were evaluated against *S. aureus* and *P. aeruginosa*, the most common pathogens found in skin wound infections, to prevent bacterial penetration and disease. The obtained results showed antimicrobial activity against both bacteria, Figure 5. However, the electrospun PCL/PVA_PEC nanofibrous meshes containing *C. majus* extract exhibit a higher inhibitory effect against *S. aureus* (99.98 ± 4.43%, 3.82 Log reduction) than against *P. aeruginosa* (95.26 ± 5.52%, 1.32 Log reduction), with $p < 0.01$. Furthermore, the results proved the potential of the crude plant extracts, such as *C. majus*, to be used as a source of natural compounds with valuable antimicrobial activity in wound management. Regarding that, the antibacterial effect of the *C. majus* was found to be related to the capability of some of its alkaloids, such as sanguinarine and chelerythrine, to change the permeability of the bacterial membrane and inhibit the synthesis of bacterial DNA [29]. Therefore, the electrospun PCL/PVA/PEC nanofibrous meshes containing *C. majus* could be useful for preventing and treating wound infections.

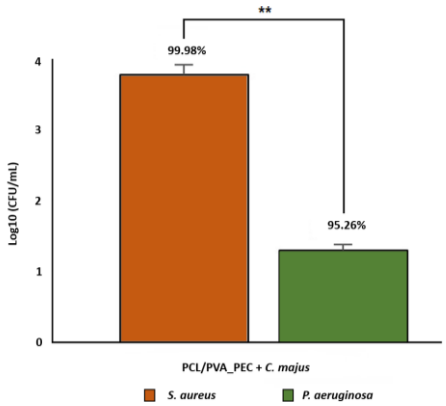

Figure 5 – Assessment of antibacterial properties of the produced *C. majus*-loaded electrospun PCL/PVA_PEC nanofibrous meshes against *S. aureus* and *P. aeruginosa*. (Data are presented as the mean ± SD, ** $p < 0.01$).

3.5. *In Vitro* Cell Viability Assay

An ideal wound dressing should be biocompatible and perform its function without compromised the cellular events involved in wound healing. Moreover, these materials are supposed to reproduce the 3D architecture of the native skin's ECM, which support cell adhesion and proliferation [55]. The *in vitro* biocompatibility of the produced electrospun PCL/PVA_PEC nanofibrous meshes was evaluated using MTT assay, and their effects on NHDF cells proliferation are shown in Figure 6. The cell viability of both the plain and the *C. majus*-loaded PCL/PVA_PEC nanofibrous meshes mats did not show any cytotoxic effect over 7 days.

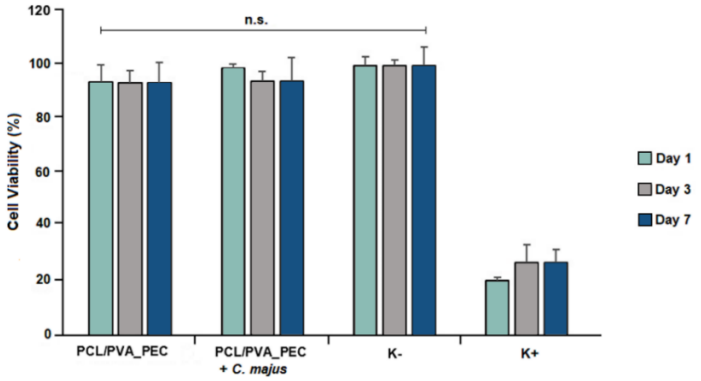

Figure 6 – Evaluation of the NHDF cell after 1, 3, and 7 days in direct contact with the produced electrospun PCL/PVA_PEC nanofibrous meshes with and without *C. majus* extract.

According to the guideline for evaluation of *in vitro* cytotoxicity of medical devices (ISO 10993-5), the biomaterials can be classified as non-cytotoxic and biocompatible when the cell viability is greater than 70%. Hence, it is possible to conclude that the produced electrospun nanofibrous meshes are safe and can be applied as wound dressing without inducing any toxicity.

4. Conclusions

The production of polymeric electrospun nanofibers conjugated with natural products, such as medicinal plants, has been regarded as a promising approach to improve the performance and efficiency of the wound dressing displaying antimicrobial activity. In this study, crude *C. majus* extract, well known for improving the bactericidal activity and the healing process, was successfully incorporated into electrospun PCL/PVA_PEC nanofibrous meshes via emulsion electrospinning for the first time. The produced dressing materials were characterized by their morphological, chemical, physical, and biological features. The manufactured electrospun PCL/PVA_PEC nanofibrous meshes exhibited morphological similarities with native skin's ECM structure and demonstrated to be able to ensure the maintenance of a moist environment at the wound site. Moreover, the *in vitro* release assay revealed that the *C. majus* extract incorporated in the nanofiber structure was gradually

released to the medium for 30 days testing period. Moreover, the produced electrospun nanofiber meshes presented mechanical properties similar to those of the human skin and showed the capability to inhibit *S. aureus* and *P. aeruginosa* growth, without compromising cell viability. Therefore, the loading and controlled release of *C. majus* extract using the electrospun PCL/PVA_PEC nanofibrous meshes could be potentially applied to prevent bacterial wound infection and consequently accelerate the healing process. Soon, *in vivo* studies will be performed to further characterize the performance of these dressing materials for wound care and management, as well as the possible allergic reactions that *C. majus* extract may cause to patients.

Author Contributions: C.M. performed the experiments; A.P.G. performed the SEM experiments; I.C.G. and R.F. supervised the study; C.M. wrote the manuscript; M.A. and I.C.G. reviewed the manuscript. All authors have read and agreed to the published version of the manuscript.

Funding: The authors are also grateful for the funding support given by FibEnTech Research Unit (Project UIDB/00195/2020). Cláudia Mouro acknowledges a PhD fellowship from the Foundation for Science and Technology (FCT) (PD/BD/113550/2015).

Data Availability Statement: The data presented in this study are available in this article. Acknowledgments: The authors would like to thank Ana Raquel Nunes for her help in the *in vitro* cell viability assay.

Conflicts of Interest: The authors declare no conflict of interest.

References

1. Felgueiras, H.P.; Amorim, M.T.P. Functionalization of electrospun polymeric wound dressings with antimicrobial peptides. *Colloid Surf. B Biointerfaces* **2017**, *156*, 133–148.
2. Gizaw, M.; Thompson, J.; Faglie, A.; Lee, S.Y.; Neuenschwander, P.; Chou, S.F. Electrospun fibers as a dressing material for drug and biological agent delivery in wound healing applications. *Bioengineering* **2018**, *5*, 9.
3. Yang, X.; Fan, L.; Ma, L.; Wang, Y.; Lin, S.; Yu, F.; Pan, X.; Luo, G.; Zhang, D.; Wang, H. Green electrospun Manuka honey/silk fibroin fibrous matrices as potential wound dressing. *Mater. Des.* **2017**, *119*, 76–84.
4. Pilehvar-Soltanahmadi, Y.; Dadashpour, M.; Mohajeri, A.; Fattahi, A.; Sheervalilou, R.; Zarghami, N. An overview on application of natural substances incorporated with electrospun nanofibrous scaffolds to development of innovative wound dressings. *Mini-Rev. Med. Chem.* **2017**, *18*, 414–427.

5. Shankhwar, N.; Kumar, M.; Mandal, B.B.; Robi, P.S.; Srinivasan, A. Electrospun polyvinyl alcohol-polyvinyl pyrrolidone nanofibrous membranes for interactive wound dressing application. *J. Biomater. Sci. Polym. Ed.* **2016**, *27*, 247–262.

6. Azimi, B.; Maleki, H.; Zavagna, L.; de la Ossa, J.G.; Linari, S.; Lazzeri, A.; Danti, S. Bio-based electrospun fibers for wound healing. *J. Funct. Biomater.* **2020**, *11*, 67.

7. Kumbar, S.G.; Nukavarapu, S.P.; James, R.; Nair, L.S.; Laurencin, C.T. Electrospun poly(lactic acid-co-glycolic acid) scaffolds for skin tissue engineering. *Biomaterials* **2008**, *29*, 4100–4107.

8. Juncos Bombin, A.D.; Dunne, N.J.; McCarthy, H.O. Electrospinning of natural polymers for the production of nanofibres for wound healing applications. *Mater. Sci. Eng. C* **2020**, *114*, 110994.

9. Fatehi, P.; Abbasi, M. Medicinal plants used in wound dressings made of electrospun nanofibers. *J. Tissue Eng. Regen. Med.* **2020**, *14*, 1527–1548.

10. Kalva, S.N.; Augustine, R.; Al Mamun, A.; Dalvi, Y.B.; Vijay, N.; Hasan, A. Active agents loaded extracellular matrix mimetic electrospun membranes for wound healing applications. *J. Drug Deliv. Sci. Technol.* **2021**, *63*, 102500.

11. Sell, S.; Barnes, C.; Smith, M.; McClure, M.; Madurantakam, P.; Grant, J.; McManus, M.; Bowlin, G. Extracellular matrix regenerated: Tissue engineering via electrospun biomimetic nanofibers. *Polym. Int.* **2007**, *56*, 1349–1360.

12. Herrmann, I.; Supriyanto, E.; Jaganathan, S.K.; Manikandan, A. Advanced nanofibrous textile-based dressing material for treating chronic wounds. *Bull. Mater. Sci.* **2018**, *41*, 18.

13. Safdari, M.; Shakiba, E.; Kiaie, S.H.; Fattahi, A. Preparation and characterization of Ceftazidime loaded electrospun silk fibroin/gelatin mat for wound dressing. *Fiber Polym.* **2016**, *17*, 744–750.

14. Liu, G.; Gu, Z.; Hong, Y.; Cheng, L.; Li, C. Electrospun starch nanofibers: Recent advances, challenges, and strategies for potential pharmaceutical applications. *J. Control. Release* **2017**, *252*, 95–107.

15. Kim, G.H.; Kang, Y.M.; Kang, K.N.; Kim, D.Y.; Kim, H.J.; Min, B.H.; Kim, J.H.; Kim, M.S. Wound dressings for wound healing and drug delivery. *J. Tissue Eng. Regen. Med.* **2011**, *8*, 1–7.

16. Boateng, J.S.; Matthews, K.H.; Stevens, H.N.E.; Eccleston, G.M. Wound healing dressings and drug delivery systems: A review. *J. Pharm. Sci.* **2008**, *97*, 2892–2923.

17. Goh, Y.F.; Shakir, I.; Hussain, R. Electrospun fibers for tissue engineering, drug delivery, and wound dressing. *J. Mater. Sci.* **2013**, *48*, 3027–3054.

18. Liu, M.; Duan, X.P.; Li, Y.M.; Yang, D.P.; Long, Y.Z. Electrospun nanofibers for wound healing. *Mater. Sci. Eng. C* **2017**, *76*, 1413–1423.

19. Basar, A.O.; Castro, S.; Torres-Giner, S.; Lagaron, J.M.; Turkoglu Sasmazel, H. Novel poly(ε-caprolactone)/gelatin wound dressings prepared by emulsion electrospinning with controlled release capacity of Ketoprofen anti-inflammatory drug. *Mater. Sci. Eng. C* **2017**, *81*, 459–468.

20. Lee, K.; Lee, S. Electrospun nanofibrous membranes with essential oils for wound dressing applications. *Fiber. Polym.* **2020**, *21*, 999–1012.

21. Zhang, W.; Ronca, S.; Mele, E. Electrospun nanofibres containing antimicrobial plant extracts. *Nanomaterials* **2017**, *7*, 42.

22. Jin, G.; Prabhakaran, M.P.; Kai, D.; Annamalai, S.K.; Arunachalam, K.D.; Ramakrishna, S. Tissue engineered plant extracts as nanofibrous wound dressing. *Biomaterials* **2013**, *34*, 724–734.

23. Aghamohamadi, N.; Sanjani, N.S.; Majidi, R.F.; Nasrollahi, S.A. Preparation and characterization of Aloe vera acetate and electrospinning fibers as promising antibacterial properties materials. *Mater. Sci. Eng. C* **2019**, *94*, 445–452.

24. Suganya, S.; Senthil Ram, T.; Lakshmi, B.S.; Giridev, V.R. Herbal drug incorporated antibacterial nanofibrous mat fabricated by electrospinning: An excellent matrix for wound dressings. *J. Appl. Polym. Sci.* **2011**, *121*, 2893–2899.

25. Jenifer, P.; Kalachaveedu, M.; Viswanathan, A.; Gnanamani, A. Mubeena fabricated approach for an effective wound dressing material based on a natural gum impregnated with Acalypha indica extract. *J. Bioact. Compat. Polym.* **2018**, *33*, 612–628.

26. Moradkhannejhad, L.; Abdouss, M.; Nikfarjam, N.; Mazinani, S.; Heydari, V. Electrospinning of zein/propolis nanofibers; antimicrobial properties and morphology investigation. *J. Mater. Sci. Mater. Med.* **2018**, *29*, 165.

27. Wang, J.; Vermerris, W. Antimicrobial nanomaterials derived from natural products-a review. *Materials* **2016**, *9*, 255.

28. Khan, A.u.R.; Xiangyang, S.; Ahmad, A.; Mo, X.-M. Electrospinning of crude plant extracts for antibacterial and wound healing applications: A review. *SM J. Biomed. Eng.* **2018**, *4*, 1–8.

29. Maji, A.K.; Banerji, P. *Chelidonium majus* L. (Greater celandine)—A review on its phytochemical and therapeutic perspectives. *Int. J. Herb. Med.* **2015**, *3*, 10–27.

30. Yang, G.; Lee, K.; Lee, M.H.; Kim, S.H.; Ham, I.H.; Choi, H.Y. Inhibitory effects of *Chelidonium majus* extract on atopic dermatitis-like skin lesions in NC/Nga mice. *J. Ethnopharmacol.* **2011**, *138*, 398–403.

31. Borghini, A.; Pietra, D.; di Trapani, C.; Madau, P.; Lubinu, G.; Bianucci, A.M. Data mining as a predictive model for *Chelidonium majus* extracts production. *Ind. Crop Prod.* **2015**, *64*, 25–32.

32. Orland, A.; Knapp, K.; König, G.M.; Ulrich-Merzenich, G.; Knöß, W. Combining metabolomic analysis and microarray gene expression analysis in the characterization of the medicinal plant *Chelidonium majus* L. *Phytomedicine* **2014**, *21*, 1587–1596.

33. Tra Thanh, N.; Ho Hieu, M.; Tran Minh Phuong, N.; Do Bui Thuan, T.; Nguyen Thi Thu, H.; Thai, V.P.; Do Minh, T.; Nguyen Dai, H.; Vo, V.T.; Nguyen Thi, H. Optimization and characterization of electrospun polycaprolactone coated with gelatin-silver nanoparticles for wound healing application. *Mater. Sci. Eng. C* **2018**, *91*, 318–329.

34. Pedram Rad, Z.; Mokhtari, J.; Abbasi, M. Fabrication and characterization of PCL/zein/gum arabic electrospun nanocomposite scaffold for skin tissue engineering. *Mater. Sci. Eng. C* **2018**, *93*, 356–366.

35. Patra, N.; Salerno, M.; Cernik, M. Electrospun polyvinyl alcohol/pectin composite nanofibers. In Electrospun Nanofibers; Elsevier Inc.: Amsterdam, The Netherlands, 2017; pp. 599–608, ISBN 9780081009116.

36. Lin, H.Y.; Chen, H.H.; Chang, S.H.; Ni, T.S. Pectin-chitosan-PVA nanofibrous scaffold made by electrospinning and its potential use as a skin tissue scaffold. *J. Biomater. Sci. Polym. Ed.* **2013**, *24*, 470–484.

37. Munarin, F.; Tanzi, M.C.; Petrini, P. Advances in biomedical applications of pectin gels. Int. *J. Biol. Macromol.* **2012**, *51*, 681–689.

38. Ajalloueian, F.; Tavanai, H.; Hilborn, J.; Donzel-Gargand, O.; Leifer, K.; Wickham, A.; Arpanaei, A. Emulsion electrospinning as an approach to Fabricate PLGA/chitosan nanofibers for biomedical applications. *BioMed Res. Int.* **2014**, *2014*, 475280.

39. Yeh, C.C.; Li, Y.T.; Chiang, P.H.; Huang, C.H.; Wang, Y.; Chang, H.I. Characterizing microporous PCL matrices for application of tissue engineering. *J. Med. Biol. Eng.* **2009**, *29*, 92–97.

40. Artamonova, E.S.; Kurkin, V.A. Developing methods for qualitative and quantitative analysis of *Chelidonium majus* herbs. *Pharm. Chem. J.* **2008**, *42*, 633–636.

41. Zuo, G.Y.; Meng, F.Y.; Han, J.; Hao, X.Y.; Wang, G.C.; Zhang, Y.L.; Zhang, Q. *In Vitro* activity of plant extracts and alkaloids against clinical isolates of extended-spectrum β-lactamase (ESBL)-producing strains. *Molecules* **2011**, *16*, 5453.

42. Committee on Herbal Medicinal Products (HMPC) Assessment Report on *Chelidonium majus* L., Herba. Available online: https: //www.ema.europa.eu/en/documents/herbal-report/final-assessment-report-chelidonium-majus-l-herba_en.pdf (accessed on 8 July 2021).

43. Agnes Mary, S.; Giri Dev, V.R. Electrospun herbal nanofibrous wound dressings for skin tissue engineering. *J. Text. Inst.* **2015**, *106*, 886–895.

44. Motealleh, B.; Zahedi, P.; Rezaeian, I.; Moghimi, M.; Abdolghaffari, A.H.; Zarandi, M.A. Morphology, drug release, antibacterial, cell proliferation, and histology studies of chamomile-loaded wound dressing mats based on electrospun nanofibrous poly(ε-caprolactone)/polystyrene blends. *J. Biomed. Mater. Res. Part B* **2014**, *102*, 977–987.

45. Dos Santos, D.M.; Leite, I.S.; de Lacerda Bukzem, A.; de Oliveira Santos, R.P.; Frollini, E.; Inada, N.M.; Campana-Filho, S.P. Nanostructured electrospun nonwovens of poly(ε-caprolactone)/quaternized chitosan for potential biomedical applications. *Carbohydr. Polym.* **2018**, *186*, 110–121.

46. Augustine, R.; Kalarikkal, N.; Thomas, S. Electrospun PCL membranes incorporated with biosynthesized silver nanoparticles as antibacterial wound dressings. *Appl. Nanosci.* **2016**, *6*, 337–344.

47. Ninan, N.; Muthiah, M.; Park, I.K.; Elain, A.; Thomas, S.; Grohens, Y. Pectin/carboxymethyl cellulose/microfibrillated cellulose composite scaffolds for tissue engineering. *Carbohydr. Polym.* **2013**, *98*, 877–885.

48. Yousefi, I.; Pakravan, M.; Rahimi, H.; Bahador, A.; Farshadzadeh, Z.; Haririan, I. An investigation of electrospun Henna leaves extract-loaded chitosan based nanofibrous mats for skin tissue engineering. *Mater. Sci. Eng. C* **2017**, *75*, 433–444.

49. Trinca, R.B.; Westin, C.B.; da Silva, J.A.F.; Moraes, Â.M. Electrospun multilayer chitosan scaffolds as potential wound dressings for skin lesions. *Eur. Polym. J.* **2017**, *88*, 161–170.

50. Wang, J.; Planz, V.; Vukosavljevic, B.; Windbergs, M. Multifunctional electrospun nanofibers for wound application—Novel insights into the control of drug release and antimicrobial activity. *Eur. J. Pharm. Biopharm.* **2018**, *129*, 175–183.

51. Xu, R.; Xia, H.; He, W.; Li, Z.; Zhao, J.; Liu, B.; Wang, Y.; Lei, Q.; Kong, Y.; Bai, Y.; et al. Controlled water vapor transmission rate promotes wound-healing via wound re-epithelialization and contraction enhancement. *Sci. Rep.* **2016**, *6*, 1–12.

52. Vakilian, S.; Norouzi, M.; Soufi-Zomorrod, M.; Shabani, I.; Hosseinzadeh, S.; Soleimani, M.L. inermis-loaded nanofibrous scaffolds for wound dressing applications. *Tissue Cell* **2018**, *51*, 32–38.

53. Nikmaram, N.; Roohinejad, S.; Hashemi, S.; Koubaa, M.; Barba, F.J.; Abbaspourrad, A.; Greiner, R. Emulsion-based systems for fabrication of electrospun nanofibers: Food, pharmaceutical and biomedical applications. *RSC Adv.* **2017**, *7*, 28951–28964.

54. Sofokleous, P.; Stride, E.; Edirisinghe, M. Preparation, characterization, and release of amoxicillin from electrospun fibrous wound dressing patches. *Pharm. Res.* **2013**, *30*, 1926–1938.

55. Poornima, B.; Korrapati, P.S. Fabrication of chitosan-polycaprolactone composite nanofibrous scaffold for simultaneous delivery of ferulic acid and resveratrol. *Carbohydr. Polym.* **2017**, *157*, 1741–1749.

Part II
Electrospun Double-Layered for Wound Dressing Applications

This part is focused on the development of the electrospun nanofibrous membranes with two different layers containing crude plant extracts. The double-layer electrospun membranes exhibited the capability to restore the structural and functional properties of the skin and presented antibacterial activity. Hence, the electrospun wound dressing membranes designed as double layers are suggested to be a superior strategy to further enhance the healing process and prevent infections.

This part includes the following scientific publications:

Cláudia Mouro, Ana P. Gomes, and Isabel C. Gouveia. Double-layer PLLA/PEO_Chitosan nanofibrous mats containing *Hypericum perforatum* L. as an effective approach for wound treatment. Polymers for Advanced Technologies (2021) 32(4):1493-1506. (**Paper 5**)

Cláudia Mouro, Raul Fangueiro, and Isabel C. Gouveia. Preparation and Characterization of Electrospun Double-layered Nanocomposites Membranes as a Carrier for *Centella asiatica* (L.). Polymers (2020) 12(11):2653. (**Paper 6**)

Paper 5 - Double-layer PLLA/PEO_Chitosan nanofibrous mats containing *Hypericum perforatum* L. as an effective approach for wound treatment

Abstract

Despite a large number of wound dressing materials in the market, an ideal dressing able to re-establish both the features and functions of the native skin remains a challenge. Concerning this, the present study aimed to produce a new double-layer nanofibrous dressing material. The upper layer was fabricated by using Poly(L-lactic acid; PLLA) to act as a hydrophobic protective barrier, while the highly porous lower layer composed of a blend of Poly(ethylene oxide) (PEO) and Chitosan (CS) containing *Hypericum perforatum* L. (HP) was produced to be used in the wound site, reduce the risk of infection, and enhance the healing process. The produced double-layer material exhibited the required chemical, physical, and mechanical properties. Besides, the results showed an inhibitory effect on *Staphylococcus aureus* and *Pseudomonas aeruginosa* growth without providing any cytotoxicity on normal human dermal fibroblast (NHDF) cells. Therefore, these findings emphasize the potential use of this material as an antimicrobial wound dressing to treat skin lesions.

Graphical Abstract

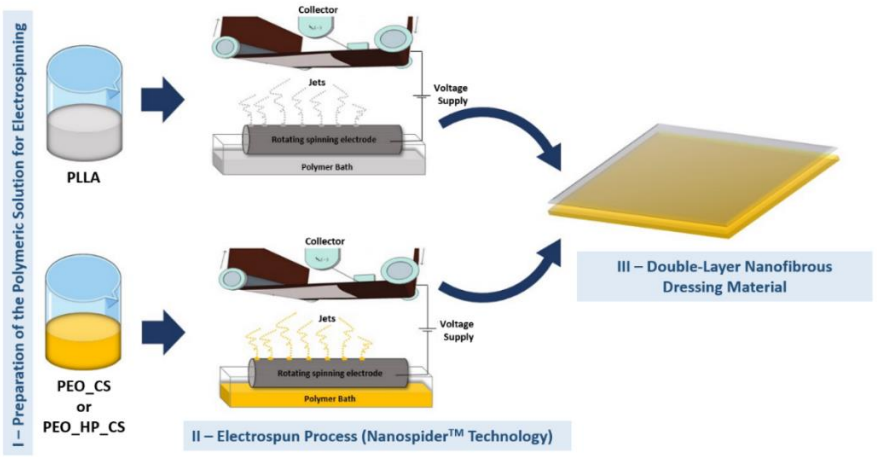

Keywords: Nanospider technology; multilayer electrospinning; crude plant extracts; *Hypericum perforatum* L.*;* wound dressings.

1. Introduction

The skin is a sensory organ capable of acting as a physical barrier against harmful external influences, provides thermo-regulation to maintain consistent body temperature, and contributes to biological, immunological, and metabolic functions [1-3]. The skin's three main layers confer these unique abilities: the epidermis, the thin outer layer, directly exposed to the external environment, the dermis, the thick middle layer, responsible for skin's strength and elasticity, and the subcutaneous tissue, the innermost layer, which contain abundant fat and act as additional insulation and mechanical protection [3]. Nevertheless, the skin's structure and functions can be compromised after injury, and consequently, a skin wound can occur. Many different types of wounds can affect skin integrity. The wounds may be superficial, partial-thickness, or full-thickness wounds, depending on the number of skin layers that are damaged [4]. However, partial-thickness and full-thickness wounds, may particularly cause severe changes in body temperature, due to fluid loss and electrolyte disorders. Besides, although the accumulation of the exudates around the wounds may represent an optimal moist and nutrient-rich environment, the damaged skin is more susceptible to bacterial growth and under these conditions increase the risk of infection, delaying the normal healing process [4-6]. The most common gram-positive bacteria present in the wound environment is the *Staphylococcus aureus*. However, *Escherichia coli* and *Pseudomonas* species are often found at the later stages of chronic wounds and tend to penetrate the skin's deeper layers, contributing to significant tissue damage [7]. Regarding that, remarkable advances have been made to prevent wound bacterial contamination. The electrospun nanofibrous mats have arisen as promising materials to re-establish the natural skin features, due to their ability to mimic the human skin's extracellular matrix (ECM) architecture that supports cell adhesion and proliferation, and encourages the formation of new tissue [1,3,4,8-13]. Moreover, the inherently high surface area and porosity, exhibited by electrospun nanofibers, might promote the hemostasis, quickly absorb wound exudates and control a moist wound environment, allowing a beneficial transport of nutrients, oxygen, and water permeation [1,3,4,8-13]. Also, these nonwovens structures are flexible, provide conformability to the wound site, present an effective physical barrier, and can reduce scar formation. In addition, the biological performance of the electrospun nanofibers can be further improved by incorporating a wide range of bioactive compounds, like growth factors, vitamins, antibiotics, analgesics, anti-inflammatory, and antimicrobial agents [1,3,4,8-13]. For this purpose, blend, coaxial, and emulsion electrospinning techniques have been extensively explored. However, recent studies report the production of multi-layered nanofibers containing bioactive agents through sequential electrospinning [14,15]. Accordingly, in this study, Nanospider technology, a modified electrospinning technique, based on a rotating spinning electrode, was used to produce a new double-layer nanocomposite dressing material containing a crude plant extract [16-18]. The Poly(L-lactic acid; PLLA), a biodegradable and biocompatible synthetic polymer, approved by the US Food and Drug Administration (FDA) for direct contact with biological fluids, was selected to produce the upper layer, due to its unique mechanical

properties [19,20]. On the other hand, a lower layer of Poly(ethylene oxide); PEO) and Chitosan (CS) was considered to be in direct contact with the injured tissue, and the crude *Hypericum perforatum* L. (HP) extract was further incorporated to enhance their biological properties and antimicrobial ability. The CS, a natural polysaccharide-based biopolymer, was blended with the PEO, a hydrophilic water-soluble synthetic polymer, to improve its electrospinnability, since the CS presents limited solubility at physiological pH and high viscosity in acid solutions [1,14,21-23]. Also, the CS has been used to stimulate the production of collagen and promote skin cell adhesion and proliferation, and it has been demonstrated to display bactericidal activity and hemostatic properties [1,14,21-23]. In turn, the crude HP extract contains multiple interesting bioactive phytochemicals, like naphthodianthrones (hypericin, pseudohypericin), phloroglucinol (hyperforin), flavonoids (hyperoside, quercitrin, rutin), and phenolic acids (chlorogenic acid), which exhibit excellent medicinal properties [24-26]. Particularly, naphthodianthrones like hypericin (Hyp) has shown notable anti-inflammatory and antimicrobial properties, which make this plant extract useful to accelerate wound healing and prevent infection. Besides, the HP extract has demonstrated to enhance fibroblast proliferation, revascularization, and collagen deposition [24-26]. Furthermore, the crude natural plant extracts, which are widely available and inexpensive, have emerged as an attractive therapeutic option to suppress the incidence of antibiotic-resistance bacteria because they possess low side effects and can exert their activity not only killing the microorganism itself, but affecting several key events in the pathogenic process [27-30]. Herein, the new double-layer PLLA/PEO_HP_CS nanofibrous material was successfully fabricated by the deposition of a PEO_HP_CS layer on a dense PLLA layer using a multilayer electrospinning method. The obtained results revealed the suitability of this material to be applied as a multifunctional wound dressing in the treatment of wounds. Likewise, these results demonstrated a unique capability of the eco-friendly and low-cost crude HP extract to promote the wound healing process while protecting the wound from infection.

2. Experimental

2.1. Materials

Hypericum perforatum L. (HP) was bought from a Portuguese botanic shop. Normal human dermal fibroblasts (NHDF) cells were purchased from ATCC – American Type Culture Collection. Poly(L-lactic acid) (PLLA) with an average molecular weight (MW) of 217,000 to 225,000 g/mol, Purasorb (PL18), was acquired from Corbion Purac. Poly(ethylene oxide) (PEO) (MW 100,000 g/mol) and Chitosan (CS) (MW 50,000-190,000 g/mol, degree of deacetylation 75%-85%) were obtained from Sigma-Aldrich. Chloroform (analytical grade), dimethylformamide (DMF; analytical grade), glacial acetic acid, and ethanol absolute were purchased from Fisher Chemical. Nutrient agar (NA), nutrient broth (NB), and agar for microbiology were obtained from Fluka. Brain Heart Infusion (BHI) broth

was bought from Panreac. Sodium chloride (NaCl), Mueller-hinton broth (MHB), tween 80, dimethyl sulfoxide (DMSO) anhydrous ≥99.9%, ethylene glycol anhydrous (99.8%), diiodomethane, trypsin, and 3-(4,5-Dimethyl-2-thiazolyl)-2,5-diphenyl-2H-tetrazolium bromide (MTT) were acquired from Sigma Aldrich. Phosphate-buffered saline (PBS) was purchased from Alfa Aesar. All solvents were used as received without further purification.

2.2. Crude HP extract

2.2.1. Preparation of crude ethanolic HP extract

The crude extract was obtained from aerial parts of the plant by the maceration method using water and ethanol in a ratio of 20:80. Briefly, approximately 2.50 g of powdered plant material was macerated with 50 mL of solvent at room temperature. Afterward, the ethanolic extract was filtered with filter paper (Whatman No. 1, 11 µm pore size), and the filtrate was evaporated by Rotavapor (Buchi Rotavapor RE 111) to obtain the dried extract. The extract yield percentage based on the starting material was 17.97%. Finally, the dried HP extract was properly stored in the Eppendorf tubes and then used for the investigation, as described below.

2.2.2. Analysis of the total content of Hypericin in the crude HP extract

The total content of Hyp from the crude HP extract was quantified by the spectrophotometric method described by Pourhojat et al. [31]. Briefly, stock solutions (6000 to 50 ppm) of dried crude HP extract were prepared. Then, the Hyp content (% Hyp [wt/wt]) was calculated from the absorbance readings of each HP solution at 587 nm, using phosphate buffer saline (PBS) pH = 5.5 as control. The Hyp content was determined through Equation (1):

$$\text{Hyp } (\%) = \frac{A}{780}\frac{100}{m} \quad (1)$$

Where A is the measured absorbance, m the weight in grams after drying of 25 mL of crude HP extract, and 780 the specific absorbance of Hyp at 587 nm.

2.3. Determination of minimum inhibitory concentration of crude ethanolic HP extract

Broth microdilution minimum inhibitory concentration (MIC) method was used to determine the *in vitro* antimicrobial activity of the crude ethanolic HP extract against *Staphylococcus aureus* (ATTC 6538) (*S. aureus*), a gram-positive bacteria, and *Pseudomonas aeruginosa* (PA25) (*P. aeruginosa*), a gram-negative bacteria, according to NCLS M07-A6 guidelines. Briefly, overnight liquid cultures of

S. aureus and *P. aeruginosa* were diluted in sterile water to get suspensions of 10^8 CFU/mL (0.5 McFarland turbidity). Then, these suspensions were further diluted 1:10 in sterile Mueller-Hinton Broth (MHB) to obtain the bacterial work suspensions of approximately 10^7 CFU/mL. The crude HP solutions were prepared in MHB and ranging from 10 to 0.1 mg/mL. Subsequently, 50 µL of these dilutions and 50 µL of the work suspensions of the *S. aureus* or *P. aeruginosa* were added for each well of the 96 well plates. A positive control (MHB with work suspension), as well as a negative control (containing only MHB), were also included. The 96-well plates were incubated for 24 hours at 37 °C. The MIC value is the lowest concentration of HP extract that visibly inhibits the bacterial growth in the wells (absence of medium turbidity and a pellet on the bottom of each well). All the experiments were performed in triplicate.

2.4. Preparation of polymer solutions

In the first step, the individual PLLA and PEO_CS solutions were freshly prepared to produce the double-layer nanofibrous wound dressing used in this study. The 10% PLLA solution (wt/vol) was prepared at room temperature by dissolution in a 9:1 (vol/vol) chloroform/DMF mixture. This solution was kept under magnetic stirring until complete polymer dissolution. On the other hand, the PEO_CS blend was prepared from 8% PEO solution (wt/vol) in 8:2 (vol/vol) ethanol/distilled water and 4% CS (wt/vol) in 14% acetic acid (vol/vol) at room temperature. Then, these solutions were blended in a weight fraction of 80:20 and stirred on a magnetic stirrer for 2 hours to obtain a homogeneous solution. The crude HP extract was further added to the PEO_CS blend to obtain a solution containing 2.5% over weight of fiber (owf) of crude HP extract.

2.5. Production of the double-layer nanofibrous mats

The double-layer PLLA/PEO_CS and PLLA/PEO_HP_CS nanofibrous materials were fabricated by Nanospider Technology (Nanospider laboratory machine NS LAB 500S from Elmarco s.r.o., Czech Republic, http://www.elmarco.com), the needleless electrospinning equipment based on a rotating spinning electrode. First, the PLLA solution was electrospun at 80.0 kV with a working distance (distance from the electrode to collector) of 13 cm and an electrode rotation rate of 55 Hz at 20 °C for 30 minutes. After that, the PEO_CS or PEO_HP_CS blend solutions were electrospun directly over recently produced electrospun PLLA fibers at 80.0 kV with a working distance of 9 cm and an electrode rotation rate of 35 Hz at 25 °C for 1 hour. The PLLA's upper layer and the lower layers of PEO_CS and PEO_HP_CS were further electrospun separately for comparative purposes.

2.6. Evaluation of the surface morphology, chemical, physical, and mechanical properties of the produced double-layer nanofibrous mats

2.6.1. Characterization of the surface morphology by scanning electron microscopy

The obtained double-layer nanofibrous mats were observed by scanning electron microscopy (SEM) using a Hitachi S2700 to analyze the fiber morphology. Briefly, the samples were fixed on aluminium stubs using double-sided tape and then sputter-coated with gold using an Emitech K550 sputter coater (Quorum Technologies Ltd, UK). All the samples were examined under SEM with an accelerating voltage of 20 kV. The average diameter and diameter distribution were obtained by analyzing SEM images using public domain software (Image J, National Institutes of Health) for 100 randomly selected fibers.

2.6.2. Attenuated total reflectance–Fourier transform infrared spectroscopy analysis

The chemical structure of the upper layer of PLLA, the crude HP extract, and the lower layers of PEO_CS with and without crude HP extract were analyzed by Fourier transform infrared spectroscopy (FTIR; Thermo-Nicolet is10 FT-IR Spectrophotometer) with an attenuated total reflectance (ATR) accessory. Data were collected over 64 scans at 4 cm^{-1} resolution over the range from 4000 and 400 cm^{-1}.

2.6.3. Porosity assessment

The porosity of the upper layer composed by PLLA and the lower layers of PEO_CS and PEO_HP_CS was determined through a liquid displacement method as previously described by Chitrattha and Phaechamud [32]. Absolute ethanol was used as the displacement liquid because it penetrated easily into the pores and, being a non-solvent of the PLLA, PEO_CS, and PEO_HP_CS did not induce shrinkage or swelling of the electrospun nanofibrous mats. In the first step, the dried samples were weighed (W_S) and immersed in a cylinder containing a known volume of displacement liquid (W_1). Each cylinder was placed in a water-bath sonicator for 40 minutes at 30 °C. After sonication, the amount of ethanol was refilled, and the cylinders were reweighed (W_2). The ethanol-impregnated samples were then removed from the cylinders while the remaining displacement liquid was recorded (W_3). The samples' porosity (ε) was determined through Equation (2) [32]:

$$\varepsilon\ (\%) = \frac{(W_2 - W_3 - W_S)}{(W_1 - W_3)} \times 100 \quad (2)$$

All the experiments were performed in triplicate, and the average values were reported.

2.6.4. Water contact-angle measurement

The contact angle measurements of the double-layer nanofibrous materials composed by the upper layer of PLLA and the lower layers of PEO_CS and PEO_HP_CS were carried out with a Dataphysics Contact Angle System OCAH-200 apparatus, operating in static mode at 25 °C, using deionized water as reference fluid. For each sample, droplets (4 μL) were placed at different locations on the material surface, and then the average was reported as the contact angle of each sample.

2.6.5. Measurement of surface free energy of adhesion

The interactions between bacteria and material surfaces were investigated from sessile drop contact angle measurements at room temperature, using three probe liquids of different polarities: two polar liquids, deionized water and ethylene glycol, and one non-polar component, diiodomethane, whose surface tension components are known. Briefly, the measured contact angles were converted into its Lifshitz-Van der Waals (γ^{LW}) and Lewis acid–base (γ^{AB}) surface free energy components using the Lifshitz-van der Waals and Lewis acid–base approaches proposed by Van Oss et al. [33-35]. The γ AB, being $\gamma^{AB} = 2\sqrt{\gamma^{+}\gamma^{-}}$, was separated into two different components, namely in the electron-donating (γ^{-}) and electron-accepting (γ^{+}) parameters. After that, the total free energy of adhesion (ΔG_{adh}^{TOTAL}) between the bacteria (*S. aureus* and *P. aeruginosa*) (B) and material surfaces (PLLA/PEO_CS and PLLA/PEO_HP_CS nanofibrous mats) (S) in an aqueous suspension (L) was calculated through the surface tension components, according to Equation (3):

$$\Delta G_{adh}^{TOTAL} = \Delta G_{adh}^{LW} + \Delta G_{adh}^{AB} \quad (3)$$

Where the Lifshitz-Van der Waals component was determined by Equation (4):

$$\Delta G_{adh}^{LW} = \left(\sqrt{\gamma_B^{LW}} - \sqrt{\gamma_S^{LW}}\right)^2 - \left(\sqrt{\gamma_B^{LW}} - \sqrt{\gamma_L^{LW}}\right)^2 - \left(\sqrt{\gamma_S^{LW}} - \sqrt{\gamma_L^{LW}}\right)^2 \quad (4)$$

And the Lewis acid-base parameter was determined by Equation 5:

$$\Delta G_{adh}^{AB} = 2\left[\sqrt{\gamma_L^{+}}\left(\sqrt{\gamma_B^{-}} + \sqrt{\gamma_S^{-}} - \sqrt{\gamma_L^{-}}\right) + \sqrt{\gamma_L^{-}}\left(\sqrt{\gamma_B^{+}} + \sqrt{\gamma_S^{+}}\right) - \sqrt{\gamma_L^{+}} - \sqrt{\gamma_B^{-}\gamma_S^{+}} - \sqrt{\gamma_B^{+}\gamma_S^{-}}\right] \quad (5)$$

According to the prediction of the thermodynamic approach, adhesive interactions will be favorable if $\Delta G_{adh}^{TOTAL} < 0$ and unfavorable if $\Delta G_{adh}^{TOTAL} > 0$ [33 − 35].

2.6.6. Water vapor transmission rate (WVTR)

The WVTR through the double-layer PLLA/PEO_CS nanofibrous mats with and without crude HP extract was measured according to the ASTM E96/E96M-15 standard method. Briefly, circular discs

of 1.2 cm diameter were cut from each sample and placed on the top of the glass test tubes containing 10 mL of deionized water. A parafilm tape was used around the open of each test tube to attach the samples and prevent any moisture loss. The electrospun nanofibrous materials were incubated at 37 °C, and the passage of water vapor from the test tube was determined at specific time points through their weight loss and according to the following equation (Equation (6)):

$$\text{Water vapor transmission rate (WVTR)} = \frac{W_{loss}}{A} \quad (6)$$

Where W_{loss} is the daily weight loss of water, and A is the area of the glass tube opening in m^2.

2.6.7. Swelling profiles of the double-layer nanofibrous mats

The swelling behavior of the double-layer PLLA/PEO_CS and PLLA/PEO_HP_CS nanofibrous materials was assessed by a gravimetric method. Briefly, pre-weighted dry samples (W_{dry}) were submerged in PBS, pH = 5.5, for 30 days at 37 °C. At specific time points, the swollen samples were taken out and reweighed after gently removing the excess liquid with a filter paper (W_{wet}). All measurements were conducted in triplicate, and the swelling ratio calculated according to Equation (7):

$$\text{Swelling Ratio (\%)} = \frac{(W_{wet} - W_{dry})}{W_{dry}} \times 100 \quad (7)$$

2.6.8. Characterization of the mechanical properties of the produced double-layer nanofibrous mats

The mechanical properties of the double-layer PLLA/PEO_CS and PLLA/PEO_HP_CS nanofibrous materials were studied under dry conditions using a universal tensile testing machine (DY-35 Adamel Lhomargy, France) according to the guidelines established by Standard Test Method for Tensile Properties of Polymer Matrix Composite Materials (ASTM standard D3039/D3039M). Before testing, the samples (n = 5) were prepared with a width of 1 cm and a length of 4 cm. The length between the clamps was set to 1 cm and performed at a strain rate of 2 mm/min. The Young's modulus, tensile strength, and elongation at break (%E) were calculated from the strain–stress curve based on the Equations (8) and (9), respectively:

$$Stress = \sigma = \frac{F}{A} \quad (8)$$

$$Strain = \varepsilon = \frac{\Delta l}{L} \quad (9)$$

Where F is the maximum load at the breakpoint; A is the area of the cross-section of a specimen on which force was applied (mm^2); Δl is the extension of length at rupture; L is the initial length between the clamps.

2.7. *In vitro* release study of HP from double-layer nanofibrous mats

The *in vitro* crude HP extract release from the double-layer PLLA/PEO_HP_CS nanofibrous mats was studied in PBS, pH 5.5, at 37 °C, with constant rotation at a speed of 100 rpm, simulating the acidic environment of a wound site. At predetermined intervals, a fixed volume of release medium was removed and replaced by fresh PBS. The released crude HP extract was measured by UV-Vis spectrometry at wavelength λmax = 587 nm, which is associated with the absorbance of naphthodianthrones, like hypericin [31]. The *in vitro* crude HP extract release curve was drawn based on the cumulative release percentage of HP in PBS solution over 30 days. Previously, a calibration curve was constructed from a series of HP standard solutions with concentrations from 0.00 mg/mL to 10.00 mg/mL. All measurements were carried out in triplicate.

2.8. Evaluation of the biological properties of the produced double-layer nanofibrous mats

2.8.1. Antibacterial properties assessment

The ability of the double-layer PLLA/PEO_HP_CS nanofibrous dressing material to inhibit *S. aureus* (ATTC 6538) and *P. aeruginosa* (PA25) growth was tested through ASTM E2180-07. Briefly, bacterial suspensions (~10^8 CFU/mL) were prepared from an overnight stationary liquid culture and transferred to the sterile agar slurries previously made with 0.85 (wt/vol) NaCl and 0.30 (wt/vol) agar-agar in deionized water. After that, a thin layer of the semi-solid agar slurries was inoculated over the PLLA's upper layer and the lower layers of PEO_CS and PEO_HP_CS, as well as a 0.22 μm filter paper (control). The samples were assessed immediately after inoculum application (T_{0h}), and after 18 to 24 hours in contact with the agar slurries at 37 °C (T_{24h}). To accomplish that, serial dilutions were carried out with 0.85 (wt/vol) NaCl, plated in NA plates, and incubated at 37 °C during 18 to 24 hours. The bacterial colonies were counted, and CFU/mL was calculated. All samples and control were tested in triplicate, and the results presented as mean values of log (CFU mL^{-1}).

2.8.2. Evaluation of cell viability after cells being in direct contact with the produced double-layer nanofibrous mats

The biocompatibility of the upper layer of PLLA and the double-layer PLLA/PEO_CS and PLLA/PEO_HP_CS nanofibrous materials was evaluated *in vitro* through the 3-(4,5-dimethylthiazol- 2-yl)-2,5-diphenyltetrazolium bromide (MTT) assay following ISO 10993−5 (Biological evaluation of medical devices-Part 5: Tests for *in vitro* cytotoxicity). Briefly, sample discs (n = 4) were placed at the center of each well in 24-well plates, covering <1/10 of its area, and sterilized under UV irradiation (254 nm, ~7 mW cm^{-2}) for 1 hour. After that, normal human dermal fibroblasts (NHDF) cells were used to seed each well containing the samples at a density of 1×10^4 cells/well. The plates were incubated at 37 °C under a humidified 5% CO_2 atmosphere. At specific intervals of time, namely after 1, 3, and 7 days of incubation, the medium of each well was removed and replaced by 1 mL of 0.5 mg/mL MTT reagent solution and incubated for 4 hours under the same conditions. Following this, the content of each well was discarded, and DMSO was added to dissolve the purple formazan crystals of MTT formed. The absorbance of each well was measured at 570 nm using a microplate reader (Biorad xMark microplate spectrophotometer). The measured absorbance was directly proportional to the number of living cells in each well. A negative control (K^-) composed by cells incubated without materials and positive control (K^+) formed by cells incubated with EtOH (96%) were also used.

2.9. Statistical analysis

Data were statistically analyzed according to the one-way ANOVA parametric test followed by multiple comparison test Turkey using GraphPad Prism 6 software (Prism Software). Statistical calculations were based on a confidence level of ≥95% (values of $p < 0.05$ were considered statistically significant).

3. Results and Discussion

3.1. Analysis of the total content of Hypericin (Hyp) in crude HP extract

The total content of Hyp, one of the main bioactive agents responsible for HP antimicrobial properties, is presented in Table 1. The Hyp content in the crude HP extract was 0.29 ± 0.06 (%), according to the calibration equation (y = 0.0001x - 0.0184) with an $r^2 = 0.99$. In fact, the obtained value was similar to that reported by Pourhojat et al. (0.23 ± 0.06 [%]) [31].

Table 1 – Determination of Hypericin (Hyp) content in crude HP extract.

Samples	Dried extract (ppm)	Dried extract (g)	Absorbance in λ_{587}	Hyp (%)
1	6000	0.30	0.81	0.34
2	4000	0.20	0.54	0.35
3	3000	0.15	0.39	0.33
4	1000	0.05	0.07	0.19
5	500	0.025	0.04	0.20
6	200	0.01	0.02	0.26
7	100	0.005	0.01	0.34
8	50	0.0025	0.01	0.31

Note: Average = 0.29 ± 0.06.

3.2. Determination of minimum inhibitory concentration of crude ethanolic HP extract

The MIC values of the crude ethanolic HP extract against *S. aureus* (Gram-positive) and *P. aeruginosa* (Gram-negative) were 2.5 and 5.0 mg/mL, respectively. Reichling et al. reported an inhibitory effect between 1.3 and 2.5 mg/mL and >60 mg/mL on the growth of *S. aureus* and *P. aeruginosa*, respectively, when different watery HP's preparations of loose teas and filtered teas were tested [36]. Although the MIC reported in the aforementioned work, against *P. aeruginosa* (>60 mg/mL), exhibits a higher value than the MIC of 5.0 mg/mL against *P. aeruginosa* found in this research work, both results revealed that the Gram-positive bacteria are more susceptible to the crude HP extract. Moreover, Milosevic et al. have reported MIC values of 1.25 and 2.5 mg/mL against *P. fluorescens* (B28), *P. phaseolicola* (B29), and *P. glycine* (B40) for ethanolic extract of HP [25]. The composition of the medicinal plant extracts can be changed by several factors, namely by growing and harvested plant location, seasonal variations, and the extraction method used. These changes can also influence the presence of phyto-constituents in the plant extracts, and consequently their antimicrobial properties [37-39].

3.3. Evaluation of the surface morphology, chemical, physical, and mechanical properties of the produced double-layer nanofibrous mats

3.3.1. Characterization of the surface morphology by scanning electron microscopy

The double-layer PLLA/PEO_CS nanofibrous materials with and without crude HP extract were successfully fabricated, as shown by SEM images in Figure 1A. A denser upper layer of PLLA with randomly oriented fibers was produced with an average fiber diameter of 1.86 ± 0.68 μm. This result

is in agreement with the data previously reported by Yee Foong and Sultana, who founded a similar mean diameter for PLLA nanofibers (1.62–4.84 μm) [16]. On the other hand, the lower layers of PEO_CS and PEO_HP_CS presented a highly porous nanofiber structure composed of homogenous fibers with a mean diameter of 141.05 ± 46.11 nm and 88.33 ± 29.45 nm, respectively. These results revealed that the less viscosity of the PEO_HP_CS solution used for nanofiber fabrication resulted in the production of the thinner fibers. A similar effect was previously reported by Sadri et al., who observed a decrease in the nanofiber diameter from 100 to 86.18 nm when 2% of green tea (GT) was incorporated into PEO/CS nanofibers [40]. Moreover, the lower average diameters exhibited by PEO_CS and PEO_HP_CS lower layers are within the preferred range of the collagen fibers present in the natural ECM (from 50 to 500 nm), and hence can recreate a new ECM environment [3,41]. The cross-section of the PLLA/PEO_CS and PLLA/PEO_HP_CS nanofibrous mats were also analyzed and proved that these wound dressing materials displayed a double-layer structure with two different layers, Figure 1B.

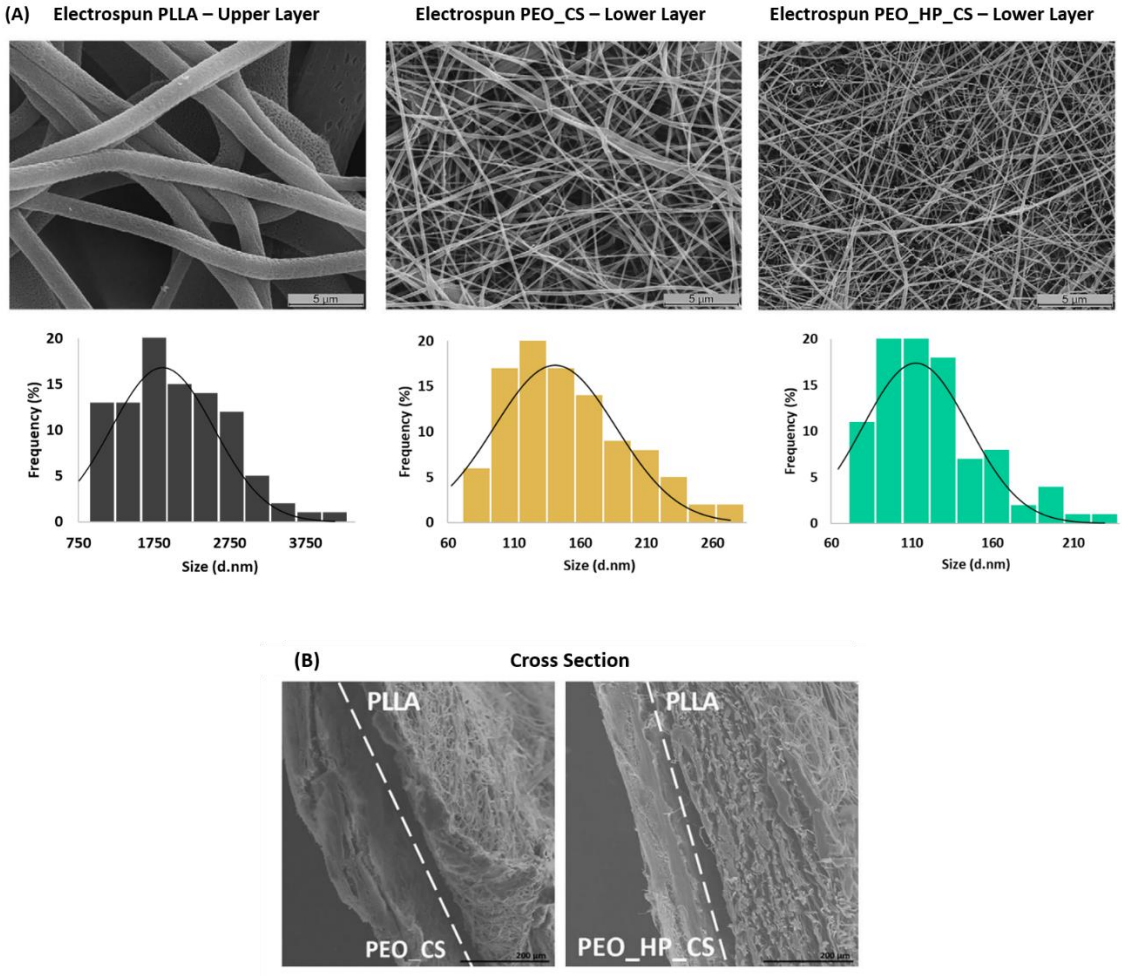

Figure 1 – Characterization of the surface morphology of the produced double-layer nanofibrous materials by scanning electron microscopy (SEM). SEM micrographs and fiber diameters distribution of the Poly(L-lactic acid) (PLLA's) upper layer and the lower layers of the PEO_CS and PEO_HP_CS, respectively (**A**). Macroscopic SEM images of the cross-sections of the produced double-layer nanofibrous mats (**B**).

3.3.2. Attenuated total reflectance-Fourier transform infrared spectroscopy Analysis

The functional groups of PLLA's upper layer, lower layers of the PEO_CS and PEO_HP_CS, and the raw HP extract were characterized by attenuated total reflectance-Fourier transform infrared spectroscopy (ATR-FTIR), as demonstrated by Figure 2. The ATR-FTIR spectrum of the PLLA's upper layer exhibits its characteristic peaks at 1750.58, 1181.56, and 1084.76 cm^{-1} associated with the stretching vibration of the C=O group, and the asymmetric and symmetric stretching vibrations of the C-O-C group, respectively. Also, the band at 1044.06 cm^{-1} corresponds to C-CH_3 stretching of the PLLA [42].

On the other hand, the spectra of the lower layers of PEO_CS and PEO_HP_CS present the typical peak between 3300.00 and 3400.00 cm^{-1} for N-H and O-H stretching of the polysaccharide molecules and crude HP extract [21,22,31]. Moreover, these spectra display two characteristic peaks around 1560.00 and 1650.00 cm^{-1} attributed to the amide groups in the PEO_CS blend, as well as a band between 2879.00 and 2880.00 cm^{-1} associated with the CH_2 stretching groups of PEO. In addition, peaks near 1341.00 and 1359.00 cm^{-1} represent the C-H group, while the band around 1145.00 cm^{-1} is due to C-O-C stretching vibration of the PEO_CS [21,22]. Therefore, the spectra of the lower layers display peaks in the same positions but differ in the intensity of them. This evidence demonstrates the successful incorporation of the crude HP extract into the PEO_CS blend. In addition, the spectrum of the crude ethanolic HP extract confirms its characteristic peaks at 3334.82 cm^{-1} (OH-stretching vibrations), 2980.77 cm^{-1} (C-H bond stretching vibrations), 1646.61 cm^{-1} (bonds in the carbonyl group), 1433.33 cm^{-1} (C-H bending vibrations), 1251.63 cm^{-1} (C-O phenolic groups), 1054.60 cm^{-1} (C-O single bonds stretching vibrations), and 890.47 cm^{-1} (aromatic rings), respectively [31,43].

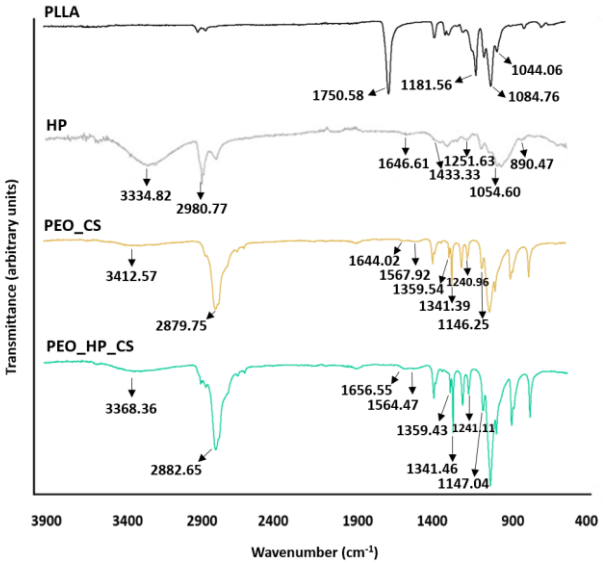

Figure 2 – ATR-FTIR analysis of the produced double-layer nanofibrous materials. Chemical composition of the PLLA's upper layer, and the PEO_CS and PEO_HP_CS's lower layers, as well as the raw crude HP extract.

3.3.3. Porosity assessment

The porous structure of the produced double-layer nanofibrous materials has a direct impact on their performance [1,10,44]. Herein, The PLLA's upper layer displays the lowest porosity (74.25% ± 13.77%), which is essential to prevent microbial penetration and growth within the wound dressing, Figure 3A. On the other hand, the lower layers of PEO_CS and PEO_HP_CS exhibit a highly porous structure with porosities values of 89.19% ± 2.43% and 93.71% ± 1.00%, respectively, Figure 3A. These results demonstrate that the porosity increases in the presence of crude HP extract, which is in agreement with the lower diameter of the PEO_HP_CS nanofibers and the higher number of void spaces existing between the nanofibers. Moreover, the PEO_HP_CS's lower layer, intended to be in direct contact with the injured tissue, exhibited a preferred porosity for cell adhesion and migration, and to provide pathways for oxygen, nutrients, and fluids exchanges. These events are essential for an effective healing process [10,44].

3.3.4. Water contact-angle measurement

The surface wettability is usually measured by the contact angle of the water (WCA) on the material surfaces [14,45]. According to literature, a WCA in the range from 40° to 60°, is characteristic of a moderate hydrophilic material. It is considered optimal for nanofiber-cell interactions, in comparison with a highly hydrophobic material surface (WCA > 90°) or very hydrophilic ones (WCA < 20°) [14,45,46]. In this context, the WCA values were measured to evaluate the wettability's surface of PLLA's upper layer and lower layers of PEO_CS and PEO_HP_CS, Figure 3B. The PLLA's upper layer displayed a WCA value higher than 90° (WCA value of 105.23 ± 2.89°), which suggests a non-wetting behavior and confirms the hydrophobic nature of PLLA fibers. On the other hand, the lowers layers of PEO_CS and PEO_HP_CS exhibited a moderate hydrophilic character as showed by the WCA values of 55.60 ± 8.89° and 50.97 ± 11.60°, respectively. Therefore, the incorporation of crude HP extract into the PEO_CS's lower layer revealed an improved surface wettability, which contributes to enhancing cell adhesion and proliferation and provides an appropriate moist wound environment.

3.3.5. Measurement of surface free energy of adhesion

Bacterial adhesion to biomaterial surfaces is a complex process that can be affected by several factors, such as the physicochemical properties of the bacteria, the material surface properties, and the surrounding environment features [47,48]. In this study, the adhesion of *S. aureus* and *P. aeruginosa* onto PLLA, PEO_CS, and PEO_HP_CS surfaces were determined thermodynamically from a liquid suspension. The free energy of adhesion to the PLLA's upper layer in the presence of *S. aureus* was unfavorable, for example, >0 mJ/m^2, $\Delta GTOTAL = 23.23 \pm 2.51$ mJ/m^2. In the same way, the free energy of adhesion between *P. aeruginosa* and PLLA's upper layer was $\Delta G^{TOTAL} = 19.82 \pm 3.03$

mJ/m². The results obtained revealed that the PLLA's layer is essential for avoiding the adhesion of the bacteria, reinforcing its suitability to act as a protective barrier.

On the other hand, the free energy of adhesion for *S. aureus* when exposed to PEO_CS and PEO_HP_CS's lower layers increased from ΔG^{TOTAL} = 44.60 ± 0.41 mJ/m² to ΔG^{TOTAL} = 48.79 ± 3.08 mJ/m², respectively. The same tendency was observed for the *P. aeruginosa* when in contact with the lower layers of PEO_CS and PEO_HP_CS, the free energy of adhesion increased from ΔG^{TOTAL} = 41.64 ± 0.40 mJ/m² to ΔG^{TOTAL} = 46.01 ± 3.22 mJ/m², respectively. These values indicated that the lower layers were further energetically unfavorable for the bacteria adhesion. This result can be explained by the highly porous structure and high surface area displayed by lower layers surface, which plays an essential role in delivering bioactive agents to the wound site, and subsequently, can avoid bacterial adhesion and growth [8]. Moreover, the excellent intrinsic antimicrobial properties exhibited by CS and HP are also able to prevent bacteria adhesion, acting as an anti-adhesive and inhibiting biofilm formation [1,31,36].

3.3.6. Water vapor transmission rate

An ideal wound dressing should be permeable to maintain a suitable moist environment and prevent wound dehydration [1,49,50]. In this way, the double-layer PLLA/PEO_CS nanofibrous mats displayed a WVTR of 1800.85 ± 133.42 g/m²/day while the double-layer PLLA/PEO_HP_CS nanofibrous mats present a WVTR of 1916.51 ± 143.02 g/m²/day. These values are slightly lower than the recommended WVTR for an appropriate wound dressing (2000-2500 g/m²/day), nonetheless, the incorporation of crude HP extract into the PEO_CS's lower layer leads to an enhancement of the WVTR value. Moreover, these results are in agreement with the WVTR values, obtained in another study, for a double-layer nanofibrous material [15].

3.3.7. Swelling profiles of the double-layer nanofibrous materials

The ability to absorb exudates and provide an optimal balance of moisture at the wound surface can be characterized through the swelling behavior of the produced materials [1]. Herein, the swelling profiles of the double-layer PLLA/PEO_CS and PLLA/PEO_HP_CS nanofibrous mats were analyzed by incubating the samples in a PBS solution at 37 °C, and their weight was monitored at predetermined time points, Figure 3C. The PLLA/PEO_HP_CS displays a higher swelling ratio (~500%) in comparison to PLLA/PEO_CS (~300%). The higher water uptake capacity of the PLLA/PEO_HP_CS can be attributed to its hydrophilic properties and highly porous structure. Also, the hydrophilic character of the crude HP extract further enhances the absorption capability [31]. On the other hand, the higher porosity of the PLLA/PEO_HP_CS increases its swelling ability due to more free space available for water uptake, which improves the dressing's ability to absorb and retain excessive amounts of exudate, which is most common during the inflammatory phase of healing

[22,40]. Hence, the double-layer PLLA/PEO_HP_CS nanofibrous mats can hold more moisture in its structure and allow a highly efficient exudate absorption, helping to avoid healthy tissue maceration, impaired cell proliferation, as well as subsequent infections.

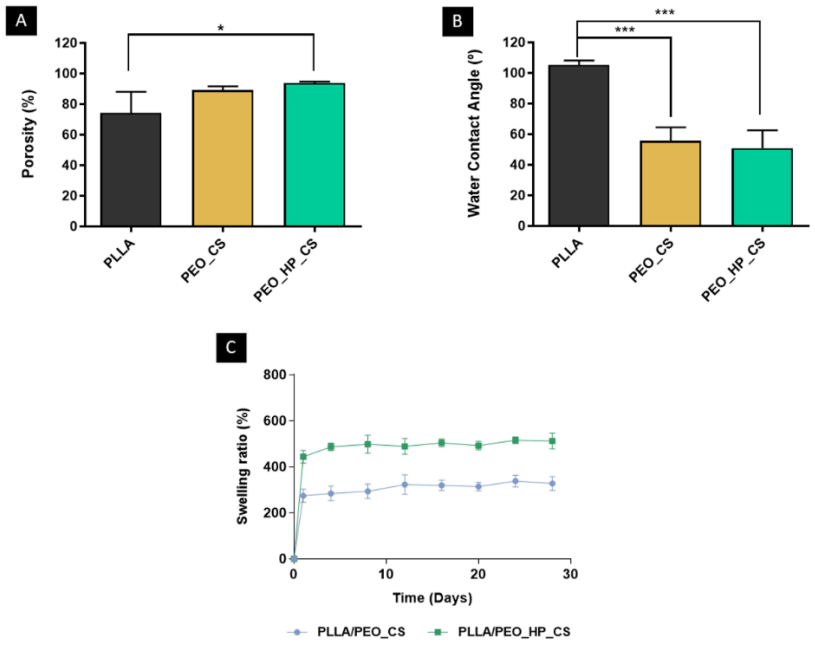

Figure 3 – Characterization of the total porosity (**A**), wettability features (**B**), and the swelling profile (**C**) of the fabricated double-layer nanofibrous materials. (Data are presented as the mean ± SD, * $p < 0.05$ and *** $p < 0.001$).

3.3.8. Characterization of the mechanical properties of the produced double-layer nanofibrous mats

The mechanical performance of the produced double-layer PLLA/PEO_CS and PLLA/PEO_HP_CS nanofibrous materials was evaluated in dry conditions through the analysis of the tensile strength, Young's modulus, and elongation at break for these materials, Table 2. The tensile strength obtained for PLLA/PEO_CS was 2.49 ± 0.17 MPa, whereas for PLLA/PEO_HP_CS this value decreased to 1.93 ± 0.18 MPa. However, the PLLA/PEO_HP_CS presented an increase of the elasticity in comparison with the PLLA/PEO_CS, exhibiting Young's modulus of 15.86 ± 0.50 MPa and 18.20 ± 2.49 MPa, respectively. Moreover, when the crude HP extract was incorporated into the double-layer PLLA/PEO_CS nanofibrous mats, a slight reduction in the elongation at break was observed. In this case, the PLLA/PEO_CS can bear a strain of 13.90% ± 2.83%, whereas the PLLA/PEO_HP_CS can carry a strain of 12.17% ± 1.33%. Through this analysis, it was verified that the produced wound dressing materials revealed similar mechanical properties, and the values showed to be very close to the native skin requirements, Table 2. Thus, from these results, we can conclude that PLLA/PEO_CS

and PLLA/PEO_HP_CS can provide and retain adequate mechanical support during the healing process, as well as facilitate their handling and application [1]. These findings are strongly related to the excellent mechanical properties of the upper layer made of PLLA [20].

Table 2 – Mechanical properties displayed by the double-layer nanofibrous materials and by the natural human skin.

	Tensile strength (MPa)	Young's modulus (MPa)	Elongation at break (%)	Thickness (mm)
PLLA/PEO_CS	2.49 ± 0.17	18.20 ± 2.49	13.90 ± 2.83	0.20 ± 0.01
PLLA/PEO_HP_CS	1.93 ± 0.18	15.86 ± 0.50	12.17 ± 1.33	0.22 ± 0.05
Native human skin	2.50-30.00[a]	0.40-20.00[a]	10.00-115.00[a]	-

[a] The native human skin' values were achieved from Reference 1.

3.4. *In vitro* release study of HP from double-layer nanofibrous mats

The release kinetics of the crude HP extract from double-layer PLLA/PEO_HP_CS dressing material was studied in PBS (pH 5.5) solution at 37 °C. As demonstrated in Figure 4, the HP release from the PLLA/PEO_HP_CS occurred in a gradual manner reaching its maximum after 5 days (76.59% ± 3.83%) [51]. This result suggests that the swelling behavior and hydrophilic character of the PEO_HP_CS can help release the crude HP extract from the lower layer. In a similar way, Sadri et al. also observed a moderate delivery of GT from CS/PEO nanofibers [40]. In addition, the slow wetting of the hydrophobic PLLA surface and the slow biodegradability rate of PLLA's upper layer can be attractive to avoid an undesirable release.

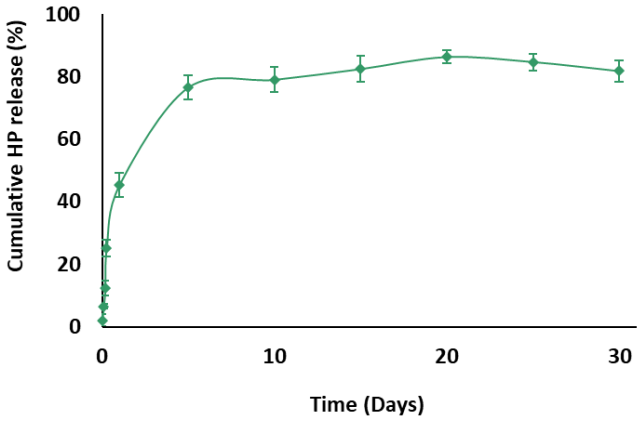

Figure 4 – *In vitro* release study of crude HP extract from produced double-layer PLLA/PEO_HP_CS nanofibrous material at a PBS buffer solution (pH = 5.5) for 30 days at 37 °C.

3.5. Evaluation of the biological properties of the produced double-layer nanofibrous mats

3.5.1. Antibacterial properties assessment

Damaged skin is particularly susceptible to microbial invasion and infections by pathogenic microorganisms, resulting in delayed healing and life-threatening complications [8]. Therefore, the antibacterial efficiency of the produced double-layer nanofibrous materials was evaluated against *S. aureus* and *P. aeruginosa*, two of the most prevalent bacteria in wound infections, Figure 5. Firstly, the capability of the PLLA's upper layer to avoid the bacterial infiltration within its structure was evaluated in comparison with the control, a 0.22 μm filter paper. As expected, the quantitative analysis showed for *S. aureus* and *P. aeruginosa* that after 24 hours of contact with the PLLA's upper layer, there was a total reduction of their viability of 6.92% ± 4.12% and 5.79% ± 1.31%, respectively. The acquired data revealed that the few bacteria were able to penetrate through the PLLA's upper layer due to its lower porosity. Consequently, the upper layer was able to act as a protective barrier avoiding bacteria growth in the wounds and ensuring a non-infectious healing environment [52]. The antimicrobial capacity of the lower layers of PEO_CS and PEO_HP_CS was also characterized to provide an aseptic environment at the wound site. The lower layer of PEO_CS exhibited a growth inhibitory effect against *S. aureus* and *P. aeruginosa* of 62.28% ± 6.10% and 47.52% ± 8.23%, respectively. However, when the crude HP extract was incorporated into the lower layer of PEO_CS, a better inhibitory effect on *S. aureus* and *P. aeruginosa* growth was observed (99.75% ± 1.30% and 90.61% ± 1.63%). This result can be explained by the intrinsic antimicrobial properties of both CS and crude HP extract. The antimicrobial activity of CS is related to its polycationic nature. Thus, the positively charged groups of CS can interact with the bacteria membranes (negatively charged), changing its permeability, and eventually leading to the leakage of the intracellular constituents [53]. Also, the naphthodianthrones, particularly hypericin, from HP can strengthen the CS's inherent antimicrobial action and enhance the antimicrobial activity displayed by a lower layer of PEO_HP_CS [24-26,54]. Therefore, the incorporation of the crude HP extract promotes wound repair while simultaneously helps to reduce wound bacterial colonization and infection.

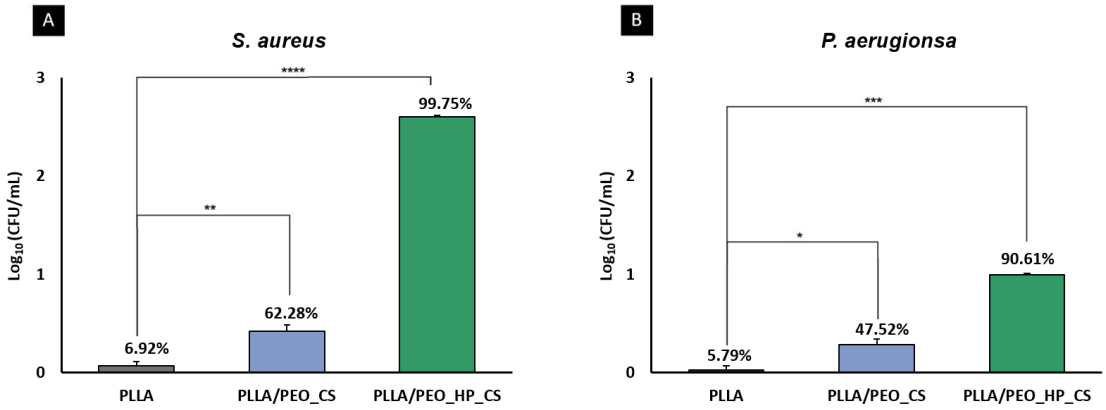

Figure 5 – Evaluation of antibacterial efficiency of the fabricated double-layer PLLA/PEO_CS nanofibrous material containing crude HP extract against *S. aureus* (**A**) and *P. aeruginosa* (**B**). (Data are presented as the mean ± SD, * $p < 0.05$, ** $p < 0.01$, *** $p < 0.001$, and **** $p < 0.0001$).

3.5.2. Evaluation of cell viability after cells being in direct contact with the produced double-layer nanofibrous mats

Wound healing is a complex biological process that involves a wide variety of cellular interactions. Among the different cell types, fibroblasts exhibit a crucial role during the healing process. They are responsible for breaking down the fibrin clot and are involved in the deposition and remodelling of ECM components, formation of collagen structures to provide structural support for other cells, as well as contracting wound tissue [55]. Herein, NHDF cells were used to evaluate the cytotoxic profile of the developed double-layer wound dressing material by using the MTT assay, Figure 6. Concerning this, the upper layer of PLLA and the double-layer PLLA/PEO_CS and PLLA/PEO_HP_CS materials did not elicit any cytotoxic effect. Moreover, the crude HP extract incorporated in the PEO_CS's lower layer did not compromise the cell viability over 7 days, confirming its biocompatibility.

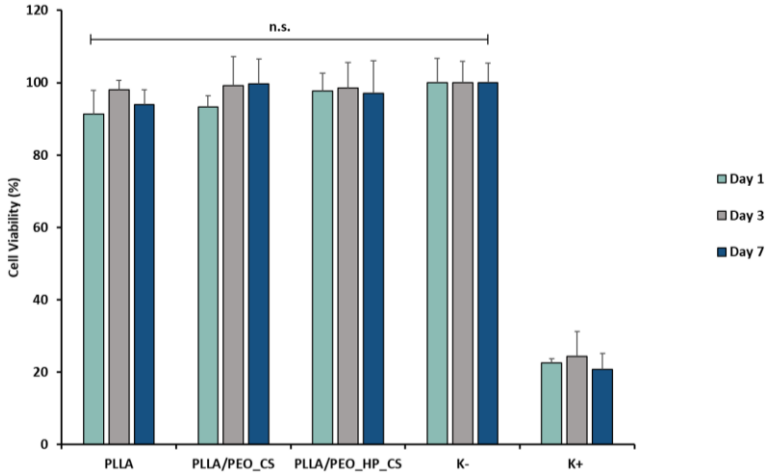

Figure 6 – Evaluation of cell viability when the NHDFs were incubated for 1, 3, and 7 days with the PLLA's upper layer, and the double-layer PLLA/PEO_CS and PLLA/PEO_HP_CS nanofibrous materials.

4. Conclusions

In this study, a double-layer nanocomposite PLLA/PEO_CS nanofibrous material containing crude HP extract was successfully developed using a multilayer electrospinning technique. The PLLA's upper layer was fabricated to protect the wound. In contrast, the lower layer of PEO_HP_CS was produced to re-establish a favorable wound environment for healing and prevent bacterial colonization or biofilm formation. The obtained results showed that the incorporation of crude HP extract in the double-layer PLLA/PEO_CS nanofibrous material exhibited a higher swelling ratio (~500%) in PBS, which is useful for maintaining favorable moisture balance within the wound site and that prevents from nanofibers sticking to the wound surface, as well as further damages. The acquired data can be related to the higher porosity (93.71% ± 1.00%) and wettability (WCA of 50.97 ± 11.60°) of the lower layer of PEO_HP_CS, as well as to the enhanced WVTR rate (1916.51 ± 143.02 g/m²/day). Besides, the incorporation of the crude HP extract into the PEO_CS's lower layer improved its ability to prevent bacterial invasion at the wound surface, as demonstrated by antibacterial activity against *S. aureus* (99.75% ± 1.30%) and *P. aeruginosa* (90.61% ± 1.63%), respectively, and this material did not show any cytotoxic effect on NHDF cells. Shortly, the application of the produced material as a wound dressing will be enhanced by performed hemolysis assay. *In vivo* studies are required to further understand the performance of the produced double-layer bioactive wound dressing material in the treatment of skin injuries. Moreover, the therapeutic ability of the crude HP extract, namely its anti-inflammatory activity, should also be evaluated, once wound infections are associated with a more significant amount of inflammation, which is responsible for delaying the healing process.

Acknowledgments

The authors would like to acknowledge Ana Raquel Nunes for her help in the cytotoxic assay. The authors are also grateful for the support given by FibEnTech Research Unit (Project UIDB/00195/2020). Cláudia Mouro also acknowledges PhD fellowship from Foundation for Science and Technology (FCT) (PD/BD/113550/2015).

References

1. dos Santos, D.M.; Leite I.S.; Bukzem, A.L.; Santos, R.P.O.; Frollini, E.; Inada, N.M.; Campana-Filho, S.P. Nanostructured electrospun nonwovens of poly(ε-caprolactone)/quaternized chitosan for potential biomedical applications. *Carbohydr. Polym.* **2018**, *186*, 110-121.
2. Jin, G.; Prabhakaran, M.P.; Kai, D.; Annamalai, S.K.; Arunachalam, K.D.; Ramakrishna, S. Tissue engineered plant extracts as nanofibrous wound dressing. *Biomaterials* **2013**, *34*, 724-734.
3. Wang, J.; Windbergs, M. Functional electrospun fibers for the treatment of human skin wounds. *Eur. J. Pharm. Biopharm.* **2017**, *119*, 283-299.

4. Chen, S.; Liu, B.; Carlson, M.A.; Gombart, A.F.; Reilly, D.A.; Xie, J. Recent advances in electrospun nanofibers for wound healing. *Nanomedicine* **2017**, *12*, 1335-1352.

5. Saeed, S.M.; Mirzadeh, H.; Zandi, M.; Barzin, J. Designing and fabrication of curcumin loaded PCL/PVA multi-layer nanofibrous electrospun structures as active wound dressing. *Prog. Biomater.* **2017**, *6*, 39-48.

6. Chen, X.; Zhao, R.; Wang, X.; Li, X.; Peng, F.; Jin, Z.; Gao, X.; Yu, J.; Wang C. Electrospun mupirocin loaded polyurethane fiber mats for anti-infection burn wound dressing application. *J. Biomater. Sci. Polym. Ed.* **2017**, *28*, 162-176.

7. Negut, I.; Grumezescu, V.; Grumezescu, A.M. Treatment strategies for infected wounds. *Molecules* **2018**, *23*, 2392.

8. Pilehvar-Soltanahmadi, Y.; Dadashpour, M.; Mohajeri, A.; Fattahi, A.; Sheervalilou, R.; Zarghami, N. An overview on application of natural substances incorporated with electrospun nanofibrous scaffolds to development of innovative wound dressings. *Mini-Rev Med. Chem.* **2018**, *18*, 414-427.

9. Hassiba, A.J.; El Zowalaty, M.E.; Nasrallah, G.K.; Webster, T.J.; Luyt, A.S.; Abdullah, A.M.; Elzatahry, A.A. Review of recent research on biomedical applications of electrospun polymer nanofibers for improved wound healing. *Nanomedicine* **2016**, *11*, 715-737.

10. Bhardwaj, N., Kundu, S.C. Electrospinning: a fascinating fiber fabrication technique. *Biotechnol. Adv.* **2010**, *28*, 325-347.

11. Liu, M.; Duan, X.P.; Li, Y.M.; Yang, D.P.; Long, Y.Z. Electrospun nanofibers for wound healing. *Mater. Sci. Eng. C* **2017**, *76*, 1413-1423.

12. Goh, Y-F.; Shakir, I.; Hussain, R. Electrospun fibers for tissue engineering, drug delivery, and wound dressing. *J. Mater. Sci.* **2013**, *48*, 3027-3054.

13. Hassiba, A.J.; El Zowalaty, M.E.; Webster, T.J.; Abdullah, A.M.; Nasrallah, G.K.; Khalil, K.A.; Luyt, A.S.; Elzatahry, A.A. Synthesis, characterization, and antimicrobial properties of novel double layer nanocomposite electrospun fibers for wound dressing applications. *Int. J. Nanomed.* **2017**, *12*, 2205-2213.

14. Trinca, R.B.; Westin, C.B.; da Silva, J.A.F.; Moraes, Â.M. Electrospun multi-layer chitosan scaffolds as potential wound dressings for skin lesions. *Eur. Polym. J.* **2017**, *88*, 161-170.

15. Mouro, C.; Fangueiro, R.; Gouveia, I.C. Preparation and characterization of electrospun double-layered nanocomposites membranes as a carrier for *Centella asiatica* (L.). *Polymers (Basel)* **2020**, *12*, 2653.

16. Foong, C.Y.; Sultana, N. Fabrication of layer-by-layer electrospun composite membranes based on polylactic acid (PLA) and poly (caprolactone) (PCL)/chitosan. *ARPN J. Eng. Appl. Sci.* **2015**, *10*, 9408-9413.

17. Li, J.; Hu, Y.; He, T.; Huang, M.; Zhang, X.; Yuan J.; Wei, Y.; Dong, X.; Liu, W.; Ko, F.; Zhou, W. Electrospun Sandwich-structure composite membranes for wound dressing scaffolds with high antioxidant and antibacterial activity. *Macromol. Mater. Eng.* **2018**, *303*, 1700270.

18. Tort, S.; Acartürk, F.; Bes¸ikci, A. Evaluation of three-layered doxycycline-collagen loaded nanofiber wound dressing. *Int. J. Pharm.* **2017**, *529*, 642-653.

19. Bolbasov, E.N.; Maryin, P.V.; Stankevich, K.S.; Kozelskaya, A.I.; Shesterikov, E.V.; Khodyrevskaya, Y.I.; Nasonova, M.V.; Shishkova, D.K.; Kudryavtseva, Y.A.; Anissimov, Y.G.; Tverdokhlebov, S.I. Surface modification of electrospun poly-(l-lactic) acid scaffolds by reactive magnetron sputtering. *Colloids Surf. B Biointerfaces* **2018**, *162*, 43-51.

20. Santos, D.; Silva, D.M.; Gomes, P.S.; Fernandes, M.H.; Santos, J.D.; Sencadas, V. Multifunctional PLLA-ceramic fiber membranes for bone regeneration applications. *J. Colloid Interface Sci.* **2017**, *504*, 101-110.

21. Yuan, T.T.; Jenkins, P.M.; DiGeorge Foushee, A.M.; Jockheck-Clark, A.R.; Stahl, J.M. Electrospun chitosan/polyethylene oxide nanofibrous scaffolds with potential antibacterial wound dressing applications. *J. Nanomater.* **2016**, *2016*, 6231040.

22. Zarghami, A.; Irani, M.; Mostafazadeh, A.; Golpour, M.; Heidarinasab, A.; Haririan, I. Fabrication of PEO/chitosan/PCL/olive oil nanofibrous scaffolds for wound dressing applications. *Fibers Polym.* **2015**, *16*, 1201-1212.

23. Aliabadi, M; Irani, M.; Ismaeili, J.; Piri, H.; Parnian, M.J. Electrospun nanofiber membrane of PEO/chitosan for the adsorption of nickel, cadmium, lead and copper ions from aqueous solution. *Chem. Eng. J.* **2013**, *220*, 237-243.

24. Yadollah-Damavandi, S.; Chavoshi-Nejad, M.; Jangholi, E.; Nekouyian, N.; Hosseini, S.; Seifaee, A.; Rafiee, S.; Karimi, H.; Ashkani-Esfahani, S.; Parsa, Y.; Mohsenikia, M. Topical *Hypericum perforatum* improves tissue regeneration in full-thickness excisional wounds in diabetic rat model. *Evid-Based Complem. Altern. Med.* **2015**, *2015*, 245328.

25. Milosevic, T.; Solujic, S.; Sukdolak, S. *In vitro* study of ethanolic extract of *Hypericum perforatum* L. on growth and sporulation of some bacteria and fungi. *Turkish J. Biol.* **2007**, *31*, 237-241.

26. Klemow, K.M.; Bartlow, A.; Crawford, J.; Kocher, N.; Shah, J.; Ritsick, M. Medical attributes of St. John's wort (*Hypericum perforatum*). *Herb. Med. Biomol. Clin.* **2011**, *11*, 1–64.

27. Zhang, W.; Ronca, S.; Mele, E. Electrospun nanofibres containing antimicrobial plant extracts. *Nanomaterials* **2017**, 7, 1-17.

28. Abd El-Hamid, M.I. Citation: El-Hamid MIA. A new promising target for plant extracts: inhibition of bacterial quorum sensing. *J. Mol. Biol. Biotechnol.* **2016**, *1(1-4)*, 1–3.

29. Anand, U.; Jacobo-Herrera, N.; Altemimi, A.; Lakhssassi, N. A comprehensive review on medicinal plants as antimicrobial therapeutics: potential avenues of biocompatible drug discovery. *Metabolites* **2019**, *9(258)*, 1–13.

30. Gupta, P.D.; Birdi, T.J. Development of botanicals to combat antibiotic resistance. *J. Ayurveda Integr. Med.* **2017**, *8(4)*, 266–275.

31. Pourhojat, F.; Sohrabi, M.; Shariati, S.; Mahdavi, H.; Asadpour, L. Evaluation of poly ε-caprolactone electrospun nanofibers loaded with *Hypericum perforatum* extract as a wound dressing. *Res. Chem. Intermed.* **2017**, *43*, 297-320.

32. Chitrattha, S.; Phaechamud, T. Porous poly(dl-lactic acid) matrix film with antimicrobial activities for wound dressing application. *Mater. Sci. Eng. C* **2016**, *58*, 1122-1130.

33. Oliveira, R.; Azeredo, J.; Teixeira, P.; Fonseca, A. The role of hydrophobicity in bacterial adhesion. *Biol. Theory.* **2001**, *1*, 11-22.

34. da Silva Domingues, J.F.; van der Mei, H.C.; Busscher, H.J.; van Kooten, T.G. Phagocytosis of bacteria adhering to a biomaterial surface in a surface thermodynamic perspective. *PLoS One* **2013**, *8*, e70046.

35. Bayoudh, S.; Othmane, A.; Bettaieb, F.; Bakhrouf, A.; Ben, O.H.; Ponsonnet, L. Quantification of the adhesion free energy between bacteria and hydrophobic and hydrophilic substrata. *Mater. Sci. Eng. C* **2006**, *26*, 300-305.

36. Reichling, J.; Weseler, A.; Saller, R. A current review of the antimicrobial activity of *Hypericum perforatum* L. *Pharmacopsychiatry* **2001**, *34*, 116-118.

37. Liu, W.; Yin, D.; Li, N.; Hou, X.; Wang, D.; Li, D.; Liu, J. Influence of environmental factors on the active substance production and antioxidant activity in *Potentilla fruticosa* L. and its quality assessment. *Sci. Rep.* **2016**, *6*, 28591.

38. Peñuelas, J.; Llusià, J. Effects of carbon dioxide, water supply, and seasonality on terpene content and emission by *Rosmarinus officinalis*. *J. Chem. Ecol.* **1997**, *23*, 979-993.

39. Dong, J.; Ma, X; Wei, Q; Peng, S; Zhang, S. Effects of growing location on the contents of secondary metabolites in the leaves of four selected superior clones of *Eucommia ulmoides*. *Ind. Crops Prod.* **2011**, *34*, 1607-1614.

40. Sadri, M.; Arab-Sorkhi, S.; Vatani, H.; Bagheri-Pebdeni, A. New wound dressing polymeric nanofiber containing green tea extract prepared by electrospinning method.

41. Papenburg, B.J.; Bolhuis-Versteeg, L.A.M.; Grijpma, D.W.; Feijen, J.; Wessling, M.; Stamatialis, D. A facile method to fabricate poly(l-lactide) nano-fibrous morphologies by phase inversion. *Acta Biomater.* **2010**, *6*, 2477-2483.

42. Jing, N.; Jiang, X.; Wang, Q.; Tang, Y.; Zhang, P. Attenuated total reflectance/Fourier transform infrared (ATR/FTIR) mapping coupled with principal component analysis for the study of *in vitro* degradation of porous polylactide/hydroxyapatite composite material. *Anal. Methods* **2014**, *6*, 5590-5595.

43. Jarzębski, M.; Smułek, W.; Baranowska, H.M.; Masewicz, L.; Kobus-Cisowska, J.; Ligaj, M.; Kaczorek, E. Characterization of St. John's wort (*Hypericum perforatum* L.) and the impact of filtration process on bioactive extracts incorporated into carbohydrate-based hydrogels. *Food Hydrocoll.* **2020**, *104*, 105748.

44. Lawrence, B.J.; Madihally, S.V. Cell colonization in degradable 3D porous matrices. *Cell. Adh. Migr.* **2008**, *2*, 9-16.

45. Wang, J.; Planz, V.; Vukosavljevic, B.; Windbergs, M. Multifunctional electrospun nanofibers for wound application – novel insights into the control of drug release and antimicrobial activity. *Eur. J. Pharm. Biopharm.* **2018**, *129*, 175-183.

46. Oliveira, S.M.; Alves, N.M.; Mano, J.F. Cell interactions with superhydrophilic and superhydrophobic surfaces. *J. Adhes. Sci. Technol.* **2014**, *28*, 843-863.

47. Sedlarik, V. Antimicrobial Modifications of Polymers. *Biodegrad. - Life Sci.* **2013**, *7*, 187–204.

48. Monte, J.; Abreu, A.C.; Borges, A.; Simões, L.C.; Simões, M. Antimicrobial activity of selected phytochemicals against *Escherichia coli* and *Staphylococcus aureus* and their biofilms. *Pathogens* **2014**, *3*, 473-498.

49. Alippilakkotte S, Kumar S, Sreejith L. Fabrication of PLA/ag nanofibers by green synthesis method using *Momordica charantia* fruit extract for wound dressing applications. *Colloids Surfaces A Physicochem. Eng. Asp.* **2017**, *529*, 771-782.

50. Vargas EAT, do Vale Baracho NC, de Brito J, de Queiroz AAA. Hyperbranched polyglycerol electrospun nanofibers for wound dressing applications. *Acta Biomater.* **2010**, *6*, 1069-1078.

51. Peršin, Z.; Ravber, M.; Stana Kleinschek, K.; Knez, Ž.; Škerget, M.; Kurecˇicˇ, M. Bio-nanofibrous mats as potential delivering systems of natural substances. *Text. Res. J.* **2017**, *87*, 444-459.

52. Ding, L.; Shan, X.; Zhao, X.; Zha, H.; Chen, X.; Wang, J; Cai, C.; Wang, X.; Li, G.; Hao, J.; Yu, G. Spongy bilayer dressing composed of chitosan – Ag nanoparticles and chitosan–*Bletilla striata* polysaccharide for wound healing applications. *Carbohydr. Polym.* **2017**, *157*, 1538-1547.

53. Rošic, R.; Kocbek, P.; Baumgartner, S.; Kristl, J. Electrospun chitosan/peo nanofibers and their relevance in biomedical application. *IFMBE Proc. Springer, Berlin, Heidelberg* **2011**.

54. Maškovic, P.Z.; Mladenovic, J.D.; Cvijovic, M.S.; Acamovic-Đokovic, G.; Solujic, S.R.; Radojkovic, M.M. Phenolic content, antioxidant and antifungal activities of acetonic, ethanolic and petroleum ether extracts of *Hypericum perforatum* L. *Hem. Ind.* **2011**, *65*, 159-164.

55. Bainbridge, P. Wound healing and the role of fibroblasts. *J. Wound Care* **2013**, *22*, 407-412.

Paper 6 - Preparation and Characterization of Electrospun Double-layered Nanocomposites Membranes as a Carrier for *Centella asiatica* (L.)

Abstract

A wide range of naturally derived and synthetic biodegradable and biocompatible polymers are today regarded as promising materials for improving skin regeneration. Alongside this, these materials have been explored in conjunction with different types of antimicrobial and bioactive agents, especially natural-derived compounds, to enhance their biological properties. Herein, a double-layered nanocomposite dressing membrane was fabricated with two distinct layers. A bottom layer from Chitosan-Sodium tripolyphosphate (CS-TPP) and Polyvinyl Alcohol (PVA) containing *Centella asiatica* (L.) (CA) was electrospun directly over a Polycaprolactone (PCL) layer to improve the biologic performance of the electrospun nanofibers. In turn, the PCL layer was designed to provide mechanical support to the damaged tissue. The results revealed that the produced double-layered nanocomposite membrane closely resembles the mechanical, porosity, and wettability features required for skin tissue engineering. On the other hand, the *in vitro* drug release profile of the PCL/PVA_CS-TPP containing CA exhibited a controlled release for 10 days. Moreover, the PVA_CS-TPP_CA's bottom layer displayed the highest antibacterial activity against *Staphylococcus aureus* (*S. aureus*) (99.96 ± 6.04%) and *Pseudomonas aeruginosa* (*P. aeruginosa*) (99.94 ± 0.67%), which is responsible for avoiding bacterial penetration while endowing bioactive properties. Finally, the 3-(4,5-Dimethyl-2-thiazolyl)-2,5-diphenyl-2H-tetrazolium bromide (MTT) assay showed that this nanocomposite membrane was not cytotoxic for normal human dermal fibroblasts (NHDF) cells. Therefore, these findings suggest the potential use of the double-layered PCL/PVA_CS-TPP_CA as an efficient bionanocomposite dressing material.

Graphical Abstract

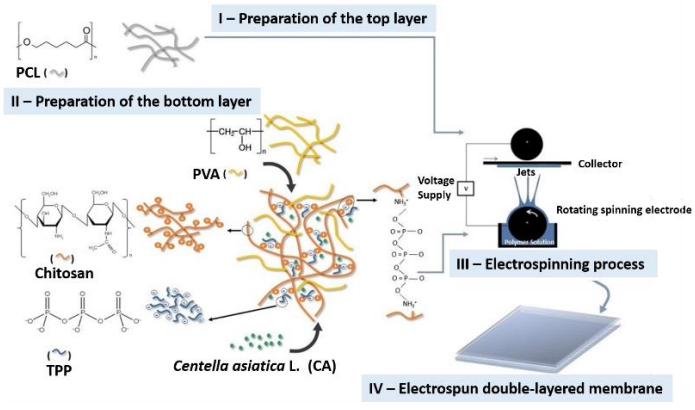

Keywords: Polycaprolactone; chitosan; sodium tripolyphosphate; poly(vinyl alcohol); *Centella asiatica*; double-layered nanocomposite membranes.

1. Introduction

Wound healing is a dynamic and complex process that requires cellular interactions between a wide variety of cell types [1–3]. These interactions are mediated through a coordinated cascade of biological events synergistically controlled by numerous bioactive molecules, such as growth factors, anti-inflammatory agents, and vitamins. However, the physiology of the healing process may be impaired by several factors [1–3]. Among them, bacterial colonization and subsequent infections remain one of the most serious complications after skin structure is compromised [1,4,5]. Generally, when pathogenic microorganisms contaminate skin wounds, the immune system mobilizes its energy trying to suppress the invasion of these pathogens instead of focusing on the re-establishment of the native skin's structural and functional features [1,4–6]. If infection occurs, microorganisms, particularly bacteria, can produce endotoxins that stimulate the expression of pro-inflammatory cytokines and encourage an extended inflammatory response. In this case, wounds exhibit increased levels of metalloproteinases (MMPs), which provide an unsuitable environment for the production of new skin's extracellular matrix (ECM) components, delaying or even interrupting the healing process [1,5,6].

Concerning this, several wound dressings displaying antimicrobial properties have been developed to protect the wound from infection and enhance the healing process. Nonetheless, it is essential to improve their performance to suppress this health problem and reduce the occurrence of life-threatening complications [1,5–7]. For this purpose, different combinations of both synthetic and natural biocompatible and biodegradable polymers have been explored to produce 3D nanofibrous membranes that mimic the architecture of the skin's ECM [1,6–8]. So far, to successfully produce nanofibers as potential wound dressings, several techniques have been used, namely self-assembly, phase separation, drawing, template synthesis, and electrospinning. Electrospinning has been considered as one of the most efficient, versatile, and cost-effective methods to produce nanocomposite dressing materials with the desirable features [1,7]. The unique structural and morphological properties of the electrospun nanofibers, like the high specific area to volume ratio, interconnected pores, and the smaller fiber diameters, closely resemble the structure of collagen fibers found in the normal skin's ECM. Alongside this, their porous structure can support cell adhesion, migration, and proliferation, and regulate the release of both growth factors and signaling molecules, which are required to achieve wound healing [1,7–11]. The electrospun nanofibers can also provide quick hemostasis, enhance exudate absorption, nutrients, and gas permeability, as well as preventing bacterial penetration and colonization. Moreover, electrospinning provides the operational ability for incorporating antimicrobial and/or bioactive agents, which enable the improvement of the biologic behavior of these wound dressing materials [1,7–9]. To accomplish that, several different approaches have been used as an alternative to traditional single-fluid electrospinning [12]. Among them, double-fluid and multiple-fluid electrospinning methods have been extensively studied to produce core–shell nanofibers and provide specific release profiles

[13,14]. In the coaxial electrospinning system, namely in modified coaxial electrospinning processes, different coaxial spinneret needles have been designed [15]. Furthermore, two needles side-by-side have been applied to produce nanofibers with Janus structures [14,16,17]. On the other hand, multiple-fluid systems with distinct spinneret arrangements like traditional and modified triaxial spinnerets and electrospun nanofibers with a common shell and two separate cores have been developed to ensure a sustained release of the incorporated agents [14,18–21]. However, those new methods for manipulating the inner chamber structure are complicated. Thus, traditional single-fluid blending electrospinning is still the mainstream method due to its straightforward operation, easy scale-up, and remarkable power for tailoring the components and compositions of resultant composite nanofibers. Additionally, manipulation of deposition on the collector with different electrospun nanofibers has been studied in recent works and is being further explored to improve the functional performances of the electrospun wound dressing materials containing antimicrobial agents [11,22–24]. Among the different antimicrobial agents incorporated so far in electrospun wound dressings, antibiotics and nanoparticles have been widely explored due to their capability to avoid bacteria penetration and colonization into the wound site [1,5,7,9]. Nonetheless, the growing threat of antibiotic resistance and their toxicity have encouraged the use of natural products to avoid bacterial contamination. Regarding that, compounds obtained from natural sources, like medicinal plants, have been regarded as a powerful natural supplement for the management and treatment of wounds [1,7,9,25,26]: mainly crude plant extracts, which are ecologically sustainable mixtures rich in interesting bioactive phytochemicals, such as tannins, alkaloids, carbohydrates and glycosides, terpenoids, steroids, flavonoids, and coumarins with multiple healing benefits [7,9,26,27]. Herein, we produced a novel bionanocomposite dressing membrane with a double-layered structure through electrospinning. Polycaprolactone (PCL), a hydrophobic synthetic polymer, was used as the main component of the first layer, due to its biocompatibility, desirable mechanical strength, and ability to act as a protective barrier [10,28–30]. On the other hand, the second layer of Polyvinyl Alcohol (PVA) and Chitosan-Sodium tripolyphosphate (CS-TPP) containing *Centella asiatica* (L.) (CA) was designed to be in direct contact with the injured skin and enhance the healing process [30,31]. CA is a member of the *Apiaceae* family, and it has been widely used for the treatment of dermatoses, skin lesions such as burns, excoriations, hypertrophic scars or eczema, and other skin diseases, like leprosy and psoriasis, as well as in non-dermatologic conditions. CA displays different terpenoids, known as centelloids, including asiaticoside, madecassoside, centelloside, centellose, brahminoside, thankunizide, sceffoleoside, brahmoside, and asiatic, centellic, brahmic, and madecassic acids which are responsible for conferring several therapeutic properties to CA [32–34]. Moreover, the extracts obtained from this medicinal plant are known for their capability to stimulate fibroblast proliferation, collagen synthesis, and angiogenesis [32]. In turn, Chitosan (CS), one of the most abundant natural polysaccharides, is known for its ability to stimulate collagen synthesis, as well as bactericidal and hemostatic properties. Alongside this, CS possesses amine functional groups on its backbone chains, which in acidic aqueous media ensure a high density of positive charges [31,35–37]. Thus, under these

conditions, CS can be ionically cross-linked with biodegradable and biocompatible polyanions, as the sodium tripolyphosphate (TPP), forming polyelectrolyte complexes as antimicrobial and/or bioactive agents delivery carriers [31,35]. Nevertheless, the CS-TPP solutions are difficult and unstable to electrospun into a fibrous structure, due to the high viscosity of the CS at low pH values [31,37–39]. To overcome this limitation, PVA, one of the most commonly used water-soluble synthetic polymers, was added to the CS-TPP blend to enhance fiber-forming ability [31,36,38,39]. Hence, in this work, we aimed to take advantage of the capability offered by double-layered PCL/PVA_CS-TPP_CA to improve the wound healing process, namely the benefits that the ionically cross-linked electrospun PVA_CS-TPP nanofibers display to control the release of the crude CA extract according to the demands for antimicrobial wound care products.

2. Materials and Methods

2.1. Materials

Centella asiatica (CA) was supplied from a Portuguese botanic shop (CHÁ HUNOS, Lda., Portugal) without any additives. Normal human dermal fibroblasts (NHDF) cells were purchased from ATCC—American Type Culture Collection. Polycaprolactone (PCL) (MW 80,000 g/mol), Chitosan (CS) (low molecular weight) were acquired from Sigma-Aldrich. Polyvinyl Alcohol (PVA) (MW 115,000 g/mol) was purchased from VWR Chemicals. Ethanol absolute, Chloroform, Dimethylformamide (DMF), and Glacial acetic acid were purchased from Fisher Chemical. Nutrient agar (NA), Nutrient broth (NB), and Agar for microbiology were provided from Fluka. Brain Heart Infusion (BHI) broth was obtained from Panreac. Mueller Hinton broth (MHB), Tween 80, Sodium Hydroxide (NaOH), Sodium Chloride (NaCl), Trypsin, and 3-(4,5-Dimethyl-2-thiazolyl)-2,5-diphenyl-2H-tetrazolium bromide (MTT) were bought from Sigma-Aldrich. Phosphate-buffered saline (PBS) and Sodium tripolyphosphate (TPP) were purchased from Alfa Aesar. All solvents were used as received from the manufacturer.

2.2. Ethanol Extraction of Crude *Centella asiatica* (CA) Plant

The dried and powdered aerial plant parts (4 g) were macerated using 40 mL of 95% ethanol as solvent at room temperature for 24 hours. Then, the supernatant from the ethanol extraction was directly filtered through Whatman filter paper, and after that, the acquired filtrate was dried under reduced pressure to obtain dry CA extract. The yield of the fresh plant was 18.81% (dry weight of the extract obtained after solvent removal per weight of plant) (w/w). Finally, the crude CA extract was stored following good storage practices and next re-suspended in 45% (v/v) ethanol for further experiments.

2.3. Minimum Inhibitory Concentration (MIC) of the Crude CA extract

Minimum inhibitory concentration (MIC) of the crude CA extract was assessed against *Staphylococcus aureus* (ATTC 6538) (*S. aureus*) and *Pseudomonas aeruginosa* (PA25) (*P. aeruginosa*) using the broth microdilution method on 96 multi-well polystyrene plates (Sigma-Aldrich), according to the CLSI M07-A6 document. Briefly, serial dilutions of crude CA extract were prepared in sterile Mueller Hinton Broth (MHB) to obtain the desired extract concentrations (between 50 and 0.15 mg/mL). Then, 50 µL of each CA dilution containing 50 µL of a bacterial suspension (adjusted to ~10^7 CFU/mL in MHB) was applied to the microplate wells in triplicate. The plates were after that incubated at 37 °C for 18–24 hours. The MIC was defined as the lowest concentration of the crude CA extract at which there was no visible growth of *S. aureus* and *P. aeruginosa* (no solution turbidity on naked eyes). MHB with bacterial suspensions was added as a positive control, whereas only MHB was used as a negative control.

2.4. Fabrication of the Double-Layered Nanocomposites Membranes

The double-layered nanocomposites membranes were fabricated using the Nanospider technology (Nanospider laboratory machine NS LAB 500S from Elmarco S.R.O., Czech Republic, http://www.elmarco.com), as a modified electrospinning method.

Top layer: Initially, a PCL solution (8% PCL (w/v)) was prepared in chloroform/DMF at 30:20 volume ratio. The resultant solution was electrospun at 75.0 kV, using a working distance of 15 cm and an electrode rotation rate of 55 Hz (electrode spin = 8.8 r/min).

Bottom layer: CS-TPP blend was prepared according to a previously reported method by Nguyen et al. [40] using sodium tripolyphosphate (TPP) as a crosslinking agent. Briefly, 0.2% (w/v) chitosan was dissolved in 0.35% acetic acid and kept overnight at room temperature. The pH of the resulting chitosan solution was then adjusted to pH 5.5 using a 0.5 M sodium hydroxide (NaOH) solution. In turn, a TPP solution was prepared in distilled water at a concentration of 0.25% (w/v). The CS-TPP was produced by dropping the TPP solution into the CS solution under vigorous stirring in a volume ratio of 6:1 for 60 min at room temperature. Afterward, the CS-TPP was blended with 10% (w/v) of PVA dissolved in distilled water at 90 °C with a volume ratio of 70:30, respectively. Additionally, the crude CA extract incorporation into CS-TPP was achieved by adding 3 mg/mL of the CA extract in the TPP solution. The CS-TPP_CA was produced following the same procedure as for the CS-TPP. After polymer solutions were obtained, they were placed in a container with a rotating spinning electrode, and electrospun on top of the recently prepared PCL's top layer at an electrode spin of 45 Hz (electrode spin = 7.2 r/min), using a working distance of 15 cm and an applied voltage of 75 kV. Finally, the fabricated double-layered nanocomposites membranes (PCL/PVA_CS-TPP and PCL/PVA_CS-TPP_CA) were characterized through *in vitro* assays to assess their appropriateness as a wound dressing material.

2.5. Characterization of the Produced Double-Layered Nanocomposites Membranes

2.5.1. Scanning Electron Microscopy (SEM) Imaging and Analysis

The surface morphology of the electrospun nanofibers of the top layer (PCL) and bottom layers (PVA_CS-TPP and PVA_CS-TPP_CA) of the developed double-layered nanocomposite membranes was observed using scanning electron microscopy (SEM) (S2700, Hitachi, Tokyo, Japan) at an accelerating voltage of 20 kV. First, the samples were mounted on aluminum stubs and sputter-coated with a thin gold layer in an Emitech K550 sputter coater (Quorum Technologies Ltd., Laughton, East Sussex, UK) for better conductivity during imaging. The fiber diameters were measured from the obtained SEM images using ImageJ software (National Institutes of Health, MD, USA) and the size-frequency distributions constructed with GraphPad Prism 6 software (GraphPad Software, La Jolla, CA, USA).

2.5.2. Attenuated Total Reflectance–Fourier Transform Infrared Spectroscopy Study

The chemical composition of the top layer (PCL), the bottom layers (PVA_CS-TPP and PVA_CS-TPP_CA), and their raw materials was analyzed using attenuated total reflectance–Fourier transform infrared spectroscopy (ATR–FTIR, Thermo-Nicolet is10 FT-IR Spectrophotometer, Waltham, MA, USA). The spectra of the samples were recorded in a spectral width ranging from 400–4000 cm^{-1} with an average of 32 scans min^{-1} and a spectral resolution of 4 cm^{-1}.

2.5.3. Differential Scanning Calorimetry (DSC)

The thermal behavior of the PCL's top layer and the bottom layers of PVA_CS-TPP with and without CA extract was evaluated by differential scanning calorimetry (DSC) (DSC 204 Phoenix Netzsch, Germany). Briefly, about 5 mg of each sample was filled in small aluminum containers, and the non-isothermal scans performed from 30 °C to 200 °C at a heating rate of 5 °C/min, with a nitrogen-replacing atmosphere.

2.5.4. Assessment of the Mechanical Characteristics of the Produced Double-Layered Nanocomposites Membranes

The tensile test was carried out in dry conditions according to the ASTM standard D3039/D3039M to evaluate the mechanical characteristics of the produced double-layered nanocomposites membranes. Briefly, samples of the PCL/PVA_CS-TPP and PCL/PVA_CS-TPP containing CA

samples (n = 5) were cut into rectangular strips of 1 cm × 4 cm, and then the thickness was measured with a micrometer (Adamel Lhomargy MI20, France). The tensile test was performed using a dynamometer (DY-35 Adamel Lhomargy, France) by using a load cell of 10-N. The samples were mounted vertically between the clamps of the tensile tester, and a speed of 2 mm/min used until the membranes were ruptured. Finally, the tensile strength, Young's modulus, and elongation at break were determined.

2.5.5. Measurement of the Total Porosity

The total porosity of the dried PCL's top layer and bottom layers of PVA_CS-TPP and PVA_CS-TPP_CA was measured using a fluid displacement method and conducted as previously described by Yeh et al. [41]. Absolute ethanol with density ρ_ε was used as displacement liquid because it can easily penetrate the porous structure without inducing negligible shrinking or swelling as a non-solvent of both layers. Briefly, a graduated cylinder with ethanol was weighed (W_1), then a dried sample with a known weight (W_s) was immersed into the cylinder containing the displacement liquid. After that, this assembly was placed in an ultrasonic bath (Ultrasons-H, P-Selecta) for 40 min at 30 °C. After this period, the volume of ethanol in the graduated cylinder was refilled and weighed as W_2. The sample saturated with ethanol was taken out from the cylinder, and its weight determined as W_3. The porosity (ε) of both layers was estimated through the following (Equations (1)–(3)):

$$V_s = \frac{(W_1 - W_2 + W_s)}{\rho_\varepsilon} \quad (1)$$

$$V_p = \frac{(W_2 - W_3 - W_s)}{\rho_\varepsilon} \quad (2)$$

$$\varepsilon\,(\%) = \frac{V_p}{(V_p + V_s)} \times 100 \;\Leftrightarrow \varepsilon\,(\%) = \frac{(W_2 - W_3 - W_s)}{(W_1 - W_3)} \times 100 \quad (3)$$

where V_s is the volume of the sample, and V_p is the volume of the sample pores. For each sample, the porosity measurements were performed in triplicate, and the average ± standard deviation (SD) shown for each sample.

2.5.6. Evaluation of Wettability Properties

The water contact angles (WCA) at the surface of both layers (PCL, PVA_CS-TPP, and PVA_CS-TPP_CA) were determined using a Data Physics Contact Angle Goniometer (OCAH-200) for surface-wetting characterization. Briefly, each sample was placed on the measuring stage, then water drops (4 µL) were seated onto the surface of the samples at different locations at 25 °C. The reported WCA values were the average of at least three independent measurements (n = 3).

2.5.7. Analysis of the *In Vitro* Swelling Behavior

The swelling degree of the produced double-layered nanocomposites membranes (PCL/PVA_CS-TPP and PCL/PVA_CS-TPP_CA) was investigated in a phosphate buffer solution (PBS) at a pH of 5.5 by using a gravimetric method. Briefly, the pre-weighted dry samples (W_o) were immersed in the PBS at 37 °C. At specific time points, the swollen samples were removed from the PBS buffer solution and reweighted after kindly wiping the excess buffer off the samples (W_t). All measurements were performed in triplicate (n = 3) and the amount of water uptake determined according to the following Equation (4):

$$\text{Swelling Ratio (\%)} = \frac{(W_t - W_0)}{W_0} \times 100 \quad (4)$$

2.5.8. Study of the *In Vitro* Biodegradation Profile

The physical integrity behaviors were analyzed from the weight loss of the produced double-layered nanocomposites membranes. Briefly, the dried samples with the initial weight of (W_o) were immersed into PBS solution (pH = 5.5) at 37 °C. At predetermined time intervals (1, 4, 7, and 10 days), the samples (n = 3) were removed from the PBS solution, rinsed with distilled water to remove residual buffer salts, oven-dried, and reweighted (W_d). Finally, the weight loss (%) of each sample was determined based on Equation (5):

$$\text{Weight loss (\%)} = \frac{(W_0 - W_d)}{W_d} \times 100 \quad (5)$$

2.5.9. Water Vapor Transmission Rate (WVTR) Analysis

The gravimetric assay based on the ASTM E96/E96M-15 standard was used to evaluate the water vapor transmission rate (WVTR) of the produced double-layered nanocomposites membranes. Briefly, sample circles (1.2 cm diameter) were cut and carefully attached to the mouths of test tubes containing 10 mL of deionized water. The circular opening of the test tubes was sealed using parafilm, and the samples–glass tubes assembly placed in an incubator at 37 °C. At predetermined intervals, the amount of water evaporation was estimated by the changes in their weight over time. The WVTR was calculated according to Equation (6):

$$\text{Water vapor transmission rate (WVTR)} = \frac{W_{loss}}{A} \ (\text{g}/m^2/day) \quad (6)$$

Where W_{loss} is the daily weight loss of water and A is the test area in m^2.

2.6. Analysis of the *In Vitro* CA Release from Double-Layered Nanocomposites Membranes

The *in vitro* release profile of the double-layered nanocomposites membranes containing crude CA extract was investigated in PBS (pH = 5.5) containing 10% (v/v) of ethanol. The amount of released CA in PBS was monitored by a UV–Vis spectrophotometer at a wavelength of 370 nm [42]. Briefly, the double-layered PCL/PVA_CS-TPP_CA membranes were kept immersed in PBS buffer at 37 °C and 100 rpm for 10 days. At specific time points, a fixed volume of released medium was taken out from the incubation medium, and an equal amount of fresh buffer solution refilled to maintain the sink condition. The amount of crude CA extract released was measured by converting its detected UV absorbance to its concentration according to the calibration curve constructed from a series of CA standard solutions (from 0.00 mg/mL to 5.00 mg/mL). After that, the data obtained were evaluated to determine the cumulative percentage of the released CA from the samples at each immersion time point. The experiments were conducted in triplicate (n = 3).

2.7. Assessment of the Antibacterial Properties of the Produced Double-Layered Nanocomposites Membranes

The antibacterial activity of both layers (PCL, PVA_CS-TPP, and PVA_CS-TPP_CA) was exanimated against *S. aureus* and *P. aeruginosa* following the guidelines established by the Standard Test Method for Determining the Activity of Incorporated Antimicrobial Agent(s) in Polymeric or Hydrophobic Materials (ASTM E2180-07 standard). Firstly, *S. aureus* and *P. aeruginosa* were cultivated in nutrient broth (NB) and brain–heart infusion broth (BHI) in a shaking incubator at 37 °C and 110 rpm for 18–24 hours, respectively. After that, the bacterial suspensions were diluted until the bacterial concentration reached ~10^8 CFU/mL, then added to the previously prepared agar slurry to facilitate surface interaction. A thin layer of inoculated agar slurry was pipetted onto the samples and then left to gel at room temperature before incubation at 37 °C for 18–24 hours. The surviving bacteria were analyzed immediately (T_{0h}) and after incubation (T_{24h}) by elution of the agar slurry inoculum from the test samples. After bacteria elution, serial dilutions were made in NaCl and pipetted on agar plates, and incubated at 37 °C for 18–24 hours. Finally, the number of surviving colonies following incubation was counted, and the counts used to establish the log (CFU/mL).

2.8. Analysis of the *In Vitro* Cell Viability

The cytotoxicity of the double-layered nanocomposites membranes (PCL/PVA_CS-TPP and PCL/PVA_CS-TPP_CA) was evaluated through colorimetric 3-(4,5-Dimethyl-2-thiazolyl)-2,5-diphenyl-2H-tetrazolium bromide (MTT) assay according to ISO 10993–5 (Biological evaluation of medical devices–Part 5: Tests for *in vitro* cytotoxicity). Firstly, the normal human dermal fibroblasts

(NHDF) cells were cultured in a medium supplemented with fetal bovine serum (FBS) in a humidified incubator at 37 °C under a 5% CO_2 atmosphere. Afterward, the samples cut into round disks (with a diameter of ~6 mm) were placed at the center of each well in 24-well plates, then sterilized by UV irradiation for 1 hour before cell seeding. After that, 1×10^4 cells/well were seeded in each well containing the sterilized membranes and incubated with 5% CO_2 at 37 °C for 1, 3, and 7 days. During these intervals of time, the medium was removed, and a mixture of fresh culture medium with the MTT reagent added to each well. After being incubated for 4 hours under the same conditions, the content of each well was again removed and replaced by DMSO to dissolve the formazan crystals. Finally, the absorbance of each membrane was measured at 570 nm using a spectrophotometric plate reader (Biorad xMark microplate spectrophotometer). Cells incubated without samples (K^-) and cells with EtOH (96%) (K^+) were chosen as control groups. The positive control (K^+) was added in separate 24 well plates to avoid false results caused by EtOH (96%).

2.9. Statistical Analysis

Statistical analysis was performed from the one-way ANOVA, followed by multiple comparison test Turkey using GraphPad Prism 6 software (GraphPad Software, La Jolla, CA, USA) with a statistical significance of $p < 0.05$.

3. Results and Discussion

3.1. Minimal Inhibitory Concentration (MIC) of the Crude CA Extract

The antimicrobial susceptibility of the crude CA extract was determined by the MIC. The MIC value against *S. aureus* was found to be 1.40 mg/mL, while the value for *P. aeruginosa* was 2.80 mg/mL. These values were lower than those obtained by Yao et al. [43], who revealed MIC values to the ethanolic extract of CA of 6.25 mg/mL and 25 mg/mL against *S. aureus* and *P. aeruginosa*, respectively. These results proved that the antibacterial activity of the medicinal plants depends on the specific active compounds present in the extract.

3.2. Characterization of the Produced Double-Layered Nanocomposites Membranes

3.2.1. Scanning Electron Microscopy (SEM) Imaging and Analysis

In this study, the surface morphologies and diameter distributions of the electrospun nanofibers from PCL's top layer and the bottom layers of PVA_CS-TPP and PVA_CS-TPP incorporated with the crude CA extract, respectively, are displayed in Figure 1a. The SEM images show that both layers exhibit a

random distribution of nanofibers with interconnected pores. The average diameters of the smooth PCL structure were determined to be 277.63 ± 85.19 nm, which is in agreement with other studies performed with PCL [44]. In turn, the average fiber diameter of the smooth and bead-free structures of PVA_CS-TPP was decreased from 323.85 ± 91.07 nm to 284.34 ± 75.79 nm when the crude CA extract was incorporated, as a result of reduction of the viscosity of the electrospinning solution. In this way, these results suggest that the produced double-layered nanocomposites membranes resemble the fibrous morphology and architecture of the natural extracellular matrix (ECM) since the nanofibers exhibit diameters within the size range of the collagen fibers of ECM (50–400 nm), being able to promote cell adhesion and proliferation [45,46].

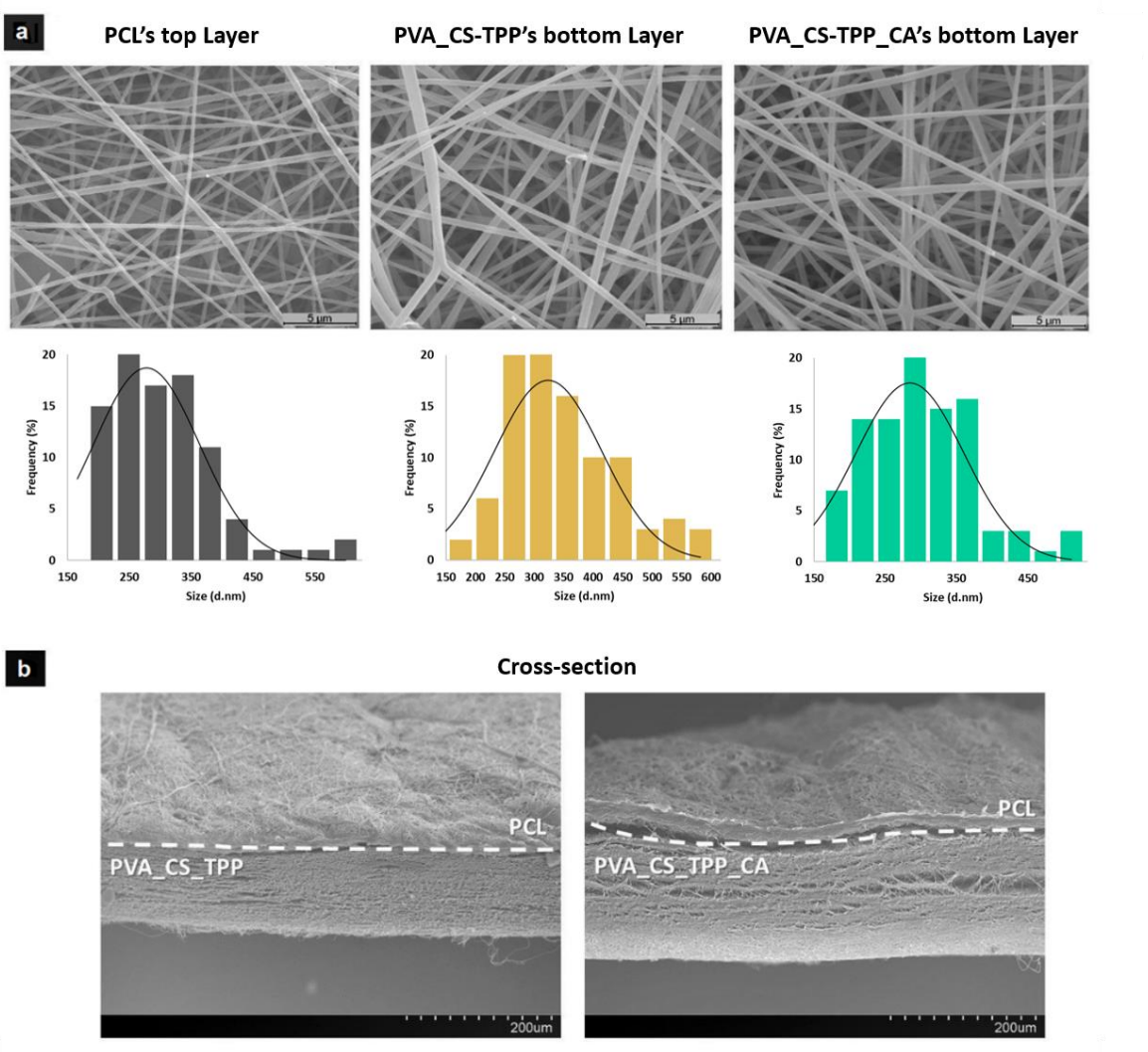

Figure 1 – Morphology and fiber diameter distribution of the PCL's top layer and the PVA_CS-TPP and PVA_CS-TPP_CA's bottom layers (**a**); and Cross-sectional SEM images of the double-layered membranes PCL/PVA_CS-TPP with crude CA extract (on the right) and without (on the left) (**b**).

According to the cross-sectional image, Figure 1b, it is possible to observe the two different layers of the produced double-layered nanocomposites membranes.

3.2.2. Attenuated Total Reflectance-Fourier Transform Infrared Spectroscopy Study

The acquired ATR-FTIR spectra of the produced double-layered nanocomposites membranes are presented in Figure 2. The spectrum of the PCL's top layer displays its characteristic bands, Figure 2a. The peaks at 2865.22 and 2943.10 cm^{-1} belongs to the symmetric and asymmetric CH_2 stretching vibration, while the band at 1722.95 cm^{-1} corresponds to the C=O stretching vibration [47].

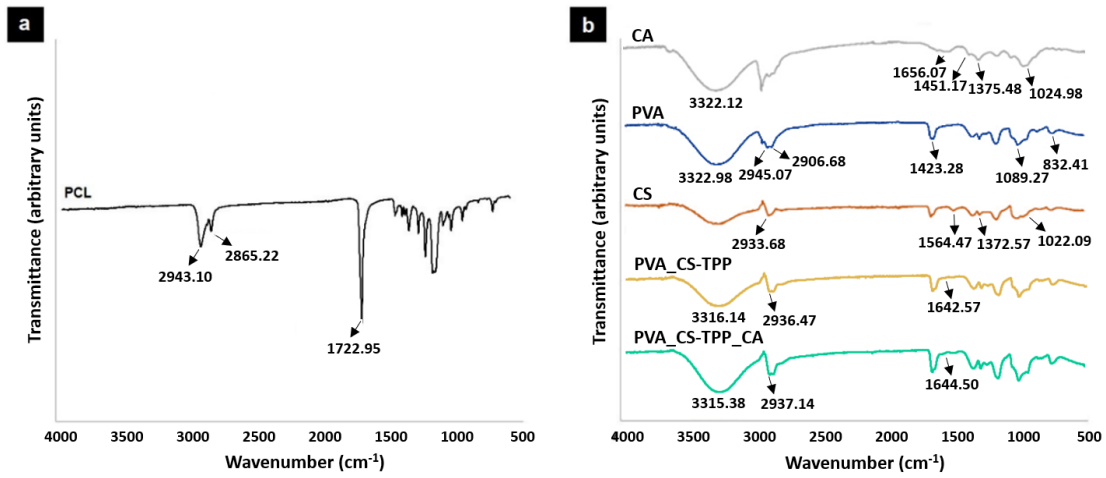

Figure 2 – ATR-FTIR analysis of the produced double-layered membranes. FTIR spectra of the PCL's top layer (**a**), the bottom layers of PVA_CS-TPP and PVA_CS-TPP_CA, and their raw materials (**b**).

In turn, the spectrum of the PVA_CS-TPP's bottom layer shows the characteristic peaks of the PVA and CS at 3316.14 and 2936.47 cm^{-1}, attributed to the O-H and CH_2 stretching vibration, respectively, and a peak at 1642.57 cm^{-1} assigned to C=O stretching of a primary amide, Figure 2b. These bands revealed that the PVA and CS-TPP were successfully dispersed in the nanofibers [31]. Moreover, when the CA extract was incorporated into the PVA_CS-TPP nanofibers, a higher intensity of the peaks was observed once the characteristic peaks of the crude CA extract overlapped with the bands of PVA_CS-TPP, Figure 2b. A similar effect was previously reported by Amina et al. [48], who showed that the characteristic peaks of PU nanofibers overlapped with the bands of aqueous extract of *Grewia mollis* (*G. mollis*), leading to a higher intensity in the PU/*G. mollis* nanofibers' spectrum. However, the spectrum of raw CA confirms its characteristics peaks at 3322.12 cm^{-1} (O-H stretching vibration of carboxylic acid group), 1656.07 cm^{-1} (C-O stretching vibration), 1451.17 cm^{-1} (C-H in-plane bending vibration), 1375.48 cm^{-1} (C-N stretching vibration, aromatic amide), and 1024.98 cm^{-1} (C-O stretchining) [49].

3.2.3. Differential Scanning Calorimetry (DSC)

The thermal properties of both layers (PCL's top layer and the bottom layers of PVA_CS-TPP and PVA_CS-TPP containing crude CA extract) were evaluated by DSC, as demonstrated in Figure 3. In PCL's top layer, the endothermic peak at 62.96 °C corresponds to the melting temperature (T_m) of PCL. This result is in agreement with the data available in the literature for electrospun PCL membranes (T_m(PCL) = 60.10 °C) [50]. On the other hand, comparing the raw PVA_CS with the PVA_CS-TPP nanofibers, it was found that the endothermic peak at 62.24 °C corresponding to the evaporation of water and acetic acid solvents [51,52]. In addition, a weak endothermic peak was found at 188.43 °C, which is due to the melting of PVA crystals [51]. Additionally, the DSC thermograms suggest that the presence of CS-TPP shifted the endothermic peaks to a higher temperature, confirming the thermal stability of the ionically cross-linked electrospun PVA_CS-TPP nanofibers. Moreover, the incorporation of the crude CA extract slightly changed the *Tm* of the PVA_CS-TPP nanofibers, indicating that the incorporation of the crude plant extract slightly enhance the thermal properties of the bottom layer of the produced double-layered nanocomposite membrane. Therefore, the electrospun PVA_CS-TPP_CA nanofibers were revealed to be thermally stable to support cell growth, which is essential for improving the healing process.

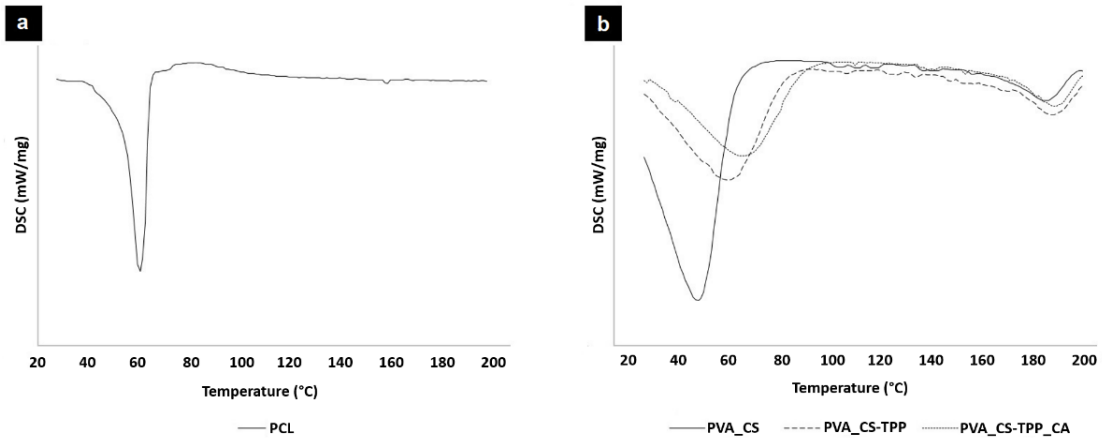

Figure 3 – Characterization of the thermal behavior of the produced double-layered membranes. DSC curves of the PCL's top layer (**a**); and the bottom layers of PVA_CS, PVA_CS-TPP, and PVA_CS-TPP_CA (**b**).

Similarly, Ghaseminezhad et al. [53] developed electrospun PCL/Gelatin nanofibers loaded with different amounts of *Althea officinalis* (AO) and demonstrated that till 15 wt % AO the thermal stability of these electrospun nanofibers was slightly improved.

3.2.4. Assessment of the Mechanical Characteristics of the Produced Electrospun Double-Layered Nanocomposites Membranes

The mechanical characteristics, like tension, elasticity, and Young's modulus, of the produced double-layered nanocomposites membranes, are summarized in Table 1. The electrospun PCL/PVA_CS-TPP membrane exhibited a tensile strength of 3.96 ± 0.99 MPa, Young's modulus of 38.16 ± 5.32 MPa, and an elongation at break of 10.39 ± 1.89%. However, the mechanical strength of the nanocomposites membranes was decreased after incorporation of the crude CA extract. The tensile strength and Young's modulus of the PCL/PVA_CS-TPP_CA were reduced to 3.03 ± 0.67 MPa and 36.36 ± 7.29 MPa, respectively. The crude CA extract also had a slight effect on the elongation at break (8.31 ± 0.61%). Nevertheless, the obtained values are close to those exhibited by native human skin, Table 1.

Table 1 – Evaluation of the mechanical properties of the produced Polycaprolactone (PCL)/ Poly(vinyl alcohol) (PVA) and Chitosan-Sodium tripolyphosphate (CS-TPP) (PVA_CS-TPP) nanofibrous membranes with and without crude *Centella asiatica* (L.) (CA) extract and comparison with the native human skin values.

	Tensile strength (MPa)	Young's modulus (MPa)	Elongation at break (%)	Thickness (mm)
PCL/PVA_CS-TPP	3.96 ± 0.99	38.16 ± 5.32	10.39 ± 1.89	0.12 ± 0.01
PCL/PVA_CS-TPP_CA	3.03 ± 0.67	36.36 ± 7.29	8.31 ± 0.61	0.10 ± 0.02
Native skin	2.50-30.00 [a]	0.40-20.00 [a]	10.00-115.00 [a]	-

[a] From reference [10].

According to what was described above, several studies have shown that the incorporation of the crude plant extracts into electrospun nanofibers decreases the mechanical strength of the membranes, due to its weaker mechanical properties [11,54]. In turn, synthetic polymers like PCL have exhibited excellent mechanical performance [55].

Thereby, the two layers of the double-layered nanocomposites membranes attached will provide good resilience and compliance to cover a wound area, resulting in effective wound healing with minimal scarring.

3.2.5. Measurement of the Total Porosity

The wound dressings' porosity is a very important parameter for an effective healing process to occur. Herein, the porosity of the PCL's top layer was found to be 64.01 ± 10.61%, Figure 4a. This value is in accordance with other studies that used the lowest porosity of the PCL as a protective layer against bacteria penetration [11,56]. On the other hand, the bottom layers of the PVA_CS-TPP and PVA_CS-TPP_CA displayed porosities of 92.92 ± 1.16% and 96.88 ± 1.14%, respectively, Figure 4a. The data obtained reveal that the porosity values of the bottom layers, which play a vital role in the healing

process, are in the preferred range of 60 to 90% for cell adhesion, migration, and proliferation. In addition, a highly porous structure is beneficial for the improvement of the production of the new ECM components [7].

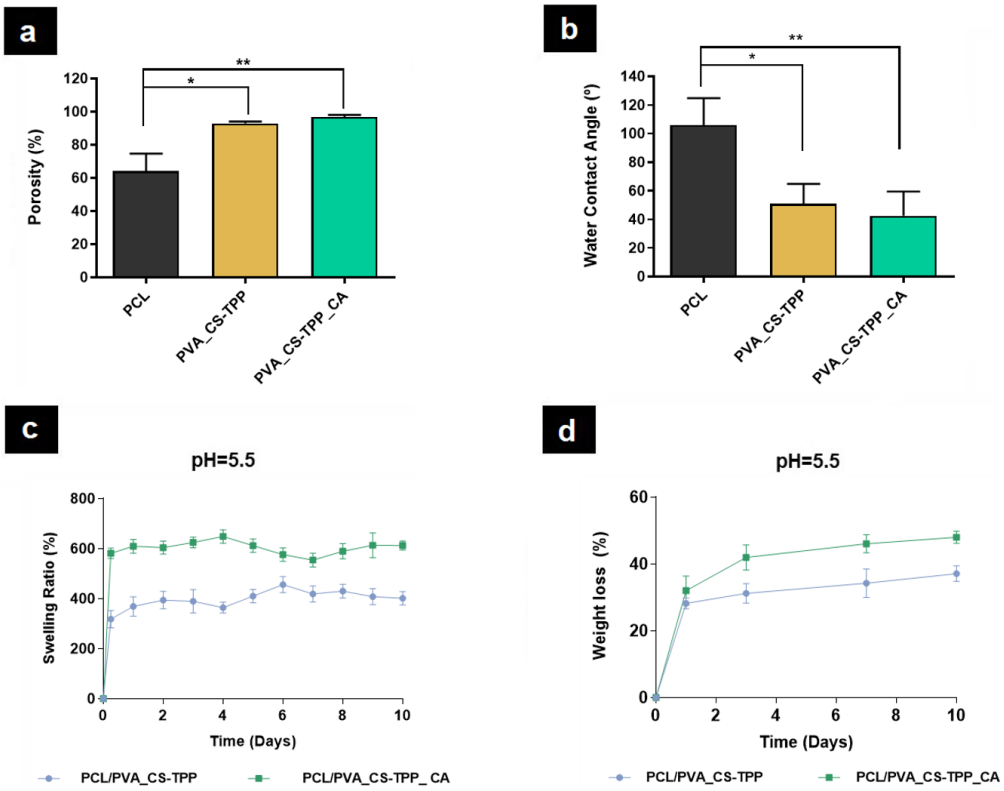

Figure 4 – Characterization of the total porosity (**a**); wettability (**b**); swelling profile (**c**); and weight loss at pH = 5.5 (**d**) of the produced double-layered membranes. (Data are represented as average ± standard derivation (SD), * $p < 0.05$ and ** $p < 0.01$).

3.2.6. Evaluation of Wettability Properties

The wettability of the wound dressing materials is a crucial parameter that affects their biological performance [57]. Herein, the surface wettability of both layers of the produced double-layered nanocomposite membranes was investigated from the WCA between the surface material and water droplets using the sessile drop technique. The PCL's top layer of nanocomposites membranes exhibited a WCA value of 105.93 ± 18.85°, confirming its hydrophobic character conferred by PCL aliphatic chains, Figure 4b. On the other hand, the bottom layers of the PVA_CS-TPP, which is in contact with the wound, showed a WCA value of 50.83 ± 13.97°. This value decreased to 42.50 ± 16.93° when the crude CA extract was incorporated in this layer (PVA_CS-TPP_CA), Figure 4b. Such behavior is associated with the hydrophilic character of the plant components. Therefore, the moderate wettability of the PVA_CS-TPP and PVA_CS-TPP_CA nanofibers is in accordance with the literature since WCA values between 40◦ and 70° could lead to better cell adhesion, migration, and

proliferation. Furthermore, values within this range are more prone to provide moist environments, enhancing the healing process, than the hydrophobic (WCA > 90°) or super hydrophilic (WCA < 20°) surfaces, as previously mentioned in the literature [56,57].

3.2.7. Analysis of the *In Vitro* Swelling Behavior

The water absorption capability of the produced electrospun double-layered nanocomposites membranes plays an important role in the absorption of wound exudates providing a moist wound environment [58]. The swelling behavior might contribute to avoiding an extreme level of the moisture at the wound surface, and the dryness of the wound, which can lead to a delay in healing [58]. The swelling profiles of the PCL/PVA_CS-TPP and PCL/PVA_CS-TPP_CA membranes were evaluated after immersion in PBS at pH = 5.5 for 10 days to simulate the acidic environment at the wound site, Figure 4c. The electrospun PCL/PVA_CS-TPP membrane containing crude CA extract displayed a higher water absorption capability (~600%) than the PCL/PVA_CS-TPP membrane (~400%). Thus, the results suggest that the incorporation of CA extract in the bottom layer of PVA_CS-TPP provided hydrophilicity to the polymer blend, contributing to a higher amount of water retained in the interconnected fibrous pores and increasing the water absorption ratio. A similar effect was previously described by Yousefi et al. [35], who found a higher water-uptake ability when Henna extracts were incorporated into CS/Poly(ethylene oxide) (PEO) nanofibrous mats. Regarding that, the CS/PEO/Henna extract nanofibrous mats were demonstrated to exhibit the capability to efficiently remove the exudate from the wound, adjusting the wound moisture.

3.2.8. Study of the *In Vitro* Biodegradation Profile

An ideal wound dressing must display suitable biodegradability and a degradation profile consistent with the wound repair and regeneration [59]. Herein, the electrospun double-layered nanocomposites membranes were fabricated from biodegradable materials, and the percentages of weight loss are presented in Figure 4d. The degradation studies showed that the PCL/PVA_CS-TPP exhibited a weight loss of 37.10 ± 2.33%, while the PCL/PVA_CS-TPP_CA undergo a weight loss of 48.04 ± 1.82%, respectively. Therefore, the hydrophilic character of crude CA extract contributed to both increases the water absorption and a slightly faster weight loss of the nanofibers. In addition, the PVA and CS present in the bottom layer are characterized by suffering higher weight losses than the PCL's top layer, which displays a slow *in vitro* degradation profile [11].

3.2.9. Water Vapor Transmission Rate (WVTR) Analysis

The membrane's permeability is another important parameter which can ensure suitable oxygenation of the wound environment and stimulate new blood vessel, sustaining the complex cellular events during the healing process [60]. In addition, the wound dressing membranes should

avoid excessive dehydration as well as the build-up of exudates [7]. The data available in the literature demonstrated that the ideal WVTR value for wound dressing materials should be between 2000–2500 g/m²/day [7]. Herein, a WVTR of 1162.94 ± 116.10 g/m²/day and 1757.12 ± 67.69 g/m²/day were measured for PCL/PVA_CS-TPP and PCL/PVA_CS-TPP_CA, respectively. These values appeared to be outside the range recommended for an ideal dressing. However, the WVTR values obtained herein are within the range displayed by commercial wound dressings (426–2047 g/m²/day) [61].

3.3. Analysis of the *In Vitro* CA Release from Electrospun Double-Layered Nanocomposites Membranes

Nowadays, loading bioactive agents into the electrospun nanofibers can be achieved through the simple blending of the polymer solution before spinning, post-spinning surface functionalization methods, or using core-shell electrospinning techniques [7]. The choice of the method is dependent on the intended application and based on the preferred bioactive agent release profile. Herein, crude CA extract, a medicinal plant, was selected to be incorporated into the PVA_CS-TPP nanofibers to improve the healing properties of the double-layered nanocomposites membranes. The cumulative release profile of the crude CA extract from the bottom's nanofibers is shown in Figure 5. The amount of CA released from the bottom layer reached 84.22 ± 2.08% after 10 days. The slower and sustained release of CA could be influenced by the nature of the plant components as well as the pore size of the nanofibers. Further, the swelling ability and consequential diffusion and degradation of the polymers on exposure to the aqueous medium (PBS pH = 5.5) can also affect the release mechanism of the crude CA extract [62,63].

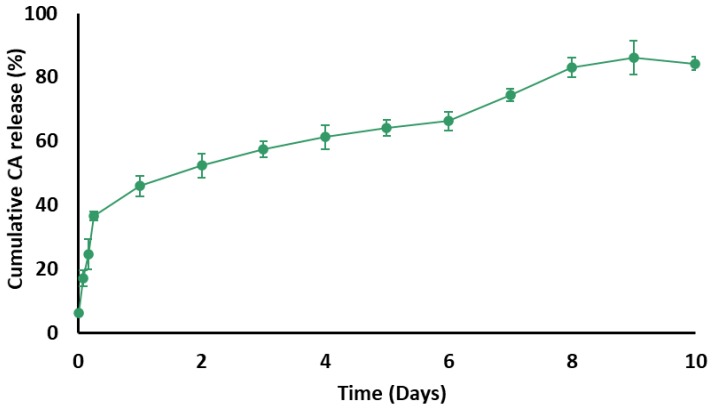

Figure 5 – Cumulative release profile of the crude CA extract from the bottom's PVA_CS-TPP nanofibers at pH = 5.5.

Regarding all the above-mentioned, the obtained release profile is crucial for the produced bottom layer to prevent wound bacterial colonization and infection.

3.4. Assessment of the Antibacterial Properties of the Produced Electrospun Double-Layered Nanocomposites Membranes

Wounded skin is usually associated with a higher level of bacterial colonization and subsequent biofilm formation, which can prolong the inflammatory phase of healing, delay collagen synthesis, and impede re-epithelialization [1,5,6]. Although the inflammatory cells inducing phagocytosis of the pathogens, high growth of bacteria at the wound site lead to an extended infiltration of immune cells and increase the production of pro-inflammatory cytokines [1,5,6]. Therefore, an ideal wound dressing material should provide an unfavorable environment for bacteria growth or inhibit the infiltration of bacteria at the wound site. In this study, the behavior of the PCL's top layer was similar to the control group (filter paper with a pore size of 0.22 µm), proving the capability to act as a protective barrier against *S. aureus* and *P. aeruginosa* due to its low porosity, Figure 6. The antibacterial activity of the bottom layers (PVA_CS-TPP and PVA_CS-TPP_CA) was also evaluated. PVA_CS-TPP showed an inhibitory effect of 61.80 ± 4.45% and 48.41 ± 9.94% against *S. aureus* and *P. aeruginosa*, respectively. However, an increased inhibitory effect on bacterial growth, 99.96 ± 6.04% and 99.94 ± 0.67% for *S. aureus* and *P. aeruginosa*, was observed when the crude CA extract was incorporated, Figure 6. This result confirmed that the CA's secondary metabolites, like triterpenoid saponins (asiatic acid, asiaticoside, and madecassoside) exhibit a high ability to inhibit bacterial growth, as previously reported in different research studies [34,64]. Hence, the PVA_CS-TPP layer containing CA extract is essential to provide an aseptic environment at the wound site.

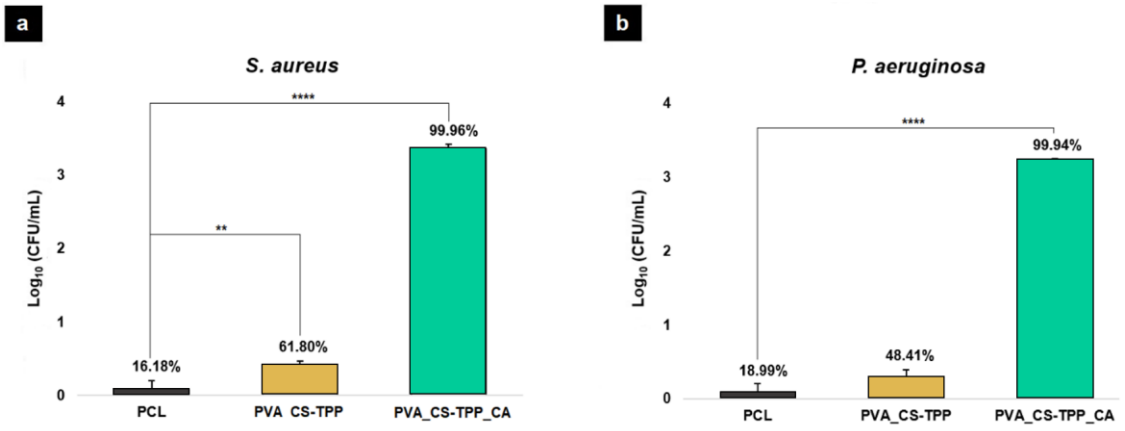

Figure 6 – Evaluation of the antibacterial potential of the PCL's top layer and the PVA_CS-TPP_CA and PVA_CS-TPP_CA's bottom layers against *Staphylococcus aureus* (*S. aureus*) (**a**) and *Pseudomonas aeruginosa* (*P. aeruginosa*) (**b**). (Data are represented as average ± standard deviation (SD), ** $p < 0.01$ and **** $p < 0.0001$).

3.5. Analysis of the *In Vitro* Cell Viability

In this study, the effect of the produced double-layered nanocomposites membranes on cell viability and proliferation was investigated through MTT assay for 1, 3, and 7 days and the results are shown in Figure 7. Overall, it was found that the PCL/PVA_CS-TPP and PCL/PVA_CS-TPP containing CA extract displayed excellent cell viability (over 90%) when tested on NHDF cells. The non-toxic properties could be attributed to the porous and hydrophilic character exhibited by the bottom layers, which can support cell adhesion and proliferation.

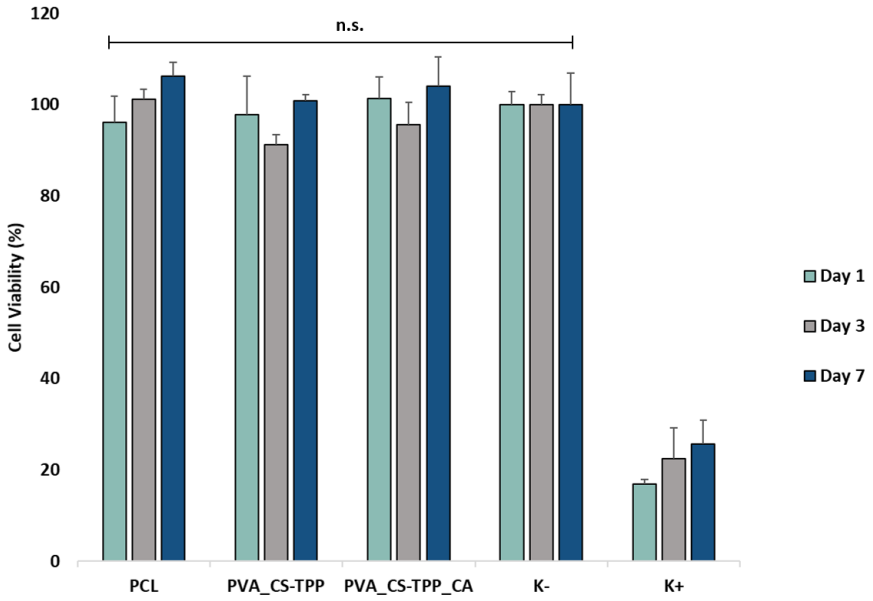

Figure 7 – Growth of normal human dermal fibroblasts (NHDF) cells on the PCL's top layer and the PVA_CS-TPP and PVA_CS-TPP_CA's bottom layers detected by 3-(4,5-Dimethyl-2-thiazolyl)-2,5-diphenyl-2H-tetrazolium bromide (MTT) assay in term of cell viability after 1, 3, and 7 days.

Similarly, Yousefi et al. [35] demonstrated that the incorporation of the Henna extracts into CS/PEO nanofibrous mats did not affect the proliferation and viability of the NHF cells, confirming that they lack cytotoxic effects.

4. Conclusions

In the present study, the electrospun double-layered nanocomposite membrane of PCL, PVA, and CS-TPP was incorporated with crude CA extract to improve skin regeneration. The obtained nanocomposite material was characterized in terms of physical, chemical, and biological features to verify its suitability to be applied as an advanced wound dressing. The results showed that the PCL's layer could act as a protective barrier against external contaminants, and simultaneously, the PVA_CS-TPP_CA's bottom layer was revealed to be effective in exudate absorption and providing a

moist environment. Moreover, PVA_CS-TPP_CA improved the antibacterial activity of the double-layered nanocomposite membrane against *S. aureus* and *P. aeruginosa*, which is advantageous to prevent microbial penetration. This novel nano-carrier was also able to achieve a controlled release of CA and closely resemble the mechanical properties of native skin. Furthermore, the produced double-layered nanocomposites membranes did not provide a cytotoxic effect on NHDF cell culture. Hence, these findings emphasize the potential to blend PCL and PVA_CS-TPP nanofibers with the beneficial properties of crude CA extract for wound healing applications. Shortly, other potential healing benefits of these double-layered nanocomposites membranes will be further tested, as well as their efficacy in animal models to establish *in vivo* data.

Author Contributions: C.M. performed the investigation and wrote the paper; R.F. supervised the paper; I.C.G. supervised and validated the data of the paper. All authors have read and agreed to the published version of the manuscript.

Funding: The authors are grateful for the support given by the FibEnTech Research Unit (Project UIDB/00195/2020). Cláudia Mouro also acknowledges a PhD fellowship from the Foundation for Science and Technology (FCT) (PD/BD/113550/2015).

Acknowledgments: The authors would like to thank Ana Raquel Nunes for her help in the cytotoxic assay and Eng. Ana Paula Gomes for her help in SEM and DSC analysis.

Conflicts of Interest: The authors declare no conflict of interest, financial or otherwise.

References

1. Sousa Coelho, D.; Veleirinho, B.; Alberti, T.; Maestri, A.; Yunes, R.; Fernando Dias, P.; Maraschin, M. Electrospinning Technology: Designing Nanofibers toward Wound Healing Application. In *Nanomaterials - Toxicity, Human Health and Environment*; IntechOpen, 2018; pp. 1–19.
2. Williamson, D.; Harding, K. Wound healing. *Medicine (Baltimore).* **2004**, *32*, 4–7.
3. Chouhan, D.; Dey, N.; Bhardwaj, N.; Mandal, B.B. Emerging and innovative approaches for wound healing and skin regeneration: Current status and advances. *Biomaterials* **2019**, *216*, 119267.
4. Mihai, M.M.; Dima, M.B.; Dima, B.; Holban, A.M. Nanomaterials for wound healing and infection control. *Materials (Basel).* **2019**, *12*, 2176.

5. Sarheed, O.; Ahmed, A.; Shouqair, D.; Boateng, J. Antimicrobial Dressings for Improving Wound Healing. In *Wound Healing - New insights into Ancient Challenges*; InTech, 2016; pp. 373–398.

6. Paladini, F.; Pollini, M. Antimicrobial Silver Nanoparticles for Wound Healing Application: Progress and Future Trends. *Materials (Basel)*. **2019**, *12*, 2540.

7. Pilehvar-Soltanahmadi, Y.; Dadashpour, M.; Mohajeri, A.; Fattahi, A.; Sheervalilou, R.; Zarghami, N. An Overview on Application of Natural Substances Incorporated with Electrospun Nanofibrous Scaffolds to Development of Innovative Wound Dressings. *Mini-Reviews Med. Chem.* **2017**, *18*, 414–427.

8. Andreu, V.; Mendoza, G.; Arruebo, M.; Irusta, S. Smart dressings based on nanostructured fibers containing natural origin antimicrobial, anti-inflammatory, and regenerative compounds. *Materials (Basel).* **2015**, *8*, 5154–5193.

9. Zhang, W.; Ronca, S.; Mele, E. Electrospun nanofibres containing antimicrobial plant extracts. *Nanomaterials* **2017**, *7*, 1–17.

10. dos Santos, D.M.; Leite, I.S.; Bukzem, A. de L.; de Oliveira Santos, R.P.; Frollini, E.; Inada, N.M.; Campana-Filho, S.P. Nanostructured electrospun nonwovens of poly(ε-caprolactone)/quaternized chitosan for potential biomedical applications. *Carbohydr. Polym.* **2018**, *186*, 110–121.

11. Miguel, S.P.; Ribeiro, M.P.; Coutinho, P.; Correia, I.J. Electrospun polycaprolactone/Aloe Vera_chitosan nanofibrous asymmetric membranes aimed for wound healing applications. *Polymers (Basel).* **2017**, *9*, 183.

12. Bai, Y.; Wang, D.; Zhang, Z.; Pan, J.; Cui, Z.; Yu, D.-G.; Annie Bligh, S.-W. Testing of fast dissolution of ibuprofen from its electrospun hydrophilic polymer nanocomposites. *Polym. Test.* **2020**, 106872.

13. Wang, K.; Wang, P.; Wang, M.; Yu, D.G.; Wan, F.; Bligh, S.W.A. Comparative study of electrospun crystal-based and composite-based drug nano depots. *Mater. Sci. Eng. C* **2020**, *113*, 110988.

14. Huang, C.K.; Zhang, K.; Gong, Q.; Yu, D.G.; Wang, J.; Tan, X.; Quan, H. Ethylcellulose-based drug nano depots fabricated using a modified triaxial electrospinning. *Int. J. Biol. Macromol.* **2020**, *152*, 68–76.

15. Kang, S.; Hou, S.; Chen, X.; Yu, D.G.; Wang, L.; Li, X.; Williams, G.R. Energy-saving electrospinning with a concentric teflon-core rod spinneret to create medicated nanofibers. *Polymers (Basel).* **2020**, *12*, 1–16.

16. Liu, Y.; Liu, X.; Liu, P.; Chen, X.; Yu, D.G. Electrospun multiple-chamber nanostructure and its potential self-healing applications. *Polymers (Basel).* **2020**, *12*, 1–13.

17. Wang, M.; Li, D.; Li, J.; Li, S.; Chen, Z.; Yu, D.G.; Liu, Z.; Guo, J.Z. Electrospun Janus zein–PVP nanofibers provide a two-stage controlled release of poorly water-soluble drugs. *Mater. Des.* **2020**, *196*, 109075.

18. Hou, J.; Yang, J.; Zheng, X.; Wang, M.; Liu, Y.; Yu, D.G. A nanofiber-based drug depot with high drug loading for sustained release. *Int. J. Pharm.* **2020**, *583*.

19. Ding, Y.; Dou, C.; Chang, S.; Xie, Z.; Yu, D.G.; Liu, Y.; Shao, J. Core-shell eudragit S100 nanofibers preparedvia triaxial electrospinning to providea colon-targeted extended drug release. *Polymers (Basel).* **2020**, *12*.

20. Wang, M.; Hou, J.; Yu, D.G.; Li, S.; Zhu, J.; Chen, Z. Electrospun tri-layer nanodepots for sustained release of acyclovir. *J. Alloys Compd.* **2020**, *846*, 156471.

21. Chang, S.; Wang, M.; Zhang, F.; Liu, Y.; Liu, X.; Yu, D.G.; Shen, H. Sheath-separate-core nanocomposites fabricated using a trifluid electrospinning. *Mater. Des.* **2020**, *192*, 108782.

22. Hassanin, A.; El-Moneim, A.A.; Ghaniem, M.; Nageh, H. Nanocomposite multilayer fibrous membrane for sustained drug release. In Proceedings of the Advanced Materials Research; Trans Tech Publications Ltd, 2014; Vol. 894, pp. 364–368.

23. Rezk, A.I.; Lee, J.Y.; Son, B.C.; Park, C.H.; Kim, C.S. Bi-layered nanofibers membrane loaded with titanium oxide and tetracycline as controlled drug delivery system for wound dressing applications. *Polymers (Basel).* **2019**, *11*.

24. López-Calderón, H.D.; Avilés-Arnaut, H.; Galán-Wong, L.J.; Almaguer-Cantú, V.; Laguna-Camacho, J.R.; Calderón-Ramón, C.; Escalante-Martínez, J.E.; Arévalo-Niño, K. Electrospun Polyvinylpyrrolidone-Gelatin and Cellulose Acetate Bi-Layer Scaffold Loaded with Gentamicin as Possible Wound Dressing. *Polymers (Basel).* **2020**, *12*, 2311.

25. Bhullar, S.K.; Buttar, H.S. Perspectives on nanofiber dressings for the localized delivery of botanical remedies in wound healing. *AIMS Mater. Sci.* **2017**, *4*, 370–382.

26. Hajialyani, M.; Tewari, D.; Sobarzo-Sánchez, E.; Nabavi, S.M.; Farzaei, M.H.; Abdollahi, M. Natural product-based nanomedicines for wound healing purposes: Therapeutic targets and drug delivery systems. *Int. J. Nanomedicine* **2018**, *13*, 5023–5043.

27. Cheesman, M.J.; Ilanko, A.; Blonk, B.; Cock, I.E. Developing new antimicrobial therapies: Are synergistic combinations of plant extracts/compounds with conventional antibiotics the solution? *Pharmacogn. Rev.* **2017**, *11*, 57–72.

28. Pedram Rad, Z.; Mokhtari, J.; Abbasi, M. Fabrication and characterization of PCL/zein/gum arabic electrospun nanocomposite scaffold for skin tissue engineering. *Mater. Sci. Eng. C* **2018**, *93*, 356–366.

29. Suryamathi, M.; Ruba, C.; Viswanathamurthi, P.; Balasubramanian, V.; Perumal, P. Tridax Procumbens Extract Loaded Electrospun PCL Nanofibers: A Novel Wound Dressing Material. *Macromol. Res.* **2019**, *27*, 55–60.

30. Foong, C.Y.; Sultana, N. Fabrication of layer-by-layer electrospun composite membranes based on polylactic acid (PLA) and poly (caprolactone) (PCL)/Chitosan. *ARPN J. Eng. Appl. Sci.* **2015**, *10*, 9408–9413.

31. Charernsriwilaiwat, N.; Rojanarata, T.; Ngawhirunpat, T.; Opanasopit, P. Preparation of chitosan-thiamine pyrophosphate/polyvinyl alcohol blend electrospun nanofibers. In Proceedings of the Advanced Materials Research; Trans Tech Publications Ltd, 2012; Vol. 506, pp. 118–121.

32. Somboonwong, J.; Kankaisre, M.; Tantisira, B.; Tantisira, M.H. Wound healing activities of different extracts of *Centella asiatica* in incision and burn wound models: an experimental animal study. *BMC Complement. Altern. Med.* **2012**, *12*, 103.

33. Roy M, A.; Krishnan, L.; Roy Roy, A. Qualitative and Quantitative Phytochemical Analysis of *Centella asiatica*. *Nat. Prod. Chem. Res.* **2018**, *06*, 1000323.

34. Sikareepaisan, P.; Suksamrarn, A.; Supaphol, P. Electrospun gelatin fiber mats containing a herbal - *Centella asiatica* - Extract and release characteristic of asiaticoside. *Nanotechnology* **2008**, *19*, 015102.

35. Yousefi, I.; Pakravan, M.; Rahimi, H.; Bahador, A.; Farshadzadeh, Z.; Haririan, I. An investigation of electrospun Henna leaves extract-loaded chitosan based nanofibrous mats for skin tissue engineering. *Mater. Sci. Eng. C* **2017**, *75*, 433–444.

36. Alavarse, A.C.; de Oliveira Silva, F.W.; Colque, J.T.; da Silva, V.M.; Prieto, T.; Venancio, E.C.; Bonvent, J.J. Tetracycline hydrochloride-loaded electrospun nanofibers mats based on PVA and chitosan for wound dressing. *Mater. Sci. Eng. C* **2017**, *77*, 271–281.

37. Qasim, S.B.; Zafar, M.S.; Najeeb, S.; Khurshid, Z.; Shah, A.H.; Husain, S.; Rehman, I.U. Electrospinning of chitosan-based solutions for tissue engineering and regenerative medicine. *Int. J. Mol. Sci.* **2018**, *19*, 1–26.

38. Abbaspour, M.; Makhmalzadeh, B.S.; Rezaee, B.; Shoja, S.; Ahangari, Z. Evaluation of the antimicrobial effect of chitosan/polyvinyl alcohol electrospun nanofibers containing mafenide acetate. *Jundishapur J. Microbiol.* **2015**, *8*, e24239.

39. Sarkar, S.D.; Farrugia, B.L.; Dargaville, T.R.; Dhara, S. Physico-chemical/biological properties of tripolyphosphate cross-linked chitosan based nanofibers. *Mater. Sci. Eng. C* **2013**, *33*, 1446–1454.

40. Nguyen, T.V.; Nguyen, T.T.H.; Wang, S.L.; Vo, T.P.K.; Nguyen, A.D. Preparation of chitosan nanoparticles by TPP ionic gelation combined with spray drying, and the antibacterial activity of chitosan nanoparticles and a chitosan nanoparticle–amoxicillin complex. *Res. Chem. Intermed.* **2017**, *43*, 3527–3537.

41. Yeh, C.C.; Li, Y.T.; Chiang, P.H.; Huang, C.H.; Wang, Y.; Chang, H.I. Characterizing microporous PCL matrices for application of tissue engineering. *J. Med. Biol. Eng.* **2009**, *29*, 92–97.

42. Kaur, I.; Suthar, N.; Kaur, J.; Bansal, Y.; Bansal, G. Accelerated Stability Studies on Dried Extracts of *Centella asiatica* Through Chemical, HPLC, HPTLC, and Biological Activity Analyses. *J. Evidence-Based Complement. Altern. Med.* **2016**, *21*, NP127–NP137.

43. Yao, C.H.; Yeh, J.Y.; Chen, Y.S.; Li, M.H.; Huang, C.H. Wound-healing effect of electrospun gelatin nanofibres containing *Centella asiatica* extract in a rat model. *J. Tissue Eng. Regen. Med.* **2015**, *11*, 905–915.

44. Pourhojat, F.; Sohrabi, M.; Shariati, S.; Mahdavi, H.; Asadpour, L. Evaluation of poly ε-caprolactone electrospun nanofibers loaded with *Hypericum perforatum* extract as a wound dressing. *Res. Chem. Intermed.* **2017**, *43*, 297–320.

45. Papenburg, B.J.; Bolhuis-Versteeg, L.A.M.; Grijpma, D.W.; Feijen, J.; Wessling, M.; Stamatialis, D. A facile method to fabricate poly(L-lactide) nano-fibrous morphologies by phase inversion. *Acta Biomater.* **2010**, *6*, 2477–2483.

46. Abrigo, M.; McArthur, S.L.; Kingshott, P. Electrospun nanofibers as dressings for chronic wound care: Advances, challenges, and future prospects. *Macromol. Biosci.* **2014**, *14*, 772–792.

47. Manotham, S.; Pengpat, K.; Eitssayeam, S.; Rujijanagul, G.; Sweatman, D.R.; Tunkasiri, T. Fabrication of Polycaprolactone/*Centella asiatica* Extract Biopolymer Nanofiber by Electrospinning. *Appl. Mech. Mater.* **2015**, *804*, 151–154.

48. Amina, M.; Al-Youssef, H.M.; Amna, T.; Hassan, S.; El-Shafae, A.M.; Kim, H.Y.; Khil, M.-S. Poly(urethane)/G. Mollis Composite Nanofibers for Biomedical Applications. *J. Nanoeng. Nanomanufacturing* **2012**, *2*, 85–90.

49. Rebia, R.A.; Sadon, N.S.B.; Tanaka, T. Natural antibacterial reagents (Centella, propolis, and hinokitiol) loaded into poly[(R)-3-hydroxybutyrate-co-(R)-3-hydroxyhexanoate] composite nanofibers for biomedical applications. *Nanomaterials* **2019**, *9*.

50. Hu, J.; Prabhakaran, M.P.; Ding, X.; Ramakrishna, S. Emulsion electrospinning of polycaprolactone: Influence of surfactant type towards the scaffold properties. *J. Biomater. Sci. Polym. Ed.* **2015**, *26*, 57–75.

51. Koosha, M.; Mirzadeh, H.; Shokrgozar, M.A.; Farokhi, M. Nanoclay-reinforced electrospun chitosan/PVA nanocomposite nanofibers for biomedical applications. *RSC Adv.* **2015**, *5*, 10479–10487.

52. Vega-Cázarez, C.A.; López-Cervantes, J.; Sánchez-Machado, D.I.; Madera-Santana, T.J.; Soto-Cota, A.; Ramírez-Wong, B. Preparation and Properties of Chitosan–PVA Fibers Produced by Wet Spinning. *J. Polym. Environ.* **2018**, *26*, 946–958.

53. Ghaseminezhad, K.; Zare, M.; Lashkarara, S.; Yousefzadeh, M.; Aghazadeh Mohandesi, J. Fabrication of althea officinalis loaded electrospun nanofibrous scaffold for potential application of skin tissue engineering. *J. Appl. Polym. Sci.* **2020**, *137*, 48587.

54. Pedram Rad, Z.; Mokhtari, J.; Abbasi, M. Preparation and characterization of *Calendula officinalis*-loaded PCL/gum arabic nanocomposite scaffolds for wound healing applications. *Iran. Polym. J. (English Ed.* **2019**, *28*, 51–63.

55. Motealleh, B.; Zahedi, P.; Rezaeian, I.; Moghimi, M.; Abdolghaffari, A.H.; Zarandi, M.A.

Morphology, drug release, antibacterial, cell proliferation, and histology studies of chamomile-loaded wound dressing mats based on electrospun nanofibrous poly(ε-caprolactone)/polystyrene blends. *J. Biomed. Mater. Res. - Part B Appl. Biomater.* **2014**, *102*, 977–987.

56. Trinca, R.B.; Westin, C.B.; da Silva, J.A.F.; Moraes, Â.M. Electrospun multilayer chitosan scaffolds as potential wound dressings for skin lesions. *Eur. Polym. J.* **2017**, *88*, 161–170.
57. Wang, J.; Planz, V.; Vukosavljevic, B.; Windbergs, M. Multifunctional electrospun nanofibers for wound application – Novel insights into the control of drug release and antimicrobial activity. *Eur. J. Pharm. Biopharm.* **2018**, *129*, 175–183.
58. Khoshnevisan, K.; Maleki, H.; Samadian, H.; Doostan, M.; Khorramizadeh, M.R. Antibacterial and antioxidant assessment of cellulose acetate/polycaprolactone nanofibrous mats impregnated with propolis. *Int. J. Biol. Macromol.* **2019**, *140*, 1260–1268.
59. Salvatore, L.; Carofiglio, V.E.; Stufano, P.; Bonfrate, V.; Calò, E.; Scarlino, S.; Nitti, P.; Centrone, D.; Cascione, M.; Leporatti, S.; et al. Potential of electrospun poly(3-hydroxybutyrate)/collagen blends for tissue engineering applications. *J. Healthc. Eng.* **2018**, *2018*, 6573947.
60. Eğri, Ö.; Erdemir, N. Production of *Hypericum perforatum* oil-loaded membranes for wound dressing material and *in vitro* tests. *Artif. Cells, Nanomedicine Biotechnol.* **2019**, *47*, 1404–1415.
61. Garcia-Orue, I.; Santos-Vizcaino, E.; Etxabide, A.; Uranga, J.; Bayat, A.; Guerrero, P.; Igartua, M.; de la Caba, K.; Hernandez, R.M. Development of bioinspired gelatin and gelatin/chitosan bilayer hydrofilms for wound healing. *Pharmaceutics* **2019**, *11*, 1–18.
62. Goh, Y.-F.; Shakir, I.; Hussain, R. Electrospun fibers for tissue engineering, drug delivery, and wound dressing. *J. Mater. Sci.* **2013**, *48*, 3027–3054.
63. Avci, H.; Ghorbanpoor, H.; Nurbas, M. Preparation of origanum minutiflorum oil-loaded core–shell structured chitosan nanofibers with tunable properties. *Polym. Bull.* **2018**, *75*, 4129–4144
64. Hou, Q.; Li, M.; Lu, Y.H.; Liu, D.H.; Li, C.C. Burn wound healing properties of asiaticoside and madecassoside. *Exp. Ther. Med.* **2016**, *12*, 1269–1274.

Part III
Cotton based composite for Wound Dressing Applications

This part englobes the development of a bilayer composite wound dressing material aimed to suppress the limitations of the frequently used textile wound dressings by deposition of an electrospun nanofiber layer containing a crude medicinal plant extract. The properties added by the electrospun nanofibers to the conventional cotton gauze bandage are highlighted.

This part includes the following scientific publications:

Cláudia Mouro, Colum P. Dunne, and Isabel C. Gouveia. Designing New Antibacterial Wound Dressings: Development of a Dual Layer Cotton Material Coated with Poly(Vinyl Alcohol)_Chitosan Nanofibers Incorporating *Agrimonia eupatoria* L. Extract. Molecules (2021) 26(1):83. (**Paper 7**)

Paper 7 - Designing New Antibacterial Wound Dressings: Development of a Dual Layer Cotton Material Coated with Poly(vinyl alcohol)_Chitosan Nanofibers Incorporating *Agrimonia eupatoria* L. Extract

Abstract

Wounds display particular vulnerability to microbial invasion and infections by pathogenic bacteria. Therefore, to reduce the risk of wound infections, researchers have expended considerable energy on developing advanced therapeutic dressings, such as electrospun membranes containing antimicrobial agents. Among the most used antimicrobial agents, medicinal plant extracts demonstrate considerable potential for clinical use, due primarily to their efficacy allied to relatively low incidence of adverse side-effects. In this context, the present work aimed to develop a unique dual-layer composite material with enhanced antibacterial activity derived from a coating layer of Poly(vinyl alcohol) (PVA) and Chitosan (CS) containing *Agrimonia eupatoria* L. (AG). This novel material has properties that facilitate it being electrospun above a conventional cotton gauze bandage pre-treated with 2,2,6,6-tetramethylpiperidinyl-1-oxy free radical (TEMPO). The produced dual-layer composite material demonstrated features attractive in production of wound dressings, specifically, wettability, porosity, and swelling capacity. Moreover, antibacterial assays showed that AG-incorporated into PVA_CS's coating layer could effectively inhibit *Staphylococcus aureus* (*S. aureus*) and *Pseudomonas aeruginosa* (*P. aeruginosa*) growth. Equally important, the cytotoxic profile of the dual-layer material in normal human dermal fibroblast (NHDF) cells demonstrated biocompatibility. In summary, these data provide initial confidence that the TEMPO-oxidized cotton/PVA_CS dressing material containing AG extract demonstrates adequate mechanical attributes for use as a wound dressing and represents a promising approach to prevention of bacterial wound contamination.

Graphical Abstract

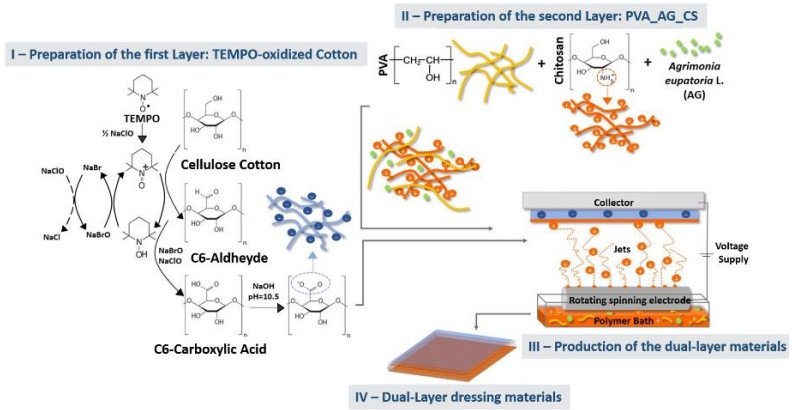

Keywords: Cotton; nanofibers; electrospinning; *Agrimonia eupatoria* L.; antibacterial wound dressings; skin infections.

1. Introduction

Although skin is a relatively robust protection against infectious agents [1,2], it is prone to compromise by physical damage or disease-related lesions that affect both the structure and function. Of these, cutaneous wounds represent a favorable microenvironment for bacterial colonization and proliferation, facilitating occurrence of infections especially in patients with impaired immune responses [3–7]. In an era of increasing multidrug-resistance, impaired treatment options, and elevated rates of morbidity and mortality [6], the development of wound dressings with intrinsic antimicrobial properties is increasingly desirable. Traditionally, wound dressings comprise gauzes, films, foams, hydrogels, and hydrocolloids and these have been used to cover the wound site to improve the healing process [3,6–8]. Nevertheless, natural textile materials (such as cotton) continue to be most used due to their low cost, limited adverse effects, easy handling and fabrication, and adequate mechanical support [8]. However, such textile wound dressings can lead to wound dehydration, adherence to wound beds in the presence of high-exudate wounds, and cause trauma and pain during removal [8]. Due to this, composite wound dressings, which combine the most advantageous features of these different materials have been developed to prevent bacterial infections while enhancing the healing process. Likewise, complementary approaches have involved innovative dressings with intrinsic antibacterial activity, integrated extrinsic antimicrobial agents, surface modification, and topical application have been explored [3,9–12]. However, the latter approach involving topical administration has proved problematic due to subsequent irritation or allergic contact dermatitis reactions that negatively impact the healing process [11,13]. Furthermore, non-healing, chronic wounds often present with considerable volumes of exudate, which can reduce the penetration rate of topically administered agents [14]. In efforts to overcome these challenges, attention has turned to the potential use of nanofiber materials produced from naturally derived or synthetic biopolymer mixtures that undergo electrospinning, with enhanced capability to promote skin regeneration while conferring protection against bacterial infection [10,15,16]. These beneficial traits are mediated somewhat through a physical similarity of the electrospun nanofibrous membranes to the native skin extracellular matrix that promotes cell adhesion and proliferation allied with the ability to deliver therapeutic and bioactive compounds directly to the wound site [10,15,16]. In addition, the simplicity, cost-effectiveness, and versatility of the electrospinning, as well as the unique features of the produced electrospun nanofibers, make this technique attractive for wound dressing applications [10,15,16].

Among the therapeutic and bioactive compounds, many are sourced from medicinal plants [10,16]. More specifically, crude plant extracts that (presumably) contain mixtures of bioactive compounds have demonstrated attractive levels of efficacy that is often greater than those exhibited by single isolated compounds from those same plants. This efficacy is likely to relate to synergic interactions between constituent compounds or possible protection of bioactive agents from enzymatic degradation during extraction processes [16–19]. One such crude extract derives from *Agrimonia*

eupatoria L., a member of the family *Rosaceae*, commonly known as agrimony (AG) has been analyzed and shown to be rich in tannins, flavonoids, phenolic acids, and triterpenoids with recognized anti-inflammatory, antioxidant, antimicrobial, and antibiofilm properties [20–23]. In this study, a new composite wound dressing material was produced that comprised two distinct layers. To accomplish that, a cotton gauze bandage that had been oxidized previously with the 2,2,6,6-tetramethylpiperidine-1-oxyl radical (TEMPO)/sodium bromide (NaBr)/sodium hypochlorite (NaClO) system was used as a substrate for the nanofibrous membrane composed of Poly(vinyl alcohol) (PVA), Chitosan (CS), and AG. Hence, the produced electrospun PVA_CS membrane combined with AG is intended to reduce the adhesion behavior of the textile dressing when applied to the wound bed and to improve the healing process, complemented by suppression of wound infection mediated by inherent antibacterial activity.

2. Results and Discussion

2.1. Minimum Inhibitory Concentration (MIC)

The *in vitro* antibacterial efficiency measures of the ethanol crude extract of AG against *Staphylococcus aureus* (*S. aureus*) and *Pseudomonas aeruginosa* (*P. aeruginosa*) were found to be 1.25 and 3.75 mg/mL, respectively, Figure 1. These results suggest that the crude AG extract is less effective against Gram-negative bacteria (*P. aeruginosa*) compared to Gram-positive (*S. aureus*), albeit that only two species were studied. Notably, a similar effect was described previously by Muruzovic et al., where MIC values of 1.25 mg/mL and 0.62 mg/mL were obtained for *P. aeruginosa* and *S. aureus*, respectively [23]. However, there is a caveat in that the geographic location, the season in which the medicinal plants are harvested, and the chosen extraction method may impact the eventual extract's chemical composition and, thereby, MIC values.

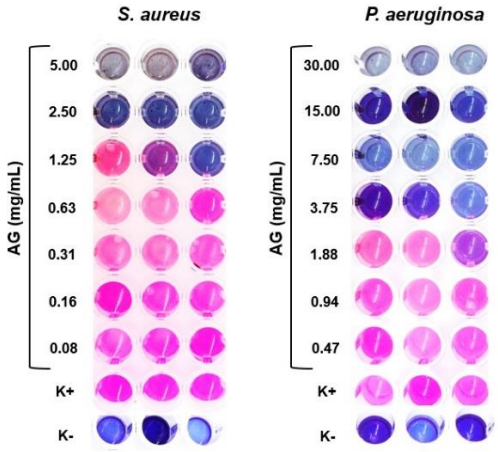

Figure 1 – Determination of the minimum inhibitory concentration (MIC) against *Staphylococcus aureus* (*S. aureus*) and *Pseudomonas aeruginosa* (*P. aeruginosa*) by resazurin-based 96-well plate microdilution method.

2.2 Characterization of the Dual-Layer Dressing Materials

2.2.1. Assessment of the Morphologic Features

The TEMPO-oxidized cotton/PVA_CS materials with and without incorporated crude AG extract were successfully fabricated with a bilayer organization as demonstrated by the cross-sectional SEM images, Figure 2A. Additionally, the coating layers of PVA_CS and PVA_AG_CS were electrospun directly over the cotton bandage gauze to enable absorption of wound exudates in a controlled manner, to maintain a suitable moist environment, and to ensure proper nutrient and gas exchange. This electrospun membrane proved to be non-toxic, biocompatible and biodegradable, with antimicrobial ability to enhance collagen synthesis, as previously reported membranes produced with PVA and CS [24]. Moreover, incorporation of the crude AG extract into this layer supplements the antimicrobial activity on the dual-layer material. With regard to physical properties specifically, the diameter of the coating layer's nanofibers was determined by SEM imaging, Figure 2B. Uniform and homogeneous nanofibers having an average diameter of 280.20 ± 82.65 nm and 208.11 ± 57.92 nm were obtained for CS_PVA and CS_AG_PVA, respectively. These diameters are within the size range displayed by collagen fibers in natural skin (50–400 nm), potentially promoting cell adhesion, migration, and proliferation [25,26].

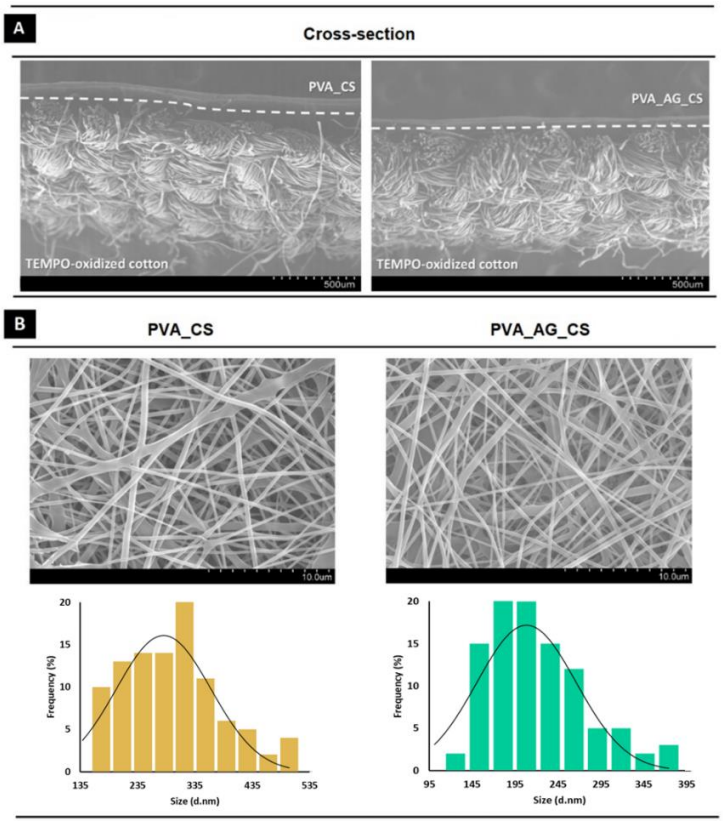

Figure 2 – Morphological characterization of the produced 2,2,6,6-tetramethylpiperidine-1-oxyl radical (TEMPO)-oxidized cotton/Poly(vinyl alcohol) (PVA)_Chitosan (CS) materials with and without crude *Agrimonia eupatoria* L. (AG) extract. SEM images of the cross-sections (**A**); surface morphologies and diameter distribution of the coating layers of PVA_CS and PVA_AG_CS nanofibers (**B**).

2.2.2. Fourier Transform Infrared Spectroscopy (ATR-FTIR)

The ATR-FTIR spectra were acquired to characterize the chemical composition of the produced nanocomposite wound dressing materials, Figure 3. The spectrum of the TEMPO-oxidized cotton reflected the characteristic peaks of unmodified cotton at around 3330 cm^{-1} (O–H stretching vibration), 2880 cm^{-1} (C–H stretching vibration), 1330 cm^{-1} (O–H deformation vibration), 1160 and 890 cm^{-1} (β-(1–4) glycoside bridge), and 1030 cm^{-1} (C–O–C stretching vibration). In addition, in the TEMPO-oxidized cotton spectrum, it is possible to detect a band at about 1600 cm^{-1} (asymmetrical COO– stretching vibration) Figure 3A. This result is associated with the TEMPO-mediated oxidation conditions, which impart a negative surface charge to the cellulose cotton [27]. In comparison, the spectrum of the coated layer displays the characteristic bands of CS around 1560 cm^{-1} (N–H bending vibrations) and 1650 cm^{-1} (C=O stretching vibrations), as well as the typical broad peak of PVA_CS in the region between 3000 and 3500 cm^{-1} (–OH and –NH stretching) Figure 3B. The presence of these bands is evidence of the effective blending of the PVA_CS. Furthermore, an increase in the intensity of the PVA_AG_CS's characteristic peaks demonstrated the successful blending of the crude AG extract into the PVA_CS nanofibers. A similar effect was described by Hadisi et al., whereby the characteristic peaks of henna overlapped with the peaks of gelatin-oxidized starch nanofibers [28].

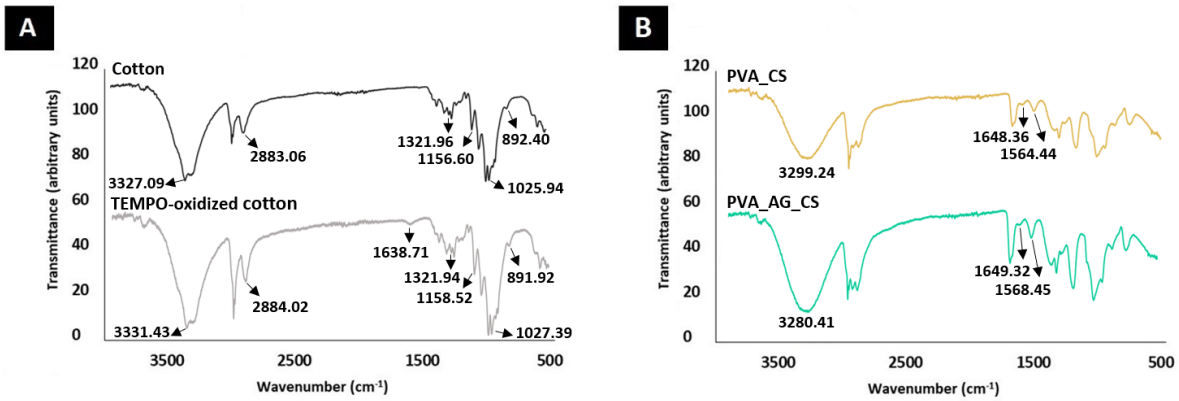

Figure 3 – Attenuated total reflection-Fourier transform infrared (ATR-FTIR) analysis of the produced dual-layer dressing materials. Cotton layer (**A**), and the nanofibrous coating layers (**B**).

2.3. Mechanical Strength Behavior

In order to confirm whether the produced dual-layer dressing materials are suitable for support of mechanisms involved in the healing process, the mechanical behavior of the TEMPO-oxidized cotton/PVA_CS with and without crude AG extract was determined in dry conditions from tensile strength, Young's modulus, and elongation at break, Table 1. The mechanical properties of the TEMPO-oxidized cotton, PVA_CS, and PVA_AG_CS nanofibers were also evaluated for further comparison purposes.

Table 1 – Characterization of the mechanical properties of the produced dual-layer dressing material and associated raw materials.

	Tensile Strength (MPa)	Young's Modulus (GPa)	Elongation at Break (%)	Thickness (mm)
TEMPO-oxidized cotton	36.98 ± 4.13	1.82 ± 0.25	2.04 ± 0.12	0.250 ± 0.011
PVA_CS	9.83 ± 16.38	0.41 ± 0.25	4.64 ± 1.40	0.051 ± 0.004
PVA_AG_CS	9.66 ± 1.95	0.35 ± 0.09	3.03 ± 0.60	0.012 ± 0.001
TEMPO-oxidized cotton/PVA_CS	22.48 ± 4.46	0.40 ± 0.14	5.80 ± 0.89	0.315 ± 0.011
TEMPO-oxidized cotton/PVA_AG_CS	26.55 ± 1.41	0.46 ± 0.11	5.95 ± 1.71	0.270 ± 0.004

The TEMPO-oxidized cotton/PVA_CS displayed a tensile strength value of 22.48 ± 4.46 MPa, whereas the TEMPO-oxidized cotton/PVA_AG_CS exhibited a value of 26.55 ± 1.41 MPa. These results, and in comparison with the tensile strength obtained for the individual layers, confirmed that an appropriate balance is required between the higher mechanical strength of the TEMPO-oxidized cotton and the weaker mechanical behavior exhibited by the PVA_CS and PVA_AG_CS nanofibrous coating layers. That requirement mirrors the tensile strengths' range of 5.00 to 30.00 MPa associated with native skin [2]. TEMPO-oxidized cotton/PVA_CS with and without crude AG extract demonstrated a similar Young's modulus of elasticity of 0.46 ± 0.11 GPa and 0.40 ± 0.14 GPa, respectively. The elongation at break assays determined that TEMPO-oxidized cotton/PVA_CS and TEMPO-oxidized cotton/PVA_AG_CS materials bore a similar strain of 5.80 ± 0.89% and 5.95 ± 1.71%, respectively. While these values are outside the range available for native skin (Young's modulus ranging between 0.4 and 20 MPa and elongations ranging from 10% to 115%) [2], other potential wound dressing materials (previously described) have similarly high Young's modulus (*e.g.*, ranging between 278.6 ± 12.5 MPa and 456.2 ± 22.5 MPa) [29].

2.4. Wetting Studies

Water droplet contact angle (WCA) between 40° and 70° has been considered as a favorable surface in contrast to very hydrophilic (WCA < 20°) and hydrophobic (WCA > 90°) surfaces [30,31]. This relates to cell adhesion, migration, and proliferation, and absorption of excess wound exudate. In this study, the TEMPO-oxidized cotton displayed a WCA value of 27.53 ± 6.84°, confirming its highly hydrophilic nature [27]. This result is indicative of the ability of the hydroxyl groups present on the cotton fabric to absorb fluids. However, it is important to remember that although the cotton bandage gauzes could be used for absorbing exudates, their efficiency can be lost when these dressings become saturated, resulting in tissue maceration and potential contribution to increase in the occurrence of infections [10]. Notably, the coating layer of PVA_CS exhibited a WCA value of 54.03 ± 11.98°, and

the PVA_AG_CS layer had a WCA score of 42.37 ± 7.52°. These results demonstrated that the presence of polar phytochemicals in the crude AG extract improves the wettability of the PVA_CS, creating an effective moist environment, which is essential to the healing process [32].

2.5. Porosity Assessment

Ideally, the dual dressing materials' porosity should allow proper gas exchange, efficient water and nutrients supply, and effective fluid absorption while maintaining the moisture balance at the wound site [10]. High porosity is also expected to support cell accommodation and migration. In that context, porosity values within the range of 60–90% have been found essential for effective healing processes [10]. In our study, the TEMPO-oxidized cotton exhibited the lowest porosity value (76.09 ± 5.64%), whereas the blend of PVA_CS and PVA_AG_CS scored highest porosity values (84.09 ± 6.71% and 92.77 ± 6.01%, respectively). These findings indicate that nanofibers with lower diameters, like PVA_AG_CS (208.11 ± 57.92 nm), lead to a higher number of void spaces available between nanofibers and result in higher porosity values. This physical feature also provides a larger specific surface area suitable for cell adhesion and growth during the healing process.

2.6. Water Vapor Transmission Rates (WVTRs)

An ideal wound dressing should keep the wound moist and also absorb excess fluids, while allowing air and vapor permeation. Specifically, water vapor transmission rates (WVTRs) ranging between 2000 and 2500 g/m^2/day facilitate water vapor exchanges and prevent exudate accumulation, which can contribute to the breakdown of the skin extracellular matrix (ECM) components or provoke skin maceration of the healthy tissue surrounding the wound [10]. In this study, the TEMPO-oxidized cotton coated with a blend of PVA_CS without and with crude AG extract had similar WVTR values of 1246.75 ± 148.63 g/m^2/day and 1304.09 ± 123.13 g/m^2/day, respectively. These results suggest that the obtained WVTRs are outside of the ideal range for a proper wound dressing material. However, it is interesting that our test coatings performed better than several commercially available wound dressings (Comfeel (Coloplast A/s) (308 g/m^2/day), Dermiflex (Johnson & Johnson, New Brunswick, Nova Jersey, EUA) (90 g/m^2/day), and Duroderm (ConvaTec Ltd., Deeside, Flintshire, UK) (886 ± 32 g/m^2/day)) [33].

2.7. Swelling and *In Vitro* Degradation Studies

The water uptake and weight loss tests of the our dual-layer dressing materials were performed over 10 days in PBS buffer at pH = 5.5 and pH = 8.0 to mimic the acidic wound environment favorable for wound healing, and the attributes of wound fluid, respectively, Figure 4A,B. The TEMPO-oxidized cotton/PVA_CS displayed a lower degree of swelling at pH = 5.5 and pH = 8.0 of ~310% and ~250%, respectively. The TEMPO-oxidized cotton/PVA_CS containing the crude AG extract presented a

water absorption ratio at pH = 5.5 and pH = 8.0 of ~400% and ~320%, respectively, Figure 4A. These behaviors can be explained by the higher hydrophilic character of the electrospun PVA_AG_CS nanofibers. In addition, the highest swelling capacity was observed at pH = 5.5, due to the protonation of the amino NH_2 and acetamido $CH_3C(O)NH$ groups of CS, which can form ammonium cations and increase the degree of swelling [34]. Hence, it was evident that TEMPO-oxidized cotton/PVA_AG_CS at both pHs provided a more appropriate environment for exudates absorption. The TEMPO-oxidized cotton/PVA_CS displayed weight losses of 16.63 ± 4.49% and 13.05 ± 3.07% at pH = 5.5 and pH = 8.0, while TEMPO-oxidized cotton/PVA_AG_CS underwent weight loss of 22.12 ± 5.96% and 16.25 ± 3.07% at pH = 5.5 and pH = 8.0, respectively, Figure 4B. This is mainly due to the addition of the biodegradable and natural components, such as PVA, CS, and crude AG plant extract to the non-degradable TEMPO-oxidized cotton. It is reasonable to conclude that the components present in the coating layer are the most important regulators of the degradation profile, which itself must be similar to the skin regeneration rate [35]. Nevertheless, the produced dual-layer dressing materials showed no significant differences in the hydrolytic degradation.

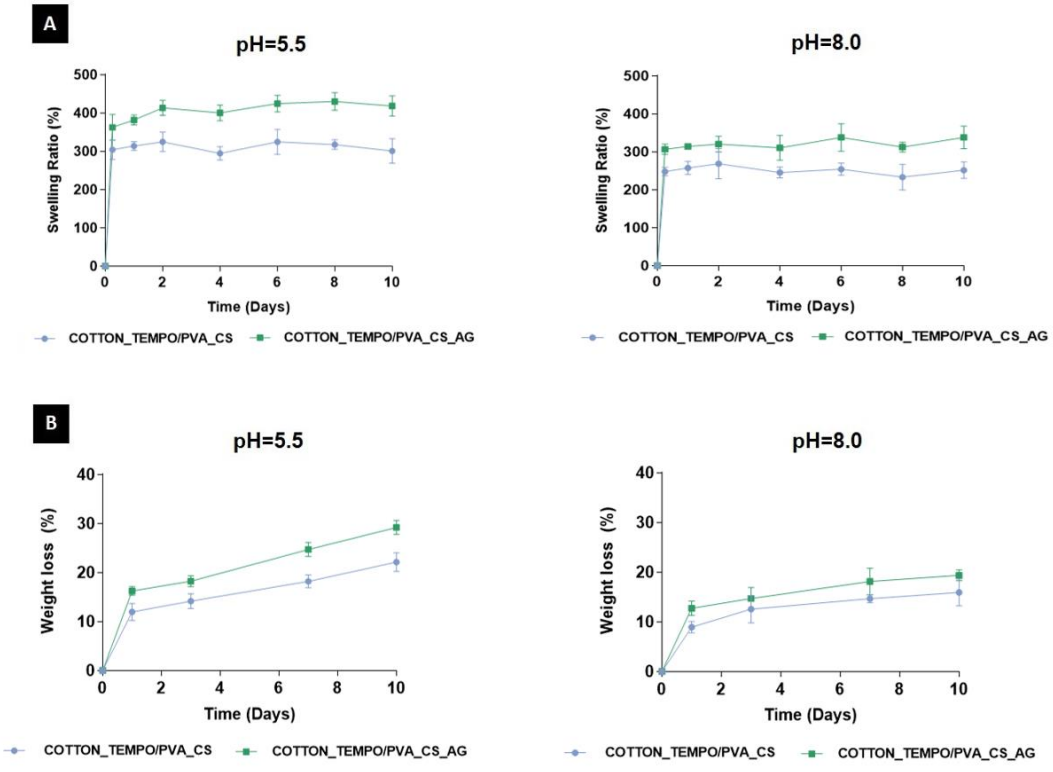

Figure 4 – Characterization of the TEMPO-oxidized cotton/PVA_CS materials with and without crude AG extract incorporated. Swelling profile (**A**); weight loss (**B**) at pH = 5.5 and pH = 8.0.

3. Study of the *In Vitro* AG Release

The release behavior of the nanofibers was investigated by immersing the produced material in PBS at pH = 5.5 (pH found on normal skin and beneficial for wound healing) and pH = 8.0 (pH of wound exudate), for 10 days, Figure 5. The result was an initial burst release observed within the first 6 h, followed by a sustained diffusion or slow release. Correspondingly, a cumulative release of the AG extract from the lower layer was 72.18 ± 3.71% and 62.68 ± 3.87% at pH = 5.5 and pH = 8.0, respectively. This behavior can be explained by the higher swelling capacity of the TEMPO-oxidized cotton/PVA_AG_CS dressing material at pH = 5.5, as well as weight loss. Hence, it appeared that the AG release rate from PVA_CS is mainly controlled by the degree of swelling and weight loss rate, being the cumulative release of the crude AG extract crucial if occurrence of infections at the wound site is to be avoided.

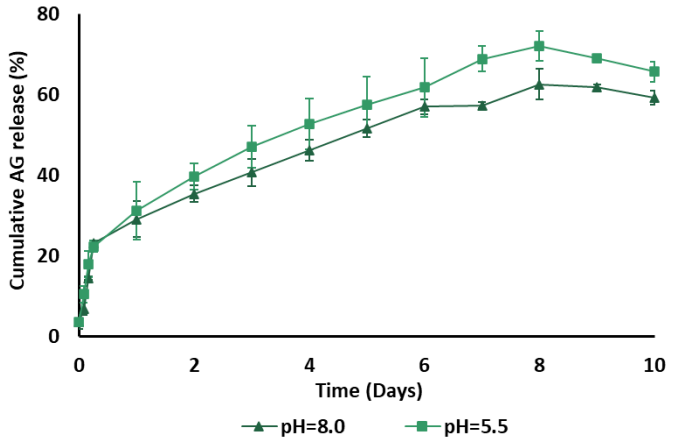

Figure 5 – Evaluation of the *in vitro* release profile of the crude AG extract incorporated into the TEMPO-oxidized cotton/PVA_CS material.

4. Antibacterial Properties of the Dual-Layer Dressing Materials

In this study, the antimicrobial properties were characterized against *S. aureus* (Gram-positive) and *P. aeruginosa* (Gram-negative), the bacteria most commonly isolated from wound infections [7,36]. The observed results (Figure 6) show an inhibitory effect after 24 h of contact of 25.32 ± 5.62% and 27.84 ± 5.77% for the TEMPO-oxidized cotton sample against *S. aureus* and *P. aeruginosa*, respectively. This suggests that the cellulose cotton may help to prevent bacterial penetration into the wound, while offering mechanical support to the wound site. In contrast, the coating layer of PVA_AG_CS exhibited a higher inhibitory effect, 99.17 ± 4.05% and 98.13 ± 0.88% for *S. aureus* and *P. aeruginosa*, while the coating layer of PVA_CS inhibited *S. aureus* and *P. aeruginosa* growth to lesser degrees (64.39 ± 10.07% and 61.25 ± 4.22%, respectively) (Figure 6). These values reflect the

intrinsic bactericidal activity of CS and crude AG extract and previous studies demonstrating that inhibitory or anti-adhesion attributes of secondary metabolites, such as flavonoids, phenolic acids, and triterpenoids of AG [21,23]. In addition, the cationic properties of CS allow it to interact with the negatively charged bacterial material surface, resulting in increased cell wall permeability, and consequent disruption and loss of intracellular components [37,38].

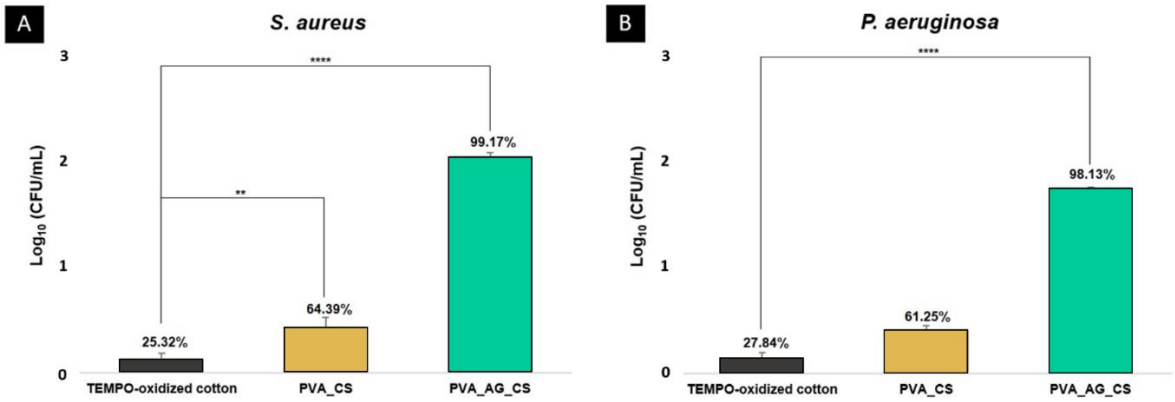

Figure 6 – Evaluation of the antibacterial properties of the TEMPO-oxidized cotton, PVA_CS, and PVA_AG_CS nanofibers against *S. aureus* (**A**); *P. aeruginosa* (**B**). Data are represented as average ± standard deviation (SD), ** $p < 0.01$ and **** $p < 0.0001$).

5. *In Vitro* Cytotoxicity Assay (MTT)

An ideal wound dressing should be biocompatible and play a major role in cellular interactions, supporting the healing process. To explore this aspect of our coatings, the normal human dermal fibroblast (NHDF) cells were chosen as implicated in producing new ECM components, and collagen fibers, which are integral events in cell migration and proliferation responsible for reestablishment of damaged tissue [7,10,36]. As shown in Figure 7, the chosen direct MTT (3-(4,5-Dimethyl-2-thiazolyl)-2,5-diphenyl-2H-tetrazolium bromide) cytocompatibility assay provided no evidence of cytotoxicity against NHDF cells. Notably, the produced dual-layer dressing materials displayed more than 80% cell viability, even after 7 days. Additionally, the TEMPO-oxidized cotton coated with PVA_AG_CS exhibited an ascending effect of proliferation from 1 to 7 days. This trend could be attributed to the higher porosity and hydrophilic character exhibited by the PVA_AG_CS nanofibers, which are considered to be proper for encouraging the cell attachment and proliferation at the nanofibrous membrane's surface.

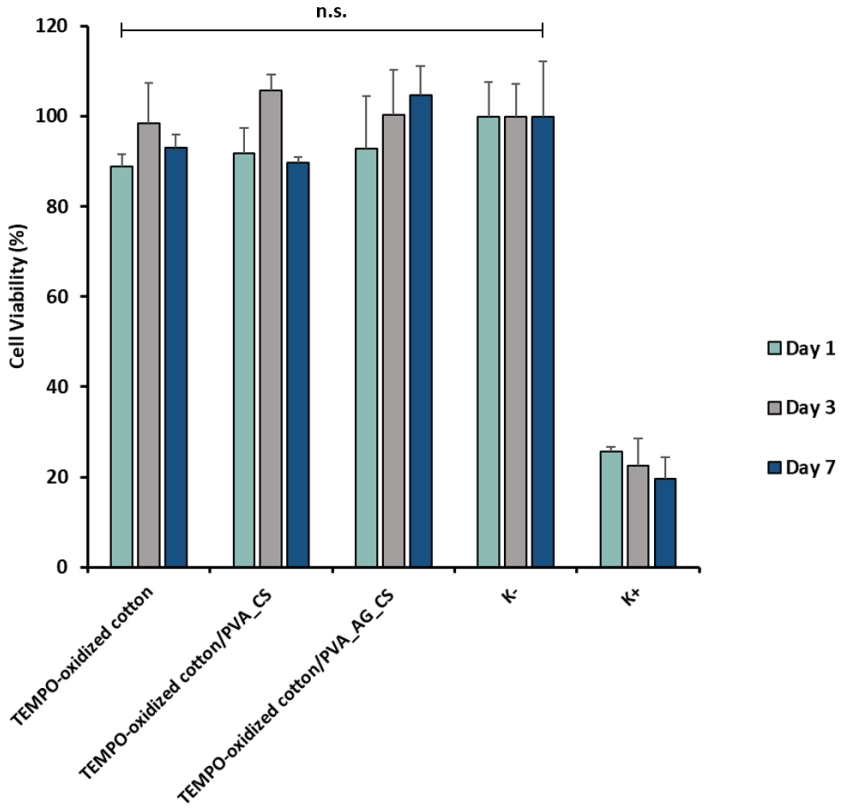

Figure 7 – Evaluation of the normal human dermal fibroblast (NHDF) cell viability after 1, 3, and 7 days in contact with the TEMPO-oxidized cotton and the produced dual-layer dressing materials.

Moreover, the toxicity levels of the produced dual-layer dressing materials were determined from the standard percentage cell viability ranges (as seen in Table 2). The obtained results showed that the tested materials displayed toxicity levels between 0 and 1, which are considered as nontoxic to the human body [39].

Table 2 – Classification of the toxicity level of the produced dual-layer dressing materials depending on the percentage of cell viability (%).

Standard Viability Data[a]		**Experimental Data**			
Cell Viability (%)	**Toxicity Level**	**Samples**		**Cell Viability (%)**	**Toxicity Level**
≥ 100	0	**TEMPO-oxidized cotton**	Day 1	88.99	1
75-99	1		Day 3	98.50	1
50-74	2		Day 7	92.98	1
25-49	3	**TEMPO-oxidized cotton/PVA_CS**	Day 1	91.83	1
1-24	4		Day 3	105.79	0
0	5		Day 7	89.69	1
		TEMPO-oxidized cotton/PVA_AG_CS	Day 1	92.78	1
			Day 3	100.45	0
			Day 7	104.64	0

[a] The standard viability data were obtained from reference [39].

6. Materials and Methods

6.1. Materials

Agrimonia eupatoria L. (AG) plant was obtained (CHÁ HUNOS, Lda., Vila Nova de Gaia, Portugal), stored and used according to the supplier's recommendations. Normal human dermal fibroblast (NHDF) cells were acquired from ATCC—American Type Culture Collection. Cotton fabric was obtained from James H. Heal & Co. Ltd. (Halifax, UK). Resazurin (7-hydroxy-3H-phenoxazin-3-one 10-oxide) dye, 2,2,6,6-tetramethylpiperidine-1-oxyl radical (TEMPO), sodium bromide (NaBr), sodium hypochlorite (NaOCl), chitosan (CS) (low molecular weight), sodium hydroxide (NaOH), hydrochloric acid (HCl), sodium chloride (NaCl), Mueller-Hinton broth (MHB), tween 80, dimethyl sulfoxide (DMSO) anhydrous ≥ 99.9%, trypsin, and 3-(4,5-Dimethyl-2-thiazolyl)-2,5-diphenyl-2H-tetrazolium bromide (MTT) were purchased from Sigma-Aldrich (Sintra, Portugal). Glacial acetic acid (CH_3COOH) and ethanol absolute were acquired from Fisher Scientific (Porto Salvo, Portugal). Poly(vinyl alcohol) (PVA) (MW 115,000 g/mol) was purchased from VWR International (Carnaxide, Portugal). Nutrient agar (NA), nutrient broth (NB), and agar for microbiology were bought from Fluka (Sintra, Portugal). Brain Heart Infusion (BHI) broth was obtained from Panreac (Barcelona, Spain). Phosphate-buffered saline (PBS) was purchased from Alfa Aesar (Ward Hill, USA). All solvents were of analytical grade and used as received without further purification.

6.2. Methods

6.2.1. Preparation of Crude AG Extract

The dried aerial parts of the medicinal AG plant (CHÁ HUNOS, Lda., Vila Nova de Gaia, Portugal) were powdered and subjected to cold maceration with ethanol/water in a ratio of 80:20 for 24 hours. The extracted solution was filtered through a membrane filter (Whatman No. 1, 11 µm pore size), and the filtrate solvent evaporated using a Rotavapor apparatus (Buchi Rotavapor RE 111). The obtained crude AG extract was used throughout the sudy.

6.2.2. Minimum Inhibitory Concentration (MIC)

Minimum inhibitory concentration (MIC) of the crude AG extract was evaluated against *S. aureus* (ATTC 6538) and *P. aeruginosa* (PA25) using the broth microdilution method according to the CLSI NCLS M7-A6 guidelines. Briefly, stock solutions of the AG were prepared (30 to 0.08 mg/mL) in sterile MHB. Then, 50 µL of each AG dilution was aliquoted in 96 multi-well polystyrene plates (Sigma-Aldrich) followed by 50 µL bacterial inoculum containing ~10^7 colony-forming unit (CFU)/mL. The plates were incubated at 37 °C for 18–24 hours. After incubation, 30 µL of 0.02% resazurin solution was added to each microplate well to aid visualization of bacterial growth. The

plates were further incubated for 2–4 hours for the observation of color change. The lowest concentration at which the blue-purple resazurin color (no bacteria growth) changed to pink (bacteria growth) was taken as the MIC value. The MIC values was defined as the lowest concentration of the AG extract resulting in complete inhibition of visible growth. AG-free wells only with MHB medium and inoculum were used as a positive control (K^+), whereas wells containing only MHB medium were used as a negative control (K^-).

6.2.3. Fabrication of the Dual-Layer Dressing Materials

First layer: Firstly, cotton fabric was pre-activated with TEMPO to provide a negative net electrostatic charge. To accomplish this, a solution of 0.0125% (w/v) TEMPO, 0.125% (w/v) NaBr, and 3.2% (v/v) NaClO was prepared, and its pH value was adjusted to 10.5 with 1 N NaOH. Then, 2 g of cellulose cotton was immersed in 50 mL of the TEMPO solution and stirred for 60 minutes. The pH of the solution was reduced to 7 using 0.1 M HCl, and the cotton fabric washed in deionized water. After the activation process, the second layer was electrospun directly over the first layer to produce the dual-layer materials.

Second layer: A blend comprising 10% (w/v) PVA (well-known fiber-forming polymer) and 2% (w/v) CS (natural cationic polysaccharide) was prepared in water and 0.1 M CH_3COOH, respectively. The pH of the CS solution was adjusted to 5 using 0.1 M HCl, resulting in a positive electrostatic charge, and added to the PVA solution in a ratio of 30:70. This blend with and without 5.0 wt.% crude AG extract was electrospun on top of the TEMPO-oxidized cotton using Nanospider™ electrospinning (Nanospider laboratory machine NS LAB 500S from Elmarco S.R.O., Liberec, Czech Republic) at an electrode rotation of 55 Hz, using a working distance of 13 cm, and an applied voltage of 75 kV, during ~1 hour. The raw PVA_CS and PVA_AG_CS were collected on polypropylene nonwoven fabric over the same conditions.

6.2.4. Characterization of the Dual-Layer Dressing Materials

Assessment of the Morphologic Features

The morphology of the dual-layer dressing materials was determined by scanning electron microscopy (SEM, S-3400N, Hitachi, Tokyo, Japan) at an accelerating voltage of 20 kV. Before imaging, a small section of the nanofibers coating layer was placed on SEM specimen stubs, and then sputter coating with a thin layer of gold using the Quorum Q150R ES sputter coater (Quorum Technologies Ltd., Laughton, East Sussex, UK) to make them electrically conductive. The average fiber diameter and the fiber size distributions of each sample were analyzed by measuring the diameter of 100 random fibers from the captured SEM micrographs using an image analysis software (Image J, National Institutes of Health, Bethesda, MD, USA).

Fourier Transform Infrared Spectroscopy (ATR-FTIR)

ATR-FTIR spectra were performed in an ATR-FTIR spectrophotometer (Thermo Nicolet is10 FT-IR Spectrophotometer, Waltham, MA, USA) to demonstrate the integration among the components used in the production of the dual-layer materials. Briefly, the samples were mounted directly on the sensor, and the spectra recorded over the range of 400–4000 cm^{-1} at a resolution of 4 cm^{-1}.

Mechanical Strength Behavior

The tensile test was performed using a uniaxial tensile machine (DY-35 Adamel Lhomargy, Roissy en Brie, France), according to ASTM standard D3039/D3039M. Briefly, the dried rectangular specimens (40 mm × 10 mm (length × width)) were placed between two clamps separated by a distance of 1 cm, and a 100 N load cell was applied to the samples at a stretching rate of 2 mm/min until the break. On each sample, measurements were made five times at room temperature. The Young's modulus (MPa) was determined by the slope of the initial linear portion of the stress–strain curve, and the tensile strength (MPa) and elongation at break (%) calculated according to the following equations (Equations (1) and (2)):

Tensile strength (MPa) = (Breaking force or the maximum load (N)/Cross-sectional area of the sample (mm^2)) (1)

Elongation at break (%) = (The extension at the breaking point (mm)/Initial length of the sample (mm)) × 100 (2)

All values were compared subsequently with the reported values of native human skin.

Wetting Studies

The surface wettability of the dual-layer materials was evaluated by the sessile drop method using a Dataphysics Contact Angle System OCAH-200. Briefly, distilled water droplets of a volume of 4 µL were dropped carefully onto the surface of each sample at different locations. The droplet landing was recorded by a high-resolution video camera attached to the analyzer within 20 seconds, and the contact angle measured by analyzing the shape of the drop. The average of the values was reported as mean ± SD.

Porosity Assessment

The porosity of each layer of the produced dual-layer materials was measured using the liquid displacement method, as reported by Yeh et al. [40]. Briefly, the dry weight of the samples was recorded, as (W_s). Then, the samples were immersed in a graduated cylinder with known volume (W_1) of absolute EtOH for 40 minutes at 30 °C, and the amount of the ethanol after impregnation was

refilled and weighted as W_2. After removing the nanofibrous mats from the displacement liquid, the volume of the ethanol remaining in the graduated cylinder was recorded as W_3. The dressing's porosity was calculated as (Equation (3)):

$$\text{Porosity } (\%) = \frac{(W_2 - W_3 - W_s)}{(W_1 - W_3)} \times 100 \quad (3)$$

Water Vapor Transmission Rates (WVTR)

Water vapor transmission rates (WVTRs) were determined according to ASTM E96 (American Society for Testing Materials)—standard test method for water vapor transmission of the materials. Briefly, circular samples were affixed to individual test tubes (diameter of opening = 1.2 cm) filled with 10 mL of distilled water and tightly sealed using parafilm tape along their periphery to prevent water loss. After that, the whole apparatus was weighed (W_i) and incubated at 37 °C. After 24 hours, the sample-glass tubes assembly was removed and weighed (W_f), and WVTR calculated as outlined below (Equation (4)):

$$\text{Water vapor transmission rate (WVTR) } (g/m^2/day) = \frac{W_i - W_f}{A} \quad (4)$$

where A is the exposure area (m^2), and W_i and W_f are the initial and final weights of the test tubes, respectively.

Swelling and *In Vitro* Degradation Studies

The dried dual-layer materials were cut into 1 × 1 cm^2 pieces, and pre-weighed (W_o). These samples were soaked in 10 mL of PBS (pH = 5.5 and pH = 8.0) solutions at 37 °C and removed from the media at predetermined time points. Excess water on the surface was wiped with filter paper, and the swollen samples weighed (W_t) immediately. The degree of water uptake was calculated as follows (Equation (5)).

$$\text{Water Uptake } (\%) = \frac{W_t - W_0}{W_0} \times 100 \quad (5)$$

Hydrolytic degradation was also monitored based on the weight change of the samples by immersing in PBS (pH = 5.5 and pH = 8.0) solutions at 37 °C. The percentage weight loss was determined based on the weight of the dried pre-weighed samples (W_o) and the weight of dried samples after removing from the PBS solutions (W_d), as follows (Equation (6)).

$$\text{Weight loss } (\%) = \frac{W_0 - W_d}{W_0} \times 100 \quad (6)$$

6.2.5. Study of the *In Vitro* AG Release

The AG release from the dual-layer materials was determined using 10 mL of PBS release medium at pH = 5.5 or pH = 8.0, with a shaking rate of 100 rpm in a thermostatic shaking incubator. At specific time points, samples were removed from the release medium, and an equal amount of fresh PBS medium was added. The concentration of AG was determined using a UV-visible spectrophotometer at a 400 nm wavelength, and the cumulative release of the AG calculated from a standard curve plotted with a known amount of AG as standard [22,41].

6.2.6. Antibacterial Properties of the Dual-Layer Dressing Materials

The antibacterial activity of the produced dual-layer materials was tested according to the Standard Test Method for Determining the Activity of Incorporated Antimicrobial Agent(s) in Polymeric or Hydrophobic Materials (ASTM E2180-07 standard). Strains of *S. aureus* and *P. aeruginosa* were used. Briefly, agar slurry solutions (0.30% agar and 0.85% NaCl) were prepared and inoculated with overnight bacterial suspensions of ~10^8 CFU/mL. Then, a thin semisolid layer of inoculated agar slurries was spread onto the surface of each sample, including a filter paper control (pore size of 0.22 µm), and allowed to gel. The test samples were incubated at 37 °C for 18–24 hours for two different contact times (t = 0 hours and t = 24 hours). After each contact time, a sterilized saline solution (NaCl) was added to the falcon tubes containing the inoculated samples, and these were shaken vigorously to enable the release of the agar slurry. Next, serial dilutions were performed with NaCl solution, pipetted out, and spread onto agar plates. The plates were incubated at 37 °C for 18–24 hours, and the log (CFU/mL) calculated for each sample.

6.2.7. *In Vitro* Cytotoxicity Assay (MTT)

The cell viability and proliferation of the dual-layer materials were analyzed using a MTT assay as recommended by the ISO 10993-5:2009 guidelines (Biological evaluation of medical devices—Part 5: Tests for *in vitro* cytotoxicity). This involves direct cell contact with the material. Briefly, the NHDF cells were cultured in complete medium supplemented with fetal bovine serum (FBS) and incubated in a humidified incubator at 37 °C with 5% CO_2. After cell seeding, the samples were cut into round disks to cover less than 10% of the well area, and then placed into a 24-well culture plate and sterilized by UV irradiation (254 nm, ≈ 7 mW cm^{-2}) for 1 h. The NHDF cells were seeded onto the samples at a density of 1 × 10^4 cells/well for 1, 3, and 7 days, and the medium changed every two days. At those specific time points, the medium was taken out, and the MTT reagent solution added to each well. The plate was covered with aluminized paper. After 4 hours under the same conditions, the MTT solution was removed and the produced formazan dissolved in DMSO. The absorbance of each plate was determined by a spectrophotometric plate reader (BioRad xMark microplate spectrophotometer)

with a test wavelength of 570 nm. Cells incubated without samples were used as a negative control (K^-), and cells incubated with EtOH (96%) selected as a positive control (K^+).

6.2.8. Statistical Analysis

Statistical data analysis utilized one-way analysis of variance (ANOVA) followed by Tukey's multiple comparison test using GraphPad Prism 6 software (GraphPad Software, La Jolla, CA, USA). Using a confidence level of ≥ 95%, values of $p < 0.05$ were considered statistically significant.

7. Conclusions

Chronic wounds and difficult-to-heal wounds continue to attract considerable interest due to associated high prevalence of bacterial infections. Based on aspirations to mitigate those risks, previous research has demonstrated the potential of wound dressing materials with antimicrobial activity. This study focused on contributing new insight regarding amalgamation of well-understood wound dressing physical properties with novel use of electrospun membrane containing an antimicrobial plant extract. The findings presented demonstrate potential to enhance skin regeneration while suppressing bacterial growth, complementing published data regarding analogous use of antibiotics, nanoparticles, and other natural compounds applied to electrospun nanofibers. In summary, our novel dual-layer TEMPO-oxidized cotton/PVA_AG_CS dressing material exhibited attributes supporting its use for mechanical protection of wounds and physical barrier protection against infectious agents (i.e., albeit so far limited to *S. aureus* and *P. aeruginosa*). In addition, the coating layer of PVA_CS containing crude AG extract presented suitable morphology and achieved diameters within the size range of the collagen fibers in the natural skin (50–400 nm). Moreover, the TEMPO-oxidized cotton/PVA_AG_CS exhibited an adequate wettability, porosity, and swelling ration for a wound dressing. These characteristics are likely to enhance the therapeutic effectiveness of the produced material. Additionally, an initial burst release of AG in the first 6 hours, followed by a sustained release profile, was also observed. Such data emphasize the suitability of the dual-layer TEMPO-oxidized cotton/PVA_AG_CS dressing material to maintain an aseptic environment at the wound site, which is crucial to avoid the wound bacterial colonization and infection.

Author Contributions: Investigation, C.M.; supervision, I.C.G.; validation, C.P.D. and I.C.G.; writing original draft, C.M., revised by C.P.D. and I.C.G.; writing, review and editing, C.P.D. and I.C.G. All authors have read and agreed to the published version of the manuscript.

Funding: The authors are grateful for the support provided by FibEnTech Research Unit (Project UIDB/00195/2020). C.M. acknowledges PhD fellowship from Foundation for Science and Technology (FCT) (PD/BD/113550/2015). C.P.G. and I.C.G. benefited from support provided by EU COST action CA15114 AMiCI "Anti-microbial coating innovations to prevent infectious diseases".

Data Availability Statement: The data presented in this study are available in this article.

Acknowledgments: The authors acknowledge the help and expertise of Ana Raquel Nunes regarding cytotoxic assays. Conflicts of Interest: The authors declare no conflict of interest, financial or otherwise.

References

1. Chitrattha, S.; Phaechamud, T. Porous poly(dl-lactic acid) matrix film with antimicrobial activities for wound dressing application. *Mater. Sci. Eng. C* **2016**, *58*, 1122–1130.
2. dos Santos, D.M.; Leite, I.S.; Bukzem, A.; de Oliveira Santos, R.P.; Frollini, E.; Inada, N.M.; Campana-Filho, S.P. Nanostructured electrospun nonwovens of poly(ε-caprolactone)/quaternized chitosan for potential biomedical applications. *Carbohydr. Polym.* **2018**, *186*, 110–121.
3. Ambekar, R.S.; Kandasubramanian, B. Advancements in nanofibers for wound dressing: A review. *Eur. Polym. J.* **2019**, *117*, 304–336.
4. Williamson, D.; Harding, K. Wound healing. *Medicine* **2004**, *32*, 4–7.
5. Bowler, P.G. Wound pathophysiology, infection and therapeutic options. *Ann. Med.* **2002**, *34*, 419–427.
6. Simões, D.; Miguel, S.P.; Ribeiro, M.P.; Coutinho, P.; Mendonça, A.G.; Correia, I.J. Recent advances on antimicrobial wound dressing: A review. *Eur. J. Pharm. Biopharm.* **2018**, *127*, 130–141.
7. Mihai, M.M.; Dima, M.B.; Dima, B.; Holban, A.M. Nanomaterials for wound healing and infection control. *Materials* **2019**, *12*, 2176.
8. Pinho, E.; Soares, G. Functionalization of cotton cellulose for improved wound healing. *J. Mater. Chem. B* **2018**, *6*, 1887–1898.
9. Goh, Y.F.; Shakir, I.; Hussain, R. Electrospun fibers for tissue engineering, drug delivery, and wound dressing. *J. Mater. Sci.* **2013**, *48*, 3027–3054.
10. Pilehvar-Soltanahmadi, Y.; Dadashpour, M.; Mohajeri, A.; Fattahi, A.; Sheervalilou, R.; Zarghami, N. An overview on application of natural substances incorporated with electrospun nanofibrous scaffolds to development of innovative wound dressings. *Mini-Reviews Med. Chem.* **2017**, *18*, 414–427.
11. Punjataewakupt, A.; Napavichayanun, S.; Aramwit, P. The downside of antimicrobial agents for wound healing. *Eur. J. Clin. Microbiol. Infect. Dis.* **2019**, *38*, 39–54.
12. Liu, M.; Duan, X.P.; Li, Y.M.; Yang, D.P.; Long, Y.Z. Electrospun nanofibers for wound healing. *Mater. Sci. Eng. C* **2017**, *76*, 1413–1423.

13. Siddiqui, A.R.; Bernstein, J.M. Chronic wound infection: Facts and controversies. *Clin. Dermatol.* **2010**, *28*, 519–526.

14. Saghazadeh, S.; Rinoldi, C.; Schot, M.; Kashaf, S.S.; Sharifi, F.; Jalilian, E.; Nuutila, K.; Giatsidis, G.; Mostafalu, P.; Derakhshandeh, H.; Yue, K.; Swieszkowski, W.; Memic, A.; Tamayol, A.; Khademhosseini, A. Drug delivery systems and materials for wound healing applications. *Adv. Drug Deliv. Rev.* **2018**, *127*, 138–166.

15. Gizaw, M.; Thompson, J.; Faglie, A.; Lee, S.Y.; Neuenschwander, P.; Chou, S.F. Electrospun fibers as a dressing material for drug and biological agent delivery in wound healing applications. *Bioengineering* **2018**, *5*, 9.

16. Zhang, W.; Ronca, S.; Mele, E. Electrospun nanofibres containing antimicrobial plant extracts. *Nanomaterials* **2017**, *7*, 42.

17. El-Hamid, M.A. A new promising target for plant extracts: Inhibition of bacterial quorum sensing. *J. Mol. Biol. Biotechnol.* **2016**, *1*, 1–3.

18. Anand, U.; Jacobo-Herrera, N.; Altemimi, A.; Lakhssassi, N. A comprehensive review on medicinal plants as antimicrobial therapeutics: Potential avenues of biocompatible drug discovery. *Metabolites* **2019**, *9*, 258.

19. Gupta, P.D.; Birdi, T.J. Development of botanicals to combat antibiotic resistance. *J. Ayurveda Integr. Med.* **2017**, *8*, 266–275.

20. Avci, H.; Gergeroglu, H. Synergistic effects of plant extracts and polymers on structural and antibacterial properties for wound healing. *Polym. Bull.* **2019**, *76*, 3709–3731.

21. Ghaima, K.K. Antibacterial and wound healing activity of some *Agrimonia eupatoria* extracts. *Baghdad Sci. J.* **2013**, *10*, 152–160.

22. Pirvu, L. Studies on Agrimoniae herba selective extracts; polyphenols content, antioxidant and antimicrobial potency, MTS test. *Acad. Rom. Sci. Ann. Biol. Sci.* **2016**, *5*, 96–107.

23. Muruzovic, M.; Mladenovic, K.G.; Stefanovic, O.D.; Vasic, S.M.; Comic, L.R. Extracts of *Agrimonia eupatoria* L. as sources of ˇ biologically active compounds and evaluation of their antioxidant, antimicrobial, and antibiofilm activities. *J. Food Drug Anal.* **2016**, *24*, 539–547.

24. Rahmani Del Bakhshayesh, A.; Annabi, N.; Khalilov, R.; Akbarzadeh, A.; Samiei, M.; Alizadeh, E.; Alizadeh-Ghodsi, M.; Davaran, S.; Montaseri, A. Recent advances on biomedical applications of scaffolds in wound healing and dermal tissue engineering. *Artif. Cells Nanomed. Biotechnol.* **2018**, *46*, 691–705.

25. Papenburg, B.J.; Bolhuis-Versteeg, L.A.M.; Grijpma, D.W.; Feijen, J.; Wessling, M.; Stamatialis, D. A facile method to fabricate poly(L-lactide) nano-fibrous morphologies by phase inversion. *Acta Biomater.* **2010**, *6*, 2477–2483.

26. Abrigo, M.; McArthur, S.L.; Kingshott, P. Electrospun nanofibers as dressings for chronic wound care: Advances, challenges, and future prospects. *Macromol. Biosci.* **2014**, *14*, 772–792.

27. Gomes, A.P.; Mano, J.F.; Queiroz, J.A.; Gouveia, I.C. Layer-by-layer deposition of antibacterial polyelectrolytes on cotton fibres. *J. Polym. Environ.* **2012**, *20*, 1084–1094.

28. Hadisi, Z.; Nourmohammadi, J.; Nassiri, S.M. The antibacterial and anti-inflammatory investigation of Lawsonia Inermis-gelatin starch nano-fibrous dressing in burn wound. *Int. J. Biol. Macromol.* **2018**, *107*, 2008–2019.

29. Tandi, A.; Kaur, T.; Ebinesan, P.R.; Thirugnanam, A.; Mondal, A.K. Drug loaded poly (vinyl alcohol)-cellulose composite hydrogels for wound dressings. In Proceedings of the 8th International Conference on Materials for Advanced Technologies of the Materials Research Society of Singapore & IUMRS & 16th International Conference in Asia (ICMAT2015 & IUMRS-ICA2015), Suntec, Singapore, 28 June–3 July 2015; pp. 2–5.

30. Trinca, R.B.; Westin, C.B.; da Silva, J.A.F.; Moraes, Â.M. Electrospun multilayer chitosan scaffolds as potential wound dressings for skin lesions. *Eur. Polym. J.* **2017**, *88*, 161–170.

31. Wang, J.; Planz, V.; Vukosavljevic, B.; Windbergs, M. Multifunctional electrospun nanofibers for wound application—Novel insights into the control of drug release and antimicrobial activity. *Eur. J. Pharm. Biopharm.* **2018**, *129*, 175–183.

32. Jin, G.; Prabhakaran, M.P.; Kai, D.; Annamalai, S.K.; Arunachalam, K.D.; Ramakrishna, S. Tissue engineered plant extracts as nanofibrous wound dressing. *Biomaterials* **2013**, *34*, 724–734.

33. Lee, J.S.; Kim, J.K.; Park, S.R.; Chang, Y.H. Preparation of collagen/poly(L-lactic acid) composite material for wound dressing. *Macromol. Res.* **2007**, *15*, 205–210.

34. Fazli, Y.; Shariatinia, Z.; Kohsari, I.; Azadmehr, A.; Pourmortazavi, S.M. A novel chitosan-polyethylene oxide nanofibrous mat designed for controlled co-release of hydrocortisone and imipenem/cilastatin drugs. *Int. J. Pharm.* **2016**, *513*, 636–647.

35. Salvatore, L.; Carofiglio, V.E.; Stufano, P.; Bonfrate, V.; Calò, E.; Scarlino, S.; Nitti, P.; Centrone, D.; Cascione, M.; Leporatti, S.; et al. Potential of electrospun poly(3-hydroxybutyrate)/collagen blends for tissue engineering applications. *J. Healthc. Eng.* **2018**, *2018*, 6573947.

36. Sarheed, O.; Ahmed, A.; Shouqair, D.; Boateng, J. Antimicrobial dressings for improving wound healing. In Wound Healing—New insights into Ancient Challenges; InTech: London, UK, 2016; pp. 373–398.

37. Arkoun, M.; Daigle, F.; Heuzey, M.C.; Ajji, A. Antibacterial electrospun chitosan-based nanofibers: A bacterial membrane perforator. *Food Sci. Nutr.* **2017**, *5*, 865–874.

38. Yousefi, I.; Pakravan, M.; Rahimi, H.; Bahador, A.; Farshadzadeh, Z.; Haririan, I. An investigation of electrospun Henna leaves extract-loaded chitosan based nanofibrous mats for skin tissue engineering. *Mater. Sci. Eng. C* **2017**, *75*, 433–444.

39. Wijesinghe, W.P.S.L.; Mantilaka, M.M.M.G.P.G.; Rajapakse, R.M.G.; Pitawala, H.M.T.G.A.; Premachandra, T.N.; Herath, H.M.T.U.; Rajapakse, R.P.V.J.; Wijayantha, K.G.U. Urea-assisted synthesis of hydroxyapatite nanorods from naturally occurring impure apatite rocks for biomedical applications. *RSC Adv.* **2017**, *7*, 24806–24812.

40. Yeh, C.C.; Li, Y.T.; Chiang, P.H.; Huang, C.H.; Wang, Y.; Chang, H.I. Characterizing microporous PCL matrices for application of tissue engineering. *J. Med. Biol. Eng.* **2009**, *29*, 92–97.

41. Kurkina, A.V. A method for the assay of total flavonoids in common agrimony herb. *Pharm. Chem. J.* **2011**, *45*, 43–46.

CHAPTER 4

Concluding Remarks and Future Trends

General discussion and concluding remarks

This doctoral thesis has been intended to understand the growing interest of using natural products in wound management and care, and more specifically, highlight the importance of incorporating these therapeutic and/or bioactive agents in wound dressing materials to both prevent wound bacterial colonization, thus anticipated to promote the reestablishment of the structural and functional integrity of the injured skin. Furthermore, it has been confirmed the potential of the electrospinning technique to produce nanofibrous membranes that are capable of reproducing or mimics the native 3D-structure of the skin's extracellular matrix (ECM) and further enhance the healing process. Regarding that, there is a tremendous progress on the development of wound dressings with effective antimicrobial properties.

To accomplish the proposed goals, different approaches, namely emulsion electrospinning and multi-layered assembly by deposition of two different nanofibrous layers and a nanofiber layer on a cotton material, were used to produce dressing materials from naturally derived and synthetic biopolymers blends, and several crude medicinal plant extracts (*Hypericum perforatum* L. (HP), *Chelidonium majus* L. (CM), *Centella asiatica* L. (CA), and *Agrimonia eupatoria* L. (AG)) as well as their derivatives, like the Eugenol (EUG), were incorporated to enhance the antibacterial efficiency and provide a favorable environment for wound healing. Concerning this, the EUG, a phenol essential oil (EO) extracted from cloves, was the first natural compound with useful therapeutic properties to be successfully applied. It was, for the first time, loaded into electrospun Polycaprolactone (PCL)/ Polyvinyl Alcohol (PVA)/ Chitosan (CS) nanofibrous mats via electrospinning from either water-in-oil (W/O) or oil-in-water (O/W) emulsions. The O/W emulsion, where PCL and EUG were dispersed into PVA/CS blend, showed particular suitability to be used as wound dressing material, due to its more uniform fibers' morphology, higher porosity, and moderate wettability. Besides, it was possible to confirm that the O/W emulsions enable the best release behavior, when oil-soluble bioactive compounds, as the EUG, are incorporated. However, the antibacterial activity of EUG loaded into the O/W emulsion against *Staphylococcus aureus* (*S. aureus*) and *Pseudomonas aeruginosa* (*P. aeruginosa*) was lower than from the W/O emulsion, which could be explained by the faster EUG's diffusion from W/O emulsion blend. Hence, emulsion electrospinning was successfully applied due to its incomparable ability to improve the solubility of the different components of the blend as well as the capability to protect both EUG's stability and bioactivity. Nonetheless, some drawbacks are pointed to the time-consuming methods and special laboratory facilities required to extract the EOs, as well as the large amount of raw plant material needed to obtain them. Besides, these plant-derived substances are easily degraded and considered to be highly susceptible to volatilization losses and thermal decomposition. To overcome these limitations and corroborate the ability of the emulsion electrospinning to incorporate natural products, two crude hydroethanolic extracts of HP and CM, known for their remarkable antimicrobial properties, were prepared by maceration and then loaded

into two different W/O emulsions consisting of Poly(L-lactic acid) (PLLA), PVA, and CS, and PCL, PVA, and Pectin (PEC), respectively.

Firstly, the HP was loaded into electrospun PLLA/PVA/CS nanofibers with two different amounts (2.5% and 5.0% owf) to achieve the optimal conditions to ensure an appropriate support and microenvironment for the healing process. The main results revealed that the produced membranes, mainly when 2.5% owf crude HP extract was incorporated, provided the desired properties for wound dressing materials due to their nanofibers morphology, porosity, wettability, vapor and gas permeation, as well as water uptake capability. Furthermore, the *in vitro* assays demonstrated that the produced membranes effectively inhibited the growth of bacteria without inducing any cytotoxic effect on normal human dermal fibroblast (NHDF) cells. Moreover, the observed sustained HP release profile from nanofibers was achieved, which is crucial to enhance the healing process.

Meanwhile, the fabricated electrospun PCL/PVA_PEC nanofibrous meshes containing 2.5% owf of the CM showed the features required to promote both the regeneration of skin tissue and to prevent wound contamination, as well as mechanical properties similar to those of the native skin. Overall, the emulsion electrospinning is an attractive approach to incorporate natural products and produce, in single-step, single-layer nanofibrous delivery systems.

On the other hand, the crude plant extracts proved to be a promising alternative to EOs due to their easy availability, low cost, and versatility. Also, these ecologically sustainable mixtures with multiple therapeutic properties have shown to be more effective than their isolated components, perhaps owing to positive synergetic interactions between the different compounds.

Although the previous nanofibrous membranes have demonstrated promising properties to be used as wound dressing materials, they are not always capable to reproduce both the structure and functions of native skin. Thus, the knowledge and the know-how acquired up to this stage of the doctoral work have allowed the development of a new approach focused on the benefits of producing double-layer nanofibrous wound dressings containing crude medicinal plant extracts.

Concerning the above mentioned, a double-layer nanofibrous material was successfully produced with an upper layer of PLLA and a lower layer of Polyethylene oxide (PEO), CS, and HP. The PLLA's upper layer revealed excellent mechanical properties as well as a suitable porosity and wettability to act as a waterproof and breathable barrier preventing bacteria penetration to the wound site. On the other hand, the PEO_HP_CS's lower layer was able to mimic the structure and properties of the native skin's ECM, easily absorb the wound exudate, and avoid the growth of *S. aureus* and *P. aeruginosa*, strengthening its suitability to improve the healing process. Similarly, a novel electrospun double-layered wound dressing membrane was produced with a top layer made of PCL that protects the wound against external threats, while CS was cross-linked with sodium tripolyphosphate (TPP) in order to be used as a carrier for CA, and then added to PVA to produce the bottom layer. Due to their features, this layer was able to modulate the release of the CA according to the demands of the healing process while also inhibit the growth of *S. aureus* and *P. aeruginosa* without eliciting any toxic effect on NHDF cells.

Finally, a nano-coating of PVA, CS, and AG onto a cotton gauze bandage was applied to suppress the limitations of the cotton dressings, which can lead to wound dehydration, cause skin maceration, and trauma and pain during dressing removal. Thus, the combination the most advantageous features of cotton (mechanical protection) with the ability of the electrospun nanofibrous layer in maintain the moist wound environment, absorb the excess exudates, and delivery bioactive compounds improves the performance of this composite material in skin regeneration. For this purpose, the cellulose cotton was oxidized by the radical 2,2,6,6-tetramethylpiperidinyl-1-oxy free radical (TEMPO), one of the most common surface chemical modification of cellulose fibers, to convert the surface hydroxyl groups into charged carboxyl entities. The negatively charged carboxyl groups were convenient to interact with the positively amino groups of CS, which was previously blended with PVA and AG to produce the nanofiber coating. The results demonstrated that the PVA_CS_AG's layer, designed to be in contact with the wound, exhibited a better ability to ensure a moist wound healing environment and exudate absorption than the PVA_CS's layer. Besides, this layer showed an enhanced bactericidal activity against *S. aureus* and *P. aeruginosa* and adequate properties to promote cell adhesion and proliferation. Hence, composite wound dressings by coating of cotton with a nanofibrous layer open the way for developing new potential composite wound dressings, including based on the previously produced materials.

Overall, it was found that all approaches enabled the successful production of the polymeric electrospun nanofibrous materials to be used as wound dressings. Also, medicinal plant extracts demonstrated to be a very powerful source of bioactive compounds that can be incorporated into nanofibrous meshes and improve the performance of these materials without inducing any cytotoxic effect and develop any resistance to bacteria.

Therefore, by analysing and correlating all the obtained results summarized in Table 1 with the desired values for an ideal wound dressing with antimicrobial properties, it can be concluded that the produced electrospun PCL/PVA_PEC nanofibrous meshes containing CM displayed a better antibacterial activity against *S. aureus* (99.98 ± 4.43%, 3.82 Log reduction) and *P. aeruginosa* (95.26 ± 5.52%, 1.32 Log reduction) than the other single-layer wound dressing materials produced via emulsion electrospinning. Furthermore, those electrospun nanofibrous meshes resulted in excellent properties to promote a perfect wound healing process, as mentioned above. The obtained fibers exhibited good morphology and a mean diameter of 190.53 ± 56.07 nm, which is within the size range displayed by the collagen fibers present in native ECM (50-400 nm). Besides, the produced electrospun nanofibrous meshes revealed a porosity above 90% (94.38 ± 4.08%) and a moderate hydrophilic character (60.30 ± 14.99°) able to sustain a moist environment at the wound site, as well as ability to provide support for cell adhesion and proliferation. Also, the electrospun PCL/PVA_PEC nanofibrous meshes incorporated with CM presented the desired value of water uptake (between 100-900%) and vapor permeation (between 2000-2500 g/m^2/day), which highlight their potential to absorb wound exudates and ensure an efficient nutrient supply and gas exchanges. Moreover, these

nanofibrous meshes showed a suitable release for wound healing, as well as good mechanical properties for handling (Young's modulus between 0.40-20.00 MPa).

Among the fabricated double-layered membranes, the bilayered electrospun membrane composed by a PCL's top layer, and a PVA_CS-TPP_CA's lower layer was able to avoid bacterial invasion and exhibited a higher inhibitory effect against *S. aureus* (99.96 ± 6.04%) and *P. aeruginosa* (99.94 ± 0.67%), reaching a 3 Log reduction. According to what was described above, the obtained results demonstrated that the PCL's top layer presented a lower porosity and a more hydrophobic character, which is essential to protect the wound against external threats. In turn, the highly porous and hydrophilic PVA_CS-TPP_CA's lower layer endows this wound dressing material with the ability to absorb a high amount of exudate (~600%). However, the ideal water vapor transmission rate (WVTR) and mechanical properties were not yet achieved. Concerning that, these features could be improved by adjusting the structural properties of this membrane, namely the nanofibers' orientation and/or the thickness of both layers, in order to perfectly mimic the structure of epidermis and dermis of the human skin.

Altogether, this work highlights the benefits of using simple, cost-effective, versatile, easy scale-up techniques to produce biocompatible and biodegradable materials with unique properties to attend to the demands of an ideal wound dressing. Moreover, it has been reinforced that the incorporation of crude plant extracts in these materials, which are eco-friendly, non-expensive, non-toxic, and efficient alternatives against drug-resistant bacteria is an effective approach to further improve their performance as antimicrobial wound dressings. Regarding this, the blending of synthetic and natural polymers and the medicinal plant extracts applied should be carefully chosen based on the capability to promote both the healing process and prevent wound infection, which remains one of the most frequent causes of wound healing failure.

Table 1 – Summary of the main results obtained with the different strategies applied.

Wound dressings Features	**PCL/PVA/CS**	**PLLA/PVA/CS**	**PCL/PVA/PEC**	**PLLA/PEO_CS**	**PCL/PVA_CS-TPP**	**Cotton/PVA_CS**
Production Method	Electrospinning using O/W emulsion	Electrospinning using W/O emulsion	Electrospinning using W/O emulsion	Double-layered	Double-layered	Double-layered
Medicinal plants and their derivatives	EUG	HP	CM	HP	CA	AG
	5% owf	2.5% owf	2.5% owf	2.5% owf	3 mg/mL	5.0 wt.%
Morphologic Features / Fibers diameters (nm)	Uniform fibers with fewer beads / 199.90 ± 48.86	Thinner and uniform fibers / 119.96 ± 29.90	Thinner and uniform fibers / 190.53 ± 56.07	Uniform fibers / PLLA's upper layer: 1860 ± 680 and PEO_HP_CS' lower layer: 88.33 ± 29.45	Uniform fibers / PCL's top layer: 277.63 ± 85.19 and PVA_CS-TPP_CA's bottom layer 284.34 ± 75.79	208.11 ± 57.92
Wettability (°)	59.37 ± 5.11	52.22 ± 8.17	60.30 ± 14.99	PLLA's upper layer: 105.23 ± 2.89 and PEO_HP_CS' lower layer: 50.97 ± 11.60	PCL's top layer: 105.93 ± 18.85 and PVA_CS-TPP_CA's bottom layer: 42.50 ± 16.93	TEMPO-oxidized cotton: 27.53 ± 6.84 and PVA_AG_CS: 42.37 ± 7.52
Porosity (%)	88.52 ± 4.09	93.30 ± 1.24	94.38 ± 4.08	PLLA's upper layer: 74.25 ± 13.77 and PEO_HP_CS' lower layer: 93.71 ± 1.00	PCL's top layer: 64.01 ± 10.61 and PVA_CS-TPP_CA's bottom layer: 96.88 ± 1.14	TEMPO-oxidized cotton: 76.09 ± 5.64 and PVA_AG_CS: 92.77 ± 6.01
WVTR ($g/m^2/day$)	-	2230.58 ± 39.49	2019.82 ± 151.01	1916.51 ± 143.02	1757.12 ± 67.69	1304.09 ± 123.13
Water uptake ability (%)	-	~500	~400	~500	~600	~320 at pH=8.0 and ~400 at pH=5.5
Mechanical properties: Young's modulus (MPa)	-	-	15.75 ± 6.46	15.86 ± 0.50	36.36 ± 7.29	$0.46\times10^3 \pm 0.11\times10^3$

In vitro release profile	Burst effect during first 8 hours followed by a sustained release during 120 hours	Sustained release during 72 hours	Faster sustained release rates over the first 10 days	Controlled burst release during 5 days	Initial burst release within the first 6 hours, followed by a gradual release up to 9 days	Initial burst release was observed within the first 6 hours, followed by a gradual release up to 8 days
Antibacterial activity (%)	Against *S. aureus* (83.08%) and *P. aeruginosa* (87.85%)	Against *S. aureus* (93.11 ± 3.53%)	Against *S. aureus* (99.98 ± 4.43%) and *P. aeruginosa* (95.26 ± 5.52%)	Against *S. aureus* (99.75 ± 1.30%) and *P. aeruginosa* (90.61 ± 1.63%)	Against *S. aureus* (99.96 ± 6.04%) and *P. aeruginosa*) (99.94 ± 0.67%)	Against *S. aureus* (99.17 ± 4.05%) and *P. aeruginosa* (98.13 ± 0.88%)
In vitro cytotoxicity	No cytotoxic effect on NHDF cells	No cytotoxic effect on NHDF cells	No cytotoxic effect on NHDF cells	No cytotoxic effect on NHDF cells	No cytotoxic effect on NHDF cells	No cytotoxic effect on NHDF cells

Future Trends

Taking into account all the work performed until now, it could be of interest to optimize nanofibers' orientation and the layer thickness of the double-layered nanofibrous membranes in order to improve the mechanical properties for handling and better control the vapor and gas permeation. This is also intended to precisely mimic the epidermal and dermal morphology of the native human skin. Likewise, it is mandatory to perform some additional studies regarding the *in vivo* inflammatory and wound-healing responses of the produced electrospun wound dressing materials to further characterize their suitability for wound management. In addition, resistance assays against multidrug-resistant bacteria should be performed for testing the efficiency of these plant extracts, although the literature does not report a direct cause-and-effect relation between the resistance of bacteria to the studied medicinal plants and essential oil.

Nonetheless, despite the promising results obtained with the different strategies applied, these wound dressing materials are not able to perfectly reproduce the native structure and all functions of the skin, although can be of benefit in chronic wound management. To improve the knowledge acquired until now and reach the ideal wound dressing, several research lines could be further explored due to their promising preliminary results, namely the combination of electrospinning with 3D-printing to charge different polymers with a variety of cells (fibroblasts, keratinocytes, endothelial, and stem cells). In fact, these new 3D nanostructures are engineered to further enhance the healing process as well as the regeneration of skin appendages, like hair follicles, sweat ducts, and sebaceous glands, after skin injury. Also, the incorporation of sensors into electrospun membranes has been studied in order to successfully monitor the healing progress of a wound, namely by controlling the pH, temperature, oxygen, wound moisture, drug delivery capability, and by detecting bacteria at the wound site.

Finally, considering the implementation and commercialization of the wound dressing materials on the market, careful and exhaustive work needs to be performed to make sure the quality, safety, and functional performance of the produced materials. Therefore, in addition to the work presented in this thesis in advanced materials science and processing that aims to develop the materials themselves, other assays, namely several validation processes, are mandatory to confirm the safety and performance of the final product. Thus, if the fabricated materials demonstrate compliance with the procedures established in national and international standards, they can be placed on the market. In Portugal, Infarmed is the competent health authority, which ensures that medical devices like wound dressing materials respect the legal requirements for introduction in the market and whose guidelines should be followed.

Overall, it is crucial that a multidisciplinary team, involving engineers, chemists, pharmacists, and clinicians continue to work together to achieve further improvements on the production methods, properties, and performance of wound dressings containing natural products, which are essential to fighting infections and display a low propensity to develop resistance to bacteria.